NOVEL INSIGHTS INTO MULTISENSORY PROCESSING IN THE SUPERIOR COLLICULUS

By

Dipanwita Ghose

Dissertation

Submitted to the Faculty of the

Graduate School of Vanderbilt University

In partial fulfillment of the requirements for

the degree of

DOCTOR OF PHILOSOPHY

in

Psychology

August, 2013

Nashville, Tennessee

Approved

Dr. Mark Wallace

Dr. Vivien Casagrande

Dr. Ford Ebner

Dr. Jon Kaas

Dr. Anna Roe

Dedicated to my parents who made me what I am today and my husband who encouraged and supported me every step of the way.

ACKNOWLEDGEMENTS

This Dissertation Thesis is the outcome of 4 years of hard work through which I have been fortunate enough to receive the love and support of a great group of people, each of whom have contributed to my success in their own special way. I would take this opportunity to express my heartfelt gratitude to each of them here.

First and foremost, I would like to express my heartfelt gratitude to Dr. Mark Wallace who has been an excellent mentor and provided me with unconditional support through the last 4 years. None of this would be possible without his help, guidance and constant encouragement. I have learnt a lot from him in the past few years that have shaped my professional development and will be forever grateful to him for the kindness and generosity I have received from him always.

Next, I would like to express my deep sense of gratitude to Dr. Ford Ebner who is the reason for my acceptance in Vanderbilt. He has been a constant pillar of support, not only academically but also in our personal lives here in a foreign country. I am forever indebted to him for the help and support that I have received from him through the past years. Along with Dr. Ebner, I would also like to thank Dr. Leslie Smith for her kindness and support as well.

I would also like to thank my PhD committee members, Dr. Vivien Casagrande, Dr. Jon Kaas and Dr. Anna Roe for all the useful feedback and help I received from them in my committee meetings. Without their invaluable inputs regarding my projects, this work would never have been possible. Additionally I would like to thank deeply, our

collaborator, Dr. Alex Maier without whose help a great part of my thesis work would be incomplete.

I would also like to thank past and present members of the Wallace lab who have made my journey fun and memorable. I thank the entire team of electrophysiology in the lab without whose time and support none of this work would ever be possible. Special thanks go to Aaron Nidiffer for helping me extensively with his MATLAB skills. He is essentially my "*Matlab guru"* and I am grateful to him for helping me with the construction of a lot of the figures for my different manuscripts.

I would like to thank the Division of Animal Care in Medical Center North especially Dr. Troy Apple and LuAnn for helping me take good care of our animals.

I would like to thank Brian Lustig and Dr. Corrie Camalier for the scientific discussions that we had over the years that helped me interpret a lot of my findings better.

I thank the administrative staff of the Department of Psychology especially Vay Welch for their constant help and support. I would also like to thank my Directors of Graduate studies past and present (Thomas Palmeri and Rene Marois) and the Chair of my Department Dr. Andrew Tomarken who was also an amazing statistics teacher.

I thank my parents, my parent-in-laws, my brothers and sisters and my whole family who have always prayed for my success and showered me with unconditional love. Without their motivation, love and encouragement, I would not be here.

I thank all my friends in Nashville and all across the world for their constant support through good times and bad that gave me strength and courage to keep moving

forward. All the crazy parties that we had together despite my busy work schedule helped me relieve my stress and preserve my sanity.

Last but not the least, I would take this opportunity to express my sincere heartfelt gratitude to my husband, Dr. Ayan Ghoshal, who has loved and supported me through thick and thin for the past 10 years of my life. He motivated me to pursue research here in USA and was instrumental in providing me useful information that helped me apply and successfully join Vanderbilt University. His scientific inputs have been invaluable over the years and his patience and support has been indispensable all through my graduate career. None of this would be possible without his unconditional love, care and support.

TABLE OF CONTENTS

LIST OF TABLES

LIST OF FIGURES

PROLOGUE

Combining information from multiple sensory modalities is an essential prerequisite to navigate the world around us. Thus, there has been an upsurge in studying multisensory processing in the brain over the last several decades. The long standing model system used to study how the brain combines information from different modalities at the level of single neurons has been the midbrain structure, the superior colliculus (SC) for various reasons discussed later. Early work has extensively characterized responses of SC neurons to stimuli from multiple modalities, the factors affecting the neurons' ability to combine multisensory information and some of the behavioral benefits of combining information from different modalities have been widely studied. However the mechanisms by which such multisensory integration is achieved and the detailed nature of the receptive field architecture of these neurons that make it possible for them to support multisensory processing still remains largely ignored. Thus, the overarching goal of this thesis is to detail the receptive field architecture of multisensory SC neurons and study mechanisms by which such multisensory integration is brought about in these neurons with the hope of shedding light on the mechanistic processes underlying multisensory information processing in the brain which remains elusive to date. The sections to follow will review the literature germane to studying mechanisms underlying multisensory integration in the SC.

First, the anatomy and connections of the SC will be described to provide detailed knowledge about the model structure here. Next, the factors affecting the processing of

multisensory stimuli in this midbrain structure will be discussed. This will include a description of the measures used to index multisensory processing to date and also review the behavioral role of SC in order to understand the functional benefits of multimodal interactions. Finally, the latter part of the introduction will focus on current and novel methods that can be used to shed light on the mechanisms underlying multisensory interactions.

Understanding the mechanistic basis of multisensory processing is important. This will help us learn the ways by which information from multiple modalities are combined by the neurons in the normal brain that facilitates behavior. This in turn will help us design ways in which multisensory processing can be facilitated when sensory deprivation occurs and that will help restore the behavioral/perceptual benefits of multisensory integration under sensory deprived conditions as well.

CHAPTER I

INTRODUCTION

GENERAL INTRODUCTION TO MULTISENSORY PROCESSING

We live in a world where we are constantly bombarded with sensory information from multiple modalities and our brains are tasked with processing sensory information and using it to guide behavior and perception. The long standing notion about the sensory brain has been that different sensory information is processed in separate brain areas and after extensive unimodal processing occurs, higher order association areas are tasked with combining information from multiple senses (Felleman and Van Essen 1991; Kuypers et al. 1965). This view was supported by early anatomical studies that revealed few if any anatomical connections between visual, auditory, somatosensory cortical areas in cats and monkeys (Kuypers et al. 1965), and by lesion studies in which damage restricted to discrete regions of cortex produced unimodal behavioral deficits (Massopust et al. 1965). However, this classical view has been challenged by growing evidence supporting convergence of inputs from different sensory modalities onto individual neurons in early cortical areas. Examples of this include: visual and somatosensory processing in auditory cortex (Allman et al. 2008a; Allman et al. 2008b;

Brosch et al. 2005; Cappe and Barone 2005; Fu et al. 2003; Ghazanfar et al. 2005; Kayser et al. 2005; Schroeder and Foxe 2002; Schroeder et al. 2001), auditory and somatosensory processing in visual cortex (Falchier et al. 2002; Morrell 1972; Rockland and Ojima 2003) and visual and auditory processing in somatosensory cortex (Zhou and Fuster 2004; 2000). Multisensory convergence is even seen at the level of the thalamus, including in structures such as the medial division of MGN (Graham 1977; Linke 1999), pulvinar (Jones 1985; Benevento and Fallon 1975; Benevento and Standage 1983; Fitzgibbon et al. 1995; Jones 2007; Rodrigo-Angulo and Reinoso-Suarez 1988), and suprageniculate nucleus (Benedek et al. 1996; Benedek et al. 1997; Berkley 1973). These early sensory convergence patterns may confer advantages of multisensory processing early on in the neuraxis. In addition to early cortical and thalamic areas mentioned above, multisensory convergence and integration has been described in higher cortical areas including the anterior ectosylvian cortex and lateral suprasylvian cortex (Jiang et al. 2002; Wallace and Stein 1994) in cats, and the superior temporal sulcus (STS)(Barraclough et al. 2005), lateral intraparietal area (LIP) (Gifford and Cohen 2004; Linden et al. 1999; Mazzoni et al. 1996; Snyder et al. 1998) ventral intraparietal area (VIP) (Avillac et al. 2005; Bremmer et al. 2002; Schlack et al. 2005), the temporo-parietal association cortex (Tpt) (Leinonen et al. 1980), ventrolateral prefrontal cortex (VLPFC) (Sugihara et al. 2006) premotor cortex ((Fogassi et al. 1996; Fuster et al. 2000; Graziano 1999; Graziano et al. 1994) in primates.

The advantages of building a system capable of processing inputs from multiple modalities from very early stages may be manifold. Multisensory integration in the thalamus may help to relay the integrated signal to the early cortical areas (Giard and

Peronnet 1999; Molholm et al. 2002) thus aiding multimodal binding. On the other hand cross modal processing in early cortical areas has been suggested as a way to increase information processing efficiency. In addition studies show that attention shifts between sensory modalities can impact local sensory processing in early cortical areas like SII (Steinmetz et al. 2000). Multisensory integration in higher cortical areas like LIP is thought to play a role in multisensory guided movements in space (Ghazanfar and Schroeder 2006) while VIP has been suggested to be involved in determining movement direction in head centered coordinates during self-motion (Zhang et al. 2004). STS has been implicated to play a role in audiovisual speech integration and biological motion processing (Barraclough et al. 2005; Calvert et al. 2000; Stevenson and James 2009), frontal eye field (FEF) is thought to play a role in visual and auditory motion processing (Lewis et al. 2000). VLPFC may be an essential part of the network involved in integration of auditory and visual communication signals (Sugihara et al. 2006) while ventral premotor cortical (vPMC)areas are supramodally involved in gestural communication and understanding action (Keysers et al. 2003; Kohler et al. 2002) and perceptual decision making (Romo et al. 2004). However researchers differ in opinion regarding the exact role of vPMC but are suggested to be an area in which sensory inputs can access various motor programs through associative links (Hickok et al. 2009; Rizzolatti et al. 1988).

Thus, all the recent studies described above, bear evidence to the fact that multisensory processing in the brain is much more prevalent than was realized. Multisensory processing is more efficient and can confer functional benefits in behavior and perception. Such functional benefits of multisensory processing are evident in our daily

lives. For example when one is watching movies on television or at the cinema and voices are perceived to originate from the actors on the screen, despite a potentially large spatial discrepancy between the image and the sound source. Another well-known example is that of speech perception in a noisy environment, often referred to as the "Cocktail Party" effect. Understanding speech, particularly in a noisy environment is significantly facilitated by viewing the speaker's face (Sumby and Pollack 1954; Grant and Seitz 2000; Schwartz et al 2004). In fact, this bimodal gain may be an important factor in the improvements in speech comprehension seen in those with significant hearing loss after visual training (Schorr et al 2005; Rouger et al 2007). It has also been shown that tactile location can be "captured" by visual location (Pavani et al 2000; Rock and Victor 1964). All these effects emphasize the strong influence of visual signals on other modalities, primarily due to the fact that humans are primarily vision dominant animals. However, visual perception can also be altered by other modalities. Depending on the temporal relationships between visual and auditory stimuli, visual temporal resolution can be improved or degraded by sounds (Scheier et al 1999). This study showed that when two lights were turned on at different locations with a small temporal delay, the accuracy of temporal order judgments between the two lights was better with a sound and another sound following the visual stimuli (A-V-V-A) than when no sound was presented. However, the subjects' performance became worse when two sounds were inserted between the two visual stimuli (V-A-A-V). In addition to improving visual temporal processing, a sudden sound can improve the detection of a subsequent flash at the same location (McDonald and Hilliard 2000). The perceived intensity of a visual stimulus has been shown to be enhanced by the presence of sound (Stein et al

1996).Presence of sound can alter the interpretation of an ambiguous visual motion (Sekuler et al 1997) and auditory motion can bias visual motion perception as well (Meyer and Wuerger 2001; Shams et al 2001). Behavioral manifestations of multisensory processing are also reflected in faster reaction times and greater accuracy of responses. Using the saccade system as model, numerous studies have demonstrated that saccadic eye movements made to a visual target that is spatially and temporally coincident with an auditory/somatosensory non target have shorter latencies than saccades that are directed towards the same visual target without an auditory/somatosensory co stimulation (Frens et al 2005; Amlot et al 2003;Colonius and Arndt 2001; Frens and Van Opstal 1998; Corneil et al 2002).

Thus, studies done to date have established the existence of multisensory processing in a wide variety of brain areas and the behavioral/perceptual benefits of such multisensory processing. However, the mechanisms underlying multisensory processing in these different brain areas remain elusive. Recent studies (Kayser et al. 2005; Lakatos et al. 2007) of multisensory processing in the auditory cortex provide evidence for a “phase resetting mechanism” of ongoing neuronal oscillation wherein the cross modal non-dominant stimulus resets the phase of ongoing neuronal oscillation to its “ambient (high-excitability) phase” thus aiding perception. Similar studies need to be done in different brain areas to understand the mechanistic basis of multisensory processing in cortical and subcortical areas.

SUPERIOR COLLICULUS: A MODEL STRUCTURE FOR STUDYING MULTISENSORY PROCESSING IN THE BRAIN

Though most of the studies discussed above describe multisensory integration in thalamus and cortex, multisensory neurons have been studied widely in the midbrain structure, the superior colliculus (SC) in cats (Meredith and Stein 1983). The SC is an ideal model for studying multisensory processing because of its high incidence of multisensory neurons (Meredith and Stein 1996) and its direct involvement in orientation behaviors (Sprague and Meikle 1965; Stein et al. 1988; Stein BE 1993). Moreover, the SC contains mutually aligned map of visual, auditory, and somatosensory space which makes it well suited for its role in multisensory processing. Individual neurons in the SC receive converging inputs from multiple sensory modalities and in turn integrate this information to guide orientation behavior via its output to target motor nuclei in the brainstem and spinal cord. The anatomy and connections of the SC help us to understand its multisensory nature and the potential functional benefits that can be derived by integrating multiple modalities in this midbrain structure.

Anatomy and connections of the superior colliculus

The superior colliculus (SC) is a laminated structure that, in mammals, is composed of seven layers based on the distribution of fibers and the packing density of the neurons in the different layers (Kanaseki and Sprague 1974; May 2006). It's non-mammalian homologue, the optic tectum is also involved mainly in visuomotor behavior (Ewert 1970; Ingle 1970; Knudsen 2004; Knudsen et al. 1993; Northcutt 2002; Saitoh et al.

2007; Stein BE 1993). However, studies in avian optic tectum show that, similar to SC it is also involved in multimodal spatial localization and control of spatial attention (Lovejoy and Krauzlis 2010; McPeek and Keller 2004; Muller et al. 2005; Sridharan et al. 2011; Stein BE 1993; Winkowski and Knudsen 2007; 2006).

Based on overall differences in neuronal morphology, afferent-efferent connections, physiological properties and behavioral involvements the SC can be divided into superficial and deep layers.

Superficial layers of the superior colliculus:

Structural observations: The first three layers of the SC comprise the superficial layers. They include stratum zonale (SZ), stratum griseum superficiale (SGS) and stratum opticum (SO). The SZ in mammals is very narrow (20-25 μm) and consists of few small and medium sized neurons (Sterling 1971) that correspond to marginal and horizontal cells described by Cajal (Cajal 1995). The SGS lies below the SZ and is 300-400 μm in depth (Huerta MF 1984). It consists of neurons of varying sizes that include horizontal cells presumed to be interneurons, the marginal cells and the stellate cells (May 2006). The SO mainly consists of fibers and some cells interspersed among the fibers (Huerta MF 1984; May 2006). These fibers predominantly include the incoming retinal axons, details of which are described later.

Afferent connections: Retinal input: On the basis of input architecture**,** the superficial layers of the superior colliculus are thought to be purely visual in nature. The retina and primary visual cortex (area 17) are the two best documented inputs to the superficial layers. The retinal input is heavily distributed to SGS with fewer terminations in SO [cat:

(Graybiel 1975; 1976); ferret: (Zhang and Hoffmann 1993); monkey: (Pollack and Hickey 1979); rat: (Lund et al. 1980)].There are species specific differences in the distribution of the retinotectal projections within the SC. Here, for brevity, I will restrict my descriptions to the cat SC. The ganglion cells of the retina provide a major input to the superficial layers of the SC primarily to SGS with lesser terminations in SO. There are 3 main types of retinal ganglion cells in cats (X, Y, W) as identified by physiological studies (Cleland et al. 1971; Enroth-Cugell and Robson 1966; Kuffler 1953). The SC in cats receives input from the Y (which are predominantly fast conducting) and W (which is predominantly slow conducting) cells (Illing 1980; Illing and Wassle 1981; Kelly and Gilbert 1975; Wassle and Illing 1980). Some studies show that in addition to the Y and W types of cells, approximately 10% of the X type of retinal ganglion cells also project to the SC (Illing 1980; Wassle and Illing 1980). However, the X cell input to the SC is more controversial with some studies showing X cells projecting to pretectum only (Bowling and Michael 1980; Tamamaki et al. 1995).

In addition, there are sub-laminar differences in retinal projections from the two eyes in cats (May 2006) .The contralateral projection is most dense in the dorsal region of SZ/SGS border, but terminals are also present in the remaining regions of SGS. The ipsilateral projection terminates in patches within ventral SGS. The ipsilateral projections alternate with the contralateral projections in a graded fashion but the segregation is not absolute (Pollack and Hickey 1979).More specifically, input from the contralateral eye arises mainly from the W cells, with very little contribution from the Y cells (Fukuda and Stone 1974; Hoffmann 1973; Wassle and Illing 1980). In contrast, the ipsilateral projection is mainly from the Y cells (Fukuda and Stone 1974). The laminar

extent of the distribution of the ipsilateral and contralateral projections differs greatly. Whereas the contralateral input terminates throughout the rostrocaudal extent of the SC, the ipsilateral input is much more limited. The large central zone of SC receives both ipsilateral and contralateral input. This is called the binocular zone. Neurons in this zone are binocularly activated by stimuli placed within the contralateral hemifield (McIlwain and Buser 1968; Rhoades and Chalupa 1979; Siminoff et al. 1966; Straschill and Hoffmann 1969). In cats, the rostral portion of the SC receives direct retinal input from contralateral temporal retina as well as input from contralateral cortical areas related to vision. This zone contains a representation of approximately 40° of the ipsilateral hemifield. The most caudal region of SC receives input from the most temporal portion of the visual field via the contralateral nasal retina; this is the monocular zone.

Cortical inputs to superficial SC: The major cortical input to the superficial SC comes from the primary visual cortex (area 17) (Graham and Casagrande 1980; Harting and Noback 1971; Martin 1968; Symonds and Kaas 1978). The cortico-collicular projection arises from Layer V pyramidal cells and ends in tight visuotopic register with the retinal inputs within superficial layers of SC (Hollander 1974; Kawamura and Konno 1979). There is differential distribution of the cortical projections within the superficial layers of SC. In cats more cortical terminals are present in areas of the SC which contains a representation of the central part of the visual field than in regions representing more peripheral parts (Updyke 1977). This is the same part of the SC that receives a diminished input from the retina and thus it is suggested that the relative influences of cortical and retinal afferents on collicular neurons vary as a function of their location

(Graybiel 1975; Harting and Guillery 1976; Kanaseki and Sprague 1974; Updyke 1977). In addition, the rostral pole of the SC (the region that contains a representation of ipsilateral hemifield), receives crossed input from Layer V of areas 17, 18, 19 (Gilbert and Kelly 1975; Hollander 1974; Powell 1976; Updyke 1977). The superficial layers SGS and SO also receive exclusive inputs from Area 20 a and b and the posterior suprasylvian area while the posterior lateral, posterior medial and anterior medial lateral suprasylvian sulcus predominantly target SO and SGS with minor projections to deeper layers (Harting et al. 1992; Hollander 1974; Norita et al. 1991) and the frontal eye fields (Kunzle and Akert 1977; Kunzle et al. 1976). Also, the corpus callosum is important for the ipsilateral hemifield representation in rostral pole of SC in cat (Antonini et al. 1979; Antonini et al. 1978)

Other afferents: In addition to the retinal and cortical inputs described above, the superficial SC also receives thalamic input from several sources. Bilateral input arises from the ventral LGN (Edwards et al. 1979; Edwards et al. 1974; Graybiel and Hartwieg 1974; Kawamura et al. 1978; Nakamura and Itoh 2004; Swanson et al. 1974). In addition, input from the pretectal complex is derived from the nucleus of the optic tract (Edwards et al. 1979; Weber and Harting 1980). Finally, the parabigeminal nucleus projects bilaterally to the SC (Graybiel 1978; Stevenson and Lund 1982).

Efferent connections: Analysis of the projections of the superficial layers of the SC reveals a diversity of targets. The SGS layer projects to the dorsal lateral geniculate nucleus [cat :(Harrell et al. 1982; Kawamura et al. 1980); galago: (Baldwin and Kaas 2012; Harting et al. 1991); monkey: (Wilson et al. 1995)]. The superficial SC also projects to the ventral LGN (Harrell et al. 1982), and provide a major projection to the

pulvinar/lateral posterior (Pul/LP) complex [cat: (Caldwell and Mize 1981; Kawamura et al. 1980; Mooney et al. 1984); galago: (Raczkowski and Diamond 1981; Rodrigo-Angulo and Reinoso-Suarez 1988); monkey: (Benevento and Standage 1983; Huerta and Harting 1983)]. In monkeys the main terminal zone of superficial SC projections is in the inferior pulvinar (Huerta and Harting 1983; Lin and Kaas 1979; May 2006). In addition to receiving projections from the superficial SC, the SC also projects to the parabigeminal nucleus (Baldwin and Kaas 2012; Casagrande et al. 1972; Harting et al. 1973).

Deep layers of the superior colliculus

Structural observations: The intermediate and deep layers of the SC include stratum griseum intermediale (SGI), stratum album intermediale (SAI), stratum griseum profundum (SGP) and stratum album profundum (SAP). The intermediate and deep layers of the SC consist of large (35-60μm in diameter), medium (20-30μm) and small (8-15μm) neurons (Norita 1980). The large neurons occupy mainly the lateral two thirds of the SC while the medium and small neurons are found throughout the intermediate and deep layers. The deep layers of the SC receive inputs from visual, auditory, somatosensory and motor brain structures.

Afferent connections: Visual: The intermediate and deep layers of the SC receive afferents from a diverse set of visual sources. Unlike the superficial layers, most of the visual inputs to the deep layers come from extrastriate visual areas (area 20, 21) that include the lateral suprasylvian area (Baleydier et al. 1983; Berson and McIlwain 1983; Kawamura and Konno 1979; Segal and Beckstead 1984; Tortelly et al. 1980) and the anterior ectosylvian visual area (Mucke et al. 1982). These projections are

predominantly ipsilateral where projections form a series of patches (Huerta MF 1984). Very little direct retinal inputs terminate in the deep layers and whatever sparse projections are present originate from the contralateral retina and are confined to upper regions of rostral half of the structure (Beckstead and Frankfurter 1983). The intermediate and deep layers also receive sparse visual input from ventral LGN and pretectum (Edwards et al. 1979; Edwards et al. 1974; Huerta MF 1984)

Auditory: The descending (i.e., cortical) component of the auditory input to deep SC comes from Field AES region of AES (Meredith and Clemo 1989). Ascending inputs that are mainly contralateral arise from the dorsomedial periolivary nucleus and a region medial to trapezoid body (Edwards et al. 1979). In contrast, ipsilateral ascending inputs originate in the inferior colliculus and nucleus of lateral lemniscus. These inputs tend to be restricted to caudal parts of deeper layers (Henkel 1983; Kudo 1981; Kudo and Niimi 1980; Moore and Goldberg 1966).

Somatosensory: The somatosensory descending afferents are primarily from the dorsal bank of AES from area SIV, which contains a well formed map of the body (Clemo and Stein 1982; McHaffie et al. 1988; Stein et al. 1983). The rostral suprasylvian sulcus also contains a body map that projects to the deep layers of the SC (Clemo and Stein 1984; Stein et al. 1983). The ascending component of the somatosensory projections to deep SC are heavy and arises from contralateral sensory trigeminal complex, dorsal column nuclei, lateral cervical nucleus and spinal cord (Blomqvist et al. 1978; Edwards et al. 1979; Huerta MF 1984).

Motor: Motor afferents to the intermediate and deep SC layers arise from numerous sources and are primarily ipsilateral, with the most prominent input being that arising from the frontal eye field (FEF) in cats and primates (Fries 1984; Huerta and Kaas 1990; Huerta et al. 1986; Kawamura and Konno 1979; Komatsu and Suzuki 1985; Leichnetz and Gonzalo-Ruiz 1996; Leichnetz et al. 1981; Moschovakis et al. 2004; Stanton et al. 1988). In cats FEF lies both in the ventral bank of the cruciate sulcus and the medial bank of the presylvian sulcus (Schlag and Schlag-Rey 1970). Corticotectal neurons are found in both these regions. These projections are primarily ipsilateral and terminate in SGI and to a lesser extent in SGP (Hartwich-Young and Weber 1986; McHaffie et al. 2001; Miyashita and Tamai 1989). In addition, heavy inputs arise from the substantia nigra of the basal ganglia (Moschovakis and Karabelas 1985). In rats this projection is entirely ipsilateral but in cats and primates a contralateral projection is more pronounced (Beckstead et al. 1981). The nucleus of the posterior commissure which is involved in upward eye movements (Christoff 1974) also projects to the ipsilateral deep SC (Huerta and Harting 1982a). The deep nuclei of cerebellum also project to the SC (Edwards et al. 1979).

Other afferents: Other afferents arise from contralateral SC, hypothalamus, locus ceruleus, raphe dorsalis, parabrachial nuclei, reticular formation, and reticular nucleus of the thalamus (Edwards et al. 1979; see May 2006 for review).

Efferent connections: The efferent connections of the intermediate and deep layers are more diverse and extensive than the superficial layers (Casagrande et al. 1972; Harting et al. 1980).There are two major descending tectofugal pathways : the ipsilateral tectopontine or tectobulbar (with medial and lateral branches) and the contralateral

tectospinal pathway, also called the predorsal bundle (Huerta MF 1984). Cross species differences exist in the efferent projections of SC. Below is a description of the the efferent connections of the intermediate and deep layers of cat SC. The predorsal bundle contains the main descending output of the SC. These axons arise from cells widely distributed in SGI and SGP in cats. They run parallel to the border of the central gray in the mesencephalic reticular formation (cMRF) before crossing to the contralateral side in the dorsal tegmental decussation beneath the oculomotor nuclei. They then descend adjacent to the midline, beneath the medial longitudinal fasciculus (MLF) all the way up to the cervical spinal cord (May 2006). The major target of the predorsal bundle is the paramedian pontine reticular formation (PPRF) (Cowie and Holstege 1992; Grantyn and Grantyn 1982). Moreover, some studies show that the crossed fibers of the predorsal bundle have collaterals that re-cross to terminate in ipsilateral pons (Cowie and Holstege 1992). A minor output from SC targets the nucleus prepositus hypoglossi (Cowie and Holstege 1992; Grantyn and Grantyn 1982).The predorsal bundle also sends collaterals to the central mesencephalic reticular formation (cMRF) which in turn contact the gaze related brainstem nuclei and spinal cord (Grantyn and Grantyn 1982; May et al. 2002). Efferent projections from SGI and SGP (which are mainly ipsilateral in nature) also target the rostral interstitial nucleus of the medial longitudinal fasiculus (riMLF) in cats (Graham 1977; Wang and Spencer 1996). Ipsilateral projections from the SC to the nucleus of the posterior commissure have also been reported (Graham 1977). Neurons in the rostral part of SGI also project to nucleus raphe interpositus (Langer and Kaneko 1984; May 2006). Rostral SC neurons also project bilaterally to the supraoculomotor area and the periaqueductal gray

(Edwards and Henkel 1978). Direct projections from SGI to abducens nucleus have also been reported (Langer et al. 1986). The intermediate and deep layers of the cat (SGI and SGP) of the SC project heavily to contralateral spinal cord and fewer ipsilateral projections have also been reported (Holstege 1988a; b; Murray and Coulter 1982; Nudo and Masterton 1988; 1989).

The tectospinal pathway in cats extends up to the cervical enlargement and terminates in Rexed's Lamina V-IX of contralateral cervical cord (Huerta and Harting 1982a; b). On the other hand, the tectobulbospinal tract in cats terminates within the medullary reticular formation (Cowie and Holstege 1992; Grantyn and Berthoz 1985; 1987). In addition the SC is intimately connected with various cerebellar nuclei and the inferior olivary nucleus (Graham 1977; Mower et al. 1979).

The ascending efferent pathway from the intermediate and deep layers of the SC reaches the suprageniculate nucleus of the thalamus, the centromedian/parafascicular complex, and the intralaminar nucleus (May 2006; Stein and Meredith 1993). Finally, a commissural pathway reaches the opposite SC. Fig 1-1 summarizes the efferent connections of the intermediate and deep layers of the cat SC.

Connectional organization of the Deep layers: Deep layers of the SC have a more complex connectional organization than the superficial SC. Similar to the superficial SC, fibers innervating the deep layers are usually restricted to specific parts of the dorsal ventral extent. For example in cats it has been shown that cells of the substantia nigra project to the dorsal border of SGI, inputs from the nucleus of the posterior commissure ramify below the nigral afferents and spinal trigeminal nucleus innervates a

zone ventral to nucleus of posterior commissure input (Huerta and Harting 1982b). In contrast to the inputs to the superficial layers, afferents to the deep lamina do not form continuous sheets across the mediolateral extent. The incoming fibers are distributed discontinuously forming a series of patches that are limited to a particular zone of the dorsal ventral extent of a particular layer. A characteristic of these patchy afferents being that those located in the medial parts are generally smaller and densely labeled than the ones situated laterally (Huerta MF 1984). In the rostrocaudal dimension, some afferents are present rostrally (commissural input, (Edwards 1977) while others are present caudally (input from inferior colliculus, (Kudo and Niimi 1980). Thus the deep layers do not form simple sublamina as the superficial layers. The afferent inputs are stratified in the dorso-ventral extent within a given deep layer. Such stratification of patchy afferents suggests that incoming fibers distribute to medial- lateral “subdivisions” of sub-lamina (Huerta MF 1984). Studies show that the efferent modules are sometimes also discretely organized as the afferent modules and certain afferent efferent modules are tightly coupled (Huerta et al. 1981; Huerta and Harting 1983). Thus, it can be inferred that that the complex connectional organization of the deep layers compared to the superficial layers are a result of their diversity of connections. The modular subdivisions of the deeper layers which are similar to the sub-lamina of the superficial layers serves to match certain inputs with certain outputs so that some autonomy of particular information channels prevail. The modules occupy specific dorsal ventral levels of a particular lamina. In addition, different modules may occupy different medial lateral positions within a layer, permitting different modules to interdigitate. This could allow the same dorsal ventral region of a deep layer to contain two entirely separate

information channels which effectively increases the number of segregated information channels that can flow through a given layer.

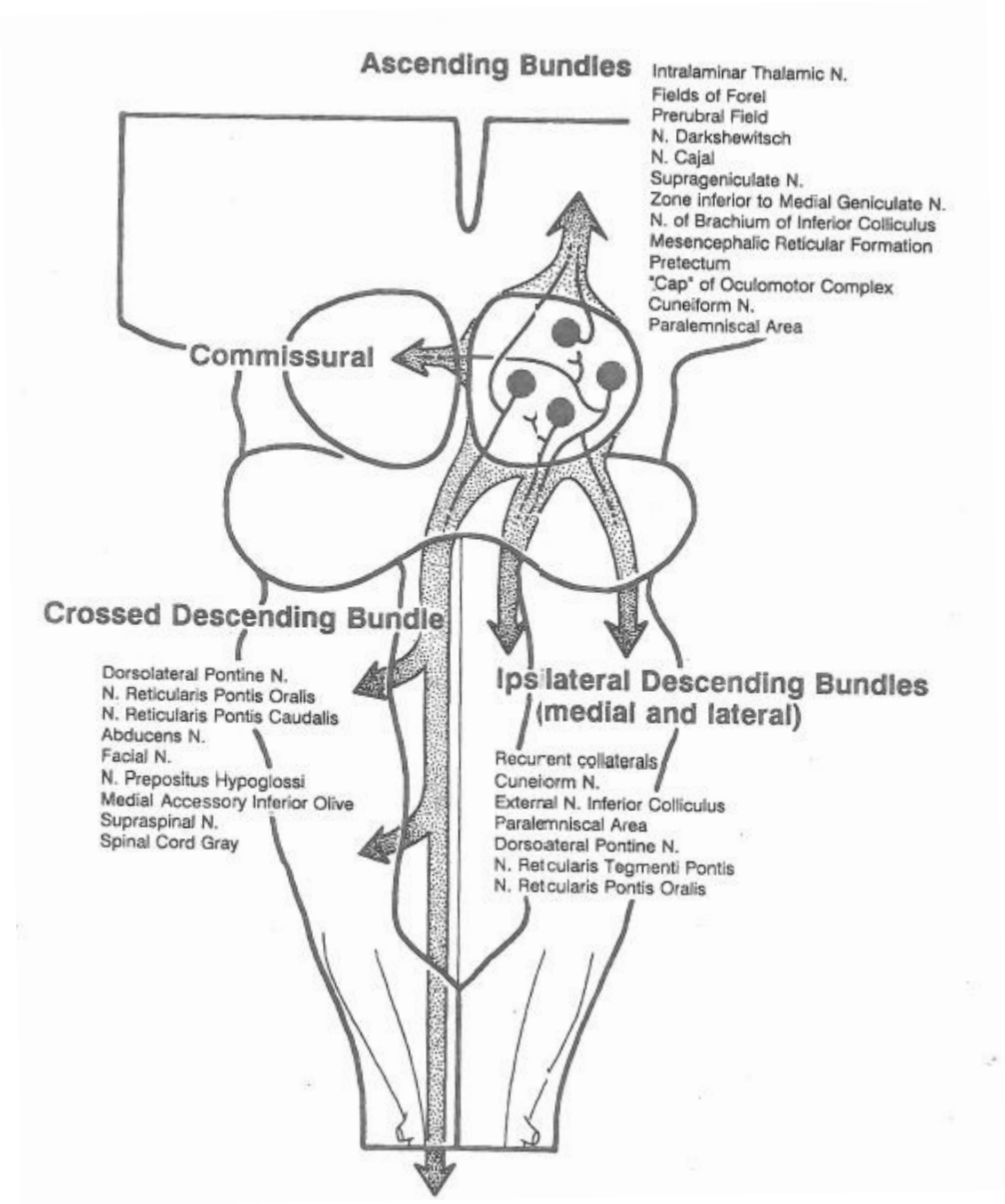

Figure 1-1: Efferent connections of the intermediate and deep layers of the superior colliculus (SC) in cats.

Adapted from: Stein and Meredith. The Merging of the Senses. *Book* 1993.

Intrinsic connections within the SC:

The most widely held view regarding intrinsic connections within the SC is that the superficial and deep layers function as independent entities as with the exception of a single study by Sprague et al (Sprague 1975). Anatomical experiments failed to demonstrate axons of superficial cells terminating in the deep layers in any significant numbers (Behan and Appell 1992). In addition, depressing the activity of superficial layer neurons in cats by deactivating their cortical inputs had no obvious influence on the functional integrity of the deep layer neurons (Ogasawara et al. 1984). This led to the view that there is no connectivity between the superficial and deep layers cells. However, recent studies confirm the presence of reciprocal connections between the superficial layers and the deep layers in different species [cats: (Behan and Appell 1992; Behan and Kime 1996) monkey: (Moschovakis et al. 1988) ferrets: (Doubell et al. 2003)]. Using PHA-L labeling, direct superficial to deep layer connections were demonstrated in cats (Behan and Appell 1992). These axons were of very fine caliber and branched infrequently with few small terminals. Intracellular labeling studies using HRP show that dendrites of deep layer neurons in cat extend into stratum opticum and to a lesser extent SO dendrites extend into stratum griseum intermedium (Grantyn and Grantyn 1982; Grantyn et al. 1984). In addition, though HRP studies failed to reveal axonal projections from deep to superficial layers in cats, using PHA-L Behan and Kime (1996) and Behan and Appell (1987) were able to demonstrate some axon terminals of the intermediate layer neurons extending into the superficial layers. In tree shrews, it has been suggested that SO serves as the connecting link between the superficial and deep layers of SC (Hall and Lee 1993; 1997). Intracellular labeling of superficial gray

layer neurons with biocytin revealed extensive projections from SGS to SO while projections to the intermediate layers were comparatively very sparse. Intracellular biocytin labeling of neurons in SO revealed that the axons of the optic layer cells terminate densely within SO and also project in a horizontally restricted fashion to overlying SGS and subjacent SGI. Labeling of SGI neurons revealed that apical dendrites of the intermediate layer neurons extend to SO and so can receive signals from superficial SC while some neurons in upper SGI had axon terminals extending up to SO as well (Lee and Hall 1995). Thus, these intrinsic connections serve as potential pathways through which visual information from superficial SC can reach the deeper layers and multisensory information from intermediate/deep layers can reach the superficial layers of SC. The potential physiological relevance of these intrinsic projections is investigated in detail in Chapter IV.

SENSORY TOPOGRAPHY IN THE SUPERIOR COLLICULUS

Superficial layers

As discussed above, the diverse anatomical connections of the superior colliculus provides the substrate for sensory convergence in the superior colliculus. However, the superficial layers are thought to be strictly visual in nature and representation of visual space is topographic or map-like. The representation of visual space in the superficial layers of SC is studied by plotting the positions of receptive fields (RFs) primarily their centers found along a vertical electrode penetration and then comparing the clusters of

receptive fields found along penetrations made in different locations in the structure (Stein BE 1993). The visual map generated in this manner reveals that neurons whose receptive fields are nasal in visual space are located rostral and those with temporal visual fields are represented caudally (Feldon and Kruger 1970). Therefore, the representation of the horizontal meridian of visual space runs from the front of the structure to the rear (Stein and Meredith 1993). Similarly representation of vertical meridian of visual space is oriented along the medial to lateral aspect with upper visual field represented more medially and lower field more laterally. However, there are interspecies differences in terms of presence and magnitude of geometric expansion of central visual field, and the representation of one or two eyes in the same SC. Cats, monkeys and many other species including humans make heavy use of their central retinas in fixating and examining objects of interest and there is a corresponding increase in the amount of tissue devoted in representing this region of retina. Also, in rats the rostral half of SC represents much of the ipsilateral or nasal visual field and the caudal half represents contralateral or temporal visual space (Siminoff et al. 1966). In cats only the representation in the rostral pole of the structure extends 10 degree into ipsilateral field (Feldon et al 1970) and the representation in monkey ends at the vertical meridian (Cynader and Berman 1972).

Deep layers

Visual topography: The RFs of the deep layer neurons are far larger than the superficial layers with a fourfold increase in RF diameter on average. In addition, as the electrode advances through the tissue, RF centers vary considerably with respect to one another, often shifting erratically within the same column of vertical tissue (Meredith and Stein

1990). This makes the standard way of RF mapping which is dependent on position of RF center unsuitable for mapping deep layer RF because the center of the RF are often out of register with each other but much of the area of their RF is overlapping which fails to be captured by this technique. Also, a map of the RF centers would underestimate the extent of SC activated by a single point in visual space (Stein and Meredith 1993). The point image method (McIlwain 1975) was the most suitable in mapping the deep layer visual RF (Meredith and Stein 1990). This technique determines how much of SC is activated by a single point in visual space. It was found that large blocks of tissue represent the same point in visual space (Meredith and Stein 1990). As in a map, the block of tissue activated shifts as the point (or image) in the visual field shifts. The presence of a block of tissue representing a point in visual space reflects the rather coarse detail of this map (Stein and Meredith 1993). Thus, 2 electrode penetrations would have be spaced very far apart for them to locate neurons whose RFs do not share common points in visual space (Stein and Meredith 1993). The deep layer visual map differs from the superficial layer map in that it is not only coarser but also represents the far periphery. It encompasses the entire contralateral visual field and also extends into ipsilateral space about 40 degrees (Stein and Meredith 1993; Meredith and Stein 1990). Although the visuotopy is similar in the superficial and deep layers of SC the topographic register is most secure rostrally and becomes increasingly poorer at more caudal and lateral locations (Meredith and Stein 1990). It can be seen that the ipsilateral and central visual space occupies the rostral and rostrolateral aspects of the deep layers while temporal visual space is found more caudally. Points superior or inferior are represented medially or laterally. Despite some differences, the overall

pattern in which visual space is represented is similar in the superficial and deep layers and their visuotopies are closely aligned in the representation of central visual space (Stein and Meredith 1993).

Somatosensory topography: The somatosensory RFs are also large and organized into somatotopic map. This was described before the visual topography was mapped out in the deep layers and was done with reference to the visual map in the superficial layers (Stein et al. 1976b). Visual RFs were mapped superficially in each electrode penetration and somatosensory RF found in the deep layers was then related to the centers of the overlying visual RFs in the same electrode penetrations. A very regular relationship was found between the visual and somatotopic maps. Regions of the deep layers representing the face were found lying under visual RFs representing area centralis. Using the point image technique it was found that the head has the largest representation occupying nearly the entire rostral half of the structure, and the scalp is medial to the chin. The second largest representation is that of the forelimb localized to the lateral aspects of the caudal two thirds of the structure. The reminder of the body is compressed into a region overlapping part of the forelimb and extending into small remaining caudal zone (Meredith et al. 1991). There is considerable degree of overlap among the representations of one or more adjacent body regions. For example, neurons with RFs on the forelimb may be found rostrally, within the region devoted for face. Thus, a stimulus on any given body region can activate an expanse of tissue far greater than that predicted on the basis of the tissue devoted primarily to that body part. This widespread activation helps to increase the likelihood of detecting an event by activating many neurons (Stein and Meredith 1993).

Auditory topography: The auditory system is different from the visual and somatosensory systems in that there are no spatial maps in any of the auditory structures. Rather there is a tonotopic map of sound frequencies at different auditory brain structures. Thus the construction of a spatial auditory map in the SC has to be the result of a computation based on differences in the intensity and timing of sound as it reaches the two ears. Thus, sensitivity to interaural time and intensity differences are features that the SC auditory neurons respond to and help to form auditory maps (Gordon 1973; King and Palmer 1983; 1985; Middlebrooks and Knudsen 1984). Interaural delays results from differences in the lengths of the paths of sound to each ear. Interaural delays are nearly equal for all sounds located at constant azimuths. Sounds located at different azimuths produce different interaural delays. Thus, interaural delays provide cues to auditory azimuth but not elevation. Intensity effects provide both monoaural and binaural cues to location of sound (Middlebrooks and Knudsen 1984). Depending on location of source the intensity increases or decreases by the collecting and shadowing properties of the head and external ears (Middlebrooks and Pettigrew 1981; Wiener et al. 1966). These effects increase with increasing sound frequency. Thus, frequency spectrum of a sound is shaped differently depending on the location of a source in azimuth and elevation. In cat SC monoaural tuning provides cues for elevation tuning and might contribute to azimuth tuning (Middlebrooks and Knudsen 1984). Examination of the most responsive or best areas of the RF of auditory neurons shows that, a spatiotopic map is evident in the auditory neurons of SC (Middlebrooks and Knudsen 1984). Neurons in the SC are selective for location of sound source and this selectivity shifts systematically as a function of neuron position to form a continuous

map of auditory space. The horizontal dimension of space is mapped rostrocaudally and vertical dimension is mapped mediolaterally. The spatial response profile of auditory neurons in the SC demonstrates that there are neurons (hemifield units) in the SC that have their receptive fields extending behind the cat's head while certain others have their RFs(frontal units) restricted entirely in front of the interaural plane. A minority of the neurons have unbounded RFs (omnidirectional). Spatial topography is most evident when the responses of the neurons are evaluated quantitatively relative to their maximum firing rates. The optimal stimulus locations of neurons, their best areas vary continuously in elevation and azimuth as a function of neuron position throughout SC and best areas correspond with visual RF.

Multisensory map formation: The convergence of inputs from different sensory modalities in the deep layer neurons of the SC renders multisensory properties to majority of the deep layer neurons. There is a great deal of correspondence in the visual, auditory and somatosensory maps of a trimodal neuron. The horizontal and vertical meridians of the different sensory representations in the SC are quite similar which suggests a representation of "multisensory space" in a manner demonstrated in Fig 1-2.

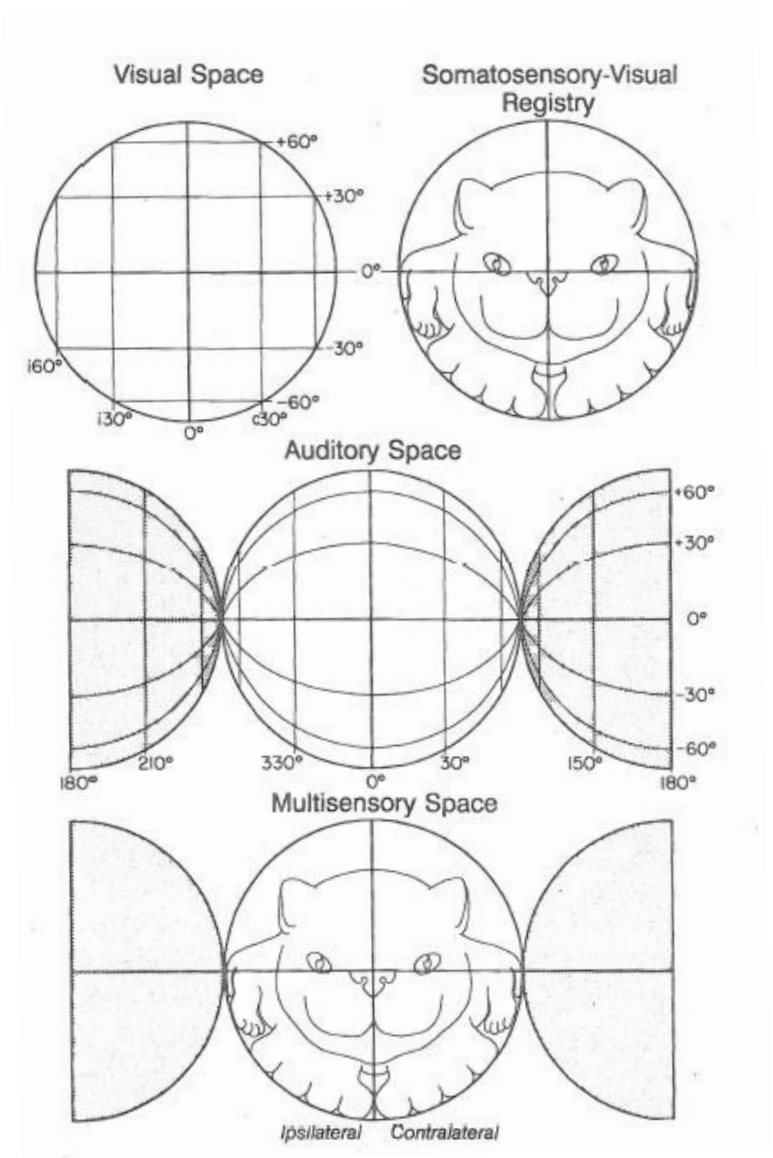

Figure 1-3: A multisensory spatial coordinate system.

Visual space is depicted by a double pole co-ordinate system with intersection of vertical and horizontal meridians at area centralis. Superior and inferior visual space is represented by plus and minus signs respectively. Representation of the body as it would appear if mapped in visual coordinates. This map was obtained by plotting the body part at the center of the visual RF in each visual somatosensory neuron sampled. Auditory space shown in double polar co-ordinates. Positions anterior to interaural axis are depicted within the clear circle, while those posterior are represented by darkened crescents on each side which were detached from one another and folded forward to flatten auditory space into a two dimensional representation. Finally auditory space is aligned with overlapping visual and somatosensory representations to produce a schematic of multisensory space.

Adapted from: Stein and Meredith. The Merging of the Senses. *Book* 1993.

The sensory maps in these neurons demonstrate a great deal of overlap but it is important to know that due to the large RF structure this overlap is far from complete. Thus in a multisensory neuron that responds to both visual and auditory stimulus the visual and auditory RFs will overlap but not completely. A possible advantage of this imprecision is that minor shifts of peripheral sensory organs are not very disruptive to overall register among sensory representations or among different RFs of individual multisensory neurons. Small movements of one set of sensory organs will increase the degree of RF overlap in some neurons while simultaneously degrading it in others, yet the registry among the maps themselves remain largely intact (Stein and Meredith 1993). This ensures that stimuli of any modality in the same location in space will activate neurons in same region of SC. This kind of organization seems economical in specifying the location of peripheral stimuli and organizing and activating the motor program required for orientation behavior. However, since these multisensory neurons have large RFs which are not organized in a point to point manner, a small stimulus activates a large number of neurons over a wide block of tissue. Thus, the activity of a single neuron or a small group of neurons cannot predict the exact location of the stimulus. Localization requires activation of a large number of neurons producing an activity pattern that can be distinguished from the surround. Correct localization is achieved by distribution of active neurons and differential levels of activity of these neurons (Stein and Meredith 1993). This is achieved by the RFs having “best areas” and thus the same stimulus may fall within the best area of some neurons but not others though all these neurons occupy similar regions in sensory field.

PHYSIOLOGICAL PROPERTIES OF NEURONS IN THE SC

Superficial layers

As discussed above, the superficial layers of the SC receives input from visual structures and is thought to be purely visual in nature. A number of features characterize the response properties of neurons in these layers. First, the majority of the visually responsive neurons in the superficial SC (87%) exhibit single excitatory region within their RF while some (12%) exhibit multiple excitatory regions that are spatially segregated as plotted by a moving narrow slit of light (Dreher and Hoffmann 1973). Superficial SC neurons generally exhibit ON-OFF responses to flashing spots of light and lack the center surround organization of retinal RF (Kuffler 1953). As regards inhibition, majority of the superficial SC neurons studied showed inhibitory regions within their RF (Dreher and Hoffmann 1973). In 30% the inhibitory zones surrounded the excitatory region. In 10% the inhibitory zones bordered the excitatory region on 3 sides, in another 10% two opposite sides of the excitatory region were flanked by inhibition and in 5.3% the inhibitory region was apparent only on 1 side of the excitatory region. Finally in 16% inhibition was revealed only when stimulus moved in the non-preferred direction.

A second major feature is that the majority of SC neurons respond to a wide range of stimulus velocities but systematic studies reveal 3 types of SC neurons: units that prefer slow stimulus velocity, those which prefer medium stimulus velocities and others that prefer fast stimulus velocities. Neurons responding to slow velocity stimuli are sharply

tuned in their preference to the particular stimulus velocity than the neurons in the other two groups and along with the medium velocity preferring cells are completely or partially direction selective. These neurons have both excitatory and inhibitory regions within their RF. The fast preferring group of cells responds to a wide variety of stimulus velocities, is non-direction selective, and lack inhibitory regions within their RF (Dreher and Hoffmann 1973).

A third major feature of superficial SC neurons is that the majority are direction selective and respond vigorously to stimuli moving through the excitatory region in one (preferred) direction but weakly or not at all to movement of stimuli in the opposite (null) direction (Dreher and Hoffmann 1973).

The receptive field architecture of superficial SC neurons imposes restrictions to the optimal size of the stimulus that activates the superficial layer SC neurons. As discussed above majority of SC receptive fields have suppressive regions flanking the activating region at least on one side. Thus, when suppressive regions were present outside each border of the activating regions, the response of the unit showed no spatial summation or suppression as long as the stimulus was within the activating region. But when the surround on either side was invaded, summation of the suppressive effects was seen (Sterling and Wickelgren 1969). In some neurons, the response of the neuron increased as the stimulus size enlarged until the highest response was obtained from stimulus that was the size of the activating region. In some other cells, the most effective stimulus was smaller than the activating region (Sterling and Wickelgren 1969). For other superficial SC neurons responses were little affected by change in stimulus size. Each of these cell categories included direction selective and non-direction

selective cells while the responses of most cells were relatively unaffected by changes in stimulus contours (Sterling and Wickelgren 1969).

Most cells in superficial SC respond optimally to very low spatial frequencies and have low spatial resolution and so act as good low pass filters in the spatial frequency domain. This fits well with the type of input that these cells receive coming mainly from the Y and W type of retinal ganglion cells (Waleszczyk et al. 2007).

In regards to the temporal properties of the superficial SC neurons, most respond to stationary stimuli in a transient fashion while moving stimuli evokes a more sustained response (Sterling and Wickelgren 1969). Regarding the response of superficial SC neurons to varying temporal frequencies, studies show that SC neurons respond to a wide range of temporal frequencies. Preference of some cells to high temporal frequencies reflects the predominance of Y type of input to these cells (Waleszczyk et al 2007). Thus the SC neurons serve as important source of visual information in the high temporal frequencies relayed via extrageniculate visual thalamus to cortical neurons in lateral suprasylvian and anterior ectosylvian cortices (AEV) that participate in motion analysis (Hicks et al. 1986; Norita et al. 1996; Norita et al. 1986).

Deep layers

As discussed above, the deep layer neurons receive inputs from multiple modalities and majority of the neurons (50%) are multisensory in nature in cats with visual-auditory multisensory neurons (30%) being the most common type (Meredith and Stein 1996). This reflects the cat's heavy dependence on visual and auditory cues for orientation and contrasts sharply with that of other species. For example, in rodents, visual-

somatosensory neurons are most prevalent (Drager and Hubel 1975; Weldon and Best 1992). This reflects the critical input from whiskers in these animals for orientation and object identification. Similarly visual-infrared neurons are common in rattlesnake because they make extensive use of thermal cues to locate and capture warm blooded prey (Hartline et al 1978; Newman and Hartline 1981). The prevalence of multisensory neurons in the intermediate/deep layers of SC also varies with species with primate SC having much lower number of multisensory neurons (28%)(Wallace et al 1996).Thus, as alluded to previously, due to the high prevalence of multisensory neurons in cat SC, it serves as a great model to study multisensory processing. Described below are the major physiological properties of the multisensory neurons in cats.

Visual receptive field properties: The RFs of visually-responsive neurons in the deep layers are large and are not arranged into separate on and off regions. Rather early studies suggest that they appear to be organized in a homogenous manner. The most effective stimulus is smaller than the diameter of the RF. Moving stimulus are most effective in stimulating these neurons. The neurons are direction selective and respond better to rapidly moving stimuli compared to stimuli moving with low velocity. Repeated presentation of stimulus produces response habituation. Such RF properties of visual neurons is well suited to underlie attentive and orientation behaviors. The neurons are most responsive to novel moving stimuli that preferentially elicit orientation response and code for movement direction and velocity that are necessary for predicting location of a moving target to intercept or avoid it (Stein and Meredith 1993).

Finally, it is relevant to summarize the similarities and differences in the physiological properties of the superficial and deep layer visual responses in cat SC here. The

majority (98%) of superficial and deep layer neurons are binocular in nature (Meredith and Stein 1996). The size of visual receptive fields in the superficial layers are much smaller (average diameter 23 degrees) than that in the deep layers (average diameter 78 degrees) (Sterling 1969; Meredith and Stein 1990; 1996). The mean latency of visual responses in the superficial layers is shorter (40ms) than that in the deep layers (70ms) (Sterling and Wickelgren 1969;Sterling 1971; Meredith et al 1987; Wurtz and Albano 1980). Both the superficial and deep layer neurons were best activated by moving visual stimuli that were smaller in size than their receptive fields but they responded to stationary light flashes as well (Sterling and Wickelgren 1969; Meredith and Stein 1996). The majority of neurons in both superficial and deep layers exhibited stimulus velocity preferences and were direction selective (Dreher and Hoffman 1973; Sterling and Wickelgren 1969; Meredith and Stein 1996; Stein and Meredith 1993).

Auditory receptive field properties: Though most of the structures in the auditory pathway are tonotopic in nature, the auditory neurons in SC are poorly responsive to pure tones. Rather they respond to complex sounds composed of multiple frequencies (Gordon 1973; Horn and Hill 1966; Stein and Arigbede 1972; Wickelgren 1971). They are more specialized for signaling spatial locations of sound rather than identifying their spectral composition. They respond to moving stimuli and exhibit some directional selectivity (Gordon 1973; Rauschecker and Harris 1989). Unlike auditory neurons in other structures they habituate to repeated stimulation and are best suited for detecting novel sounds. They have broad tuning curves that are biased towards the higher frequencies and have higher than average thresholds (Mast and Chung 1973; Wise and Irvine 1983). The majority of neurons are binaural in nature and they are exquisitely

sensitive to interaural time and intensity differences. Sounds to the left of the midline are louder and arrive earlier in the left ear as they are not shadowed by head. By systematically varying interaural intensity differences Wise and Irvine (Wise and Irvine 1983; 1985) identified 4 types of neuronal groups. The first group EO/I is excited by inputs from the contralateral ear, does not respond to inputs from ipsilateral ear alone and exhibits inhibition between the 2 ears when they are stimulated together. For the other 3 groups facilitation occurs among inputs from the 2 ears. EE/F neurons respond to either ear alone but better to their combination; EO/F neurons to contralateral ear alone do not respond to ipsilateral ear alone and are facilitated by stimulation of the 2 ears together; OO/F neurons do not respond to either ear alone but do respond to combined inputs. By integrating inputs from the 2 ears the auditory neurons in SC construct spatially restricted RF (King and Palmer 1983; 1985; Middlebrooks and Knudsen 1984) with heterogeneity in excitability and clearly defined regions of maximal response called “best areas”. The exception is the EE/F type which will respond to stimuli anywhere in auditory space (omnidirectional), EO/F and OO/F have RFs whose best areas are within 20 degrees of frontal midline (frontal units) and EO/I neurons have RFs restricted to portions of contralateral hemifield (hemifield unit). Because EO/I type is restricted by inhibition from the ipsilateral ear, its contralateral excitatory region is flanked by large ipsilateral inhibitory zone.

Somatosensory receptive field properties: The somatosensory responsive neurons respond well to stimulation of hair and/or skin and have well defined RFs (Stein and Arigbede 1972). They respond well to low velocity stimuli but prefer intermediate or high velocity stimuli (Stein et al. 1976b). They respond transiently to maintained stimuli and

show rapid habituation to stimulations at high rates. Thus, they are best suited to deal with novel stimuli that elicit orientation responses (Clemo and Stein 1986; 1984; Stein et al. 1976b). The RFs are large and non-homogenous like the auditory RFs and have clearly defined best regions (Clemo and Stein 1991). Progressively larger stimuli within the best region evoke higher number of impulses. Only very few somatosensory neurons have suppressive surrounds or directional selectivity (Clemo and Stein 1987).

BEHAVIORAL ROLE OF SC

Superficial layers

In accordance with the long held view of parallel streams of visual information processing early lesion studies established that the SC forms an essential part of the visual system that codes for “where” objects are in the visual world due to its role in spatial localization and orientation response (Schneider 1969; Sprague 1996). Most SC neurons show properties that mostly resemble Y type of retinal ganglion cell input which is similar to neurons in Area 18, posteromedial lateral suprasylvian and AEV of cortex and suggests its role along with these other visual areas in motion perception and action (Benedek et al. 1988; Burke et al. 1998; Mucke et al. 1982). The preference for low spatial frequencies combined with large range of temporal frequencies indicates that a population of SC cells would respond well to large objects moving at a wide range of velocities. The robust responsiveness of SC cells to a broad range of temporal frequencies increases the chances of stimulus detection regardless of its properties. SC

neurons with spectral RFs showing speed tuning are most probably involved in detection of stimuli moving with a particular velocity while other SC neurons are most likely involved in detection of stimuli moving in a broad range of velocities (Waleszczyk et al. 2007).Convergence in the superficial layers of SC of excitatory input from different visual information channels with complementary temporal properties and velocity response profiles (W and Y retinal ganglion cells) can be regarded as a first step to a more global integration of multimodal sensory information in deeper layers. One of the reasons for this convergence is most likely strong participation of SC in visuomotor behavior such as reflex adjustment of head and eyes which is often performed in shortest possible time. The pathway from retina to the superficial layers and then deep layers of SC is relatively short and thus appropriate for fast orientation responses to visual stimuli. The functional segregation of the superficial and deep layers of the SC was described in an early study by (Casagrande et al. 1972) in when they found that superficial lesions of SC in the tree shrew resulted in deficits in form discrimination while deep layer lesions resulted in inability to track objects. Though, the findings of this study are hard to replicate due to the difficulty of restricting lesions strictly to the superficial /deep layers, the general role of SC in visual form discrimination and perception has been suggested by numerous studies (Anderson et al. 1971; Berlucchi et al. 1972; Sprague 1991; Sprague et al. 1970; Sprague et al. 1977; Tunkl and Berkley 1977).

Deep layers

The long standing role attributed to the SC is that in localization and orientation behavior. Early studies by Sprague and Meikle (Sprague and Meikle 1965) demonstrated that unilateral lesions of the SC resulted in profound sensory neglect on

the contralateral side. This was evidence to show that the SC is crucial for localization of sensory stimulus. Moreover, the deep layers of the SC by virtue of its connections with different sensory systems and output to motor structures is aptly suited to integrate sensory information in order to guide movement. As discussed in detail above, the multisensory nature of the deep layers allows SC to act as a sensorimotor integrator that plays an important and specific role in allowing the animal to orient to visual, auditory, somatosensory stimuli (Casagrande et al. 1972; Harting et al. 1973; Stein et al. 1976a). Moreover it is well known that SC-mediated behaviors are facilitated under multisensory circumstances, with improvements being seen in both the speed and accuracy of responses (Bell et al. 2005; Burnett et al. 2004; Burnett et al. 2007; Diederich and Colonius 2004; Frens et al. 1995; Gingras et al. 2009; Hughes et al. 1994; Jiang et al. 2002; Nozawa et al. 1994; Stein et al. 1988; Wilkinson et al. 1996). The critical role of SC in mediating such multisensory benefits was established in a series of lesion studies where the lesions were restricted to the deep layers of the SC (Burnett et al 2004, 2007). Such restricted lesions resulted in loss of integrative capacity of the multisensory neurons. They were still capable of responding to multiple modalities but their responses under multisensory conditions were no different from that under the strongest unisensory condition (Burnett et al 2007). This was reflected in orientation behavior as well, where the animals were capable of orienting to sensory cues but the benefit that is observed under normal multisensory circumstances (increased accuracy) was lost (Burnett et al 2004).

MULTISENSORY PROCESSING IN THE DEEP LAYERS OF SC

We live in an environment which is changing dynamically. Stimuli occur at various positions in space and time and our brains are tasked with creating perceptual order out of this bewildering array of dynamically changing stimuli to produce an integrated, comprehensive assessment of the external world. This can be achieved by attending to some stimuli while ignoring others. This requires the brain to successfully determine stimuli that are related to one another and ones that are not. Certain combinations of stimuli become more salient because neuronal responses to them are enhanced while others remain less salient by neuronal depression. The SC neurons are capable of exhibiting such neuronal enhancements and depressions in response to combinations of stimuli from multiple modalities in order to guide behavior. This ability of SC neurons to combine information from multiple modalities in order to guide behavior is defined as “multisensory integration”.SC consists of multisensory neurons that may be grouped into two major classes: neurons that show overt responses to more than one sensory modality and these are defined as overt multisensory neurons. These neurons have been the focus of majority of the early multisensory studies. The second class of neurons show overt responses to one dominant sensory modality but their responses are modulated by presentation of sensory stimulus of a second modality. These are defined as modulatory multisensory neurons. Regardless of the class to which they belong, both these groups of multisensory neurons engage in multisensory integration which is quantified as follows.

Quantification of multisensory integration

Multisensory neurons in the SC respond to presentation of unisensory stimulus alone but when presented with a multisensory stimulus combination, the response generated is dramatically altered. If the multisensory response is statistically significantly greater than the best unisensory response, it is defined as response enhancement. But, if the multisensory response is statistically significantly lower than the best unisensory response, it is defined as response depression. Both multisensory response enhancement and depression is generally quantified using the following two metrics:

a) Interactive Index (ii) which is the percent difference in the mean number of stimulus driven action potentials evoked by cross modal stimulus and that evoked by the most effective modality specific stimulus component. Spontaneous activity is always subtracted. Thus the strongest unisensory response is the referent for determining the magnitude of multisensory enhancement or depression. Statistical tests are used to determine significant differences between the strongest unisensory and multisensory conditions. The formula used to calculate the magnitude of multisensory enhancement and depression is:

$$ii = (CM - SMmax) \div (SMmax) \times 100$$

where CM is the mean number of impulses in response to the cross modal stimulus and SMmax is the mean number of impulses in response to the most effective modality specific stimulus (Meredith and Stein 1986a,b; Stein and Meredith 1993). Thus if CM=10 and SMmax=5, MSI = 100%.

A second measure of multisensory integration is called mean statistical contrast (msc). This measure takes into account both of the unisensory responses and compares this to the predicted addition of these two responses. This model creates a predicted multisensory response based on the addition of the two unisensory responses, which can then be contrasted against the observed response using the mean statistical contrast (or *multisensory contrast*, msc) measure. Statistical tests are used to determine significant differences. The msc is calculated as follows:

$$msc = \sum[(SA - A) - (V - VA)] \div n$$

where SA is the spontaneous activity, A is the auditory response, V is the visual response, VA is the multisensory response, and n is the number of trials. This model assumes independence between inputs from each sensory modality and utilizes additive factors logic to distinguish between *superadditive* (contrast > 0) and *subadditive* (contrast < 0) responses (Carriere et al. 2008; Perrault et al. 2003; 2005; Stanford et al. 2005). Thus, msc characterizes the type of integration present, beyond simply determining enhancement versus depression of the response, by incorporating both component unisensory responses (rather than only the strongest) as a metric for categorizing integration effects. For example if the combined response is 15 spikes/ trial whereas the visual only response is 3 spikes/trial and auditory only response is 4 spikes/trial then the multisensory response is categorized as super-additive.

Now, that we know that the SC neurons can combine information from multiple modalities, it is important to realize that these neurons are endowed with a complex task. They should not only be capable of successfully combining information from

stimuli that are related, but also prevent binding stimuli that are unrelated .For example, stimuli that occur at the same time and place are likely to be interrelated by common causality and hence should be combined while those that occur at different times and / or at different places are likely to remain unrelated and should not be combined. Early studies of multisensory processing in the SC identified certain cues/factors that helped the SC neurons select multimodal stimuli that are related and hence should be combined while ignoring others that are unrelated. These factors were also termed as principles of multisensory integration.

Principles of integration

The principles of multisensory integration have been investigated extensively at the single neuron level in animal models (Meredith et al. 1987; Meredith and Stein 1986a; b) and have recently been extended to human neuroimaging studies (Bushara et al. 2001; Stevenson and James 2009). The original work and these follow-up studies have identified three main principles that govern the process of multisensory integration. These are known collectively as the spatial principle, temporal principle and principle of inverse effectiveness as discussed below.

Spatial principle: In its earliest form, the spatial “rule” suggested a strong relationship between the proximity of multisensory stimuli and the interactions that resulted from their combination (Meredith and Stein 1986a). In this seminal study it was demonstrated that the nature and magnitude of multisensory interactions was dependent on the position of the stimuli relative to one another. Spatially coincident stimuli produced response enhancements while spatially disparate stimuli produced response

depressions. In a later study by the same group (Meredith and Stein 1996), these findings were clarified to show that multisensory integration depended on the relationship of different stimuli to their corresponding receptive fields, rather than to the absolute spatial relationship of the stimuli to one another. This is to say that, if a multisensory stimulus combination (visual-auditory) is presented such that the visual stimulus is within its visual receptive field and the auditory stimulus is within its auditory receptive field, it will most likely produce response enhancement, even when they are not at the exact same spatial location. However, if the visual stimulus is within its receptive field while the auditory stimulus is outside its receptive field, it will likely result in response depression.

As discussed in an earlier section, the multisensory neurons of the deep layers of the superior colliculus have large unisensory receptive fields (Meredith and Stein 1990) that result in a great degree of overlap between the visual, auditory, somatosensory receptive fields of these neurons. The greatest amount of multisensory enhancement is produced by stimuli located in the area of receptive field overlap. However, as long as both unisensory stimuli are within their respective receptive fields, there is no systematic relationship between magnitude of enhancement and amount of cross modal stimulus disparity (Kadunce et al. 2001). From these studies it was established that the spatial register among a multisensory neuron's different receptive fields served as a critical feature in determining the resultant multisensory interaction. The aforementioned work by Kadunce et al underscored the fact that the spatial resolution of multisensory integration at the level of individual neuron is rather coarse. However, if one envisions this at the population level, it is possible that the spatial resolution of the system is

substantially greater. This is due to the fact that the high degree of spatial overlap of the receptive fields of SC neurons insures that spatially coincident multisensory stimuli will fall within the excitatory receptive fields of a large number of multisensory SC neurons and thereby evoke a large multisensory population response. On the contrary, progressive increases in spatial disparity of multisensory stimuli should progressively decrease these population responses for two reasons. First, increasing spatial disparity decreases the likelihood that the two different stimuli will encroach on the two excitatory receptive fields of the same neuron, thus decreasing the likelihood of multisensory enhancement and lowering the magnitude of population response. Second, increasing spatial disparity increases the incidence of multisensory inhibition generated when one stimulus is within its excitatory receptive field while the other stimulus is within its inhibitory receptive field (Kadunce et al. 1997). Consequently, the multisensory population response reflects an underlying spatial resolution that cannot be predicted by the absolute sizes of the multiple sensory receptive fields of individual SC neurons or their areas of receptive field overlap.

Temporal principle: Early studies showed that the relative timing of paired multisensory stimuli was another important determinant of the degree of multisensory integration exhibited by individual neurons. The major principle that appears to govern the temporal processing of multisensory information was revealed in a study that parametrically manipulated the temporal relationship between paired multisensory stimuli and looked at the consequent response on the firing profiles of cat multisensory SC neurons (Meredith et al. 1987). It was found that typically the largest gain seen upon multisensory combinations was obtained when the peak discharge periods of the

individual sensory responses overlapped. As the stimulus onset asynchronies (SOAs) became increasingly different and the peak discharge periods became less overlapping, the magnitude of the enhancement was generally found to decline. In fact, if the temporal disparity between the stimuli was sufficiently large, response enhancement could transition to response depression. Although in many circumstances the maximum response enhancement was obtained when there was minimal temporal disparity between the stimuli (i.e., simultaneity or an SOA of 0), in other neurons the largest interactions were seen with SOAs that were somewhat temporally disparate (e.g., 50 or 100 ms). It is speculated that this preference for asynchronous combinations can be accounted for by differences in the input latencies for the two modalities. For example, given average visual latencies of 70 ms for deep layer SC neurons and average auditory latencies of 15 ms, a peak temporal "tuning" function of around 50 ms is not surprising.

Principle of Inverse effectiveness: The third principle of multisensory integration is that of inverse effectiveness. Here, the weaker the component unisensory stimuli in eliciting a response, the larger the magnitude of the multisensory integration. This principle of inverse effectiveness was demonstrated in the early studies of multisensory integration by using anesthetized cat preparations and recording from the deep layers of the superior colliculus (Meredith and Stein 1986b). This work found that as the effectiveness of the single modality stimuli increased, the amount of multisensory integration decreased. Hence, minimally effective visual and auditory stimulus combinations produced the largest enhancements, whereas maximally effective stimulus combinations produced weaker (or non-existent) enhancements. Similar

results were obtained from studies done in SC of awake cat (Wallace et al. 1998) and non-human primate studies (Wallace and Stein 1996).

Caveats in the interpretation of the principle of inverse effectiveness: Though the principle of inverse effectiveness appears to be robust and true for most multisensory cells there might be a possible confound due to mathematical constraints and biological limitations (Holmes 2009). Neurons cannot produce negative numbers of spikes or respond higher than at certain rates. If the unisensory response of a neuron is equal to the minimum possible response, then the multisensory response can only be the same or higher. On the other side of the spectrum very large unisensory responses cannot be significantly “improved” by multisensory stimulus combinations because individual neurons have a limitation in the maximum number of spikes that it can fire. These “floor and ceiling effects” may produce confounds in interpretation of the magnitudes of multisensory enhancement or depression. However, such confounds can be avoided by accounting for the dynamic range of responsiveness of neurons and making adjustments in the stimulus parameters accordingly (Alvarado et al. 2007a; Alvarado et al. 2007b; Perrault et al. 2003; 2005).

Though, these principles have been classically studied in the SC neurons, later studies show that they hold true for multisensory processing in other brain areas across different species. For example, the operation of these principles have been shown in the anterior ectosylvian sulcus in cats (Wallace et al. 1992) ventral intraparietal area (Avillac et al. 2007) and auditory cortex (Ghazanfar et al. 2005; Kayser et al. 2005) in non-human primates to name but a few.

Neuron specific factors affecting multisensory integration

In addition to these principles, later studies demonstrated that certain neuron specific factors can also alter the nature and magnitude of multisensory integration. Different SC neurons respond very differently to stimuli with similar physical characteristics. Given the importance of the unisensory response in determining the ultimate multisensory product (inverse effectiveness), later studies demonstrated that spontaneous activity of the neuron and it's dynamic range are important determinants of the amount of multisensory integration (Perrault et al 2003, 2005). These studies showed that there was an inverse relationship between spontaneous activity and sensory responsiveness of a neuron and the magnitude of multisensory integration that it can produce. Thus neurons with lower spontaneous activity exhibited higher magnitudes of multisensory enhancements compared to those that exhibited high spontaneous activity for the same stimulus pair. Also, neurons that demonstrated low unisensory responsiveness could elicit higher levels of multisensory integration and sensory responsiveness was a larger contributor of the magnitude of integration compared to spontaneous activity (Perrault et al 2003). These intrinsic differences in the capacity of neurons to engage in multisensory integration, motivated studies that were designed to evaluate the underlying computations performed by these neurons to produce multisensory integration over a wide range of stimulus efficacies(Stanford et al 2005). Such studies revealed that individual multisensory neurons in the SC can engage in multisensory integration that is superadditive, additive or subadditive. The underlying computation is primarily determined by the efficacy of the modality specific inputs. Superadditivity is common within a narrow range of stimulus efficacies occurring mostly when modality

specific influences are weak. However, with more effective stimuli and over the majority of the responsiveness range displayed by the neurons, simple summation of bimodal inputs was the predominant nature of multisensory integration (Stanford et al 2005; Stanford and Stein 2007). These results suggest that multisensory integrative abilities of the SC neurons can be largely accounted for by a basic linear model and helps to better understand the mechanisms underlying multisensory integrative abilities of the SC neurons. However, a simple linear model cannot account for the apparently unique role of cortical inputs for affecting multisensory integrative abilities of SC neurons as discussed below.

Cortical dependence of SC multisensory interactions

Studies show that integrative abilities of multisensory neurons of the deep layers of the SC depend on cortex (Stein et al. 2002-review). More specifically, two extra primary areas in cats, the Anterior Ectosylvian Sulcus (AES) and the rostral lateral suprasylvian sulcus (rLS) that has multiple sensory representations project to the deep layer neurons in SC and affects neuronal responses (Clemo and Stein 1986; 1984; Stein et al. 1983). The AES consists of a somatosensory area SIV (Clemo and Stein 1982; 1984), visual area AEV (Mucke et al 1982), and auditory area FAES (Clarey and Irvine 1986). Involvement of these cortical areas in multisensory integration of the deep layer SC neurons came from both behavioral and physiological studies. In one such behavioral study, it was shown that during AES deactivation cats lost their normal ability to use a spatially coincident auditory cue to enhance orientation to contralateral visual targets (Wilkinson et al. 1996). In contrast their visual orientation abilities remained intact and there was no evidence of changes in behavior to ipsilateral multisensory stimuli. In

addition the inhibitory effects of spatially disparate auditory stimulus in contralateral hemifield were compromised. However, deactivation of the primary visual, auditory and other cortical areas that project to deep layers of SC did not produce such behavioral changes. Physiological studies earlier (Wallace and Stein 1994) had already demonstrated that individual neurons in SC lost their ability to integrate cross modal cues after AES deactivation by cooling probes. This was clearly a multisensory loss as the response of neurons to modality specific stimuli remained unaffected with such cortical deactivation. A later study (Jiang W 2000; Jiang et al. 2002) extended the finding to rLS and demonstrated that similar results occur if rLS is deactivated by cooling. Some SC neurons show these effects when AES is deactivated, some show it when rLS is deactivated and some others when both are deactivated together. Behavioral studies (Jiang et al 2000,2002) assessing orientation responses done with cats in normal and cortically deactivated conditions demonstrated under normal conditions an auditory stimulus presented in spatial coincidence with the visual target, performance improved drastically but in the same cat during cortical deactivation (either AES or rLS) such behavioral improvements were not achieved. These effects were specifically multisensory as orientation to visual target alone remains unchanged. Thus it appears that eliminating essential cortical influences damages integrative abilities of SC neurons which in turn affect SC mediated orientation behavior. This is also evident from studies done in developing cats which show that multisensory integrative abilities are not present in newborn cats but appear during the first few months of postnatal life when functional corticotectal influences are first established (Wallace and Stein 1997; 2000) .In addition neonatal ablation of these cortical areas (AES and rLS) disrupts

maturation of multisensory integrative abilities of developing cats and on reaching maturity the incidence of multisensory neurons in deep layers of SC of these cats substantially decrease and they lack normal integrative abilities. However ablation of either AES or rLS in neonatal cats had no such profound effects and at maturity those animals had almost normal numbers of multisensory neurons in the deep layers and the RF overlap was normal and the integrative abilities of the neurons remain intact. Thus, in early life both these areas possess capabilities to overcome the loss of each other but at least one of them is required for normal development of multisensory integration in the deep layers of the SC (Jiang et al. 2006).Thus, AES/rLS may be thought of as gating the integrative abilities of multisensory neurons in the SC. However, the synaptic mechanisms underlying this gating phenomenon remain largely unexplored. This served as the motivation for our study described in Chapter VI.

CURRENT AND NOVEL WAYS TO STUDY MULTISENSORY PROCESSING IN THE SC: RATIONALE FOR THE CURRENT THESIS WORK

Spatial and spatiotemporal receptive fields

Though most of the multisensory literature characterizes the principles of multisensory integration in various different model systems as well as different brain structures, however most of the work done to date treats the principles of integration in an isolated manner. Recent work however emphasizes the importance of the need to begin thinking about these principles in an integrated manner. This motivated the study of spatial

receptive fields (SRF) of multisensory neurons in cortex. In one such study, Carriere et al. (2008) demonstrated that in the anterior ectosylvian cortex in cats, even within the receptive fields of single cortical neurons, the integrative ability of the neuron varies as a function of stimulus location such that regions of the receptive field that have lower unisensory responses show higher integrative capacities while regions with higher unisensory responses show lower integration. This is in accordance with the principle of inverse effectiveness and suggests that there is an intimate relationship between the principles such that they can no longer be considered in isolation from one another. Even at the level of a single neuron, receptive field characteristics would vary depending on spatial location of the stimulus and temporal dynamics of the neuronal response (Royal et al 2009) and inverse effectiveness may form a predictive framework for guiding multisensory integration. However, at present, this has proven to be true only in cortex. Whether this interdependence of the factors affecting multisensory integration is a general ubiquitous mechanism of generation of receptive fields **both** in cortex and subcortical structures remains an open question. This was the principal motivation of our study described here in Chapter II.

As discussed above, earlier studies emphasized the temporal relationship of the stimuli and showed them to be an important factor guiding multisensory integration. However, recent views have emerged that consider the temporal profile of the multisensory response itself to be an important determinant of multisensory integration. Multisensory integration is generally quantified as change in response magnitude averaged over the entire response epoch. The limitation of such an approach is that the temporal profile of the multisensory response is often ignored in such analysis. Recent studies have begun

to explore the temporal dynamics of multisensory integration (Rowland et al. 2007a; Rowland and Stein 2007). This study focused upon determining when during the multisensory response that the neuron is showing the largest enhancements, and how the integrative profile of a given response changes over time. If the neuron shows multisensory integration early in the course of the response, one might see shorter response latencies that map on to the behavioral facilitations seen under multisensory conditions (i.e., speeded reaction times). Integration during the latter part of the response would imply higher order computations involved in multisensory processing for example “binding” or dependence on association areas of cortex in case of SC (Rowland et al. 2007a; Rowland et al. 2007b; Rowland and Stein 2007) The computations performed at different latency epochs could also shift dramatically during the course of the response such that the early phase may be superadditive while later period may be additive or subadditive (Rowland et al. 2007a).

Extending this view, a recent study examining the spatiotemporal receptive field (STRF) architecture of cortical multisensory neurons showed that multisensory responses had higher peak firing rates, shorter response latencies and longer discharge durations. Moreover, the multisensory response could be divided into multiple phases. The earliest phase was characterized by a short superadditive integration burst, followed by a waning period of additive and subadditive interactions. A second phase of large integration appeared late in the response profile and reflected the extended duration of the multisensory response (Royal et al. 2009). Thus it is now becoming clear that the temporal profile of the multisensory response plays an important role in multisensory integration. Further studies need to be done to clearly elucidate the temporal properties

of the multisensory response profile and its effects on multisensory integration. This idea served as the principal motivation for the study described in Chapter III.

As described in detail above, most of the studies done to date quantify multisensory integration using either ii or msc or both. However, it must be recognized that both of these analytical approaches still rely on changes in the mean firing profile of the neurons under study. Studies within sensory systems have illustrated that information can be encoded in forms that differ from these traditional spike-based measures – a series of findings that are beginning to be extended into multisensory systems.

Changes in synaptic processes

Local field potentials: As described above, for SC neurons, emphasis of multisensory work in other brain areas has also been on neurons that are overtly responsive to stimuli from two or more sensory modalities. However, recent studies have highlighted that multisensory interactions can manifest in neurons that are only overtly responsive to a single sensory modality (Allman et al. 2008a; Allman et al. 2008b; Carriere et al. 2007; Carriere et al. 2008; Clemo et al. 2008). In these neurons, the second sensory modality has the capacity to modulate the responses of the driving modality – another important form of multisensory interaction. Indeed, a recent paradigm shift in the multisensory field has stemmed from the suggestion that such modulatory influences can impact sensory processes even in very early sensory cortical domains typically characterized as “unisensory” (Falchier et al. 2002; Fu et al. 2003; Ghazanfar et al. 2005; Kayser and Logothetis 2007; Molholm et al. 2002; Rockland and Ojima 2003; Schroeder and Foxe 2002; Schroeder et al. 2001).

In addition to illustrating a different form of multisensory influence in the domain of action potential and spiking, these studies serve to reinforce the importance of sub-threshold influences underlying multisensory processes. Although such influences can be inferred from changes in the spiking response, they can be measured more directly through the use of local field potentials (LFPs), an increasingly implemented tool that samples pooled voltage changes surrounding the electrode (Berens et al. 2008a; b). There are two major components of the LFP signal: 1) *a high frequency* component (0.6-1 to 3 KHz) estimated to represent local spiking activity of a population of neurons surrounding the electrode tip within a radius of 150-300 μm (Gray et al. 1995; Henze et al. 2000), and 2) a *low frequency* component (<200 Hz) that is thought to be a measure of the excitatory and inhibitory postsynaptic potential changes in the vicinity of the electrode tip(about 250-500μm) (Berens et al. 2008a; b; Logothetis 2003; 2008). Extracellular recordings can be used to detect both spiking activity and local field potential changes, depending on the filtering parameters applied to the signal, with each carrying distinct functional implications. In addition to its amplitude and latency, the raw LFP signal can be decomposed into its component frequency bands similar to electroencephalogram (EEG) waves. The most commonly referred to of these are *delta* (1-4 Hz), *theta* (4-8 Hz), *alpha* (8-12 Hz), *beta* (12-30 Hz), and *gamma* (>30 Hz).

Much that is known about the role of LFPs in sensory processing comes from work done within single sensory modalities. In primary visual cortex of awake macaques, low frequency LFP oscillations dominate activity even in the absence of stimulation (Berens et al. 2008a; b; Henrie and Shapley 2005; Young et al. 1992). With the onset of visual stimulation, this shifts to fast gamma oscillations (Berens et al. 2008a; b). Gamma band

activity shows the highest stimulus selectivity in primate V1, being associated with the coding of stimulus orientation preference and ocular dominance (Berens et al. 2008a; b). Moreover, gamma power has been reported to increase in different visual areas during perceptual (Gail et al. 2004; Wilke et al. 2006), memory (Pesaran et al. 2002) and attentional (Fries et al. 2001; Fries et al. 2008) processes. Feature selectivity (for both stimulus direction and speed) (Liu and Newsome 2006), attentional allocation (Fries et al. 2001; Taylor et al. 2005) and object category selectivity (Kreiman et al. 2006) have also been related to changes in LFPs in visual cortex. In the auditory system, A1 of awake rhesus monkeys was shown to have frequency tuning of high frequency LFPs matching that of single or multi-unit activity, demonstrating that frequency tuning properties of auditory cortex can be inferred across both domains (Kayser and Logothetis 2007).Furthermore, in the somatosensory system, SII of awake monkeys, high gamma frequency oscillations are closely synchronized with the occurrence of action potentials, which suggests that high gamma power in LFPs may be an index of population firing rate (Pesaran 2009; Ray et al. 2008). Moreover, since LFPs are essentially an index of local synaptic processing, they provide information about local inputs in a given brain area (Pesaran 2009), making the link between LFP and spiking activity an essential bridge between analyzing inputs to and outputs from a particular brain area (reflected in LFP and spiking activity, respectively). Such studies conducted in the principal sensory modalities have established important relationships between firing rate and LFP encoding of stimulus properties, as well as perceptual and attentional correlates of LFPs that can be extended to multisensory applications.

Local field potentials: implications for multisensory processing: Though LFPs have been widely used within individual sensory systems, their application to the multisensory realm remains limited. Recent studies have begun to examine changes in the amplitude and frequency of LFP oscillations in different brain areas in response to multisensory stimuli. For instance, Ghazanfar and colleagues demonstrated multisensory integration of faces and voices using LFP and single unit activity analyses in the auditory cortex of rhesus monkeys (Ghazanfar et al. 2005). Kayser and colleagues also reported visual modulation of activity in the auditory cortex of rhesus monkeys, demonstrated by changes in the amplitude of the LFP signal (enhancement and suppression) under cross-modal conditions (Kayser et al. 2008). Beyond simple changes in LFP amplitude, recent work has highlighted the utility of LFP analysis to shed insight on mechanistic questions within multisensory systems. For instance, Lakatos and colleagues demonstrated that in A1 of macaque monkeys the phase of ongoing LFP oscillations is reset by somatosensory inputs (Lakatos et al. 2007). Thus, the activity of subsequent auditory inputs can be either enhanced or suppressed depending on their timing relative to the oscillatory cycle. Such phase-locking (i.e., synchronization) ultimately serves to amplify neuronal representations, facilitate sensory discrimination, and increase response speed and accuracy (Lakatos et al. 2008; Schroeder and Lakatos 2009a; b). However most of these studies have been focused on cortical structures and so there is a growing need for applying similar methods to study mechanisms underlying multisensory processing in the SC to decipher similarities and/or differences underlying multisensory integration in cortex and subcortical structures. This served as our principal motivation for the studies described in Chapters IV and V

Changes in response variability

An integral concept when studying sensory (and multisensory) encoding is reliability. In multisensory psychophysical studies, reliability is generally framed from the perspective of cue weighting, with the relative cue weights being a function of the reliability of the various sensory inputs (Burge et al. 2010; Burr and Alais 2006; Ernst and Banks 2002; Shams et al. 2005). In a simple multisensory context, one can envision a situation in which one of the sensory inputs (e.g., vision) is providing much more reliable information than the other modality (e.g., audition), such as in the localization of an object in space. The concept of cue reliability can be readily extended into the neural domain, in which the metric of interest is the variability (in essence the opposite of reliability) of the neuronal response upon repeated stimulus presentations, since the variability of the response would directly impact how reliably a stimulus is encoded. Response variability of spike counts is captured in the *Fano factor* (FF):

$FF = \sigma^2/\mu$

FF represents the ratio of variance (σ^2) to the mean (μ) of spike counts computed across trials and averaged over a specific time window (Fano 1947). A Fano factor of one indicates neuronal responses as reliable as would be found from a Poisson process (Eden and Kramer 2010; Kara et al. 2000). From an information encoding perspective, changes in response reliability are potentially very meaningful, as they could be used as weighting factors in neural processes responsible for cue combination (Fetsch et al 2012). One tangible example of the use of Fano factor as a tool has come from studies that have tied response variability to functional relevance and behavioral outcomes. In

the prefrontal cortex of macaques, FF values were shown to change during the components of a motion discrimination task (Hussar and Pasternak 2010).Changes in response variability have been shown to have important implications for sensory processing in individual sensory systems (Churchland et al. 2006; Hussar and Pasternak 2010; Kara et al. 2000; Mochol et al. 2010; Steinmetz and Moore 2010). Recent work has extended this conceptual framework to multisensory systems and has shown that reduction in response variability results in multisensory information gain in the auditory cortex of rhesus monkeys (Kayser et al. 2010). These findings illustrate the potential utility of Fano factor as an additional measure to define information content in multisensory systems. This serves as the motivation for our study described in Chapter VI here.

SPECIFIC AIMS OF THIS THESIS

Thus, from the discussion above, it is clear that although a great deal is known about the responses of SC neurons to multisensory stimulus combinations and factors that affect such responses, little is known about the receptive field architecture that supports the generation of such responses. The work described here represents a series of studies aimed at characterizing the receptive field architecture of multisensory neurons in the SC which will help us understand the mechanistic basis of multisensory integration.

As discussed in detail above, recent studies of multisensory processing in anterior ectosylvian cortex in cats suggest complex heterogeneous receptive field architecture of the cortical multisensory neurons. This complex RF architecture has important implications for the nature of multisensory integration performed by these neurons (Carriere et al 2008). Moreover, the characterization of the temporal dynamics of neuronal responses in these cortical neurons show an inherent dynamism in the temporal profile of multisensory cortical responses, such that two distinct phases of multisensory integration are observed (Royal et al 2009). The early superaaditive phase of integration is thought to play an important role in multisensory behavioral benefits such as faster reaction times observed in numerous psychophysical studies (Colonius and Arndt 2001; Corneil et al. 2002; Frens and Van Opstal 1998; Frens et al. 1995). The second phase of integration is reflected in the longer duration of cortical multisensory responses, which may serve to provide perceptual benefits. These recent findings in the

cortex formed the basis for the work in SC described in Chapter II and Chapter III of this thesis. The motivation was to reveal if such heterogeneity and temporal properties were a general characteristic of cortical and sub cortical multisensory processing or whether these are specialized features of "*cortical"* multisensory processing. Towards this aim, Chapters II and III provide a detailed description of the receptive field architecture of the multisensory neurons in the SC, revealing an inherent heterogeneity of these receptive fields, both in spatial and temporal domains that have not been appreciated to date. Along with detailing this receptive field architecture, these studies provide evidence that this architecture powerfully shapes the multisensory properties of these neurons. In the course of these studies, we were surprised to see evidence for multisensory activity in the superficial layers of the SC. As described earlier, these layers have been considered to be exclusively visual. However, the recent anatomical observations for presence of extensive inter-laminar connections in the SC as described in details above, may serve as a potential anatomical substrate for the physiological evidence for multisensory interactions in the superficial layers. Hence, for Chapter IV we focus on the superficial layers and provide physiological evidence for multisensory processing in the superficial layers of SC. We use both traditional spike based measures and novel local field potential based measures to characterize the subthreshold and suprathreshold nature of multisensory interactions in the superficial layers of SC.

In our discussion above, we find that the neurons of the intermediate and deep layers of the SC receive converging multimodal inputs from a wide variety of brain areas. Moreover, the integrative abilities of these multisensory neurons are critically dependent on their inputs from association cortices such as AES and /rLS. However, the nature of

synaptic processing in the intermediate and deep layers of SC, when these various inputs from multiple modalities are activated has remained ignored to date. Characterizing the nature of synaptic processing in the intermediate and deep layers of SC is important to understand the mechanisms underlying the cortical gating of integrative abilities of these neurons. Thus, this idea motivated the study described in Chapter V. To conclude, the study described in Chapters VI of this thesis provides evidence for changes in response variability of SC neurons under multisensory conditions. Thus changes in response variability may be another mechanism by which multisensory neurons combine information from multiple modalities.

Finally, in the General Discussion, the implications for the complex nature of the heterogeneous receptive field architecture of SC neurons, its impact on multisensory processing, importance of studying the mechanistic basis of multisensory processing and in turn the possible behavioral benefits obtained from such a system are explained.

BIBILOGRAPHY

Allman BL, Bittencourt-Navarrete RE, Keniston LP, Medina AE, Wang MY, and Meredith MA. Do cross-modal projections always result in multisensory integration? *Cereb Cortex* 18: 2066-2076, 2008a.

Allman BL, Keniston LP, and Meredith MA. Subthreshold auditory inputs to extrastriate visual neurons are responsive to parametric changes in stimulus quality: sensory-specific versus non-specific coding. *Brain Res* 1242: 95-101, 2008b.

Alvarado JC, Stanford TR, Vaughan JW, and Stein BE. Cortex mediates multisensory but not unisensory integration in superior colliculus. *J Neurosci* 27: 12775-12786, 2007a.

Alvarado JC, Vaughan JW, Stanford TR, and Stein BE. Multisensory versus unisensory integration: contrasting modes in the superior colliculus. *J Neurophysiol* 97: 3193-3205, 2007b.

Amlot R, Walker R, Driver J, and Spence C. Multimodal visual-somatosensory integration in saccade generation. *Neuropsychologia* 41: 1-15, 2003.

Anderson ME, Yoshida M, and Wilson VJ. Influence of superior colliculus on cat neck motoneurons. *J Neurophysiol* 34: 898-907, 1971.

Antonini A, Berlucchi G, Marzi CA, and Sprague JM. Importance of corpus callosum for visual receptive fields of single neurons in cat superior colliculus. *J Neurophysiol* 42: 137-152, 1979.

Antonini A, Berlucchi G, and Sprague JM. Indirect, across-the-midline retinotectal projections and representation of ipsilateral visual field in superior colliculus of the cat. *J Neurophysiol* 41: 285-304, 1978.

Avillac M, Ben Hamed S, and Duhamel JR. Multisensory integration in the ventral intraparietal area of the macaque monkey. *J Neurosci* 27: 1922-1932, 2007.

Avillac M, Deneve S, Olivier E, Pouget A, and Duhamel JR. Reference frames for representing visual and tactile locations in parietal cortex. *Nat Neurosci* 8: 941-949, 2005.

Baldwin MK, and Kaas JH. Cortical projections to the superior colliculus in prosimian galagos (Otolemur garnetti). *J Comp Neurol* 520: 2002-2020, 2012.

Baleydier C, Kahungu M, and Mauguiere F. A crossed corticotectal projection from the lateral suprasylvian area in the cat. *J Comp Neurol* 214: 344-351, 1983.

Barraclough NE, Xiao D, Baker CI, Oram MW, and Perrett DI. Integration of visual and auditory information by superior temporal sulcus neurons responsive to the sight of actions. *J Cogn Neurosci* 17: 377-391, 2005.

Beckstead RM, Edwards SB, and Frankfurter A. A comparison of the intranigral distribution of nigrotectal neurons labeled with horseradish peroxidase in the monkey, cat, and rat. *J Neurosci* 1: 121-125, 1981.

Beckstead RM, and Frankfurter A. A direct projection from the retina to the intermediate gray layer of the superior colliculus demonstrated by anterograde transport of horseradish peroxidase in monkey, cat and rat. *Exp Brain Res* 52: 261-268, 1983.

Behan M, and Appell PP. Local projections of neurons in the deep layers of cat superior colliculus: A study using Phaseolus vulgaris leucoagglutinin (PHA-L). Soc.Neurosci.Abstr.13:430, 1987.

Behan M, and Appell PP. Intrinsic circuitry in the cat superior colliculus: projections from the superficial layers. *J Comp Neurol* 315: 230-243, 1992.

Behan M, and Kime NM. Intrinsic circuitry in the deep layers of the cat superior colliculus. *Vis Neurosci* 13: 1031-1042, 1996.

Bell AH, Meredith MA, Van Opstal AJ, and Munoz DP. Crossmodal integration in the primate superior colliculus underlying the preparation and initiation of saccadic eye movements. *J Neurophysiol* 93: 3659-3673, 2005.

Benedek G, Fischer-Szatmari L, Kovacs G, Perenyi J, and Katoh YY. Visual, somatosensory and auditory modality properties along the feline suprageniculate-anterior ectosylvian sulcus/insular pathway. *Prog Brain Res* 112: 325-334, 1996.

Benedek G, Mucke L, Norita M, Albowitz B, and Creutzfeldt OD. Anterior ectosylvian visual area (AEV) of the cat: physiological properties. *Prog Brain Res* 75: 245-255, 1988.

Benedek G, Pereny J, Kovacs G, Fischer-Szatmari L, and Katoh YY. Visual, somatosensory, auditory and nociceptive modality properties in the feline suprageniculate nucleus. *Neuroscience* 78: 179-189, 1997.

Benevento LA, and Fallon JH. The ascending projections of the superior colliculus in the rhesus monkey (Macaca mulatta). *J Comp Neurol* 160: 339-361, 1975.

Benevento LA, and Standage GP. The organization of projections of the retinorecipient and nonretinorecipient nuclei of the pretectal complex and layers of the

superior colliculus to the lateral pulvinar and medial pulvinar in the macaque monkey. *J Comp Neurol* 217: 307-336, 1983.

Berens P, Keliris GA, Ecker AS, Logothetis NK, and Tolias AS. Comparing the feature selectivity of the gamma-band of the local field potential and the underlying spiking activity in primate visual cortex. *Front Syst Neurosci* 2: 2, 2008a.

Berens P, Keliris GA, Ecker AS, Logothetis NK, and Tolias AS. Feature selectivity of the gamma-band of the local field potential in primate primary visual cortex. *Front Neurosci* 2: 199-207, 2008b.

Berens P, Logothetis NK, Tolias AS. Local field potentials, BOLD and spiking activity – relationships and physiological mechanisms. 2010

Available from Nature Precedings http://hdlhandlenet/10101/npre201052161>

Berkley KJ. Response properties of cells in ventrobasal and posterior group nuclei of the cat. *J Neurophysiol* 36: 940-952, 1973.

Berlucchi G, Sprague JM, Levy J, and DiBerardino AC. Pretectum and superior colliculus in visually guided behavior and in flux and form discrimination in the cat. *J Comp Physiol Psychol* 78: 123-172, 1972.

Berson DM, and McIlwain JT. Visual cortical inputs to deep layers of cat's superior colliculus. *J Neurophysiol* 50: 1143-1155, 1983.

Blomqvist A, Flink R, Bowsher D, Griph S, and Westman J. Tectal and thalamic projections of dorsal column and lateral cervical nuclei: a quantitative study in the cat. *Brain Res* 141: 335-341, 1978.

Bowling DB, and Michael CR. Projection patterns of single physiologically characterized optic tract fibres in cat. *Nature* 286: 899-902, 1980.

Bremmer F, Klam F, Duhamel JR, Ben Hamed S, and Graf W. Visual-vestibular interactive responses in the macaque ventral intraparietal area (VIP). *Eur J Neurosci* 16: 1569-1586, 2002.

Brosch M, Selezneva E, and Scheich H. Nonauditory events of a behavioral procedure activate auditory cortex of highly trained monkeys. *J Neurosci* 25: 6797-6806, 2005.

Burke W, Dreher B, and Wang C. Selective block of conduction in Y optic nerve fibres: significance for the concept of parallel processing. *Eur J Neurosci* 10: 8-19, 1998.

Burnett LR, Stein BE, Chaponis D, and Wallace MT. Superior colliculus lesions preferentially disrupt multisensory orientation. *Neuroscience* 124: 535-547, 2004.

Burnett LR, Stein BE, Perrault TJ, Jr., and Wallace MT. Excitotoxic lesions of the superior colliculus preferentially impact multisensory neurons and multisensory integration. *Exp Brain Res* 179: 325-338, 2007.

Bushara KO, Grafman J, and Hallett M. Neural correlates of auditory-visual stimulus onset asynchrony detection. *J Neurosci* 21: 300-304, 2001.

Caldwell RB, and Mize RR. Superior colliculus neurons which project to the cat lateral posterior nucleus have varying morphologies. *J Comp Neurol* 203: 53-66, 1981.

Calvert GA, Campbell R, and Brammer MJ. Evidence from functional magnetic resonance imaging of crossmodal binding in the human heteromodal cortex. *Curr Biol* 10: 649-657, 2000.

Cappe C, and Barone P. Heteromodal connections supporting multisensory integration at low levels of cortical processing in the monkey. *Eur J Neurosci* 22: 2886-2902, 2005.

Carriere BN, Royal DW, Perrault TJ, Morrison SP, Vaughan JW, Stein BE, and Wallace MT. Visual deprivation alters the development of cortical multisensory integration. *J Neurophysiol* 98: 2858-2867, 2007.

Carriere BN, Royal DW, and Wallace MT. Spatial heterogeneity of cortical receptive fields and its impact on multisensory interactions. *J Neurophysiol* 99: 2357-2368, 2008.

Casagrande VA, Harting JK, Hall WC, Diamond IT, and Martin GF. Superior colliculus of the tree shrew: a structural and functional subdivision into superficial and deep layers. *Science* 177: 444-447, 1972.

Christoff N. A clinicopathologic study of vertical eye movements. *Arch Neurol* 31: 1-8, 1974.

Churchland MM, Yu BM, Ryu SI, Santhanam G, and Shenoy KV. Neural variability in premotor cortex provides a signature of motor preparation. *J Neurosci* 26: 3697-3712, 2006.

Clarey JC, and Irvine DR. Auditory response properties of neurons in the anterior ectosylvian sulcus of the cat. *Brain Res* 386: 12-19, 1986.

Cleland BG, Dubin MW, and Levick WR. Sustained and transient neurones in the cat's retina and lateral geniculate nucleus. *J Physiol* 217: 473-496, 1971.

Clemo HR, Sharma GK, Allman BL, and Meredith MA. Auditory projections to extrastriate visual cortex: connectional basis for multisensory processing in 'unimodal' visual neurons. *Exp Brain Res* 191: 37-47, 2008.

Clemo HR, and Stein BE. Effects of cooling somatosensory cortex on response properties of tactile cells in the superior colliculus. *J Neurophysiol* 55: 1352-1368, 1986.

Clemo HR, and Stein BE. Receptive field properties of somatosensory neurons in the cat superior colliculus. *J Comp Neurol* 314: 534-544, 1991.

Clemo HR, and Stein BE. Responses to direction of stimulus movement are different for somatosensory and visual cells in cat superior colliculus. *Brain Res* 405: 313-319, 1987.

Clemo HR, and Stein BE. Somatosensory cortex: a 'new' somatotopic representation. *Brain Res* 235: 162-168, 1982.

Clemo HR, and Stein BE. Topographic organization of somatosensory corticotectal influences in cat. *J Neurophysiol* 51: 843-858, 1984.

Colonius H, and Arndt P. A two-stage model for visual-auditory interaction in saccadic latencies. *Percept Psychophys* 63: 126-147, 2001.

Corneil BD, Van Wanrooij M, Munoz DP, and Van Opstal AJ. Auditory-visual interactions subserving goal-directed saccades in a complex scene. *J Neurophysiol* 88: 438-454, 2002.

Cowie RJ, and Holstege G. Dorsal mesencephalic projections to pons, medulla, and spinal cord in the cat: limbic and non-limbic components. *J Comp Neurol* 319: 536-559, 1992.

Cynader M, and Berman N. Receptive-field organization of monkey superior colliculus. *J Neurophysiol* 35: 187-201, 1972.

Diederich A, and Colonius H. Bimodal and trimodal multisensory enhancement: effects of stimulus onset and intensity on reaction time. *Percept Psychophys* 66: 1388-1404, 2004.

Doubell TP, Skaliora I, Baron J, and King AJ. Functional connectivity between the superficial and deeper layers of the superior colliculus: an anatomical substrate for sensorimotor integration. *J Neurosci* 23: 6596-6607, 2003.

Drager UC, and Hubel DH. Physiology of visual cells in mouse superior colliculus and correlation with somatosensory and auditory input. *Nature* 253: 203-204, 1975a.

Drager UC, and Hubel DH. Responses to visual stimulation and relationship between visual, auditory, and somatosensory inputs in mouse superior colliculus. *J Neurophysiol* 38: 690-713, 1975b.

Dreher B, and Hoffmann KP. Properties of excitatory and inhibitory regions in the receptive fields of single units in the cat's superior colliculus. *Exp Brain Res* 16: 333-353, 1973.

Eden UT, and Kramer MA. Drawing inferences from Fano factor calculations. *J Neurosci Methods* 190: 149-152, 2010.

Edwards SB. The commissural projection of the superior colliculus in the cat. *J Comp Neurol* 173: 23-40, 1977.

Edwards SB, Ginsburgh CL, Henkel CK, and Stein BE. Sources of subcortical projections to the superior colliculus in the cat. *J Comp Neurol* 184: 309-329, 1979.

Edwards SB, and Henkel CK. Superior colliculus connections with the extraocular motor nuclei in the cat. *J Comp Neurol* 179: 451-467, 1978.

Edwards SB, Rosenquist AC, and Palmer LA. An autoradiographic study of ventral lateral geniculate projections in the cat. *Brain Res* 72: 282-287, 1974.

Enroth-Cugell C, and Robson JG. The contrast sensitivity of retinal ganglion cells of the cat. *J Physiol* 187: 517-552, 1966.

Ewert JP. Neural mechanisms of prey-catching and avoidance behavior in the toad (Bufo bufo L.). *Brain Behav Evol* 3: 36-56, 1970.

Falchier A, Clavagnier S, Barone P, and Kennedy H. Anatomical evidence of multimodal integration in primate striate cortex. *J Neurosci* 22: 5749-5759, 2002.

Fano U. Ionization yield of rations. II. The fluctuations of the number of ions. Physical Review 72:26-29, 1947.

Feldon P, and Kruger L. Topography of the retinal projection upon the superior colliculus of the cat. *Vision Res* 10: 135-143, 1970.

Felleman DJ, and Van Essen DC. Distributed hierarchical processing in the primate cerebral cortex. *Cereb Cortex* 1: 1-47, 1991.

Fetsch CR, Pouget A, DeAngelis GC, Angelaki DE. Neural correlates of reliability-based cue weighting during multisensory integration. Nat Neurosci 15:146-154, 2012.

Fitzgibbon T, Tevah LV, and Sefton AJ. Connections between the reticular nucleus of the thalamus and pulvinar-lateralis posterior complex: a WGA-HRP study. *J Comp Neurol* 363: 489-504, 1995.

Fogassi L, Gallese V, Fadiga L, Luppino G, Matelli M, and Rizzolatti G. Coding of peripersonal space in inferior premotor cortex (area F4). *J Neurophysiol* 76: 141-157, 1996.

Frens MA, and Van Opstal AJ. Visual-auditory interactions modulate saccade-related activity in monkey superior colliculus. *Brain Res Bull* 46: 211-224, 1998.

Frens MA, Van Opstal AJ, and Van der Willigen RF. Spatial and temporal factors determine auditory-visual interactions in human saccadic eye movements. *Percept Psychophys* 57: 802-816, 1995.

Fries P, Neuenschwander S, Engel AK, Goebel R, and Singer W. Rapid feature selective neuronal synchronization through correlated latency shifting. *Nat Neurosci* 4: 194-200, 2001.

Fries P, Womelsdorf T, Oostenveld R, and Desimone R. The effects of visual stimulation and selective visual attention on rhythmic neuronal synchronization in macaque area V4. *J Neurosci* 28: 4823-4835, 2008.

Fries W. Cortical projections to the superior colliculus in the macaque monkey: a retrograde study using horseradish peroxidase. *J Comp Neurol* 230: 55-76, 1984.

Fu KM, Johnston TA, Shah AS, Arnold L, Smiley J, Hackett TA, Garraghty PE, and Schroeder CE. Auditory cortical neurons respond to somatosensory stimulation. *J Neurosci* 23: 7510-7515, 2003.

Fukuda Y, and Stone J. Retinal distribution and central projections of Y-, X-, and W-cells of the cat's retina. *J Neurophysiol* 37: 749-772, 1974.

Fuster JM, Bodner M, and Kroger JK. Cross-modal and cross-temporal association in neurons of frontal cortex. *Nature* 405: 347-351, 2000.

Gail A, Brinksmeyer HJ, and Eckhorn R. Perception-related modulations of local field potential power and coherence in primary visual cortex of awake monkey during binocular rivalry. *Cereb Cortex* 14: 300-313, 2004.

Ghazanfar AA, Maier JX, Hoffman KL, and Logothetis NK. Multisensory integration of dynamic faces and voices in rhesus monkey auditory cortex. *J Neurosci* 25: 5004-5012, 2005.

Ghazanfar AA, and Schroeder CE. Is neocortex essentially multisensory? *Trends Cogn Sci* 10: 278-285, 2006.

Giard MH, and Peronnet F. Auditory-visual integration during multimodal object recognition in humans: a behavioral and electrophysiological study. *J Cogn Neurosci* 11: 473-490, 1999.

Gifford GW, 3rd, and Cohen YE. Effect of a central fixation light on auditory spatial responses in area LIP. *J Neurophysiol* 91: 2929-2933, 2004.

Gilbert CD, and Kelly JP. The projections of cells in different layers of the cat's visual cortex. *J Comp Neurol* 163: 81-105, 1975.

Gingras G, Rowland BA, and Stein BE. The differing impact of multisensory and unisensory integration on behavior. *J Neurosci* 29: 4897-4902, 2009.

Gordon B. Receptive fields in deep layers of cat superior colliculus. *J Neurophysiol* 36: 157-178, 1973.

Graham J. An autoradiographic study of the efferent connections of the superior colliculus in the cat. *J Comp Neurol* 173: 629-654, 1977.

Graham J, and Casagrande VA. A light microscopic and electron microscopic study of the superficial layers of the superior colliculus of the tree shrew (Tupaia glis). *J Comp Neurol* 191: 133-151, 1980.

Grant KW, and Seitz PF. The use of visible speech cues for improving auditory detection of spoken sentences. *J Acoust Soc Am* 108: 1197-1208, 2000.

Grantyn A, and Berthoz A. Burst activity of identified tecto-reticulo-spinal neurons in the alert cat. *Exp Brain Res* 57: 417-421, 1985.

Grantyn A, and Berthoz A. Reticulo-spinal neurons participating in the control of synergic eye and head movements during orienting in the cat. I. Behavioral properties. *Exp Brain Res* 66: 339-354, 1987.

Grantyn A, and Grantyn R. Axonal patterns and sites of termination of cat superior colliculus neurons projecting in the tecto-bulbo-spinal tract. *Exp Brain Res* 46: 243-256, 1982.

Grantyn R, Ludwig R, and Eberhardt W. Neurons of the superficial tectal gray. An intracellular HRP-study on the kitten superior colliculus in vitro. *Exp Brain Res* 55: 172-176, 1984.

Graybiel AM. Anatomical organization of retinotectal afferents in the cat: an autoradiographic study. *Brain Res* 96: 1-23, 1975.

Graybiel AM. Evidence for banding of the cat's ipsilateral retinotectal connection. *Brain Res* 114: 318-327, 1976.

Graybiel AM. A satellite system of the superior colliculus: the parabigeminal nucleus and its projections to the superficial collicular layers. *Brain Res* 145: 365-374, 1978.

Graybiel AM, and Hartwieg EA. Some afferent connections of the oculomotor complex in the cat: an experimental study with tracer techniques. *Brain Res* 81: 543-551, 1974.

Graziano MS. Where is my arm? The relative role of vision and proprioception in the neuronal representation of limb position. *Proc Natl Acad Sci U S A* 96: 10418-10421, 1999.

Graziano MS, Yap GS, and Gross CG. Coding of visual space by premotor neurons. *Science* 266: 1054-1057, 1994.

Hall WC, and Lee P. Interlaminar connections of the superior colliculus in the tree shrew. I. The superficial gray layer. *J Comp Neurol* 332: 213-223, 1993.

Hall WC, and Lee P. Interlaminar connections of the superior colliculus in the tree shrew. III: The optic layer. *Vis Neurosci* 14: 647-661, 1997.

Harrell JV, Caldwell RB, and Mize RR. The superior colliculus neurons which project to the dorsal and ventral lateral geniculate nuclei in the cat. *Exp Brain Res* 46: 234-242, 1982.

Harting JK, and Guillery RW. Organization of retinocollicular pathways in the cat. *J Comp Neurol* 166: 133-144, 1976.

Harting JK, Hall WC, Diamond IT, and Martin GF. Anterograde degeneration study of the superior colliculus in Tupaia glis: evidence for a subdivision between superficial and deep layers. *J Comp Neurol* 148: 361-386, 1973.

Harting JK, Huerta MF, Frankfurter AJ, Strominger NL, and Royce GJ. Ascending pathways from the monkey superior colliculus: an autoradiographic analysis. *J Comp Neurol* 192: 853-882, 1980.

Harting JK, Huerta MF, Hashikawa T, and van Lieshout DP. Projection of the mammalian superior colliculus upon the dorsal lateral geniculate nucleus: organization of tectogeniculate pathways in nineteen species. *J Comp Neurol* 304: 275-306, 1991.

Harting JK, and Noback CR. Subcortical projections from the visual cortex in the tree shrew (Tupaia glis). *Brain Res* 25: 21-33, 1971.

Harting JK, Updyke BV, and Van Lieshout DP. Corticotectal projections in the cat: anterograde transport studies of twenty-five cortical areas. *J Comp Neurol* 324: 379-414, 1992.

Hartline PH, Kass L, and Loop MS. Merging of modalities in the optic tectum: infrared and visual integration in rattlesnakes. *Science* 199: 1225-1229, 1978.

Hartwich-Young R, and Weber JT. The projection of frontal cortical oculomotor areas to the superior colliculus in the domestic cat. *J Comp Neurol* 253: 342-357, 1986.

Henkel CK. Evidence of sub-collicular auditory projections to the medial geniculate nucleus in the cat: an autoradiographic and horseradish peroxidase study. *Brain Res* 259: 21-30, 1983.

Henrie JA, and Shapley R. LFP power spectra in V1 cortex: the graded effect of stimulus contrast. *J Neurophysiol* 94: 479-490, 2005.

Hickok G, Okada K, and Serences JT. Area Spt in the human planum temporale supports sensory-motor integration for speech processing. *J Neurophysiol* 101: 2725-2732, 2009.

Hicks TP, Stark CA, and Fletcher WA. Origins of afferents to visual suprageniculate nucleus of the cat. *J Comp Neurol* 246: 544-554, 1986.

Hoffmann KP. Conduction velocity in pathways from retina to superior colliculus in the cat: a correlation with receptive-field properties. *J Neurophysiol* 36: 409-424, 1973.

Hollander H. On the origin of the corticotectal projections in the cat. *Exp Brain Res* 21: 433-439, 1974.

Holmes NP. The principle of inverse effectiveness in multisensory integration: some statistical considerations. *Brain Topogr* 21: 168-176, 2009.

Holstege G. Brainstem-spinal cord projections in the cat, related to control of head and axial movements. *Rev Oculomot Res* 2: 431-470, 1988a.

Holstege G. Direct and indirect pathways to lamina I in the medulla oblongata and spinal cord of the cat. *Prog Brain Res* 77: 47-94, 1988b.

Horn G, and Hill RM. Responsiveness to sensory stimulation of units in the superior colliculus and subjacent tectotegmental regions of the rabbit. *Exp Neurol* 14: 199-223, 1966.

Huerta MF, Frankfurter AJ, and Harting JK. The trigeminocollicular projection in the cat: patch-like endings within the intermediate gray. *Brain Res* 211: 1-13, 1981.

Huerta MF, and Harting JK. The projection from the nucleus of the posterior commissure to the superior colliculus of the cat: patch-like endings within the intermediate and deep grey layers. *Brain Res* 238: 426-432, 1982a.

Huerta MF, and Harting JK. Projections of the superior colliculus to the supraspinal nucleus and the cervical spinal cord gray of the cat. *Brain Res* 242: 326-331, 1982b.

Huerta MF, and Harting JK. Sublamination within the superficial gray layer of the squirrel monkey: an analysis of the tectopulvinar projection using anterograde and retrograde transport methods. *Brain Res* 261: 119-126, 1983.

Huerta MF HJ. Comparative Neurology of Optic tectum. 1984.

Huerta MF, and Kaas JH. Supplementary eye field as defined by intracortical microstimulation: connections in macaques. *J Comp Neurol* 293: 299-330, 1990.

Huerta MF, Krubitzer LA, and Kaas JH. Frontal eye field as defined by intracortical microstimulation in squirrel monkeys, owl monkeys, and macaque monkeys: I. Subcortical connections. *J Comp Neurol* 253: 415-439, 1986.

Hughes HC, Reuter-Lorenz PA, Nozawa G, and Fendrich R. Visual-auditory interactions in sensorimotor processing: saccades versus manual responses. *J Exp Psychol Hum Percept Perform* 20: 131-153, 1994.

Hussar C, and Pasternak T. Trial-to-trial variability of the prefrontal neurons reveals the nature of their engagement in a motion discrimination task. *Proc Natl Acad Sci U S A* 107: 21842-21847, 2010.

Illing RB. Axonal bifurcation of cat retinal ganglion cells as demonstrated by retrograde double labelling with fluorescent dyes. *Neurosci Lett* 19: 125-130, 1980.

Illing RB, and Wassle H. The retinal projection to the thalamus in the cat: a quantitative investigation and a comparison with the retinotectal pathway. *J Comp Neurol* 202: 265-285, 1981.

Ingle D. Visuomotor functions of the frog optic tectum. *Brain Behav Evol* 3: 57-71, 1970.

Jiang W JH, Stein BE. Influences from the anterior ectosylvian sulcus and rostral lateral suprasylvian sulcus are critical for multisensory orientation behavior. *Soc Neurosci Abstr 26 : 1220* 2000.

Jiang W, Jiang H, and Stein BE. Neonatal cortical ablation disrupts multisensory development in superior colliculus. *J Neurophysiol* 95: 1380-1396, 2006.

Jiang W, Jiang H, and Stein BE. Two corticotectal areas facilitate multisensory orientation behavior. *J Cogn Neurosci* 14: 1240-1255, 2002.

Jones EG. The Thalamus. New York:Plenum Press, 1985

Jones EG. Neuroanatomy: Cajal and after Cajal. *Brain Res Rev* 55: 248-255, 2007.

Kadunce DC, Vaughan JW, Wallace MT, Benedek G, and Stein BE. Mechanisms of within- and cross-modality suppression in the superior colliculus. *J Neurophysiol* 78: 2834-2847, 1997.

Kadunce DC, Vaughan JW, Wallace MT, and Stein BE. The influence of visual and auditory receptive field organization on multisensory integration in the superior colliculus. *Exp Brain Res* 139: 303-310, 2001.

Kanaseki T, and Sprague JM. Anatomical organization of pretectal nuclei and tectal laminae in the cat. *J Comp Neurol* 158: 319-337, 1974.

Kara P, Reinagel P, and Reid RC. Low response variability in simultaneously recorded retinal, thalamic, and cortical neurons. *Neuron* 27: 635-646, 2000.

Kawamura K, and Konno T. Various types of corticotectal neurons of cats as demonstrated by means of retrograde axonal transport of horseradish peroxidase. *Exp Brain Res* 35: 161-175, 1979.

Kawamura S, Fukushima N, Hattori S, and Kudo M. Laminar segregation of cells of origin of ascending projections from the superficial layers of the superior colliculus in the cat. *Brain Res* 184: 486-490, 1980.

Kawamura S, Fukushima N, Hattori S, and Tashiro T. A ventral lateral geniculate nucleus projection to the dorsal thalamus and the midbrain in the cat. *Exp Brain Res* 31: 95-106, 1978.

Kayser C, and Logothetis NK. Do early sensory cortices integrate cross-modal information? *Brain Struct Funct* 212: 121-132, 2007.

Kayser C, Logothetis NK, and Panzeri S. Visual enhancement of the information representation in auditory cortex. *Curr Biol* 20: 19-24, 2010.

Kayser C, Petkov CI, Augath M, and Logothetis NK. Integration of touch and sound in auditory cortex. *Neuron* 48: 373-384, 2005.

Kayser C, Petkov CI, and Logothetis NK. Visual modulation of neurons in auditory cortex. *Cereb Cortex* 18: 1560-1574, 2008.

Kelly JP, and Gilbert CD. The projections of different morphological types of ganglion cells in the cat retina. *J Comp Neurol* 163: 65-80, 1975.

Keysers C, Kohler E, Umilta MA, Nanetti L, Fogassi L, and Gallese V. Audiovisual mirror neurons and action recognition. *Exp Brain Res* 153: 628-636, 2003.

King AJ, and Palmer AR. Cells responsive to free-field auditory stimuli in guinea-pig superior colliculus: distribution and response properties. *J Physiol* 342: 361-381, 1983.

King AJ, and Palmer AR. Integration of visual and auditory information in bimodal neurones in the guinea-pig superior colliculus. *Exp Brain Res* 60: 492-500, 1985.

Knudsen EI. Sensitive periods in the development of the brain and behavior. *J Cogn Neurosci* 16: 1412-1425, 2004.

Knudsen EI, Knudsen PF, and Masino T. Parallel pathways mediating both sound localization and gaze control in the forebrain and midbrain of the barn owl. *J Neurosci* 13: 2837-2852, 1993.

Kohler E, Keysers C, Umilta MA, Fogassi L, Gallese V, and Rizzolatti G. Hearing sounds, understanding actions: action representation in mirror neurons. *Science* 297: 846-848, 2002.

Komatsu H, and Suzuki H. Projections from the functional subdivisions of the frontal eye field to the superior colliculus in the monkey. *Brain Res* 327: 324-327, 1985.

Kreiman G, Hung CP, Kraskov A, Quiroga RQ, Poggio T, and DiCarlo JJ. Object selectivity of local field potentials and spikes in the macaque inferior temporal cortex. *Neuron* 49: 433-445, 2006.

Kudo M. Projections of the nuclei of the lateral lemniscus in the cat: an autoradiographic study. *Brain Res* 221: 57-69, 1981.

Kudo M, and Niimi K. Ascending projections of the inferior colliculus in the cat: an autoradiographic study. *J Comp Neurol* 191: 545-556, 1980.

Kuffler SW. Discharge patterns and functional organization of mammalian retina. *J Neurophysiol* 16: 37-68, 1953.

Kunzle H, and Akert K. Efferent connections of cortical, area 8 (frontal eye field) in Macaca fascicularis. A reinvestigation using the autoradiographic technique. *J Comp Neurol* 173: 147-164, 1977.

Kunzle H, Akert K, and Wurtz RH. Projection of area 8 (frontal eye field) to superior colliculus in the monkey. An autoradiographic study. *Brain Res* 117: 487-492, 1976.

Kuypers HG, Szwarcbart MK, Mishkin M, and Rosvold HE. Occipitotemporal Corticocortical Connections in the Rhesus Monkey. *Exp Neurol* 11: 245-262, 1965.

Lakatos P, Chen CM, O'Connell MN, Mills A, and Schroeder CE. Neuronal oscillations and multisensory interaction in primary auditory cortex. *Neuron* 53: 279-292, 2007.

Lakatos P, Karmos G, Mehta AD, Ulbert I, and Schroeder CE. Entrainment of neuronal oscillations as a mechanism of attentional selection. *Science* 320: 110-113, 2008.

Langer T, Kaneko CR, Scudder CA, and Fuchs AF. Afferents to the abducens nucleus in the monkey and cat. *J Comp Neurol* 245: 379-400, 1986.

Langer TP, and Kaneko CR. Brainstem afferents to the omnipause region in the cat: a horseradish peroxidase study. *J Comp Neurol* 230: 444-458, 1984.

Lee P, and Hall WC. Interlaminar connections of the superior colliculus in the tree shrew. II: Projections from the superficial gray to the optic layer. *Vis Neurosci* 12: 573-588, 1995.

Leichnetz GR, and Gonzalo-Ruiz A. Prearcuate cortex in the Cebus monkey has cortical and subcortical connections like the macaque frontal eye field and projects to fastigial-recipient oculomotor-related brainstem nuclei. *Brain Res Bull* 41: 1-29, 1996.

Leichnetz GR, Spencer RF, Hardy SG, and Astruc J. The prefrontal corticotectal projection in the monkey; an anterograde and retrograde horseradish peroxidase study. *Neuroscience* 6: 1023-1041, 1981.

Leinonen L, Hyvarinen J, and Sovijarvi AR. Functional properties of neurons in the temporo-parietal association cortex of awake monkey. *Exp Brain Res* 39: 203-215, 1980.

Lewis JW, Beauchamp MS, and DeYoe EA. A comparison of visual and auditory motion processing in human cerebral cortex. *Cereb Cortex* 10: 873-888, 2000.

Lin CS, and Kaas JH. The inferior pulvinar complex in owl monkeys: architectonic subdivisions and patterns of input from the superior colliculus and subdivisions of visual cortex. *J Comp Neurol* 187: 655-678, 1979.

Linden JF, Grunewald A, and Andersen RA. Responses to auditory stimuli in macaque lateral intraparietal area. II. Behavioral modulation. *J Neurophysiol* 82: 343-358, 1999.

Linke R. Differential projection patterns of superior and inferior collicular neurons onto posterior paralaminar nuclei of the thalamus surrounding the medial geniculate body in the rat. *Eur J Neurosci* 11: 187-203, 1999.

Liu J, and Newsome WT. Local field potential in cortical area MT: stimulus tuning and behavioral correlations. *J Neurosci* 26: 7779-7790, 2006.

Logothetis NK. The underpinnings of the BOLD functional magnetic resonance imaging signal. *J Neurosci* 23: 3963-3971, 2003.

Logothetis NK. What we can do and what we cannot do with fMRI. *Nature* 453: 869-878, 2008.

Lovejoy LP, and Krauzlis RJ. Inactivation of primate superior colliculus impairs covert selection of signals for perceptual judgments. *Nat Neurosci* 13: 261-266, 2010.

Lund RD, Land PW, and Boles J. Normal and abnormal uncrossed retinotectal pathways in rats: an HRP study in adults. *J Comp Neurol* 189: 711-720, 1980.

Martin GF, Jr. The pattern of neocortical projections to the mesencephalon of the opossum, Didelphis virginiana. *Brain Res* 11: 593-610, 1968.

Massopust LC, Jr., Wolin LR, and Meder J. Spontaneous Electrical Activity of the Brain in Hibernators and Nonhibernators during Hypothermia. *Exp Neurol* 12: 25-32, 1965.

Mast TE, and Chung DY. Binaural interaction in the superior colliculus of the chinchilla. *Brain Res* 62: 227-230, 1973.

May PJ. The mammalian superior colliculus: laminar structure and connections. *Prog Brain Res* 151: 321-378, 2006.

May PJ, Baker RG, and Chen B. The eyelid levator muscle: servant of two masters. *Mov Disord* 17 Suppl 2: S4-7, 2002.

Mazzoni P, Bracewell RM, Barash S, and Andersen RA. Spatially tuned auditory responses in area LIP of macaques performing delayed memory saccades to acoustic targets. *J Neurophysiol* 75: 1233-1241, 1996.

McDonald JJ, and Ward LM. Involuntary listening aids seeing: evidence from human electrophysiology. *Psychol Sci* 11: 167-171, 2000.

McHaffie JG, Kruger L, Clemo HR, and Stein BE. Corticothalamic and corticotectal somatosensory projections from the anterior ectosylvian sulcus (SIV cortex) in neonatal cats: an anatomical demonstration with HRP and 3H-leucine. *J Comp Neurol* 274: 115-126, 1988.

McHaffie JG, Thomson CM, and Stein BE. Corticotectal and corticostriatal projections from the frontal eye fields of the cat: an anatomical examination using WGA-HRP. *Somatosens Mot Res* 18: 117-130, 2001.

McIlwain JT. Visual receptive fields and their images in superior colliculus of the cat. *J Neurophysiol* 38: 219-230, 1975.

McIlwain JT, and Buser P. Receptive fields of single cells in the cat's superior colliculus. *Exp Brain Res* 5: 314-325, 1968.

McPeek RM, and Keller EL. Deficits in saccade target selection after inactivation of superior colliculus. *Nat Neurosci* 7: 757-763, 2004.

Meredith MA, and Clemo HR. Auditory cortical projection from the anterior ectosylvian sulcus (Field AES) to the superior colliculus in the cat: an anatomical and electrophysiological study. *J Comp Neurol* 289: 687-707, 1989.

Meredith MA, Clemo HR, and Stein BE. Somatotopic component of the multisensory map in the deep laminae of the cat superior colliculus. *J Comp Neurol* 312: 353-370, 1991.

Meredith MA, Nemitz JW, and Stein BE. Determinants of multisensory integration in superior colliculus neurons. I. Temporal factors. *J Neurosci* 7: 3215-3229, 1987.

Meredith MA, and Stein BE. Interactions among converging sensory inputs in the superior colliculus. *Science* 221: 389-391, 1983.

Meredith MA, and Stein BE. Spatial determinants of multisensory integration in cat superior colliculus neurons. *J Neurophysiol* 75: 1843-1857, 1996.

Meredith MA, and Stein BE. Spatial factors determine the activity of multisensory neurons in cat superior colliculus. *Brain Res* 365: 350-354, 1986a.

Meredith MA, and Stein BE. Visual, auditory, and somatosensory convergence on cells in superior colliculus results in multisensory integration. *J Neurophysiol* 56: 640-662, 1986b.

Meredith MA, and Stein BE. The visuotopic component of the multisensory map in the deep laminae of the cat superior colliculus. *J Neurosci* 10: 3727-3742, 1990.

Meyer GF, and Wuerger SM. Cross-modal integration of auditory and visual motion signals. *Neuroreport* 12: 2557-2560, 2001.

Middlebrooks JC, and Knudsen EI. A neural code for auditory space in the cat's superior colliculus. *J Neurosci* 4: 2621-2634, 1984.

Middlebrooks JC, and Pettigrew JD. Functional classes of neurons in primary auditory cortex of the cat distinguished by sensitivity to sound location. *J Neurosci* 1: 107-120, 1981.

Miyashita E, and Tamai Y. Subcortical connections of frontal 'oculomotor' areas in the cat. *Brain Res* 502: 75-87, 1989.

Mochol G, Wojcik DK, Wypych M, Wrobel A, and Waleszczyk WJ. Variability of visual responses of superior colliculus neurons depends on stimulus velocity. *J Neurosci* 30: 3199-3209, 2010.

Molholm S, Ritter W, Murray MM, Javitt DC, Schroeder CE, and Foxe JJ. Multisensory auditory-visual interactions during early sensory processing in humans: a high-density electrical mapping study. *Brain Res Cogn Brain Res* 14: 115-128, 2002.

Mooney RD, Fish SE, and Rhoades RW. Anatomical and functional organization of pathway from superior colliculus to lateral posterior nucleus in hamster. *J Neurophysiol* 51: 407-431, 1984.

Moore RY, and Goldberg JM. Projections of the inferior colliculus in the monkey. *Exp Neurol* 14: 429-438, 1966.

Morrell F. Visual system's view of acoustic space. *Nature* 238: 44-46, 1972.

Moschovakis AK, Gregoriou GG, Ugolini G, Doldan M, Graf W, Guldin W, Hadjidimitrakis K, and Savaki HE. Oculomotor areas of the primate frontal lobes: a transneuronal transfer of rabies virus and [14C]-2-deoxyglucose functional imaging study. *J Neurosci* 24: 5726-5740, 2004.

Moschovakis AK, and Karabelas AB. Observations on the somatodendritic morphology and axonal trajectory of intracellularly HRP-labeled efferent neurons

located in the deeper layers of the superior colliculus of the cat. *J Comp Neurol* 239: 276-308, 1985.

Moschovakis AK, Karabelas AB, and Highstein SM. Structure-function relationships in the primate superior colliculus. I. Morphological classification of efferent neurons. *J Neurophysiol* 60: 232-262, 1988.

Mower G, Gibson A, and Glickstein M. Tectopontine pathway in the cat: laminar distribution of cells of origin and visual properties of target cells in dorsolateral pontine nucleus. *J Neurophysiol* 42: 1-15, 1979.

Mucke L, Norita M, Benedek G, and Creutzfeldt O. Physiologic and anatomic investigation of a visual cortical area situated in the ventral bank of the anterior ectosylvian sulcus of the cat. *Exp Brain Res* 46: 1-11, 1982.

Muller JR, Philiastides MG, and Newsome WT. Microstimulation of the superior colliculus focuses attention without moving the eyes. *Proc Natl Acad Sci U S A* 102: 524-529, 2005.

Murray EA, and Coulter JD. Organization of tectospinal neurons in the cat and rat superior colliculus. *Brain Res* 243: 201-214, 1982.

Nakamura H, and Itoh K. Cytoarchitectonic and connectional organization of the ventral lateral geniculate nucleus in the cat. *J Comp Neurol* 473: 439-462, 2004.

Newman EA, and Hartline PH. Integration of visual and infrared information in bimodal neurons in the rattlesnake optic tectum. *Science* 213: 789-791, 1981.

Norita M. Neurons and synaptic patterns in the deep layers of the superior colliculus of the cat. A Golgi and electron microscopic study. *J Comp Neurol* 190: 29-48, 1980.

Norita M, Kase M, Hoshino K, Meguro R, Funaki S, Hirano S, and McHaffie JG. Extrinsic and intrinsic connections of the cat's lateral suprasylvian visual area. *Prog Brain Res* 112: 231-250, 1996.

Norita M, McHaffie JG, Shimizu H, and Stein BE. The corticostriatal and corticotectal projections of the feline lateral suprasylvian cortex demonstrated with anterograde biocytin and retrograde fluorescent techniques. *Neurosci Res* 10: 149-155, 1991.

Norita M, Mucke L, Benedek G, Albowitz B, Katoh Y, and Creutzfeldt OD. Connections of the anterior ectosylvian visual area (AEV). *Exp Brain Res* 62: 225-240, 1986.

Northcutt RG. Understanding vertebrate brain evolution. *Integr Comp Biol* 42: 743-756, 2002.

Nozawa G, Reuter-Lorenz PA, and Hughes HC. Parallel and serial processes in the human oculomotor system: bimodal integration and express saccades. *Biol Cybern* 72: 19-34, 1994.

Nudo RJ, and Masterton RB. Descending pathways to the spinal cord: a comparative study of 22 mammals. *J Comp Neurol* 277: 53-79, 1988.

Nudo RJ, and Masterton RB. Descending pathways to the spinal cord: II. Quantitative study of the tectospinal tract in 23 mammals. *J Comp Neurol* 286: 96-119, 1989.

Ogasawara K, McHaffie JG, and Stein BE. Two visual corticotectal systems in cat. *J Neurophysiol* 52: 1226-1245, 1984.

Pavani F, Spence C, and Driver J. Visual capture of touch: out-of-the-body experiences with rubber gloves. *Psychol Sci* 11: 353-359, 2000.

Perrault TJ, Jr., Vaughan JW, Stein BE, and Wallace MT. Neuron-specific response characteristics predict the magnitude of multisensory integration. *J Neurophysiol* 90: 4022-4026, 2003.

Perrault TJ, Jr., Vaughan JW, Stein BE, and Wallace MT. Superior colliculus neurons use distinct operational modes in the integration of multisensory stimuli. *J Neurophysiol* 93: 2575-2586, 2005.

Pesaran B. Uncovering the mysterious origins of local field potentials. *Neuron* 61: 1-2, 2009.

Pesaran B, Pezaris JS, Sahani M, Mitra PP, and Andersen RA. Temporal structure in neuronal activity during working memory in macaque parietal cortex. *Nat Neurosci* 5: 805-811, 2002.

Pollack JG, and Hickey TL. The distribution of retino-collicular axon terminals in rhesus monkey. *J Comp Neurol* 185: 587-602, 1979.

Powell TP. Bilateral cortico-tectal projection from the visual cortex in the cat. *Nature* 260: 526-527, 1976.

Raczkowski D, and Diamond IT. Projections from the superior colliculus and the neocortex to the pulvinar nucleus in Galago. *J Comp Neurol* 200: 231-254, 1981.

Ramon y Cajal S. The Superior Colliculus. Histology of the Nervous System.Translated by Swanson N, Swanson LW, 1995

Rauschecker JP, and Harris LR. Auditory and visual neurons in the cat's superior colliculus selective for the direction of apparent motion stimuli. *Brain Res* 490: 56-63, 1989.

Ray S, Hsiao SS, Crone NE, Franaszczuk PJ, and Niebur E. Effect of stimulus intensity on the spike-local field potential relationship in the secondary somatosensory cortex. *J Neurosci* 28: 7334-7343, 2008.

Rhoades RW, and Chalupa LM. Conduction velocity distribution of the retinal input to the hamster's superior colliculus and a correlation with receptive field characteristics. *J Comp Neurol* 184: 243-263, 1979.

Rizzolatti G, Camarda R, Fogassi L, Gentilucci M, Luppino G, and Matelli M. Functional organization of inferior area 6 in the macaque monkey. II. Area F5 and the control of distal movements. *Exp Brain Res* 71: 491-507, 1988.

Rock I, and Victor J. Vision and Touch: An Experimentally Created Conflict between the Two Senses. *Science* 143: 594-596, 1964.

Rockland KS, and Ojima H. Multisensory convergence in calcarine visual areas in macaque monkey. *Int J Psychophysiol* 50: 19-26, 2003.

Rodrigo-Angulo ML, and Reinoso-Suarez F. Connections to the lateral posterior-pulvinar thalamic complex from the reticular and ventral lateral geniculate thalamic nuclei: a topographical study in the cat. *Neuroscience* 26: 449-459, 1988.

Romo R, Hernandez A, and Zainos A. Neuronal correlates of a perceptual decision in ventral premotor cortex. *Neuron* 41: 165-173, 2004.

Rouger J, Fraysse B, Deguine O, and Barone P. McGurk effects in cochlear-implanted deaf subjects. *Brain Res* 1188: 87-99, 2008.

Rowland BA, Quessy S, Stanford TR, and Stein BE. Multisensory integration shortens physiological response latencies. *J Neurosci* 27: 5879-5884, 2007a.

Rowland BA, Stanford TR, and Stein BE. A model of the neural mechanisms underlying multisensory integration in the superior colliculus. *Perception* 36: 1431-1443, 2007b.

Rowland BA, and Stein BE. Multisensory integration produces an initial response enhancement. *Front Integr Neurosci* 1: 4, 2007.

Royal DW, Carriere BN, and Wallace MT. Spatiotemporal architecture of cortical receptive fields and its impact on multisensory interactions. *Exp Brain Res* 198: 127-136, 2009.

Saitoh K, Menard A, and Grillner S. Tectal control of locomotion, steering, and eye movements in lamprey. *J Neurophysiol* 97: 3093-3108, 2007.

Scheier CR, Nijwahan R and Shimojo S. Sound alters visual temporal resolution. *Investigative Ophthalomology and Visual Science Meeting. Fort Lauderdale FL*. 1999.

Schlack A, Sterbing-D'Angelo SJ, Hartung K, Hoffmann KP, and Bremmer F. Multisensory space representations in the macaque ventral intraparietal area. *J Neurosci* 25: 4616-4625, 2005.

Schlag J, and Schlag-Rey M. Induction of oculomotor responses by electrical stimulation of the prefrontal cortex in the cat. *Brain Res* 22: 1-13, 1970.

Schneider GE. Two visual systems. *Science* 163: 895-902, 1969.

Schorr EA, Fox NA, van Wassenhove V, and Knudsen EI. Auditory-visual fusion in speech perception in children with cochlear implants. *Proc Natl Acad Sci U S A* 102: 18748-18750, 2005.

Schroeder CE, and Foxe JJ. The timing and laminar profile of converging inputs to multisensory areas of the macaque neocortex. *Brain Res Cogn Brain Res* 14: 187-198, 2002.

Schroeder CE, and Lakatos P. The gamma oscillation: master or slave? *Brain Topogr* 22: 24-26, 2009a.

Schroeder CE, and Lakatos P. Low-frequency neuronal oscillations as instruments of sensory selection. *Trends Neurosci* 32: 9-18, 2009b.

Schroeder CE, Lindsley RW, Specht C, Marcovici A, Smiley JF, and Javitt DC. Somatosensory input to auditory association cortex in the macaque monkey. *J Neurophysiol* 85: 1322-1327, 2001.

Schwartz JL, Berthommier F, and Savariaux C. Seeing to hear better: evidence for early audio-visual interactions in speech identification. *Cognition* 93: B69-78, 2004.

Segal RL, and Beckstead RM. The lateral suprasylvian corticotectal projection in cats. *J Comp Neurol* 225: 259-275, 1984.

Sekuler AB, and Sekuler R. Collisions between moving visual targets: what controls alternative ways of seeing an ambiguous display? *Perception* 28: 415-432, 1999.

Shams L, Kamitani Y, Thompson S, and Shimojo S. Sound alters visual evoked potentials in humans. *Neuroreport* 12: 3849-3852, 2001.

Siminoff R, Schwassmann HO, and Kruger L. An electrophysiological study of the visual projection to the superior colliculus of the rat. *J Comp Neurol* 127: 435-444, 1966.

Snyder LH, Grieve KL, Brotchie P, and Andersen RA. Separate body- and world-referenced representations of visual space in parietal cortex. *Nature* 394: 887-891, 1998.

Sprague JM. Mammalian tectum: intrinsic organization, afferent inputs, and integrative mechanisms. Anatomical substrate. *Neurosci Res Program Bull* 13: 204-213, 1975.

Sprague JM. Neural mechanisms of visual orienting responses. *Prog Brain Res* 112: 1-15, 1996.

Sprague JM. The role of the superior colliculus in facilitating visual attention and form perception. *Proc Natl Acad Sci U S A* 88: 1286-1290, 1991.

Sprague JM, Berlucchi G, and Di Berardino A. The superior colliculus and pretectum in visually guided behavior and visual discrimination in the cat. *Brain Behav Evol* 3: 285-294, 1970.

Sprague JM, Levy J, DiBerardino A, and Berlucchi G. Visual cortical areas mediating form discrimination in the cat. *J Comp Neurol* 172: 441-488, 1977.

Sprague JM, and Meikle TH, Jr. The Role of the Superior Colliculus in Visually Guided Behavior. *Exp Neurol* 11: 115-146, 1965.

Sridharan D, Boahen K, and Knudsen EI. Space coding by gamma oscillations in the barn owl optic tectum. *J Neurophysiol* 105: 2005-2017, 2011.

Stanford TR, Quessy S, and Stein BE. Evaluating the operations underlying multisensory integration in the cat superior colliculus. *J Neurosci* 25: 6499-6508, 2005.

Stanford TR, and Stein BE. Superadditivity in multisensory integration: putting the computation in context. *Neuroreport* 18: 787-792, 2007.

Stanton GB, Goldberg ME, and Bruce CJ. Frontal eye field efferents in the macaque monkey: II. Topography of terminal fields in midbrain and pons. *J Comp Neurol* 271: 493-506, 1988.

Stein BE, and Arigbede MO. Unimodal and multimodal response properties of neurons in the cat's superior colliculus. *Exp Neurol* 36: 179-196, 1972.

Stein BE, Goldberg SJ, and Clamann HP. The control of eye movements by the superior colliculus in the alert cat. *Brain Res* 118: 469-474, 1976a.

Stein BE, Huneycutt WS, and Meredith MA. Neurons and behavior: the same rules of multisensory integration apply. *Brain Res* 448: 355-358, 1988.

Stein BE MA. The Merging of the Senses. *Book* 1993.

Stein BE, Magalhaes-Castro B, and Kruger L. Relationship between visual and tactile representations in cat superior colliculus. *J Neurophysiol* 39: 401-419, 1976b.

Stein BE, Spencer RF, and Edwards SB. Corticotectal and corticothalamic efferent projections of SIV somatosensory cortex in cat. *J Neurophysiol* 50: 896-909, 1983.

Stein BE, Wallace MW, Stanford TR, and Jiang W. Cortex governs multisensory integration in the midbrain. *Neuroscientist* 8: 306-314, 2002.

Steinmetz NA, and Moore T. Changes in the response rate and response variability of area V4 neurons during the preparation of saccadic eye movements. *J Neurophysiol* 103: 1171-1178, 2010.

Steinmetz PN, Roy A, Fitzgerald PJ, Hsiao SS, Johnson KO, and Niebur E. Attention modulates synchronized neuronal firing in primate somatosensory cortex. *Nature* 404: 187-190, 2000.

Sterling P. Receptive fields and synaptic organization of the superficial gray layer of the cat superior colliculus. *Vision Res* Suppl 3: 309-328, 1971.

Sterling P, and Wickelgren BG. Visual receptive fields in the superior colliculus of the cat. *J Neurophysiol* 32: 1-15, 1969.

Stevenson JA, and Lund RD. A crossed parabigemino-lateral geniculate projection in rats blinded at birth. *Exp Brain Res* 45: 95-100, 1982.

Stevenson RA, and James TW. Audiovisual integration in human superior temporal sulcus: Inverse effectiveness and the neural processing of speech and object recognition. *Neuroimage* 44: 1210-1223, 2009.

Straschill M, and Hoffmann KP. Functional aspects of localization in the cat's tectum opticum. *Brain Res* 13: 274-283, 1969.

Sugihara T, Diltz MD, Averbeck BB, and Romanski LM. Integration of auditory and visual communication information in the primate ventrolateral prefrontal cortex. *J Neurosci* 26: 11138-11147, 2006.

Sumby WH and Pollack I. Visual contribution to speech intelligibility in noise. *J Acoust Soc Am* 26:212-215. 1954

Swanson LW, Cowan WM, and Jones EG. An autoradiographic study of the efferent connections of the ventral lateral geniculate nucleus in the albino rat and the cat. *J Comp Neurol* 156: 143-163, 1974.

Symonds LL, and Kaas JH. Connections of striate cortex in the prosimian, Galago senegalensis. *J Comp Neurol* 181: 477-512, 1978.

Tamamaki N, Uhlrich DJ, and Sherman SM. Morphology of physiologically identified retinal X and Y axons in the cat's thalamus and midbrain as revealed by intraaxonal injection of biocytin. *J Comp Neurol* 354: 583-607, 1995.

Taylor K, Mandon S, Freiwald WA, and Kreiter AK. Coherent oscillatory activity in monkey area v4 predicts successful allocation of attention. *Cereb Cortex* 15: 1424-1437, 2005.

Tortelly A, Reinoso-Suarez F, and Llamas A. Projections from non-visual cortical areas to the superior colliculus demonstrated by retrograde transport of HRP in the cat. *Brain Res* 188: 543-549, 1980.

Tunkl JE, and Berkley MA. The role of superior colliculus in vision: visual form discrimination in cats with superior colliculus ablations. *J Comp Neurol* 176: 575-587, 1977.

Updyke BV. Topographic organization of the projections from cortical areas 17, 18 and 19 onto the thalamus, pretectum and superior colliculus in the cat. *J Comp Neurol* 173: 81-122, 1977.

Waleszczyk WJ, Nagy A, Wypych M, Berenyi A, Paroczy Z, Eordegh G, Ghazaryan A, and Benedek G. Spectral receptive field properties of neurons in the feline superior colliculus. *Exp Brain Res* 181: 87-98, 2007.

Wallace MT, Meredith MA, and Stein BE. Integration of multiple sensory modalities in cat cortex. *Exp Brain Res* 91: 484-488, 1992.

Wallace MT, Meredith MA, and Stein BE. Multisensory integration in the superior colliculus of the alert cat. *J Neurophysiol* 80: 1006-1010, 1998.

Wallace MT, and Stein BE. Cross-modal synthesis in the midbrain depends on input from cortex. *J Neurophysiol* 71: 429-432, 1994.

Wallace MT, and Stein BE. Development of multisensory neurons and multisensory integration in cat superior colliculus. *J Neurosci* 17: 2429-2444, 1997.

Wallace MT, and Stein BE. Onset of cross-modal synthesis in the neonatal superior colliculus is gated by the development of cortical influences. *J Neurophysiol* 83: 3578-3582, 2000.

Wallace MT, and Stein BE. Sensory organization of the superior colliculus in cat and monkey. *Prog Brain Res* 112: 301-311, 1996.

Wang SF, and Spencer RF. Spatial organization of premotor neurons related to vertical upward and downward saccadic eye movements in the rostral interstitial nucleus of the medial longitudinal fasciculus (riMLF) in the cat. *J Comp Neurol* 366: 163-180, 1996.

Wassle H, and Illing RB. The retinal projection to the superior colliculus in the cat: a quantitative study with HRP. *J Comp Neurol* 190: 333-356, 1980.

Weber JT, and Harting JK. The efferent projections of the pretectal complex: an autoradiographic and horseradish peroxidase analysis. *Brain Res* 194: 1-28, 1980.

Weldon DA, and Best PJ. Changes in sensory responsivity in deep layer neurons of the superior colliculus of behaving rats. *Behav Brain Res* 47: 97-101, 1992.

Wickelgren BG. Superior colliculus: some receptive field properties of bimodally responsive cells. *Science* 173: 69-72, 1971.

Wiener FM, Pfeiffer RR, and Backus AS. On the sound pressure transformation by the head and auditory meatus of the cat. *Acta Otolaryngol* 61: 255-269, 1966.

Wilke M, Logothetis NK, and Leopold DA. Local field potential reflects perceptual suppression in monkey visual cortex. *Proc Natl Acad Sci U S A* 103: 17507-17512, 2006.

Wilkinson LK, Meredith MA, and Stein BE. The role of anterior ectosylvian cortex in cross-modality orientation and approach behavior. *Exp Brain Res* 112: 1-10, 1996.

Wilson JR, Hendrickson AE, Sherk H, and Tigges J. Sources of subcortical afferents to the macaque's dorsal lateral geniculate nucleus. *Anat Rec* 242: 566-574, 1995.

Winkowski DE, and Knudsen EI. Top-down control of multimodal sensitivity in the barn owl optic tectum. *J Neurosci* 27: 13279-13291, 2007.

Winkowski DE, and Knudsen EI. Top-down gain control of the auditory space map by gaze control circuitry in the barn owl. *Nature* 439: 336-339, 2006.

Wise LZ, and Irvine DR. Auditory response properties of neurons in deep layers of cat superior colliculus. *J Neurophysiol* 49: 674-685, 1983.

Wise LZ, and Irvine DR. Topographic organization of interaural intensity difference sensitivity in deep layers of cat superior colliculus: implications for auditory spatial representation. *J Neurophysiol* 54: 185-211, 1985.

Wurtz RH, and Albano JE. Visual-motor function of the primate superior colliculus. *Annu Rev Neurosci* 3: 189-226, 1980.

Young MP, Tanaka K, and Yamane S. On oscillating neuronal responses in the visual cortex of the monkey. *J Neurophysiol* 67: 1464-1474, 1992.

Zhang HY, and Hoffmann KP. Retinal projections to the pretectum, accessory optic system and superior colliculus in pigmented and albino ferrets. *Eur J Neurosci* 5: 486-500, 1993.

Zhang T, Heuer HW, and Britten KH. Parietal area VIP neuronal responses to heading stimuli are encoded in head-centered coordinates. *Neuron* 42: 993-1001, 2004.

Zhou YD, and Fuster JM. Somatosensory cell response to an auditory cue in a haptic memory task. *Behav Brain Res* 153: 573-578, 2004.

Zhou YD, and Fuster JM. Visuo-tactile cross-modal associations in cortical somatosensory cells. *Proc Natl Acad Sci U S A* 97: 9777-9782, 2000.

CHAPTER II

HETEROGENEITY IN THE SPATIAL RECEPTIVE FIELD ARCHITECTURE OF MULTISENSORY COLLICULAR NEURONS AND ITS EFFECTS ON MULTISENSORY INTEGRATION

This chapter has been submitted to the Journal "Neuroscience" as: ***Ghose D and Wallace MT.*** *Heterogeneity in the spatial receptive field architecture of multisensory collicular neurons and its effects on multisensory integration.*

Introduction

Multisensory integration refers to the process by which information from the different senses converges and is synthesized in the brain, often resulting in dramatic changes for behavior and perception (Calvert et al., 2000, Stein and Stanford, 2008; Stein BE 2012; Murray and Wallace 2012). The neural underpinnings of multisensory integration have been widely studied, with much of the work being carried out in the mammalian superior colliculus (SC) (Meredith and Stein, 1983, 1986b, a, Meredith et al., 1987, Meredith and Stein, 1996, Perrault et al., 2003, 2005), a major convergence site for visual, auditory and somatosensory information. Seminal studies characterizing the responses of individual SC neurons showed that they integrate their different sensory inputs based on a number of factors, the most important of which appeared to be founded on the physical characteristics of the stimuli that are combined (Meredith and

Stein, 1986b, a, Meredith et al., 1987, Meredith and Stein, 1996).From this work three key “principles” of multisensory integration were identified. The spatial and temporal principles highlight the importance of physical and temporal stimulus proximity, such that stimuli that are spatially and temporally coincident typically give rise to the greatest response gains when combined. The principle of inverse effectiveness reflects the fact that the greatest proportionate gains in response are typically seen when stimuli that are weakly effective in eliciting a response on their own are combined (Meredith and Stein, 1986b, a, Meredith et al., 1987, Meredith and Stein, 1996).Although initially established in individual SC neurons, these principles appear to provide a universal framework for understanding multisensory interactions, in that they have also been shown to apply to multisensory neurons in other brain regions, to behavioral, psychophysical and perceptual phenomena, and in neuroimaging studies indexing the activity of large neuronal ensembles (Wallace et al., 1992, Bushara et al., 2001, Murray et al., 2001, Molholm et al., 2002, Hairston et al., 2003a, Hairston et al., 2003b, Macaluso et al., 2004, Bolognini et al., 2005, Kayser et al., 2005, 2007, Serino et al., 2007a, Serino et al., 2007b, Mozolic et al., 2008, Stevenson and James, 2009; Murray and Wallace 2012)

However, despite the fact that these principles have provided extraordinary insight, they are not the only factors that affect the integrative operations that characterize multisensory neurons and networks. Along these lines, recent work has begun to suggest that there is interdependency between the various stimulus dependent factors that shape the final integrated response (Perrault et al., 2005, Carriere et al., 2008, Royal et al., 2009). In addition, along with these stimulus-specific factors, other studies

have illustrated the importance of neuron-specific factors in dictating multisensory interactions, with neuronal responsiveness and dynamic range being previously underappreciated contributors (Perrault et al., 2003, 2005). Collectively, these studies have brought to light a previously unrecognized complexity to the factors that underlie multisensory integration in individual neurons, a complexity very likely to provide important mechanistic clues as to the cellular operations that result in the ultimate product of a multisensory interaction.

These prior studies provide the framework for the hypothesis that motivated the current study: that the location of a paired audiovisual stimulus within the receptive fields of SC neurons will dramatically alter neuronal responsiveness – with a consequent effect on the magnitude of the resultant interaction. To address this question, physically identical stimuli were presented at multiple locations within the receptive fields of individual neurons during single unit extracellular recordings, thus resulting in the creation of spatial receptive field (SRF) plots that details how changes in stimulus location impact response strength. These SRFs were then used to provide the predictive framework for the responses generated by various multisensory stimulus combinations, and comparison with these predictions revealed the nature of the integrative response (e.g., superadditive, subadditive, etc.). The results revealed that SC neurons exhibit significant heterogeneity in their SRFs, and that this heterogeneity played a key deterministic role in the magnitude of the resultant interaction.

Methods

General procedures: Experiments were conducted in adult cats (n=3) raised under standard housing conditions. All experiments were done in an anesthetized and paralyzed semichronic preparation. The experiments consisted of single unit extracellular recordings from the superior colliculus (SC) in the midbrain. Experiments were performed on a weekly basis on each animal. All surgical and recording procedures were performed in compliance with the Guide for the Care and Use of Laboratory Animals and under a protocol approved by the Institutional Animal Care and Use Committee at Vanderbilt University Medical Center, which is accredited by the American Association for Accreditation of Laboratory Animal Care.

Implantation and recording procedures: For anesthesia during the initial surgical procedure animals were first induced with ketamine hydrochloride (20 mg/kg, administered intramuscularly(im)) and acepromazine maleate (0.04mg/kg im). For implantation of the recording chamber over the SC animals were intubated and artificially respired. A stable plane of surgical anesthesia was achieved using inhalation isoflurane (1%-3%). Body temperature, expiratory CO2, blood pressure and heart rate were continuously monitored (VSM7, Vetspecs/SCIL), recorded and maintained within ranges consistent with a deep and stable plane of anesthesia. A craniotomy was made to allow access to SC and a head holder was attached to the cranium using stainless steel screws and orthopedic cement to hold the animal during recording sessions

without obstructing the face and ears. Postoperative care (antibiotics and analgesics) was done in close consultation with veterinary staff.

For recording animals were administered an initial dose of ketamine (20mg/kg im) and acepromazine maleate (0.04mg/kg im) and maintained throughout the procedure with constant rate infusion of ketamine (5mg/kg/hr iv) delivered through a cannula placed in the saphenous vein. The head holding system was then used to suspend the animal comfortably in the recumbent position. To prevent ocular drift animals were paralyzed using pancuronium or vecuronium bromide (0.1mg/kg/hr, iv for pancuronium bromide and 0.1-0.2mg/kg/hr for vecuronium bromide) and artificially respired for the duration of recording. Parylene insulated tungsten electrodes (Z = 3-5 MΩ) were advanced into the SC using an electronically controlled mechanical microdrive. Single unit neural activity (Signal to noise ratio >= 3:1) was recorded (Sort Client software, Plexon Inc., Texas), amplified and routed to an oscilloscope, audio monitor and computer for performing online and offline analysis. On the completion of the recording session the animals were given 60-100 ml of lactated Ringer solution subcutaneously to facilitate recovery.

Stimulus presentation and search strategy: Extracellular single unit recordings targeted multisensory (visual-auditory) neurons in the intermediate and deep layers of the SC. A multisensory neuron was defined as one in which the response in the multisensory condition (mean spikes/trial) was statistically different from the best unisensory response as determined by the Wilcoxon Rank test. Neurons were defined as “overt multisensory neurons” if they showed a change in spiking to both the visual and auditory stimuli when presented individually. In contrast, “modulatory multisensory neurons” showed an overt response to stimulation in one of the modalities, and this

response was altered by presentation of a stimulus in the second modality. Once a neuron was isolated (SNR $\geq$ 3:1), the borders of its receptive field were coarsely mapped by presenting visual and auditory stimuli. Visual stimuli consisted of the illumination of stationary light emitting diodes (LEDs; 100 ms duration, luminance 104 cd/m^2) while auditory stimuli were delivered through positionable speakers and consisted of 100 ms duration broadband noise (20Hz-20kHz) with an intensity of 67dB SPL on a background of 45 dB SPL. Both the LEDs and speakers were mounted on a hoop placed 60 cm in front of the cat at azimuthal locations ranging from 0° to 90° (10° increments) on either side of the midline. The hoop could be rotated along different elevations that allowed sampling numerous locations within and just outside the receptive field. Stimuli and stimulus combinations were randomly presented at different azimuthal locations along a given elevation. This procedure allowed the spatial receptive field (SRF) architecture of the neuron to be defined (Fig. 2-1). Visual and auditory stimuli were presented in a randomized interleaved manner at multiple azimuthal locations along a single elevation at a time. Multisensory combinations always consisted of visual and auditory stimuli being presented at the same spatial location. Unisensory and multisensory stimulus conditions were randomly interleaved until a minimum of 60 trials (20 visual, 20 auditory, 20 multisensory) were collected for a given stimulus location. Consecutive stimulus presentations were separated by at least 1.5 s to avoid response habituation.

During each recording session, after the boundaries of each neuron's receptive fields were mapped, a location of robust responsiveness was chosen within the spatial receptive field and this location was tested using 6 different stimulus onset asynchronies

(SOAs). These included the combinations: V50A0, V0A0, V0A50, V0A100, V0A150 and V0A200 where V50A0 represents the auditory stimulus preceding the visual stimulus by 50ms, V0A0 represents simultaneous presentation of visual and auditory stimuli, and V0A50, V0A100, V0A150, V0A200 represents conditions in which the visual stimulus preceded the auditory stimulus. Based on this preliminary testing the SOA that optimized the opportunity for multisensory interactions was used to test all other locations for that neuron.

Data acquisition and analysis: A custom built PC-based real time data acquisition system controlled the structure of the trials and the timing of the stimulus (Labview. National Instruments). The analog waveform picked up by the electrode was transferred to a Plexon MAP system (Plexon Inc.,Texas) where they were digitized at 40kHz. Single units were isolated online using Sort Client software (Plexon Inc., Texas) and also stored for further offline analysis. Neuronal responses were detailed through construction of peristimulus time histograms (PSTHs) for each condition (visual only (V), auditory only (A), paired visual-auditory (VA)) for each location tested within the SRF. Baseline for each PSTH was calculated as mean firing rate during the 500 ms immediately preceding the stimulus onset for each of the 3 conditions. Response threshold was set at 2 SD above this baseline in order to delimit the stimulus evoked response. The time at which the PSTH crossed above the 2 SD line (and remained so for at least 30ms) was determined to be response onset. Response offset was the latest time at which the PSTH fell below the 2SD line and stayed below this line for >=30ms. Response duration was defined as time interval between response onset and response offset. Mean stimulus evoked response was calculated as the average number of spikes

elicited per trial during the defined response duration interval. Mean spontaneous firing rate was subtracted from the response.

Spatial Receptive Field (SRF) analyses: To create the SRF plots, the mean stimulus evoked firing rates are normalized to the highest stimulus evoked response recorded from all tested conditions and locations. This procedure resulted in response values ranging from 0 to 1, which was then used to produce pseudo color spatial receptive field (SRF) plots that show relative activity as a function of stimulus location. SRF plots were created for each of the unisensory conditions (visual and auditory) and for the multisensory condition. In addition, a predicted SRF plot was created by summing the visual and auditory SRFs. The predicted SRF was then subtracted from the actual multisensory SRF to generate a contrast plot. In this contrast plot the warmer colors represent superadditive interactions while the cooler colors represent subadditive interactions (Carriere et al., 2008). To help better visualize these SRF plots, the SRF structure was then interpolated using a 2D gaussian filter (filter size=100, resize factor=100).

Spatiotemporal Receptive Field (STRF) analyses*:* For these STRF plots, pseudo color representations were created for each neuron by normalizing the spikes generated in the epoch spanning from 100ms prestimulus to 200ms poststimulus across all azimuthal locations, all conditions (visual, auditory, multisensory and predicted), and for each tested elevation separately. The predicted STRF obtained by summing the visual and auditory STRFs was then subtracted from the actual multisensory STRF to produce the contrast STRF. In the contrast STRF warmer colors represent superadditive interactions while cooler colors represent subadditive interactions. The contrast plots

are scaled from -1 to 1 where statistically significant negative values are sub-additive interactions and statistically significant positive values are superadditive interactions.

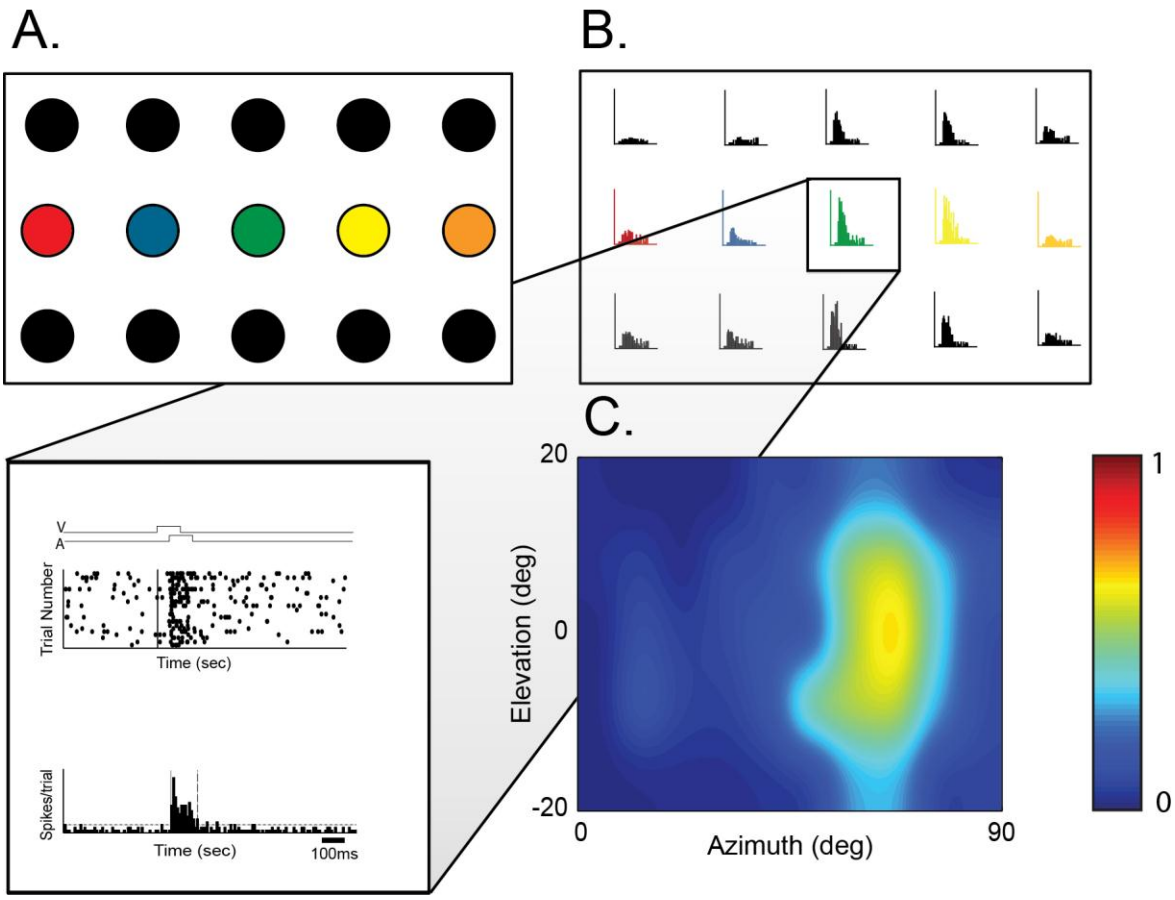

Figure 2-1. The construction of spatial receptive field (SRF) plots.

A. The schematic depicts multiple locations within the spatial receptive field of a neuron. The dots are color coded to represent different azimuths in a single elevation. The top and bottom rows represent an upper and lower elevation, respectively. **B.** Exemplar single unit activity (SUA) recorded at each of the tested locations, depicted as peristimulus time histograms (PSTHs). The inset shows a representative multisensory response at a single location. Stimulus onset and offset [visual (V), auditory (A)] is depicted by square waves on the top. Below the stimulus representation is a raster plot in which each dot represents an action potential and each row of dots represents a single trial. The solid vertical line marks stimulus onset. Shown below the rasters is the PSTH for this location. The dashed horizontal line represents the threshold criterion for response (2SD above the baseline), the solid vertical line represents response onset and the dotted vertical line represents response offset. **C**. The evoked response is then normalized across all locations and all conditions to produce a response continuum from 0 to 1 where 0 represents no response and 1 represents the maximum response. This is then represented as a pseudo

color SRF plot in which warmer colors represent greater response magnitudes and cooler colors represent lower response magnitudes.

Measures for evaluating multisensory integration: Two measures were used to quantify multisensory integration. The first was the interactive index (ii), which measures how the multisensory response differs from the best unisensory response. The magnitude of this change was calculated as

$$[(CM - SMmax)/SMmax)] X100 = \% \text{ interaction}$$

where CM is the mean response evoked by the combined modality (i.e., multisensory) stimulus and SMmax is the mean response evoked by the most effective single modality stimulus (Meredith and Stein, 1983, 1986b). Statistical comparisons between the mean stimulus evoked responses of the multisensory and best unisensory conditions were done using a Wilcoxon Rank test for each spatial location tested within the receptive field. The second measure used is mean statistical contrast (msc). This metric evaluates the multisensory response as a function of the response predicted by the addition of the two unisensory responses. Multisensory contrast is calculated using the formula

$$msc = \frac{\sum AV_i - (A_i + V_i)}{n}$$

where, A_i is the evoked auditory response on a given trial (i), V_i is the evoked visual response on a given trial, AV_i is the evoked multisensory response on a given trial and n is the number of trials. The model assumes independence between the visual and auditory inputs and uses additive factors logic to distinguish between subadditive

(contrast < 0), additive (contrast = 0) and superadditive (contrast > 0) modes of response (Perrault et al., 2003, 2005, Stanford et al., 2005, Stanford and Stein, 2007). Significant differences from a contrast value of 0 were determined by the Wilcoxon Rank test for each location.

Analyses of SRF "hotspots": After neuronal responses were collected across different locations in order to derive the SRF plots, the mean stimulus evoked spike counts were then normalized across all locations and all conditions. For each condition, all locations exhibiting at least 70% of the maximum response were considered to be within the hotspot of the receptive field. Moreover, two locations exhibiting >70% of maximum response had to be separated by a minimum of 10° in either elevation or azimuth in order to be considered as separate hotspots.

In order to determine the degree of overlap between the visual and auditory hotspots, the area of the hotspots was first computed for both the visual and auditory SRF. Next, the modality that exhibited the smaller hotspot was chosen, and the amount of the total area of that hotspot that overlapped with the hotspot of the other modality was expressed as a percentage of its total area. For example if the area of the visual hotspot was 100 deg^2 of which only 10 deg^2 overlapped with the auditory hotspot, the percentage of overlap was 10%.

Results

The spatial receptive fields (SRFs) of multisensory superior colliculus neurons are large and heterogeneous

Data was collected from 72 multisensory (visual-auditory) neurons in the intermediate and deep SC layers of 3 adult cats. A detailed mapping of each of the SRFs (i.e., visual, auditory and visual-auditory) was possible for 64 of these neurons, which often entailed isolation of the neuron for periods of several hours. In accordance with the previous literature (Meredith and Stein, 1983, Stein BE 1993, Kadunce et al., 2001; Meredith and Stein 1996;Meredith and Stein 1986; Meredith and Stein 1990; Stein BE 1993), the majority of these multisensory neurons demonstrated considerable overlap in the spatial extent of their visual and auditory receptive fields.

Following a coarse delimitation of a neuron's receptive fields, an SRF plot for each modality was then created using physically identical stimuli that differed only in spatial location. These analyses revealed significant differences in both the unisensory (i.e., visual alone, auditory alone) and multisensory (combined visual-auditory) responses as a function of stimulus location within the SRF. Figure 2-2 illustrates several representative examples of these SRF plots for individual SC neurons.

For practical purposes, SC neurons were divided into two general classes: overt neurons and modulatory neurons. Overt neurons are responsive to stimulation in both the visual and auditory modalities, whereas in modulatory neurons responses can be

driven by only one modality yet have this driven response significantly influenced when a stimulus from the other modality is presented at or around the same time.

For overt neurons, the visual (26/33=78.8%), auditory (15/33=45.5%), and multisensory (22/33=66.7%) SRFs were characterized by a single region of elevated response (single hotspot) surrounded by regions of weaker response (see methods for a description of how the hotspots were defined and delineated; Fig. 2-2A). In the remaining overt neurons the SRF architecture was more complex, with multiple regions of elevated responses (multiple hotspots) (Fig. 2-2B).

For modulatory neurons (which could either be visual modulatory (23/31=74.2%) or auditory modulatory (8/31=25.8%) depending on the driving modality), the pattern of results was very similar. The majority of auditory modulatory neurons (6/8=75%) exhibited single hotspots under both auditory and multisensory conditions while the remainder exhibited multiple hotspots under both these conditions. Similarly, the vast majority of the visual modulatory neurons (21/23=91.3%) exhibited single hotspots under both visual and multisensory conditions. The other two neurons exhibited multiple hotspots under both these conditions . Figure 2-3A shows the population distribution for these SRFs divided into single and multiple hotspots for both overt and modulatory neurons.

A more detailed analysis of these SRFs revealed that there was a considerable degree of overlap between the visual and auditory receptive fields in overt neurons (such extent could not be examined in modulatory neurons because of their lack of a driven response in two modalities). Thus, for the large majority of these overt neurons

(23/33 = 70%), there was almost complete overlap (i.e., >90%) between the visual and auditory hotspots (Fig 2-3B).There were no apparent differences (e.g., location in SC, SRF size) between neurons that showed greater and lesser correspondence in these unisensory hotspots.

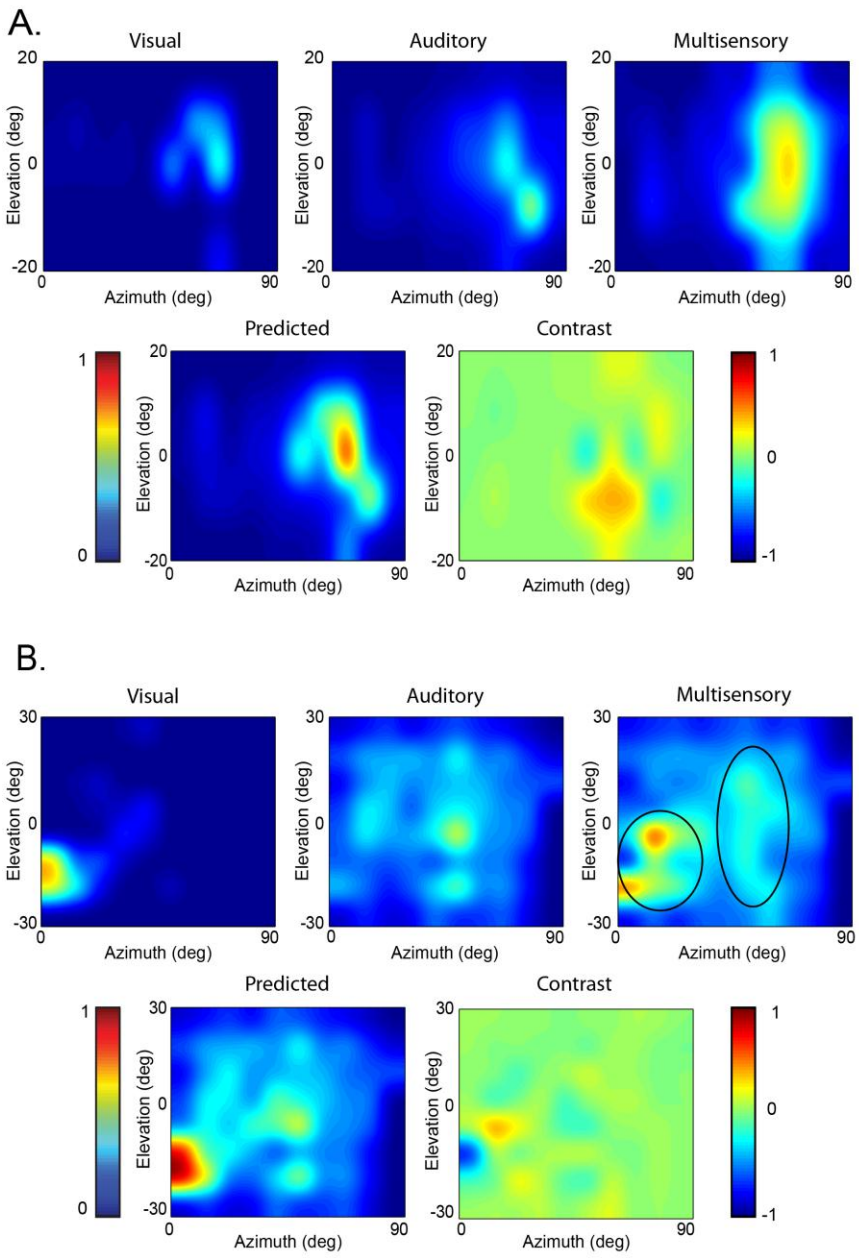

Figure 2-2: SRF plots for a pair of representative SC neurons.

A. Shown on the top row is responses to the visual, auditory and multisensory conditions. In each of these conditions, the neuronal response changes as a function of stimulus location within the receptive field. This neuron exhibits a single hotspot in the multisensory condition. Shown on the bottom row is the predicted multisensory response based on additive factors logic, as well as a contrast plot showing how the actual multisensory response differs from the predicted response. Note the regions of superadditivity (warmer colors) and subadditivity (cooler colors) in this representation. **B**. Representative example of a second multisensory neuron showing a more complex SRF architecture with multiple hotspots in the multisensory condition (highlighted by the circles). As for the neuron represented in A, the contrast plot highlights that the multisensory SRF differs substantially from the predicted SRF.

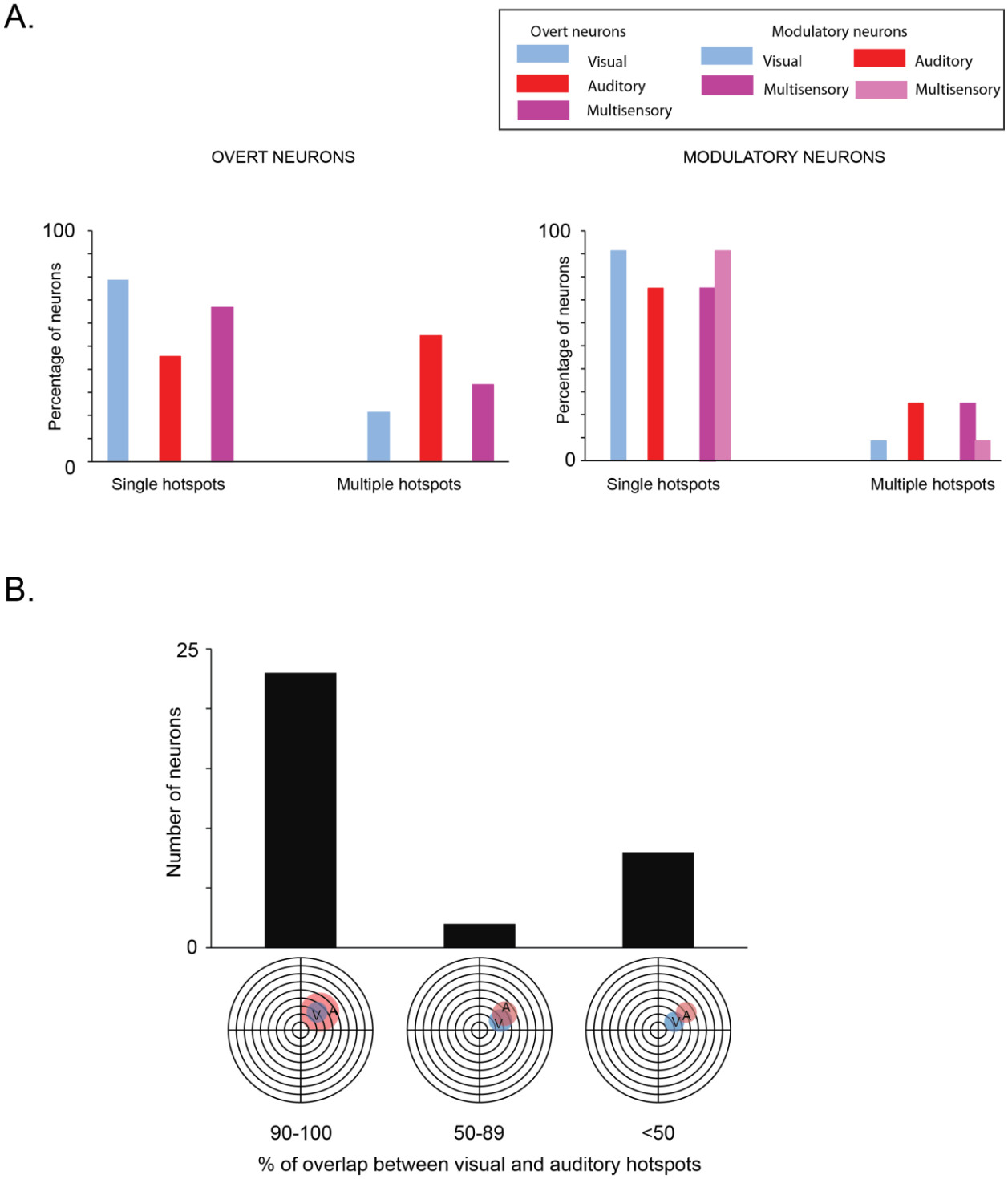

Figure 2-3. Characteristics of Spatial Receptive Fields

A. Percentage of neurons exhibiting single or multiple hotspots for the unisensory (visual alone, auditory alone) and multisensory conditions for overt and modulatory neurons(visual and auditory). **B.** Frequency distribution of the area of overlap (in %) between the visual and auditory hotspots for multisensory SC neurons. A visual depiction of the overlap is shown along the x axis.

In neurons with single hotspots, the total area of the visual hotspot was significantly smaller (mean area = 32.5 deg^2) when compared with the size of the auditory (mean area = 81.7 deg^2) and multisensory (mean area = 101.7 deg^2) hotspots (visual vs. auditory: Student t test , t=-2.20,p=0.03, visual vs multisensory : Student t test: t=-2.06, p=0.05). The size of the auditory and multisensory hotspots were not significantly different (Student t test t=0.89, p=.388).

Despite this similarity in size of the auditory and multisensory hotspots, response levels differed significantly between conditions. For neurons with single hotspots, when expressed as normalized values (in order to be able to compare across neurons), response magnitude within the multisensory hotspots was highest (0.94), followed by visual (0.65) and then auditory (0.33). Each of these values differed significantly from the other (Student t test: V vs VA: t=-3.12,p<0.01, A vs VA: t=-7.3, p<0.01, V vs A: t=2.83,p<0.01).

Similarly 86% of the neurons with multiple hotspots in either the visual or auditory SRFs, also exhibited multiple hotspots within their multisensory SRFs. For these neurons with multiple hotspots, the size of the largest hotspots was compared. This analysis revealed that area of the auditory hotspots were largest compared to that of visual and multisensory hotspots but the differences were not statistically significant(mean area of auditory hotspot =83.7deg^2 ; mean area of visual hotspot =34.3deg^2; mean area of multisensory hotspot =70deg^2 ;Student t test: V vs A: t=-1.59,p=0.13 V vs VA = t=-0.69; p=0.49; A vs VA: t=0.25, p=0.8). However, when strength of responses were compared it was found that the multisensory responses were strongest (mean =0.93) followed by visual (0.65) and auditory responses (0.39).

All these differences were statistically significant. (Student t test: V vs VA: t=-2.99, p<0.01, A vs VA: t=-8.31 p<0.01,V vs A: t=-2.95 p<0.01)

For modulatory neurons (visual and auditory), 87.1% (27/31) of the neurons exhibited single hotspots under both unisensory and multisensory conditions. In contrast to the overt neurons, the area of the visual (mean area=33.5 deg^2) and multisensory (mean area =36.5 deg^2) hotspots for the visual modulatory neurons (visual stimulus being the driving modality) were not significantly different (Student t test: t=-0.35, p=0.72). Similarly, for auditory modulatory neurons, the area of the auditory (mean area= 134.2 deg^2) and multisensory (mean area =144.2deg^2) hotspots were not significantly different (Student t test: t=-0.2, p=0.84). In contrast to the data for overt neurons, for visual modulatory neurons, the strength of responses within the visual (mean normalized response= 0.96) and multisensory (mean normalized response=0.85) hotspots were not significantly different from each other (Student t test: t =1.7, p=0.08). However, for auditory modulatory neurons, the response strength of multisensory hotspots (0.98) was significantly higher than that of auditory hotspots (mean normalized response =0.94; Student t test: t=-2.2, p=0.03).

The architecture of the visual and auditory SRFs was next used to provide a prediction of the multisensory SRF based on a simple summation of the unisensory SRFs. In virtually all neurons, the measured multisensory SRF differed significantly from the predicted multisensory SRF, as evident by the contrast plots that compared these measured and modeled responses (Fig. 2-2). When compared to the size of the best unisensory SRFs, the mean size of the multisensory SRFs were 14.6% larger for overt

neurons For modulatory neurons the mean size of the multisensory SRFs were 11% larger than that of the best unisensory SRFs.

As described in the sections above, by quantifying the total size of the SRFs, the size of the hotspots, and the strength of response at the hotspots under different stimulus conditions for both overt and modulatory neurons, an important difference emerged between the two neuronal classes. The total size of the SRFs as well as the size of the hotspots under visual and auditory conditions did not differ when compared between overt and modulatory neurons (SRF sizes: Student t test: visual: $t=1.64$, $p=0.1$; auditory: $t=1.07$, $p=0.2$) (Hotspot sizes: Student t test: visual: $t=0.13$, $p=0.89$; auditory: $t=-1.2$, $p=0.2$). However, the strength of the responses within the hotspots were significantly larger for modulatory neurons than for overt neurons under both visual and auditory conditions (visual: Student t test: $t=-4.38$, $p<0.01$, auditory: Student t test: $t=-6.4$, $p<0.01$). This suggests that the modulatory neurons that are dominated by one sensory modality exhibit higher sensory responsiveness to that dominant modality when compared to overt neurons. This is important for the differences in the nature of multisensory interactions exhibited by these two groups of neurons as described in detail later.

For both overt and modulatory neurons, the most dramatic difference was not in the size of the multisensory SRF, but rather in the magnitude of the responses elicited under multisensory conditions when compared with those predicted from the component unisensory responses.

Relationship between SRF heterogeneity and multisensory interactions

An analysis of the SRF plots revealed that multisensory interactions differed dramatically from location-to-location (Fig. 2-4-2-5). For the overt neuron represented in figure 2-4, pairings of visual and auditory stimuli at locations within the SRFs where the individual responses are weak (circle and asterisk) resulted in significant multisensory enhancements. In contrast, pairings of these stimuli at locations that showed robust auditory responses (triangle) resulted in no significant interactions. These differences are further reinforced by the contrast plot that compares the multisensory responses to the predicted additive model. Here it can be seen that significant superadditive interactions accompany the pairing of weakly effective stimuli, whereas the interaction is purely additive at the location in which responses to the auditory stimulus is robust. For the modulatory neuron depicted in figure 2-5, despite the qualitative differences in this neuron from the overt neuron represented in figure 4, the influence of SRF architecture on the nature of the multisensory interactions was very similar. Thus, whereas stimulus pairings at locations within the SRF that showed weak auditory responses (triangle) resulted in a significant superadditive response enhancement, pairings at highly effective locations resulted in significant subadditive interactions (circle and asterisk). Collectively, these single neuron examples are highly representative of the behavior of the entire neuronal population, and underscore the conclusion that multisensory interactions are critically dependent on the effectiveness of stimuli at different locations within the SRF.

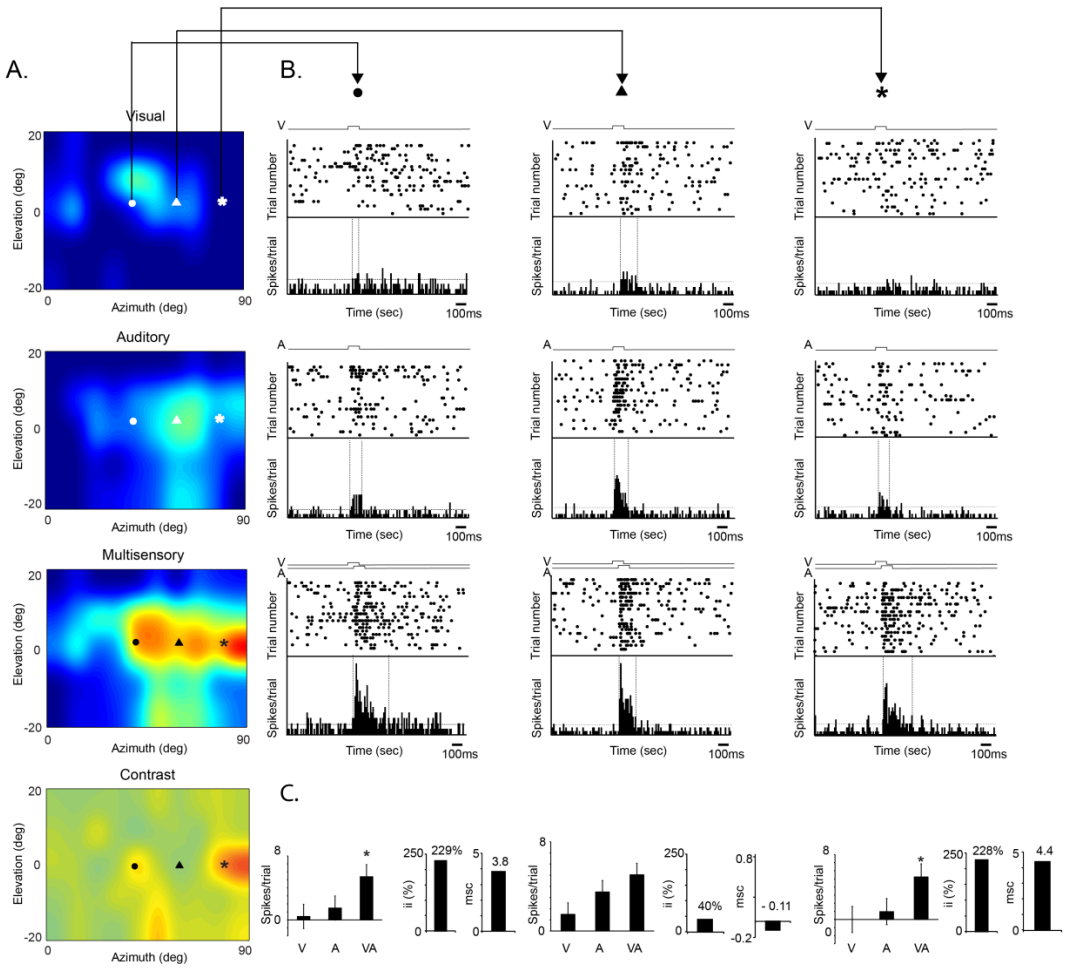

Figure 2-4. Influence of Spatial Receptive Field architecture on nature of multisensory interactions

A. Visual, auditory and multisensory SRF plotted for a representative multisensory SC neuron with overt responses to both visual and auditory stimuli. Symbols (circle, triangle, star) depict 3 locations within the SRF where visual and auditory stimuli were delivered individually (in the unisensory conditions) and in combination (for the multisensory condition). The contrast plot at the bottom is obtained by subtracting the predicted SRF (V+A) from the multisensory SRF (VA). **B.** Rasters and PSTHs show this neuron's response at each of the 3 locations (represented by symbols) in each of the 3 stimulus conditions represented in the top, middle and bottom panels. Bar graphs illustrating the mean visual, auditory and multisensory response for each location and the magnitude of multisensory interaction as calculated using both interactive index (ii) and multisensory contrast (msc). Asterisks represent statistically significant ($p<0.05$) changes in the multisensory condition. Note that despite the physical characteristics of the stimulus being identical, the responses are dramatically different for each of the different locations. Note also that the nature of the multisensory interactions differed dramatically from location-to-location. Whereas locations with lower visual and auditory responses (circle and star panels) show large superadditive interactions, locations with high visual and auditory responses (triangle panel) shows no significant interaction.

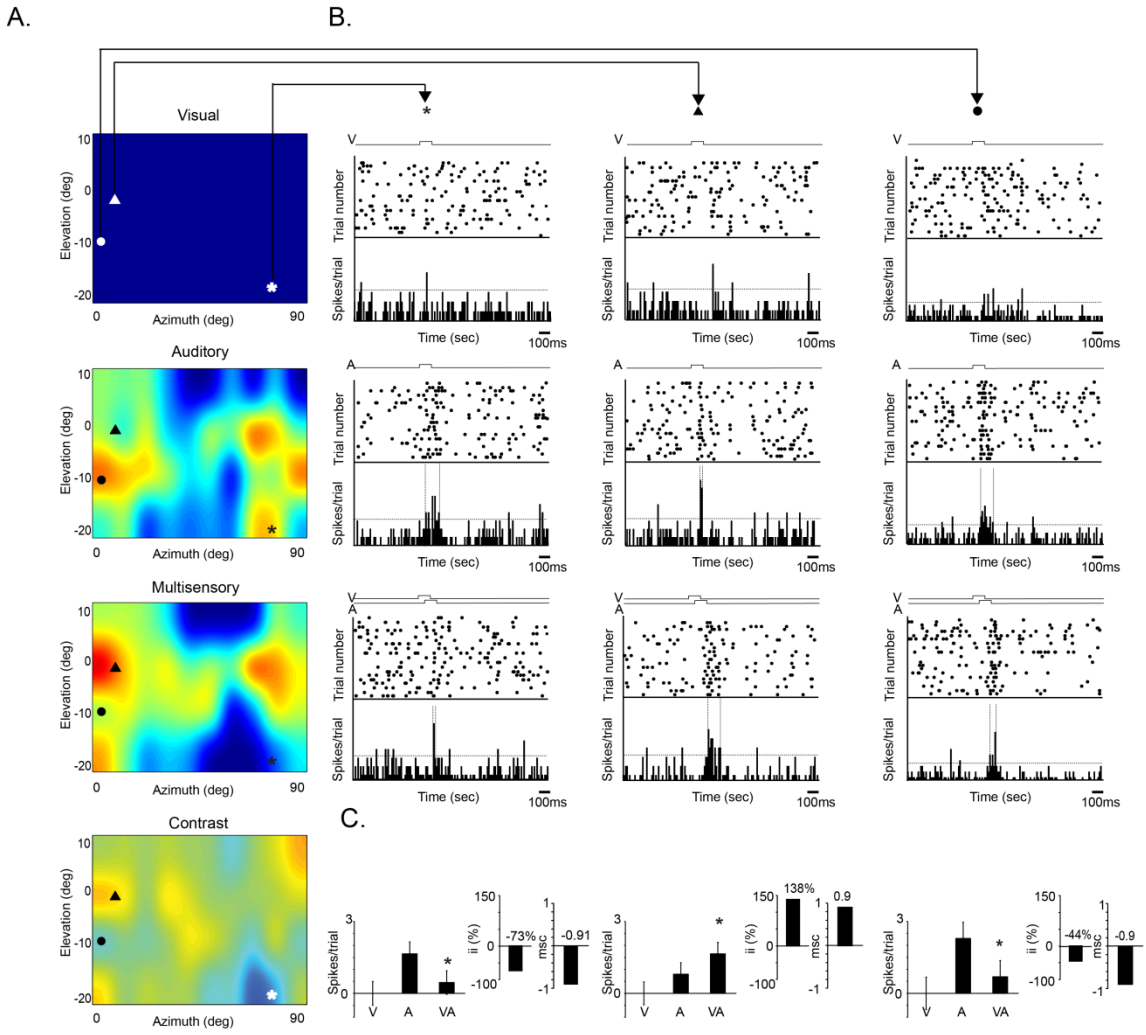

Figure 2-5. A second example of the influence of spatial receptive field architecture on the nature of multisensory interactions.

Conventions are identical to those for Fig 2-4. Note that this neuron is an example from the modulatory class, in which no frank response to the visual stimulus is evident. Nonetheless, the visual stimulus had the ability to modulate responses to the auditory stimulus. Note also the more complex and heterogeneous SRF architecture of this neuron. Nonetheless, the same general guidelines evident for the neuron shown in Fig 2-4 are evident here, with weakly responsive regions of the SRF being where the largest multisensory interactions are seen.

Inverse effectiveness forms the basis of spatial influences on multisensory interactions

The data illustrated in figures 2-4 and 2-5 strongly suggest that the magnitude of the unisensory response (i.e., stimulus effectiveness) plays an integral role in the degree of gain seen in the resultant multisensory interaction, and that spatial location *per se* is a less important determinant of these interactions. To reinforce the role of effectiveness in multisensory gain (i.e., interactive magnitude), an analysis of all of the tested interactions was conducted. For the overt neurons (n=33) a total of 1843 locations were tested, of which 46.0% (843/1843) exhibited statistically significant interactions. In contrast, for modulatory neurons (n=31), a total of 985 receptive field locations were tested, of which only 27.2% (268/985) exhibited significant multisensory interactions. This difference between overt and modulatory neurons was highly significant (Chi Square test : Chisquare=92.4, $p<0.01$).

In addition to this difference in the incidence of integration within the SRF for overt and modulatory neurons, substantial differences were noted in the magnitude of integration for these two populations. For both, a significant negative correlation was found between the best unisensory response and the amount of multisensory integration as quantified by interactive index (overt neurons $R = -0.3568$, $p<0.0001$; modulatory neurons $R = -0.2773$, $p<0.0001$) (Fig2-6 A and B left panel). However, overt neurons exhibited a greater degree of multisensory gain when compared with modulatory neurons (overt neurons mean ii = 102.4%; modulatory neurons mean ii = 74.0%). This difference was statistically significant (Student t test : $t=-3.73$, $p<0.01$).

Furthermore, and likely contributing to this difference, the percentage of receptive field locations exhibiting significant response depressions was much more frequent for modulatory neurons (39.5%) compared to that of overt neurons (15.1%). Thus, this population data is in keeping with the hypothesis that the principle of inverse effectiveness forms the predictive framework for the changes in multisensory integration that take place as a function of changes in stimulus location within the SRFs of SC multisensory neurons.

Along with an analysis of interactive magnitude, which plots gain (or loss) as a function of the best unisensory response, we also conducted parallel analyses to quantify responses relative to an additive model measured by the mean statistical contrast (msc) measure. In this framework, both unisensory responses contribute to the predicted multisensory responses, and these multisensory responses can be characterized as superadditive, additive or subadditive. Analyzed in this way, for overt neurons the majority of the significant interactions were superadditive (488/630 = 76.1%) with the remainder being subadditive in nature. In addition to these significant interactions, a substantial number of the multisensory responses were purely additive in nature (213/843 = 25.2%).

For modulatory neurons, only superadditive (162/268=or 60.5%) or subadditive (106/268or 39.5%) were in evidence (since these neurons were only driven by one modality), with the percentage of subadditive interactions being higher in these neurons than in overt neurons(Overt vs modulatory: ChiSquare Test : Chisquare=27.2, $p<0.01$) (Fig 2-6B right panel)

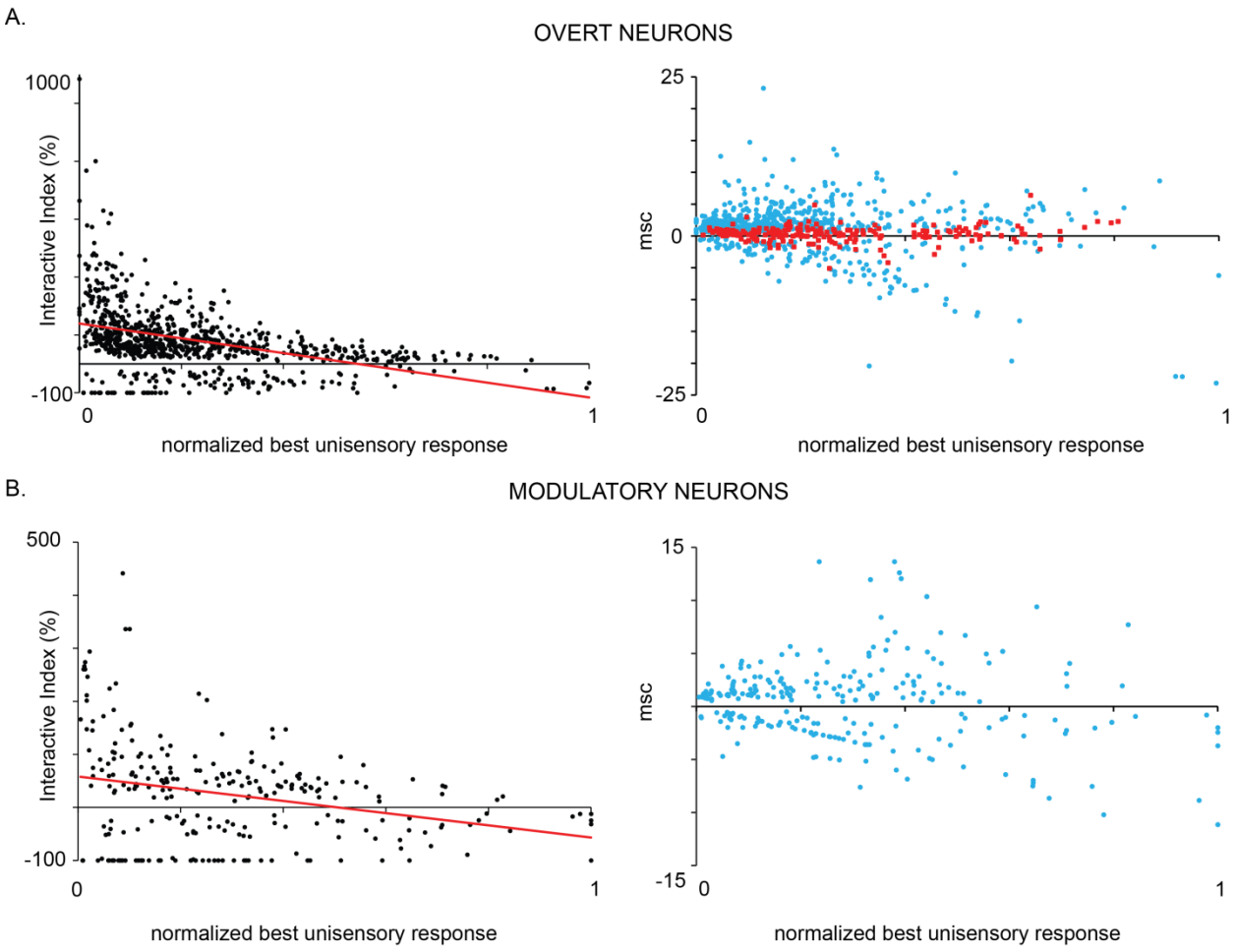

Figure 2-6. Principle of Inverse Effectiveness: Interactive Index and mean statistical contrast as a function of best unisensory response

A.Population data for all 33 overt multisensory neurons recorded from the intermediate/ deep layers of the SC and which plots statistically significant interactive index (ii) and mean statistical contrast (msc) as a function of the normalized best unisensory response. For ii, positive values signify response enhancements while negative values signify response depressions. The red line represents the trend of the dataset represented by the equation y=-255.01x + 139.19.For msc, the blue circles represent superadditive and subadditive interactions while the red circles represent additive interactions. B. Population data for all 31 modulatory multisensory neurons recorded from the intermediate/ deep layers of the SC and which plots statistically significant interactive index (ii) and mean statistical contrast (msc) as a function of the normalized best unisensory response. For ii, positive values signify response enhancements while negative values signify response depressions. The red line represents the trend of the dataset represented by the equation y=-114.89x + 58.093. For msc, the blue circles represent superadditive and subadditive interactions.By definition, modulatory neurons do not exhibit additive interactions.

SRFs represent two spatial dimensions of the complex spatiotemporal receptive fields (STRFs) that characterize SC neurons

In addition to examining how spatial location influences the entire epoch of response for SC neurons, we were also interested in testing how different spatial locations influence the temporal profile of the unisensory and multisensory responses. Hence, in a subset of the neurons (n=15) in which a complete set of SRFs was derived, the temporal response profile of the neuron as a function of changes in one spatial dimension (i.e. azimuth) was examined. The partial multisensory spatiotemporal receptive field (STRF) plot derived in this manner again showed dramatic differences from that predicted based on the unisensory responses (fig. 2-7). Of greatest interest here is the temporal evolution of the multisensory response, which differed depending upon whether the stimuli were positioned within or outside of a SRF hotspot. For locations that are within these unisensory hotspots, interactions shifted from subadditive in the earliest phase of the response (when unisensory firing is robust) to superadditive in later response epochs (when unisensory firing is weaker). In contrast, for locations where unisensory responses were weak, the temporal evolution of the multisensory response is such that there is an initial period of superadditivity followed by subadditivity. Collectively, these temporally-based analyses reinforced the results of the spatially-based manipulation in highlighting responsiveness (i.e., effectiveness) as the key factor in dictating the magnitude of the multisensory interaction.

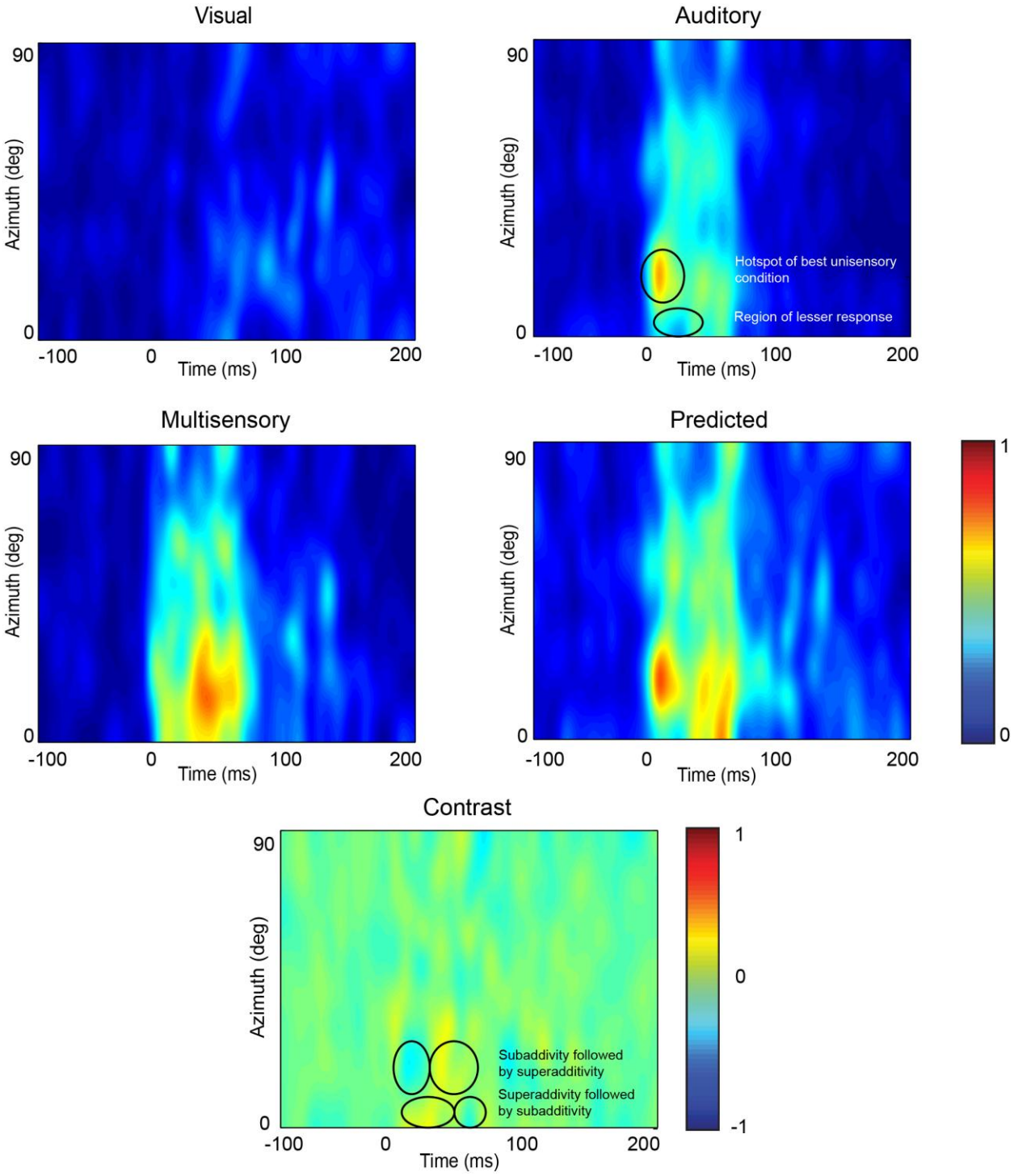

Figure 2-7. Spatiotemporal receptive field architecture of SC neurons

Example of a series of spatiotemporal receptive field (STRF) plots for a multisensory SC neuron. For these plots a single dimension of stimulus location (i.e., azimuth) is plotted on the y-axis and peristimulus time is plotted on the x-axis (stimulus onset = 0). Note that the temporal characteristics of the neuronal response changes as a function of both space and time for each of the different conditions. Once again note that the multisensory STRF differs considerably from the predicted STRF obtained by summing the

visual and auditory STRF, with the differences best highlighted in the contrast plot at the bottom. Here we see that the temporal dynamics of the response also play an important role in multisensory interactions, such that weakly responsive regions of the STRF are those in which the largest multisensory interactions are seen. The circles in the contrast plot highlight this for two azimuthal locations, and in which the temporal dynamics of the multisensory interaction follow the temporal dynamics of the unisensory response profiles.

Discussion

The current study represents the first to provide a more detailed characterization of the complex spatial receptive field architecture of superior colliculus multisensory neurons than has been previously carried out. The study illustrates that this architecture plays an important role in the multisensory interactions that characterize these neurons. Furthermore, the work shows that it is space's impact on sensory responsiveness that appears to be the most important factor in these interactions. Furthermore, we show the SRF architecture for two of the major multisensory neuron classes in the SC – overt and modulatory neurons, and highlight differences in the integrative features of these neuronal classes.

The heterogeneous nature of the receptive fields of SC multisensory neurons

Numerous previous studies have described the large receptive fields of multisensory neurons in the intermediate and deep layers of the superior colliculus (Meredith and Stein, 1990, Wallace and Stein, 1996, Wilkinson et al., 1996; Goldberg and Wurtz,1972; Gordon, 1973). In addition, several studies have hinted at the heterogeneity of these receptive fields, with differing responses to identical stimuli placed at different locations within the receptive field (Kadunce et al., 2001, Perrault et al., 2003, 2005, Krueger et

al., 2009, Royal et al., 2009; Meredith and Stein 1986; 1996). However, this heterogeneous nature for the receptive fields of SC multisensory neurons has not been systematically explored. In the current study we provide a more comprehensive (but far from complete) analysis to detail the complex architecture of these receptive fields, and show that these neurons can have spatial receptive fields with single or multiple hot spots.

Previous work on multisensory neurons of the cat SC suggests that there is a great degree of overlap between the visual and auditory receptive fields of these neurons (Meredith and Stein 1996; Meredith and Stein 1986; Stein and Meredith 1993). However, this overlap is far from complete, a result reinforced in the current study, and which may be the result of anesthesia-dependent effects or a lack of precise spatial coding in the large receptive fields of SC neurons (and which may be attributable to slight differences in input overlap). Such discrepancies between the visual and auditory receptive fields have been reported in previous studies as well (Meredith and Stein 1996; Gordon 1973; Rauschecker and Harris 1989). Since it is known that auditory receptive fields are influenced by pinnae position (Middlebrooks and Knudsen 1987), and since the pinnae sag inferolaterally during paralysis, the lateral displacement of auditory receptive fields may be a simple result of paralysis (Meredith and Stein 1996). However, it is also possible that these misalignments in certain neurons may reflect a more complex coding scheme for signaling dynamic multisensory stimuli. For example, azimuthal displacements in receptive fields may be important in signaling the direction and/or velocity of a stimulus moving along a specific trajectory. Regardless of the slight misregistry in some neurons, our current results show that this general feature of

receptive field overlap and spatial congruence extends to the hotspots of the receptive fields as well. Thus, for majority of neurons studied here, not only was there a good correspondence in the extent of the visual and auditory receptive fields, but there was also a considerable degree of alignment of the visual and auditory hotspots. Such an overlap is ideal to signal the spatial congruency of an audiovisual stimulus complex (as well as to code for incongruency), one of the key features of the mammalian SC for guiding accurate orientation movements of the eyes, ears, head and body (Sprague and Meikle 1965; Casagrande et al 1972; Harting et al 1973; Stein et al 1976a).

This type of complex receptive field architecture is not uncommon in sensory systems. Indeed, even in the superficial layers of the SC, where receptive fields are substantially smaller in size when compared with the deeper layers, receptive field heterogeneity has been described and implicated in the coding of visual motion and direction (Dreher and Hoffmann, 1973). In addition, and very consistent with the findings of the current study, recent work reveals excitatory and inhibitory domains within the visual receptive fields of neurons of the intermediate and deep layers of the SC in macaques (Churan et al., 2012). This architecture is speculated to play a role in target selection processes that ultimately give rise to oculomotor behaviors (i.e., gaze shifts).

Evidence from structures other than the SC also demonstrates that complex receptive field architecture is a common characteristic within sensory representations. Early work in the cat lateral geniculate nucleus illustrated a surprising complexity to the receptive fields of these neurons, a structure presumed to play a role in the spatial and temporal filtering processes carried out within the LGN (Stevens and Gerstein, 1976). Recent studies have also shown that the spatiotemporal architecture of LGN neurons may

contribute to orientation tuning (Soodak et al., 1987, Shou and Leventhal, 1989, Smith et al., 1990, Sillito et al., 1993, Sun et al., 2004, Naito et al., 2007, Suematsu et al., 2012). Similar studies conducted in thalamic and cortical somatosensory structures (i.e., VPM and SI) have elucidated complex spatiotemporal receptive field architecture for the constituent neurons (Simons, 1985, Simons and Carvell, 1989, Nicolelis et al., 1993a, b, Nicolelis and Chapin, 1994). Such receptive field architecture has been implicated to play a critical role in tactile discrimination and pattern recognition (Ghazanfar and Nicolelis, 1997, Shimegi et al., 1999, Ghazanfar and Nicolelis, 2001).

In each of these examples, the complex spatial architecture of these neuronal receptive fields appears integral for the coding of dynamic stimuli, in that this type of organization can provide meaningful information about stimulus direction and velocity (Hyvarinen and Poranen, 1978, Phillips et al., 1988, DiCarlo and Johnson, 2000). Indeed, with the addition of the temporal dimension (see discussion below), the spatiotemporal receptive field becomes a powerful tool for coding the salient details of a dynamic stimulus complex, an organization that maps well onto the role of the SC in guiding gaze shifts to stimuli of interest.

Spatial receptive field heterogeneity and its relevance for multisensory interactions

Although the receptive field architecture of multisensory SC neurons is quite complex, the consequences of this organization for multisensory integration appear to follow a simple mechanistic principle. Thus, for locations within the SRF in which unisensory responsiveness is weak, stimulus combinations typically result in large response

enhancements (i.e., multisensory gain that is frequently superadditive). Conversely, for locations within the SRF of high unisensory responsiveness, this gain is weak or absent (with corresponding additive or subadditive interactions). These data thus provide a compelling argument for the preeminence of inverse effectiveness as a core determinant of multisensory integration (Meredith and Stein, 1986b, a, 1996, Wallace and Stein, 1996), and relegate spatial location/proximity to a less important role. The reductionist nature of this finding has important mechanistic implications, in that it suggests a single overarching process that governs how multisensory neurons integrate their diverse sensory inputs. In addition to establishing the primacy of effectiveness (at least over space), these data also illustrate the extraordinary interdependency of the previously characterized “rules” or “principles” of multisensory integration (Meredith and Stein, 1983, 1986b, a, Meredith et al., 1987, Meredith and Stein, 1996, Wallace and Stein, 1996). In many respects such a concept is intuitive, in that changes in one of these factors (e.g., space) have a consequent impact on the others. However, since these rules were necessarily derived in isolation (by manipulating one variable at a time), the importance of the current study is in establishing the nature of this vital interdependency. Indeed, this interdependency seems to be true regardless of brain structure, in that it has been previously shown to apply to cortical multisensory neurons as well (Carriere et al., 2008).

Although the functional roles of this interdependency and the importance of effectiveness remain to be determined, they create an interesting local form of gain control that serve to increase the potential impact and functional relevance of weakly responsive regions of the unisensory SRFs.

Nature of integration within the SRF architecture of multisensory neurons

This study also shows that the nature of multisensory integration within the SRF of SC neurons differ depending on the type of multisensory neuron under study (overt vs modulatory). Thus, when compared with modulatory neurons, overt neurons exhibited more response enhancements and super additive interactions. Why such distinctions exist between these different neuronal types is not clear. One possibility is that modulatory neurons lack the synaptic drive necessary to support super-additive interactions. This seems unlikely given the inverse effectiveness observations described earlier. A second related possibility is that modulatory neurons receive their non-dominant modality inputs from the local processing architecture, and this local architecture is insufficient to support large interactions. Congruent with this explanation is prior work showing the multisensory integration in the SC, as evidenced in large super-additive response enhancements, is largely a result of convergent inputs from descending cortical sources (Wallace and Stein 1994). Finally, our results show that the strength of responses of modulatory neurons is significantly higher under unisensory conditions when compared to that of the overt neurons. Hence addition of a spatially coincident second modality stimulus may result in more frequent response depressions and subadditive interactions. Future work should be structured to examine in detail these intriguing differences in the integrative potential of overt vs. modulatory neurons..

Previous work shows that the underlying nature of the computations performed by SC multisensory neurons critically depends on the dynamic range of the individual neuron (Perrault et al 2005). Thus, neurons that show superadditive or superadditive/subadditive interactions have small dynamic ranges while neurons which

show additive and subadditive interactions have larger dynamic ranges. However, all of these earlier studies characterized the nature of integration in overt multisensory neurons only. To the best of our knowledge, this is the first study describing the nature of integration performed by modulatory multisensory neurons in the cat SC. Thus, in the light of our current results and based on previous findings it can be hypothesized that modulatory neurons, which exhibit many more subadditive interactions when compared to overt neurons, may have a wider dynamic range. However, this remains to be empirically tested.

Spatial receptive fields and their possible role in multisensory-mediated SC behaviors

The long standing role attributed to the SC has been in the detection and localization of a stimulus or stimulus complex and the subsequent production of an orientation response involving movements of the eyes, head and ears (Sprague and Meikle, 1965, Casagrande et al., 1972, Sprague, 1996). Prior work has shown that SC-mediated behaviors are facilitated under multisensory circumstances, with improvements being seen in both the speed and accuracy of responses (Stein et al., 1988, Hughes et al., 1994, Nozawa et al., 1994, Frens et al., 1995, Wilkinson et al., 1996, Jiang et al., 2002, Diederich and Colonius, 2004, Bell et al., 2005). The current study provides a more mechanistic view into this process, by illustrating ***how*** the complex receptive fields of SC neurons may contribute to these behavioral improvements. The most straightforward interpretation of these results is that the multisensory SRF serves as a "smoothing" filter, boosting gain for regions of weak response and thus equilibrating performance across space. Although an intriguing possibility, this interpretation requires

empirical validation by examining behavioral performance while recording the activity of SC multisensory neurons. Current work in the laboratory is exploring this linkage. A similar boosting of multisensory responses in regions of the receptive field that have weaker unisensory responses after pairing visual and auditory stimuli across space has been seen in auditory cortex of anesthetized ferret (Bizley and King, 2008, King and Walker, 2012). They demonstrated that spatially coincident visual and auditory cues increased the amount of information conveyed by the neurons about stimulus location. The authors suggested that such multisensory information enhancement could underlie improved localization accuracy observed when visual and auditory stimuli are presented in the same spatial location. A similar explanation can be valid for our results as well.

Spatial receptive fields as a component of the spatiotemporal receptive field

Although the current description of the SRFs of multisensory SC neurons represents an important step in furthering our mechanistic understanding of these neurons, a complete description will only be obtained with the inclusion of the temporal dimension as well. Here we begin this analysis by creating partial spatiotemporal receptive fields (STRFs) for a subset of the recorded neurons. Although very preliminary, these STRFs illustrates that complex temporal dynamics characterize the response profile of SC neurons, a finding in keeping with numerous studies looking at the response characteristics of these neurons (Sterling, 1971, Walker et al., 1995, Waleszczyk et al., 1999, Waleszczyk et al., 2003, Rowland et al., 2007, Rowland and Stein, 2007, Waleszczyk et al., 2007, Wang et al., 2010)

However, from the perspective of multisensory processing, once again it appears that this complexity can be substantially resolved by taking into account a single factor – sensory responsiveness. Thus, temporal epochs of the response in which firing is low under unisensory conditions are those that have the highest potential for gain upon stimulus pairing. Such a finding is concordant with prior work looking at the temporal elements of the multisensory response (Rowland et al., 2007, Rowland and Stein, 2007, Royal et al., 2009). One important caveat for the current data is that the STRF mappings conducted here are quite low resolution and limited to a single spatial dimension (multiple azimuths across a single elevation). Ongoing work in the lab is focused on creating more complete STRF representations where these temporal properties are analyzed for both azimuth and elevation.

Sensory signals in the natural environment are complex with time varying properties, and necessitate brain mechanisms to code for these spatiotemporal features in order to guide adaptive behavior. Indeed, the concept of spatiotemporal (or spectrotemporal) receptive fields is becoming a standard in studies of sensory processing, where this architecture provides important clues into both functional circuitry and functional utility (Dawis et al., 1984, McLean and Palmer, 1989, Reid and Shapley, 1992, Eckhorn et al., 1993, Golomb et al., 1994, Victor JD, 1994, Cai et al., 1997, Reid et al., 1997, Ringach et al., 1997, Cottaris and De Valois, 1998, Li Y, 2008). In the auditory system, the spectrotemporal RF architecture of auditory cortical neurons has been suggested to code for species-specific vocal signals used for prey hunting and/or communication among conspecifics (Suga et al., 1987). In addition, work in the primate auditory system have implicated STRFs in the encoding of stimulus edges, stimulus transitions in

frequency or intensity and conjunctions of different stimulus features (deCharms et al., 1998). In the somatosensory system, STRF architecture has been implicated to play a role in identifying patterns of tactile stimulation (Nicolelis et al., 1993a, b, Nicolelis and Chapin, 1994). The current study represents the first to extend the description and analysis of STRFs to the multisensory layers of the mammalian SC, a structure in which the well-established spatial architecture and behavioral output make it particularly amenable to psychometric-neurometric studies to further elucidate the importance of STRFs in dynamic stimulus encoding.

Conclusion

To summarize, in this study we show that multisensory neurons of the cat SC have complex spatial and spatiotemporal receptive fields, and that this receptive field architecture plays an integral role in the integrative abilities of these neurons. Thus, changes in sensory responsiveness brought about by changes in stimulus location represent an important determinant of the nature and amount of multisensory integration. Hence, regions of the receptive field that show weak unisensory responsiveness are those that show the greatest response gain under multisensory conditions.

Bibliography

Bell AH, Meredith MA, Van Opstal AJ, Munoz DP (2005) Crossmodal integration in the primate superior colliculus underlying the preparation and initiation of saccadic eye movements. J Neurophysiol 93:3659-3673.

Bizley JK, King AJ (2008) Visual-auditory spatial processing in auditory cortical neurons. Brain Res 1242:24-36.

Bolognini N, Frassinetti F, Serino A, Ladavas E (2005) "Acoustical vision" of below threshold stimuli: interaction among spatially converging audiovisual inputs. Exp Brain Res 160:273-282.

Bushara KO, Grafman J, Hallett M (2001) Neural correlates of auditory-visual stimulus onset asynchrony detection. J Neurosci 21:300-304.

Cai D, DeAngelis GC, Freeman RD (1997) Spatiotemporal receptive field organization in the lateral geniculate nucleus of cats and kittens. J Neurophysiol 78:1045-1061.

Calvert GA, Campbell R, Brammer MJ (2000) Evidence from functional magnetic resonance imaging of crossmodal binding in the human heteromodal cortex. Curr Biol 10:649-657.

Carriere BN, Royal DW, Wallace MT (2008) Spatial heterogeneity of cortical receptive fields and its impact on multisensory interactions. J Neurophysiol 99:2357-2368.

Casagrande VA, Harting JK, Hall WC, Diamond IT, Martin GF (1972) Superior colliculus of the tree shrew: a structural and functional subdivision into superficial and deep layers. Science 177:444-447.

Churan J, Guitton D, Pack CC (2012) Spatiotemporal structure of visual receptive fields in macaque superior colliculus. J Neurophysiol 108:2653-2667.

Cottaris NP, De Valois RL (1998) Temporal dynamics of chromatic tuning in macaque primary visual cortex. Nature 395:896-900.

Dawis S, Shapley R, Kaplan E, Tranchina D (1984) The receptive field organization of X-cells in the cat: spatiotemporal coupling and asymmetry. Vision Res 24:549-564.

deCharms RC, Blake DT, Merzenich MM (1998) Optimizing sound features for cortical neurons. Science 280:1439-1443.

DiCarlo JJ, Johnson KO (2000) Spatial and temporal structure of receptive fields in primate somatosensory area 3b: effects of stimulus scanning direction and orientation. J Neurosci 20:495-510.

Diederich A, Colonius H (2004) Bimodal and trimodal multisensory enhancement: effects of stimulus onset and intensity on reaction time. Percept Psychophys 66:1388-1404.

Dreher B, Hoffmann KP (1973) Properties of excitatory and inhibitory regions in the receptive fields of single units in the cat's superior colliculus. Exp Brain Res 16:333-353.

Eckhorn R, Frien A, Bauer R, Woelbern T, Kehr H (1993) High frequency (60-90 Hz) oscillations in primary visual cortex of awake monkey. Neuroreport 4:243-246.

Frens MA, Van Opstal AJ, Van der Willigen RF (1995) Spatial and temporal factors determine auditory-visual interactions in human saccadic eye movements. Percept Psychophys 57:802-816.

Ghazanfar AA, Nicolelis MA (1997) Nonlinear processing of tactile information in the thalamocortical loop. J Neurophysiol 78:506-510.

Ghazanfar AA, Nicolelis MA (2001) Feature article: the structure and function of dynamic cortical and thalamic receptive fields. Cereb Cortex 11:183-193.

Goldberg ME, Wurtz RH(1972) Activity of superior colliculus in behaving monkey. I. Visual receptive fields of single neurons. J Neurophysiol 35: (4) 542-559.

Golomb D, Wang XJ, Rinzel J (1994) Synchronization properties of spindle oscillations in a thalamic reticular nucleus model. J Neurophysiol 72:1109-1126.

Gordon B (1973) Receptive fields in deep layers of superior colliculus. J Neurophysiol 36: (2) 157-178.

Hairston WD, Laurienti PJ, Mishra G, Burdette JH, Wallace MT (2003a) Multisensory enhancement of localization under conditions of induced myopia. Exp Brain Res 152:404-408.

Hairston WD, Wallace MT, Vaughan JW, Stein BE, Norris JL, Schirillo JA (2003b) Visual localization ability influences cross-modal bias. J Cogn Neurosci 15:20-29.

Hughes HC, Reuter-Lorenz PA, Nozawa G, Fendrich R (1994) Visual-auditory interactions in sensorimotor processing: saccades versus manual responses. J Exp Psychol Hum Percept Perform 20:131-153.

Hyvarinen J, Poranen A (1978) Movement-sensitive and direction and orientation-selective cutaneous receptive fields in the hand area of the post-central gyrus in monkeys. J Physiol 283:523-537.

Jiang W, Jiang H, Stein BE (2002) Two corticotectal areas facilitate multisensory orientation behavior. J Cogn Neurosci 14:1240-1255.

Kadunce DC, Vaughan JW, Wallace MT, Stein BE (2001) The influence of visual and auditory receptive field organization on multisensory integration in the superior colliculus. Exp Brain Res 139:303-310.

Kayser C, Petkov CI, Augath M, Logothetis NK (2005) Integration of touch and sound in auditory cortex. Neuron 48:373-384.

Kayser C, Petkov CI, Augath M, Logothetis NK (2007) Functional imaging reveals visual modulation of specific fields in auditory cortex. J Neurosci 27:1824-1835.

King AJ, Walker KM (2012) Integrating information from different senses in the auditory cortex. Biol Cybern 106:617-625.

Krueger J, Royal DW, Fister MC, Wallace MT (2009) Spatial receptive field organization of multisensory neurons and its impact on multisensory interactions. Hear Res 258:47-54.

Li Y VHS, Mazurek M, White LE, Fitzpatrick D (2008) Experience with moving visual stimuli drives the early development of cortical direction selectivity. Nature 456:952-956.

Macaluso E, George N, Dolan R, Spence C, Driver J (2004) Spatial and temporal factors during processing of audiovisual speech: a PET study. Neuroimage 21:725-732.

McLean J, Palmer LA (1989) Contribution of linear spatiotemporal receptive field structure to velocity selectivity of simple cells in area 17 of cat. Vision Res 29:675-679.

Meredith MA, Nemitz JW, Stein BE (1987) Determinants of multisensory integration in superior colliculus neurons. I. Temporal factors. J Neurosci 7:3215-3229.

Meredith MA, Stein BE (1983) Interactions among converging sensory inputs in the superior colliculus. Science 221:389-391.

Meredith MA, Stein BE (1986a) Spatial factors determine the activity of multisensory neurons in cat superior colliculus. Brain Res 365:350-354.

Meredith MA, Stein BE (1986b) Visual, auditory, and somatosensory convergence on cells in superior colliculus results in multisensory integration. J Neurophysiol 56:640-662.

Meredith MA, Stein BE (1990) The visuotopic component of the multisensory map in the deep laminae of the cat superior colliculus. J Neurosci 10:3727-3742.

Meredith MA, Stein BE (1996) Spatial determinants of multisensory integration in cat superior colliculus neurons. J Neurophysiol 75:1843-1857.

Middlebrooks JC, Knudsen EI (1987) Changes in external ear position modify the spatial tuning of auditory units in cat's superior colliculus. J Neurophysiol 57: (3) 672-687.

Molholm S, Ritter W, Murray MM, Javitt DC, Schroeder CE, Foxe JJ (2002) Multisensory auditory-visual interactions during early sensory processing in humans: a high-density electrical mapping study. Brain Res Cogn Brain Res 14:115-128.

Mozolic JL, Hugenschmidt CE, Peiffer AM, Laurienti PJ (2008) Modality-specific selective attention attenuates multisensory integration. Exp Brain Res 184:39-52.

Murray MM, Foxe JJ, Higgins BA, Javitt DC, Schroeder CE (2001) Visuo-spatial neural response interactions in early cortical processing during a simple reaction time task: a high-density electrical mapping study. Neuropsychologia 39:828-844.

Murray MM and Wallace MT(editors). (2012) The Neural Bases of Multisensory Processes. Boca Raton(FL): CRC Press.

Naito T, Sadakane O, Okamoto M, Sato H (2007) Orientation tuning of surround suppression in lateral geniculate nucleus and primary visual cortex of cat. Neuroscience 149:962-975.

Nicolelis MA, Chapin JK (1994) Spatiotemporal structure of somatosensory responses of many-neuron ensembles in the rat ventral posterior medial nucleus of the thalamus. J Neurosci 14:3511-3532.

Nicolelis MA, Lin RC, Woodward DJ, Chapin JK (1993a) Dynamic and distributed properties of many-neuron ensembles in the ventral posterior medial thalamus of awake rats. Proc Natl Acad Sci U S A 90:2212-2216.

Nicolelis MA, Lin RC, Woodward DJ, Chapin JK (1993b) Induction of immediate spatiotemporal changes in thalamic networks by peripheral block of ascending cutaneous information. Nature 361:533-536.

Nozawa G, Reuter-Lorenz PA, Hughes HC (1994) Parallel and serial processes in the human oculomotor system: bimodal integration and express saccades. Biol Cybern 72:19-34.

Perrault TJ, Jr., Vaughan JW, Stein BE, Wallace MT (2003) Neuron-specific response characteristics predict the magnitude of multisensory integration. J Neurophysiol 90:4022-4026.

Perrault TJ, Jr., Vaughan JW, Stein BE, Wallace MT (2005) Superior colliculus neurons use distinct operational modes in the integration of multisensory stimuli. J Neurophysiol 93:2575-2586.

Phillips JR, Johnson KO, Hsiao SS (1988) Spatial pattern representation and transformation in monkey somatosensory cortex. Proc Natl Acad Sci U S A 85:1317-1321.

Rausschecker JP, Harris LR (1989) Auditory and visual neurons in cat's superior colliculus selective for the direction of apparent motion stimuli. Brain Res 490: 56-63.

Reid RC, Shapley RM (1992) Spatial structure of cone inputs to receptive fields in primate lateral geniculate nucleus. Nature 356:716-718.

Reid RC, Victor JD, Shapley RM (1997) The use of m-sequences in the analysis of visual neurons: linear receptive field properties. Vis Neurosci 14:1015-1027.

Ringach DL, Hawken MJ, Shapley R (1997) Dynamics of orientation tuning in macaque primary visual cortex. Nature 387:281-284.

Rowland BA, Stanford TR, Stein BE (2007) A model of the neural mechanisms underlying multisensory integration in the superior colliculus. Perception 36:1431-1443.

Rowland BA, Stein BE (2007) Multisensory integration produces an initial response enhancement. Front Integr Neurosci 1:4.

Royal DW, Carriere BN, Wallace MT (2009) Spatiotemporal architecture of cortical receptive fields and its impact on multisensory interactions. Exp Brain Res 198:127-136.

Serino A, Bassolino M, Farne A, Ladavas E (2007a) Extended multisensory space in blind cane users. Psychol Sci 18:642-648.

Serino A, Farne A, Rinaldesi ML, Haggard P, Ladavas E (2007b) Can vision of the body ameliorate impaired somatosensory function? Neuropsychologia 45:1101-1107.

Shimegi S, Ichikawa T, Akasaki T, Sato H (1999) Temporal characteristics of response integration evoked by multiple whisker stimulations in the barrel cortex of rats. J Neurosci 19:10164-10175.

Shou TD, Leventhal AG (1989) Organized arrangement of orientation-sensitive relay cells in the cat's dorsal lateral geniculate nucleus. J Neurosci 9:4287-4302.

Sillito AM, Cudeiro J, Murphy PC (1993) Orientation sensitive elements in the corticofugal influence on centre-surround interactions in the dorsal lateral geniculate nucleus. Exp Brain Res 93:6-16.

Simons DJ (1985) Temporal and spatial integration in the rat SI vibrissa cortex. J Neurophysiol 54:615-635.

Simons DJ, Carvell GE (1989) Thalamocortical response transformation in the rat vibrissa/barrel system. J Neurophysiol 61:311-330.

Smith EL, 3rd, Chino YM, Ridder WH, 3rd, Kitagawa K, Langston A (1990) Orientation bias of neurons in the lateral geniculate nucleus of macaque monkeys. Vis Neurosci 5:525-545.

Soodak RE, Shapley RM, Kaplan E (1987) Linear mechanism of orientation tuning in the retina and lateral geniculate nucleus of the cat. J Neurophysiol 58:267-275.

Sprague JM (1996) Neural mechanisms of visual orienting responses. Prog Brain Res 112:1-15.

Sprague JM, Meikle TH, Jr. (1965) The Role of the Superior Colliculus in Visually Guided Behavior. Exp Neurol 11:115-146.

Stanford TR, Quessy S, Stein BE (2005) Evaluating the operations underlying multisensory integration in the cat superior colliculus. J Neurosci 25:6499-6508.

Stanford TR, Stein BE (2007) Superadditivity in multisensory integration: putting the computation in context. Neuroreport 18:787-792.

Stein BE, Huneycutt WS, Meredith MA (1988) Neurons and behavior: the same rules of multisensory integration apply. Brain Res 448:355-358.

Stein BE MA (1993) The Merging of the Senses. Book.

Stein BE, Stanford TR (2008) Multisensory integration: current issues from the perspective of the single neuron. Nat Rev Neurosci 9:255-266.

Stein BE(2012) The New Handbook of Multisensory Processing.

Sterling P (1971) Receptive fields and synaptic organization of the superficial gray layer of the cat superior colliculus. Vision Res Suppl 3:309-328.

Stevens JK, Gerstein GL (1976) Spatiotemporal organization of cat lateral geniculate receptive fields. J Neurophysiol 39:213-238.

Stevenson RA, James TW (2009) Audiovisual integration in human superior temporal sulcus: Inverse effectiveness and the neural processing of speech and object recognition. Neuroimage 44:1210-1223.

Suematsu N, Naito T, Sato H (2012) Relationship between orientation sensitivity and spatiotemporal receptive field structures of neurons in the cat lateral geniculate nucleus. Neural Netw 35:10-20.

Suga N, Niwa H, Taniguchi I, Margoliash D (1987) The personalized auditory cortex of the mustached bat: adaptation for echolocation. J Neurophysiol 58:643-654.

Sun C, Chen X, Huang L, Shou T (2004) Orientation bias of the extraclassical receptive field of the relay cells in the cat's dorsal lateral geniculate nucleus. Neuroscience 125:495-505.

Victor JD PK, Katz E, Mao B (1994) Population encoding of spatial frequency, orientation and color in macaque V1. J Neurophysiol 72:2151-2166.

Waleszczyk WJ, Nagy A, Wypych M, Berenyi A, Paroczy Z, Eordegh G, Ghazaryan A, Benedek G (2007) Spectral receptive field properties of neurons in the feline superior colliculus. Exp Brain Res 181:87-98.

Waleszczyk WJ, Wang C, Burke W, Dreher B (1999) Velocity response profiles of collicular neurons: parallel and convergent visual information channels. Neuroscience 93:1063-1076.

Waleszczyk WJ, Wang C, Young JM, Burke W, Calford MB, Dreher B (2003) Laminar differences in plasticity in area 17 following retinal lesions in kittens or adult cats. Eur J Neurosci 17:2351-2368.

Walker S, Bruce V, O'Malley C (1995) Facial identity and facial speech processing: familiar faces and voices in the McGurk effect. Percept Psychophys 57:1124-1133.

Wallace MT, Meredith MA, Stein BE (1992) Integration of multiple sensory modalities in cat cortex. Exp Brain Res 91:484-488.

Wallace MT, Stein BE (1994) Cross-modal synthesis in the midbrain depends on input from cortex J Neurophysiol 71:429-432.

Wallace MT, Stein BE (1996) Sensory organization of the superior colliculus in cat and monkey. Prog Brain Res 112:301-311.

Wang L, Sarnaik R, Rangarajan K, Liu X, Cang J (2010) Visual receptive field properties of neurons in the superficial superior colliculus of the mouse. J Neurosci 30:16573-16584.

Wilkinson LK, Meredith MA, Stein BE (1996) The role of anterior ectosylvian cortex in cross-modality orientation and approach behavior. Exp Brain Res 112:1-10.

CHAPTER III

IMPACT OF RESPONSE DURATION ON MULTISENSORY INTEGRATION

This chapter is published in the "Journal of Neurophysiology" as: ***Ghose D, Barnett ZP and Wallace MT****. Impact of response duration on multisensory integration. J Neurophysiol 108:2534-2544, 2012.*

Introduction

The superior colliculus (SC) is a mammalian midbrain nucleus well recognized for its role in the generation of coordinated eye and head movements (Sparks and Mays, 1983; Munoz and Guitton, 1985, 1989; Marino et al., 2012; Marino et al., 2012; Marino et al., 2008). In addition, the SC is a watershed site for the convergence of sensory information, with visual, auditory and somatosensory inputs terminating in its intermediate and deep layers (Edwards et al., 1974; Tortelly et al., 1980; Mucke et al., 1982; Huerta MF, 1984). As a result of this convergence, many neurons in the SC are multisensory, receiving inputs from two and even three different sensory modalities (Meredith MA and Stein BE., 1986; Meredith and Stein 1983; Wallace et al., 1993). These neurons do far more than passively reflect these different inputs, with many actively integrating them in order to give rise to dramatically transformed outputs

(Meredith MA and Stein BE., 1986; Meredith and Stein., 1983; Wallace et al., 1993; Stein BE and Meredith MA., 1993; Meredith et al., 1987; Meredith MA and Stein BE., 1996). The presumptive importance of multisensory integration lies in the close ties between the SC and behavior, where changes in the firing characteristics of SC neurons are likely to be important for the facilitations that can be observed in saccadic, gaze-related and orientation behaviors (Hughes et al., 1994; Frens et al., 1995; Goldring et al., 1996; Frens and Van Opstal, 1998; Corneil et al., 2002).

In addition to neurons that are overtly responsive to multiple sensory cues, there is an additional population of SC neurons that are responsive to cues in only a single sensory modality (i.e., as indexed by spiking responses), but whose responses are strongly modulated under multisensory conditions (Carriere et al., 2008; Royal et al., 2009). The role of these modulated neurons in multisensory processing remains unresolved. Regardless of whether neurons are frankly responsive or modulatory, the nature by which they combine their different sensory inputs has been shown to be strongly dependent upon the physical characteristics of these inputs (Meredith MA and Stein BE., 1986; Meredith et al., 1987; Meredith MA and Stein BE., 1996). Thus, stimulus factors such as space, time and relative effectiveness are key determinants in dictating the final integrative product.

One characteristic feature of SC neurons is their large receptive fields (Meredith and Stein., 1990, Stein and Meredith., 1993, Kadunce et al., 1997, Kadunce et al., 2001, Krueger et al., 2009). Although classically treated as simply bounded areas within which sensory responses can be evoked, recent work has revealed a surprising degree of heterogeneity to the responses seen within these receptive fields (Carriere et al., 2008,

Royal et al., 2009 Krueger et al., 2009). As a means of examining this heterogeneity, these prior studies used the construct of a “spatial receptive field’ (SRF), which represents the profile of neuronal responses for a series of stimulus locations. Marked differences in response were seen as a function of location, with firing rates varying by 4-5 fold with changes in stimulus location. More importantly, these studies showed that these differences in neuronal responsiveness were an important factor in the integrated multisensory response, with SRF locations showing the weakest unisensory (i.e., visual alone, auditory alone) responses having the greatest capacity for multisensory enhancements.

Along with highlighting the importance of spatial location within the SRF in dictating response effectiveness, these prior studies (Ghose et al., 2010) also illustrated differences in temporal response dynamics that are also likely to be important factors in multisensory integration. Thus, these prior studies, along with others (Rowland et al 2007a), found that changes in both response latency and duration were key components in the enhanced multisensory response, with shorter latency and longer duration typically accompanying multisensory conditions. In the course of this work, we also began to see distinctions in response durations as a function of spatial location, such that certain locations within the SRF appeared to show short duration responses, whereas other locations were characterized by much longer duration responses. Such differences in response dynamics are likely to have strong implications for the integrated multisensory response, with the hypothesis that shorter duration responses may be coupled to the largest multisensory gains (because of inverse effectiveness). Alternatively, longer duration responses may be associated with greater integrative

potential due to a lower overall firing rate, thus allowing for greater amplification. The current study set out to test between these competing hypotheses by systematically examining the temporal dynamics of response in a population of multisensory SC neurons, and linking the temporal characteristics of response to multisensory integration.

Methods

***General procedures*:** Experiments were conducted in adult cats (n=2) raised under standard housing conditions. All experiments were done in an anesthetized and paralyzed semi-chronic preparation and consisted of single unit extracellular recordings from the superior colliculus (SC). Experiments were run on a weekly basis on each animal. All surgical and recording procedures were performed in compliance with the Guide for the Care and Use of Laboratory Animals at Vanderbilt University Medical Center, which is accredited by the American Association for Accreditation of Laboratory Animal Care. All procedures were approved by the Vanderbilt Institutional Animal Care and Use Committee.

Implantation and Recording procedures: For surgical anesthesia, animals were induced with ketamine hydrochloride (20 mg/kg, administered intramuscularly (im)) and acepromazine maleate (0.04 mg/kg im). For implantation of the recording chamber over the SC, animals were intubated and artificially respired. A stable plane of surgical anesthesia was achieved using inhalation isofluorane (1%-3%). Body temperature,

expiratory CO2, blood pressure and heart rate were continuously monitored (VSM7, Vetspecs/SCIL), recorded and maintained within ranges consistent with a deep and stable plane of anesthesia. A craniotomy was made to allow access to SC and a head holder was attached to the cranium using stainless steel screws and orthopedic cement to hold the animal during recording sessions without obstructing the face and ears. Postoperative care (antibiotics and analgesics) was done in close consultation with veterinary staff.

For recording experiments, animals were anesthetized with ketamine (20mg/kg im) and acepromazine maleate (0.04 mg/kg im) and maintained throughout the procedure with constant rate infusion of ketamine (5mg/kg/hr iv) delivered through cannula placed in the saphenous vein. Though the effects of ketamine anesthesia on multisensory processes is the subject of some debate (i.e., see Populin et al., 2002,2005, Stanford et al., 2005,2007) we have seen very little differences in receptive fields or the integrative capacity of multisensory neurons in the SC when comparing data from ketamine anesthetized and awake preparations (Wallace et al., 1994,1998). The head holding system was then used to maintain the animal in a comfortable recumbent position. To prevent ocular drift (which can impact the mapping of receptive fields), animals were paralyzed using pancuronium bromide (0.1mg/kg/hr, iv) and artificially respired for the duration of recording. Before inducing paralysis, a stable plane of anesthesia was verified in each animal. To achieve this, in an initial session a continuous infusion of ketamine was delivered and adjusted while a number of key physiological parameters indicative of anesthetic state (heart rate, EKG, temperature, blood pressure) were monitored. The basal rate of infusion for future recording sessions was thus determined.

In addition, before introducing the paralytic during recording sessions, these procedures were once again carried out prior to paralysis in order to ensure adequate depth of anesthesia. The rate of infusion was adjusted throughout the experiment depending on the established physiological parameters to ensure a stable plane of anesthesia. Since during recording there are no wounds or pressure points, with careful monitoring and adjustment based on vital signs ketamine is able to provide a sufficient sedation level. Parylene insulated tungsten electrodes (Z = 2-5 MΩ) were advanced into the SC using an electronically controlled mechanical microdrive. Single unit neural activity (signal to noise ratio >= 3:1) was recorded (Sort client software,Plexon Inc.,Texas), amplified and routed to an oscilloscope, audio monitor and computer for performing online and offline analysis. At the end of the recording session (approximately 8-10 hrs), paralysis was reversed and the animal was weaned from the ventilator. Anesthesia was discontinued, and upon return of stable respiration and locomotion the animal was returned to its home cage. Animals were given 60-100ml of lactated Ringer solution subcutaneously in order to facilitate recovery.

Stimulus presentation and search strategy: Extracellular single unit recordings targeted visual-auditory (VA) multisensory neurons in the deep layers of the SC. A multisensory neuron was defined as one in which the response in the multisensory condition (mean number of spikes/trial) was statistically different from the best unisensory response (mean number of spikes/trial) as determined by the Wilcoxon Rank test ($p<0.05$). Multisensory neurons were further divided into two categories. Frank or overt multisensory neurons were those that showed an overt response to both visual and the auditory stimuli. Modulatory multisensory neurons were those in which

the response to the driving modality was modulated by a stimulus in the other modality. Once a neuron was isolated, the borders of its receptive field were coarsely mapped. Visual stimuli consisted of the illumination of stationary light emitting diodes (LEDs: 100 ms duration) while auditory stimuli were delivered through speakers and consisted of 100 ms duration broadband noise (20Hz-20KHz) with an intensity of 67 dB SPL. Both the LEDs and speakers were mounted on a hoop 0.6 m away from the center of the animal's head, with locations spanning azimuthal space from 0-90° on either side of the midline. Stimulus location typically varied by 10° (azimuth and elevation) for each tested position. The hoop could be rotated along different elevations. This stimulus configuration allowed for the sampling of numerous locations within and just outside the coarsely-delimited receptive fields, creating a spatial receptive field (SRF) for each of the effective modalities as well as for the multisensory condition. The physical characteristics of the stimuli were always identical in all respects except for spatial location. Visual and auditory stimuli were presented in a randomized interleaved manner at multiple azimuthal locations along a single elevation at a time. Multisensory combinations always consisted of visual and auditory stimuli presented at the same spatial location (i.e., spatial coincidence). A minimum of 60 trials (20 visual, 20 auditory, 20 multisensory) were collected for any given stimulus location. Consecutive stimulus presentations were separated by a minimum of 1.5 s to avoid response habituation.

Data acquisition and analysis: A custom built PC-based real time data acquisition system controlled the structure of the trials and the timing of the stimulus (Labview. National Instruments). Analog waveforms were transferred to a Plexon MAP system (Plexon Inc.,Texas) where they were digitized at 40KHz. Single units were isolated

online using Sort Client software (Plexon Inc., Texas) and also stored for further offline analysis. Neuronal responses were characterized through construction of peristimulus time histograms (PSTHs) for each condition (visual (V) only, auditory only (A), visual-auditory (VA)) for each location tested within the SRF. Response baseline was calculated as the mean firing rate during the 500 ms immediately preceding the stimulus onset for each of the 3 conditions. Thresholds for the PSTHs were set at 2SD above the respective baselines to delimit the stimulus evoked response. Following stimulus onset, the time at which the PSTH crosses above the 2SD line (and remains so for at least 30ms) was noted as the response onset. Response offset was the time at which the PSTH fell below the 2SD line and stayed below this line for >=30ms. Response duration was defined as the time interval between response onset and response offset. Mean stimulus evoked response was calculated as the average number of spikes elicited per trial during the defined response duration interval. Mean spontaneous firing rate was always subtracted.

Measures of multisensory integration: Two measures were used to quantify multisensory integration. The first was the interactive index (ii), which measures how the multisensory response differs from the best unisensory response. The magnitude of this change was calculated as [(CM-SMmax)/SMmax)] X100 = % interaction where CM is the mean response evoked by combined modality stimulus and SMmax is the mean response evoked by the most effective single modality stimulus (Meredith et al 1983,1986b). Statistical comparisons between the mean stimulus evoked responses of the multisensory condition and the best unisensory condition were done using a non-parametric Wilcoxon Rank Test. The second measure used was mean statistical

contrast (msc). This metric evaluates the multisensory response as a function of the response predicted by the addition of the two unisensory responses. Multisensory contrast is calculated using the formula: ∑[(SA-A)-(V-VA)]/n where SA is spontaneous activity, A is auditory response, V is visual response, VA is multisensory response and n is the number of trials. The model assumes independence between the visual and auditory inputs and uses additive factors logic to distinguish between subadditive (contrast < 0), additive (contrast = 0) and superadditive (contrast > 0) modes of response (Perrault Jr et al 2003,2005; Stanford et al 2005,2007). Significant differences from a contrast value of 0 were determined by the Wilcoxon Rank test.

Temporal epoch analysis: For a subset of neurons (those with long discharge durations) the total response was divided into 3 equivalent temporal epochs: early, mid and late. Both the ii and msc values were calculated for each of these epochs to determine how the integrative abilities of these multisensory neurons changed over time.

Results

Multisensory SC neurons exhibit distinct firing modes

A total of 54 multisensory (visual-auditory) neurons (n=21 for animal 1 and n=33 for animal 2) were isolated from the intermediate and deep layers of the superior colliculus (SC) (below stratum opticum) and held for the duration of the extensive analyses that

comprise this study (1-2 hours). Of these, 30 neurons were classified as frank/overt (i.e., overtly responsive to both visual and auditory stimuli) while 24 neurons were modulatory (i.e., only driven by a single modality see methods section for definitions of frank and modulatory neurons). No differences were noted in these distributions between the two animals. Individual SC neurons exhibited a wide range of response duration in response to both unisensory and multisensory stimuli. Slightly less than 20% of the recorded neurons (10/54 exhibited only short duration (i.e., < 250 ms) responses for all locations tested within their spatial receptive field (SRF) under both best unisensory and multisensory conditions (Fig. 3-1).

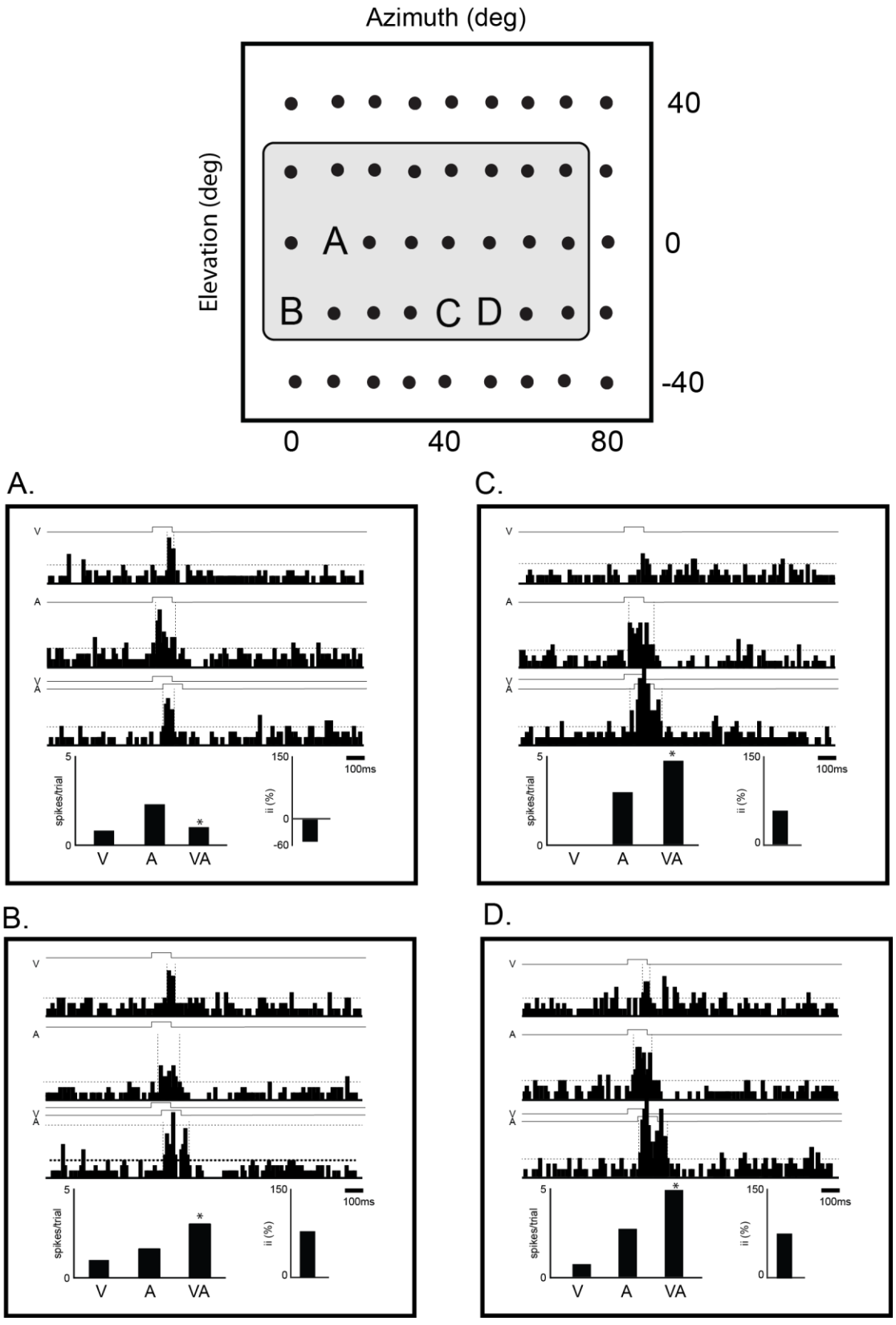
Azimuth (deg)
Elevation (deg)
40
0
-40
0
40
80
A
B
C
D
A.
C.
B.
D.
V
A
VA
spikes/trial
ii (%)
100ms

Figure 3-1: Representative example of a single neuron recorded from the intermediate and deep layers of the superior colliculus.

Representative example of a single neuron recorded from the intermediate or deep layers of the superior colliculus which shows short duration discharges at 4 of the representative locations tested within its receptive field. In fact all the locations tested within the spatial receptive field of this neuron displayed short discharge duration. The spatial receptive field of the neuron has been shown by a shaded round rectangle. The letters represent the locations for which post stimulus time histograms are shown below and bar graphs quantify the firing rates at each of the 3 stimulus conditions. Interactive index (ii) values are also depicted. For the location represented by A within the RF there is significant response depression ($p = 0.016$) and ii = -55.36%. For the location represented by B ii = 83% which is also statistically significant ($p=0.004$). For the location represented by C ii = 60.45% which is statistically significant with $p = 0.02$ as determined by Wilcoxon Rank Test. The location represented by D. exhibits significant interaction as expressed by ii = 80.61% ($p=0.004$).

In contrast, slightly more than 80% (44/54) of the neurons examined exhibited a response exceeding 250 ms in duration for at least one tested location (Fig.3-2). Nonetheless, typically in these neurons the majority of the locations (mean = 72%) within the SRF exhibited much shorter duration discharge patterns. A systematic analysis of the duration of the multisensory response for all neurons and all locations is shown in Fig 3-3.

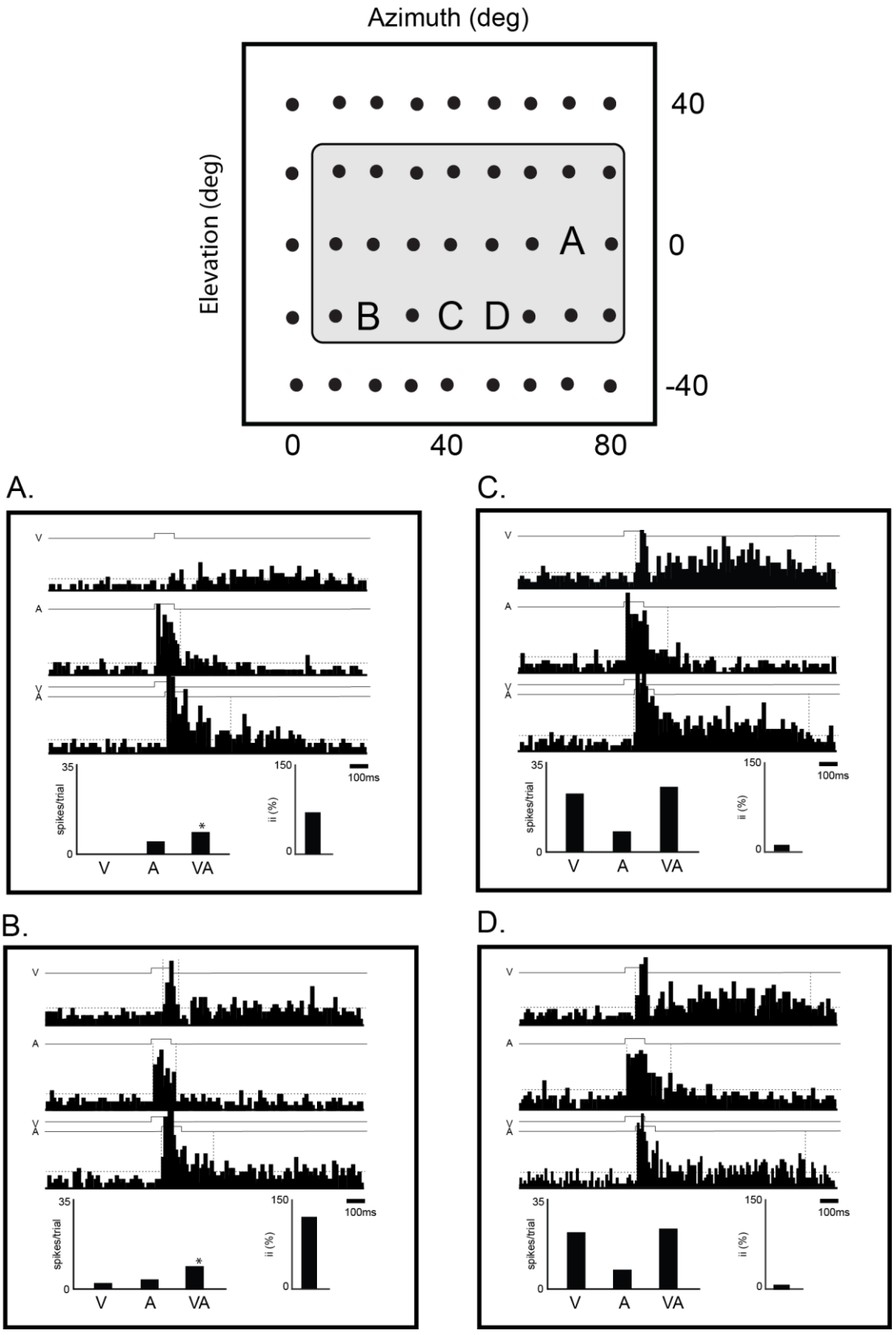
Azimuth (deg)
Elevation (deg)
40
0
-40
0
40
80
A
B
C
D
A.
C.
B.
D.
V
A
VA
spikes/trial
ii (%)
100ms

Figure 3-2: Representative example of a single neuron recorded from the intermediate or deep layers of the superior colliculus which shows dual mode of discharge.

Two of the representative locations show short response durations while the rest show long response durations. The spatial receptive field of the neuron has been shown by a shaded round rectangle. The letters represent the locations for which post stimulus time histograms are shown below and bar graphs quantify the firing rates at each of the 3 stimulus conditions. Interactive index (ii) values are also depicted. For the location represented by A ii = 75.23% and is statistically significant p = 0.0001. For the location represented by B ii = 130.81% and it is statistically significant with a p value = 0.0001. The location represented by C ii = 11.52 % and it is statistically non-significant. The same is true for the location represented by D. where ii = 6.4% and p= 0.67.

Analysis of response latencies revealed no apparent differences based on the duration of response. Thus, using the arbitrary division of 250 ms as a means to divide responses into short and long duration, the mean visual latency was approximately 75 ms for both groups (Students t test p=0.7552). Similarly, the mean auditory latency for both short and long duration responses was 23 ms (Students t test p=0.8965).

Influence of temporal discharge patterns on the integrative abilities of multisensory SC neurons

These different response modes and temporal discharge patterns were found to be associated with significant differences in multisensory integrative capacity. Thus, there is an inverse relationship between response duration and interactive index (Fig 3-3). Again, in order to better clarify the relationship between discharge duration and multisensory integration, we used the arbitrary duration criterion of 250 ms to divide the population into short and long response. When divided in this way, the average gain in response relative to the better of the two unisensory responses (i.e., interactive index) was 92% for short duration responses versus 34% for long duration responses, a significant difference (Student's t test $p = 2.015 \times 10^{-19}$).

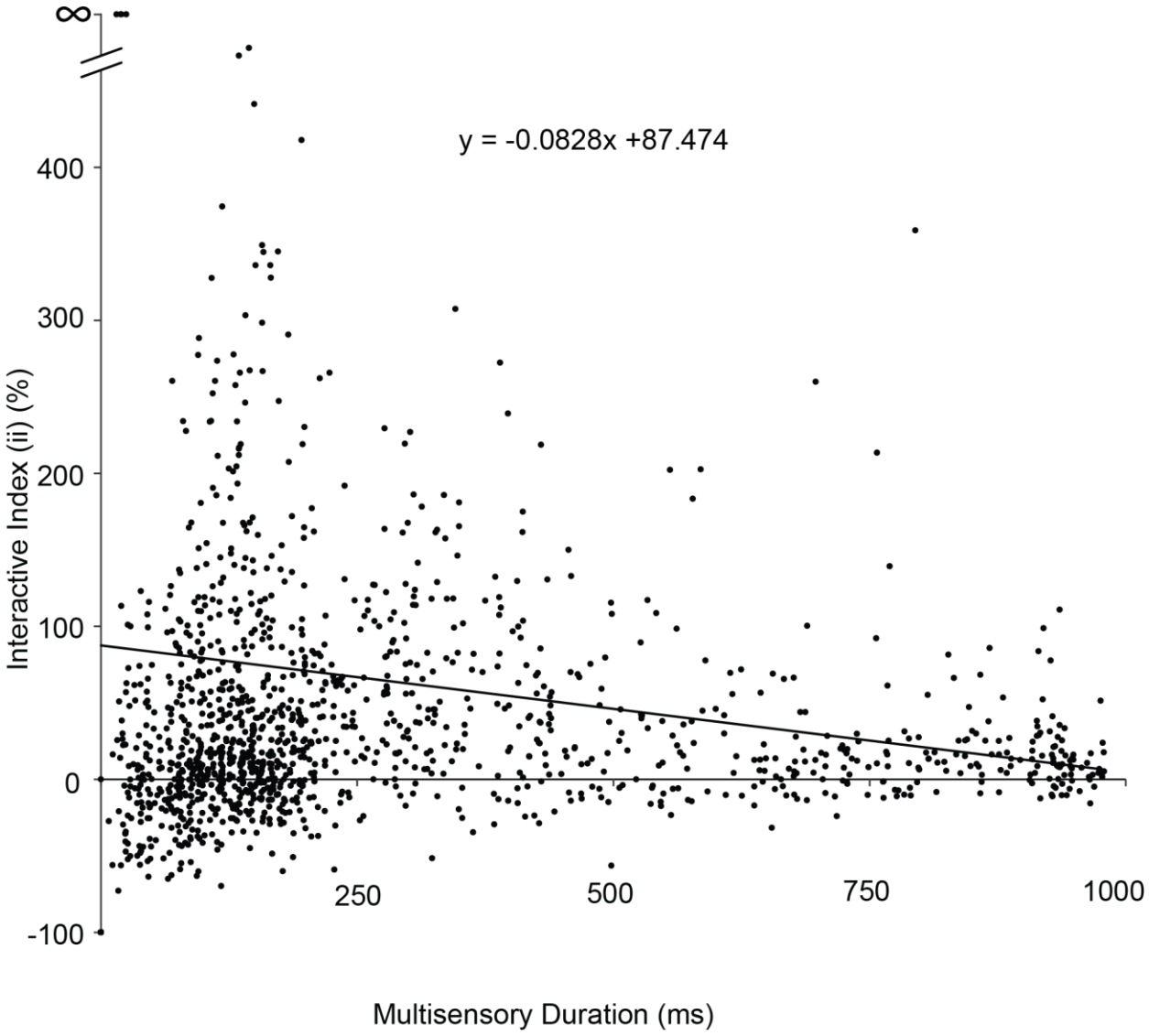

Figure 3-3: Multisensory neurons in the SC exhibit different response durations: short discharge durations and long discharge durations.

Short discharge duration is associated with high integrative abilities (mean ii = 92.43%) while long discharge duration is associated with lower integrative abilities (mean ii = 34.35%, R=-0.19, p<0.00001). The solid black line represents the trend of the dataset (y=-0.0828x +87.474).

One striking finding in the data was that there were significant differences in response duration between the best unisensory and multisensory conditions, the nature of which depended on the type of integration (Fig 3-4). Thus, for response enhancements the duration of response in the multisensory condition was significantly greater than for the best unisensory condition (Fig 3-4A), while for response depressions the response duration in the multisensory condition was significantly lower than for the best unisensory condition (Fig 3-4B). Under conditions in which there were no significant interactions, the response durations did not differ (Fig 3-4C).

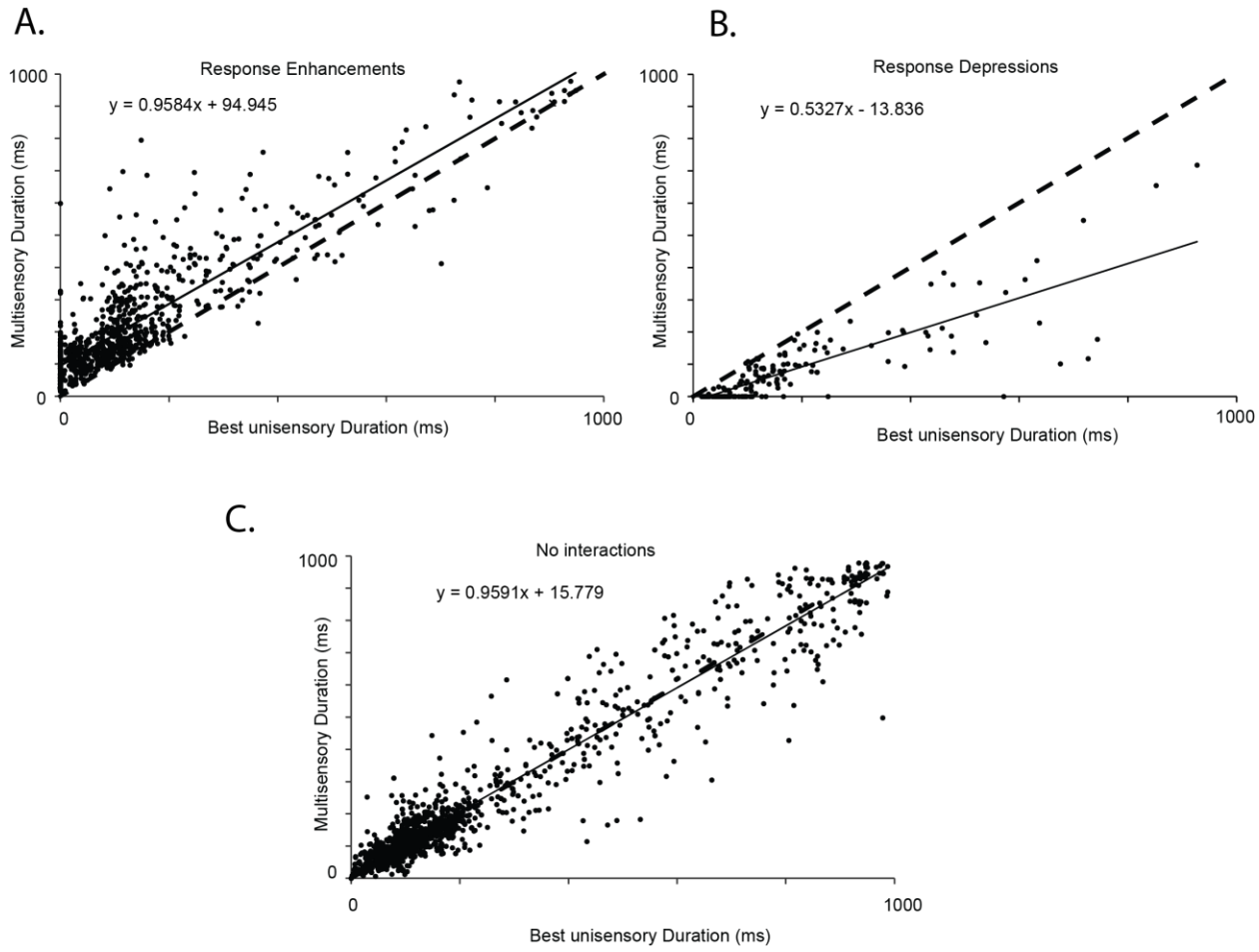

Figure3-4: Relationship between best unisensory and multisensory response durations.

A] For response enhancements, multisensory response duration was significantly longer (mean = 225.08ms) than the best unisensory condition (mean =135.79ms) as measured by the Wilcoxon Signrank Test ($p<0.00001$). The solid black line represents the trend of the dataset while the dashed black line represents the slope of 1 (y=x). **B]** For response depressions, the multisensory duration was significantly lower (mean =82.55ms) than the best unisensory duration (mean 180.94ms) $p <0.00001$. The solid black line represents the slope of the data which is <1 while the dashed line has a slope of 1(y=x).**C]** For no interactions the dashed line representing a slope of 1 and the trend of the dataset represented by the solid black line overlaps and the durations do not differ between the best unisensory (mean = 245.49ms) and multisensory (mean = 251.22ms) conditions, $p = 0.06$.

Reinforcing the role of discharge duration in determining integrative magnitude, within individual mixed response neurons (i.e., the neurons exhibiting both short and long discharge durations) the largest interactions were invariably associated with locations at which short duration responses were evoked. To exemplify this, a subset of 10 neurons are shown in Fig 3-5 and which exhibited both short and long duration discharges within their spatial receptive field. Locations at which short duration responses were elicited invariably exhibited large gains in response under multisensory conditions, where those in which long duration responses were elicited showed little gain. This pattern was typical for the entire population of neurons sampled. A comparison of interactive magnitude for the short duration responses of neurons exhibiting only short duration responses vs. neurons showing both short and long responses revealed both to have large gains. Thus, both populations exhibited large gains in interactive index (neurons with short duration responses only - mean ii = 141% vs mixed neurons with both short and long duration responses - mean ii = 112%). These differences were not significant between the two groups ($p=0.2908$ as determined by a Student's t test).

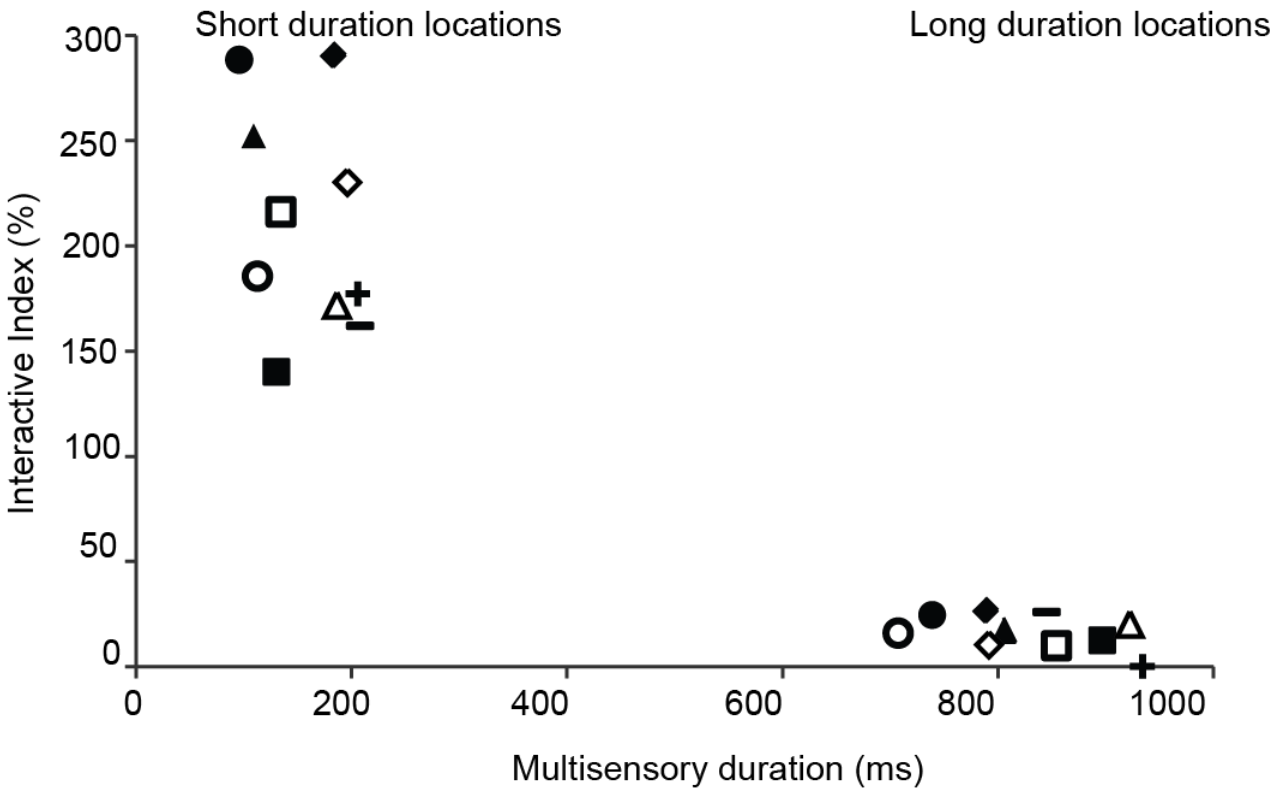

Figure 3-5: Interactive Index as a function of multisensory integration

Interactive index is plotted for locations with short discharge duration and locations with long discharge duration of a single neuron (coded by symbols) for a subset of 10 representative neurons. It can be seen from this graph that the same cell with short response duration exhibits higher integrative abilities than with long response duration when the integrative ability of the neuron is very low.

In addition to the analysis of interactive index (which uses the largest unisensory response as a referent), mean statistical contrast, which calculates multisensory integration as a function of both unisensory responses (see methods for details) was also determined for each multisensory interaction. Using this analysis, multisensory neurons showed a similar pattern of results to that seen using the interactive index. Hence, short duration responses were typically associated with significant superadditive and subadditive interactions, whereas long duration responses were mostly associated with non-significant interactions (Fig 3-6).

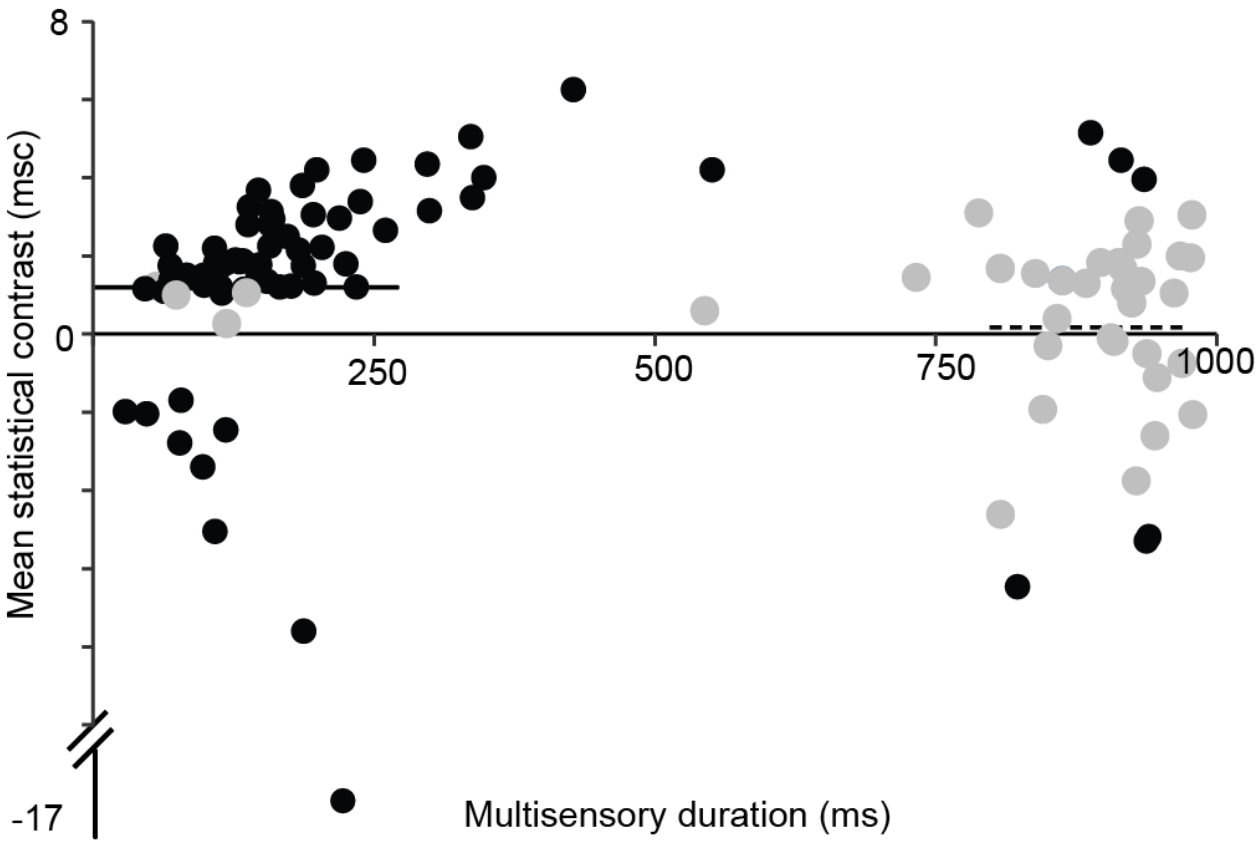

Figure 3-6: Mean statistical contrast (msc) as a function of multisensory duration.

Locations with short response durations are mostly associated with statistically significant ($p<0.05$ as tested by Wilcoxon Rank Test) superadditive and sub additive interactions (shown in black dots) while locations with long discharge durations are mostly associated with msc values that are statistically not significant ($p>0.05$ as tested by Wilcoxon Rank Test) (shown in grey dots).The solid black line represents the mean msc value (1.34) for short discharge durations while the dashed line represents the mean msc value (0.17) for the longer response durations.

Relationship between firing rate, discharge duration and integrative abilities

Since the temporal discharge pattern appeared to play an important role in the integrative abilities of the neuron under study, it was important to examine the relationship between absolute firing rate and discharge duration in these multisensory neurons. Analysis of the population means revealed higher firing rates for responses of shorter duration (41.5 spikes/s) when compared with those of longer duration (27.5 spikes/s) (Fig 3-7).

In an effort to better characterize which temporal aspects of the multisensory response were most closely related to integrative capacity, firing rate as a function of interactive magnitude was also evaluated. As opposed to the strong negative correlation between multisensory duration and interactive index ($R = -0.19$, $p<0.000001$), mean multisensory firing rate (sp/s) was not significantly correlated with interactive index ($R = .17$, $p=.2$). Furthermore, multiple regression analysis revealed that the duration of response was a significant contributor to the magnitude of the multisensory interaction ($p = .000563$) while the contribution of firing rate was non-significant ($p = .69$). This analysis helps reinforce the conclusion that the changes in the multisensory integrative abilities of SC neurons are associated with the changes in firing mode (i.e., discharge duration), and are poorly associated with absolute changes in firing rates.

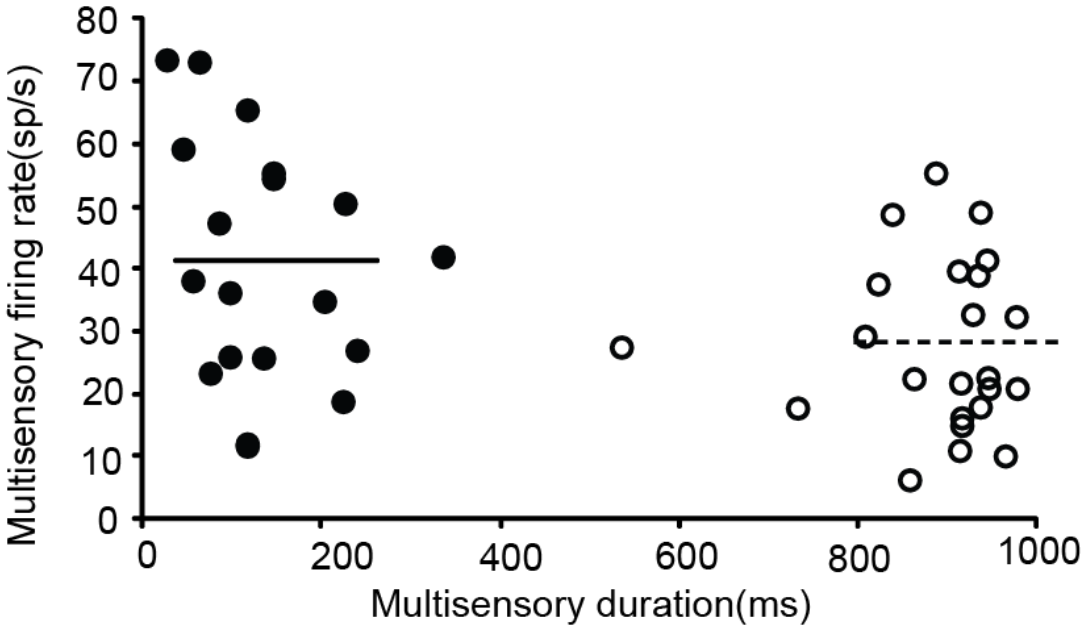

Figure 3-7: Relationship between multisensory firing rate and multisensory duration of response.

Overall short discharge duration (closed circles) is accompanied by high firing rates while long discharge durations (open circles) are accompanied by low firing rates ($R = -0.39$, $p = 0.009$). The horizontal solid line represents the mean firing rate for short discharge durations (41.5 sp/s) which is significantly higher than the mean firing rate for long responses (27.5 sp/s) (t test, $p=0.0085$).

Response dynamics under tonic mode firing conditions

In an effort to determine the evolution of multisensory integration during long duration responses, the multisensory response for neurons exhibiting long duration discharges was divided into 3 equivalent epochs: early, middle and late. The rationale for this division was to create temporal epochs comparable to the short duration responses and to examine whether interactions happening on shorter timescales were not averaged out as a result of the longer duration responses. In addition, prior work has highlighted the temporal evolution of multisensory responses in SC neurons (Royal et al. 2009), and has shown that significant interactions often accompany the earliest and latest phases of response (no distinctions in this prior work was made between short duration and long duration responses).

For this analysis, neurons were further divided based on the presence of either overt responses to stimuli in both the visual and auditory modalities (frank or overt neurons) and those with only an overt response in one modality but which was modulated by the other modality (modulatory neurons). In the vast majority (81%) of the frank/overt neurons, significant multisensory enhancements (i.e., gains in interactive index) were indeed seen during the earliest response epoch. In contrast, significant interactions were rare in the middle (6%) and late (13%) response epochs. Mean statistical contrast revealed a similar pattern, with superadditive interactions being most commonly found in the early response epoch (43%). In contrast, superadditivity was rare in the middle and late epochs of the response (13% and 6%, respectively). In striking contrast, modulatory neurons rarely showed significant interactions in any of the response epochs. Figure 8 shows the contrast measures for early, mid and late phases of

integration for a subset of mixed neurons (both frank and modulatory neurons are included).

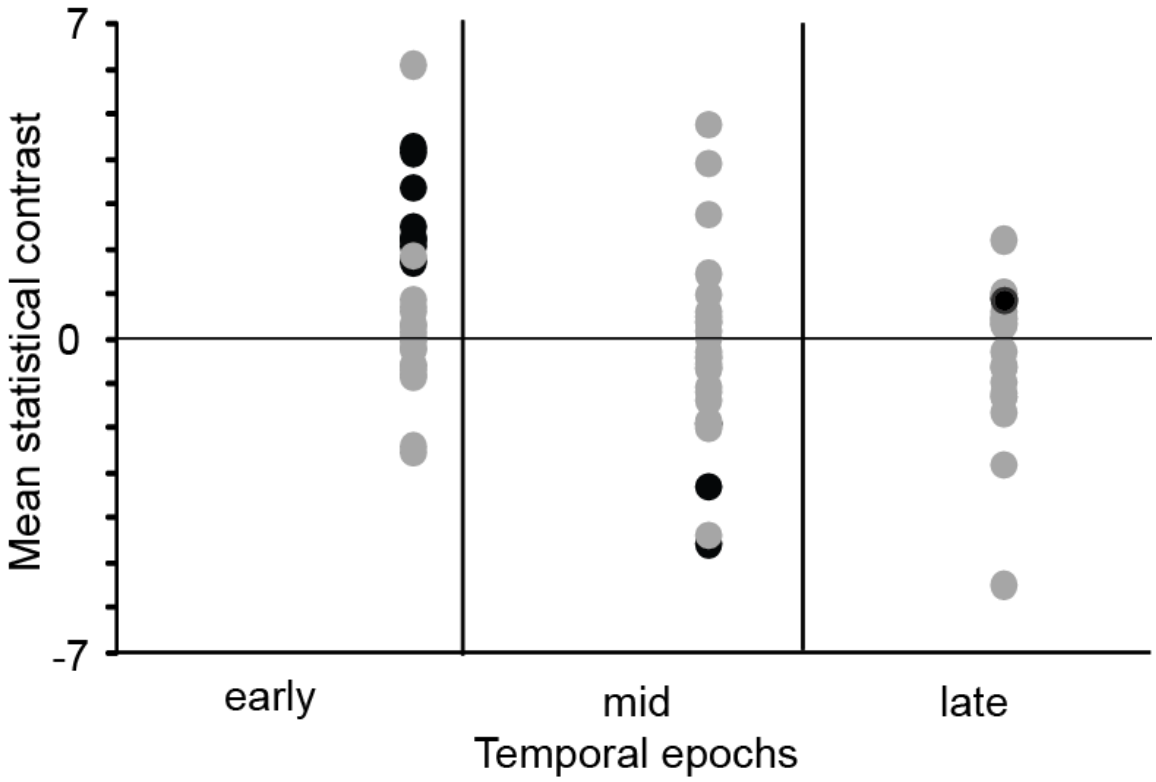

Figure 3-8: Phases of integration.

Contrast measures for the early, mid and late phases of integration for the long discharge duration of a subset of neurons. The early phase is characterized by super-additive interactions while the mid and late phases are characterized by additive interactions. Black circles represent statistically significant msc values ($p<0.05$) while grey circles represent non-significant values as measured by Wilcoxon Rank Test.

Discussion

In the current study, we show for the first time that multisensory SC neurons exhibit marked heterogeneity in the temporal characteristics of their sensory responses, and that one aspect of this heterogeneity (response duration) is intimately tied to integrative capacity. Thus, response duration was negatively associated with integrative capacity, such that short duration responses were strongly associated with high integrative capacity and long duration responses were associated with lower (or absent) integrative capacity. Although the relationship between discharge duration and multisensory integration appears to be a continuous one (see Fig 3-3), we chose to divide the population into short and long duration responses in order to best illustrate the relationship between duration and integration. Despite the fact that multisensory SC neurons and their integrative abilities has been the subject of study for over two decades, the heterogeneous nature of the large receptive fields of these neurons have been poorly characterized. Prior work that has focused on this question has largely detailed the *spatial* heterogeneity of these large receptive fields, showing that responses to the same stimuli can differ by several-fold simply based on their location within the receptive field (Kadunce et al., 2001; Krueger et al., 2009). In the current study we focus on the dimension of time, and add an additional layer of description to our understanding of how neuronal response characteristics contribute to the final integrative product. The ultimate goal of this work is to provide a complete description of how the *spatiotemporal* receptive field shapes the nature of the multisensory response, a description that will not only provide insight into the complex computations carried out

by these neurons (and thus provide important clues as to their biophysical basis), but that will also provide a more realistic description of ***how*** multisensory neurons integrate real world sensory cues.

Response duration as a determinant of multisensory integration

Prior work has highlighted that multisensory SC neurons depend critically on a number of stimulus-related factors in determining the integrative product when presented with paired multisensory stimuli. The most salient of these are space, time and effectiveness, such that the combination of multisensory stimuli that are spatially and temporally coincident, and that are weakly effective when presented on their own, result in the largest multisensory interactions (Meredith and Stein., 1986; Meredith et al., 1987; Meredith and Stein., 1996).

More recently, work has expanded these determinants to include “neuron specific” factors (Perrault et al., 2003, 2005). In these prior studies, it was established that neuronal characteristics such as spontaneous firing rate and dynamic range were important in determining the multisensory capacity of a given neuron, with those having lower spontaneous firing rates and smaller dynamic ranges exhibiting the highest multisensory gains. The current study extends upon this framework by illustrating an important association between a neuron’s temporal response dynamics, specifically discharge duration, and its multisensory integrative capacity.

The current results fit well within the recent emphasis that has focused on better detailing the temporal characteristics of multisensory integration. For example, in addition to work from our own lab (Royal et al., 2009), Rowland and colleagues (2007)

(Rowland et al., 2007a) have shown that multisensory enhancement is greatest in the initial phase of the multisensory response, a property that these authors have described as “Initial Response Enhancement (IRE).” Concordant with this are the results of the current work, in which the temporal epoch analysis demonstrates that it is the earliest part of the response that is characterized by superadditive interactions.

Placing these results in a behavioral context, early superadditive enhancements in response, coupled with a latency shift (i.e., speeding) under multisensory conditions, could readily provide the initial coding framework that ultimately results in the faster and more accurate gaze shifts that are seen under multisensory (i.e., visual-auditory) situations (Hughes et al., 1994; Frens et al., 1995; Goldring et al., 1996; Corneil et al., 2002). In such a model, these early changes in sensory encoding are ultimately transformed into premotor and motor commands that drive the resulting facilitated orientation response. The current study provides a unique view into the multisensory populations that may contribute to such behavioral gains. Thus, in addition to the short duration responses, which fit quite readily onto this interpretation, the earliest phase of the longer duration responses also exhibits superadditive interactions and could also play a role in speeded responses.

In addition to reinforcing the importance of these early multisensory interactions, one of the key findings of the current study is that majority of the multisensory SC neurons also carry a longer duration response component that is largely additive and whose role in multisensory processing remains unresolved. One possibility for such longer duration responses is that they are carrying more feature-related information about the multisensory stimulus complex. One candidate for this is motion-related information,

given the central role that the SC plays in signaling the location of a stimulus of interest, and the strong motion selectivity of its constituent neurons (Dreher and Hoffmann, 1973; Stein BE 1993). Such a speculation suggests additional experiments to examine these later response components in the context of manipulations in the structure of the multisensory pair.

These types of distinctions are likely not unique to multisensory systems. Indeed, similar results are seen within the visual system in which phasic or burst mode of firing has been linked with stimulus detection while tonic mode has been linked to stimulus analysis (Guido et al., 1995; Sherman, 1996). In addition, phasic firing has been linked to less variability, increased signal to noise ratio and better signal detection in the visual thalamus (Guido et al., 1992; Guido and Sherman, 1998). Ongoing studies are testing to see if response duration is also linked to lower variability in multisensory SC neurons.

In addition, in this study we show that, overall multisensory response durations are longer than their best unisensory counterparts under conditions of response enhancements and shorter under conditions of response depressions. Also, when no integration occur response durations between the two conditions do not differ. This finding is important because it implies that not only can multisensory response duration act as a determinant of the amount of multisensory integration (i.e., short response with high integration, long response with low integration) but also it can offer insights into the nature of integration that the neuron engages in. Thus, by knowing the response durations in the best unisensory and multisensory conditions of the neuron, it is possible to determine both the nature and integrative capacity of the neuron. This may prove to be very useful for future modeling studies (see below).

Implications of response modes for modeling multisensory processes

There has been a great deal of recent interest focused towards the modeling of multisensory integration, largely as an effort to provide more insight into the mechanistic underpinnings of the integrative capacity of multisensory neurons (Anastasio et al., 2000; Xing and Andersen, 2000; Anastasio and Patton, 2003; Diederich and Colonius, 2004; Avillac et al., 2005; Rowland et al., 2007b). Much of this work has been built around the original principles of integration (i.e., space, time and effectiveness), which provide a good first order characterization of the integrative abilities of these neurons. However, these principles are incomplete in explaining the behavior of these neurons. Indeed, this incompleteness was the motivation for follow-up studies that began to focus on neuron-specific factors, such as spontaneous activity and dynamic range (Perrault et al., 2005). As models of multisensory integration become increasingly sophisticated (see (Cuppini et al., 2010) for a recent incarnation), these stimulus- and neuron-specific factors must be incorporated in an effort to provide the most comprehensive view possible into these processes. The present study provides an important insight into one of the mechanisms (response duration changes) by which the neurons in SC may be engaging in multisensory integration. Consequently, these findings may serve as an important tool for future modeling studies that may be directed towards the development of a more complete model with higher predictive capabilities incorporating the various factors that have been empirically shown to affect the integrative abilities of these multisensory neurons in addition to the original principles of integration.

Functional implications for different response modes in SC multisensory neurons

The role of the SC in stimulus detection, localization and orientation behavior has been well documented. Multisensory-mediated improvements in these processes have also been well established, as has the role of the intermediate and deep SC in gating these behavioral improvements (Burnett et al., 2004). Despite the strong correlative links between the activity of multisensory SC neurons and these behavioral facilitations, our understanding of how (multi) sensory signals are transformed into effective motor commands remains rather poorly understood. Only through a more thorough characterization of the complexities of multisensory neurons and their integrative properties will this understanding be improved to provide a better view into the nature of these important sensorimotor transformations. This knowledge can then be used to tailor the design of experiments in awake and behaving preparations in which the relationship between sensory firing patterns, motor responses and behavioral outcomes can be assessed. . Such studies are becoming increasingly common (Iurilli et al., 2012; Wang et al., 2008; Wallace et al., 1998), but are crucially dependent upon the results of studies in anesthetized animals that allow detailed relationships to be drawn between receptive field architecture, temporal response dynamics and multisensory integration.

How short and long response modes arise in SC neurons remains unknown. One intriguing possibility is that these differing modes are in some way associated with changes in the nature of the oscillatory inputs to these neurons. Thus, it has been shown that stimulus timing plays an integral role in the phase and amplitude of ongoing oscillations, and can play a dramatic role in the amplifying (or weakening) neuronal response (Lakatos et al., 2007). Ongoing studies in the lab are analyzing local field

potentials (LFPs) in these same neurons in an effort to examine the relationship between response mode, oscillations and integrative capacity in SC neurons, with the hope of providing a better view into how LFPs may represent the nature of the multisensory encoding.

Finally, the differences in response duration and integrative abilities that are seen within the large receptive fields of these neurons are most likely a reflection of the input architecture of the visual and auditory inputs onto these neurons. The purpose of such heterogeneous receptive fields (some even with multiple “hotspots”) remains unknown, but as alluded to earlier, such heterogeneity and asymmetry may serve as the substrate for processing of dynamic (i.e., moving) stimulus elements, similar to what has been reported in the different sensory systems (Dreher and Hoffmann 1973, Krueger et al 2009) . In a recent study of motion processing, multisensory benefits are seen more in the periphery than in the center (Macneilage et al 2012), a result that may be related to the heterogeneous and asymmetrical receptive field structure that appears to characterize these complex multisensory neurons.

Bibliography

Anastasio TJ, and Patton PE. A two-stage unsupervised learning algorithm reproduces multisensory enhancement in a neural network model of the corticotectal system. *J Neurosci* 23: 6713-6727, 2003.

Anastasio TJ, Patton PE, and Belkacem-Boussaid K. Using Bayes' rule to model multisensory enhancement in the superior colliculus. *Neural Comput* 12: 1165-1187, 2000.

Avillac M, Deneve S, Olivier E, Pouget A, and Duhamel JR. Reference frames for representing visual and tactile locations in parietal cortex. *Nat Neurosci* 8: 941-949, 2005.

Burnett LR, Stein BE, Chaponis D, and Wallace MT. Superior colliculus lesions preferentially disrupt multisensory orientation. *Neuroscience* 124: 535-547, 2004.

Carriere BN, Royal DW, and Wallace MT. Spatial heterogeneity of cortical receptive fields and its impact on multisensory interactions. *J Neurophysiol* 99: 2357-2368, 2008.

Corneil BD, and Munoz DP. The influence of auditory and visual distractors on human orienting gaze shifts. *J Neurosci* 16: 8193-8207, 1996.

Corneil BD, Van Wanrooij M, Munoz DP, and Van Opstal AJ. Auditory-visual interactions subserving goal-directed saccades in a complex scene. *J Neurophysiol* 88: 438-454, 2002.

Cuppini C, Ursino M, Magosso E, Rowland BA, and Stein BE. An emergent model of multisensory integration in superior colliculus neurons. *Front Integr Neurosci* 4: 6, 2010.

Diederich A, and Colonius H. Bimodal and trimodal multisensory enhancement: effects of stimulus onset and intensity on reaction time. *Percept Psychophys* 66: 1388-1404, 2004.

Dreher B, and Hoffmann KP. Properties of excitatory and inhibitory regions in the receptive fields of single units in the cat's superior colliculus. *Exp Brain Res* 16: 333-353, 1973.

Edwards SB, Rosenquist AC, and Palmer LA. An autoradiographic study of ventral lateral geniculate projections in the cat. *Brain Res* 72: 282-287, 1974.

Frens MA, and Van Opstal AJ. Visual-auditory interactions modulate saccade-related activity in monkey superior colliculus. *Brain Res Bull* 46: 211-224, 1998.

Frens MA, Van Opstal AJ, and Van der Willigen RF. Spatial and temporal factors determine auditory-visual interactions in human saccadic eye movements. *Percept Psychophys* 57: 802-816, 1995.

Ghose D, Fister MC, Wallace MT. The influence of spatial receptive field architecture on the temporal dynamics of multisensory interactions in the superior colliculus.(Abstract) 370.2. *2010 Neuroscience Meeting Planner. San Diego, CA: Society for Neuroscience, 2010*. *Online.*

Goldring JE, Dorris MC, Corneil BD, Ballantyne PA, and Munoz DP. Combined eye-head gaze shifts to visual and auditory targets in humans. *Exp Brain Res* 111: 68-78, 1996.

Guido W, Lu SM, and Sherman SM. Relative contributions of burst and tonic responses to the receptive field properties of lateral geniculate neurons in the cat. *J Neurophysiol* 68: 2199-2211, 1992.

Guido W, Lu SM, Vaughan JW, Godwin DW, and Sherman SM. Receiver operating characteristic (ROC) analysis of neurons in the cat's lateral geniculate nucleus during tonic and burst response mode. *Vis Neurosci* 12: 723-741, 1995.

Guido W, and Sherman SM. Response latencies of cells in the cat's lateral geniculate nucleus are less variable during burst than tonic firing. *Vis Neurosci* 15: 231-237, 1998.

Harrington LK, and Peck CK. Spatial disparity affects visual-auditory interactions in human sensorimotor processing. *Exp Brain Res* 122: 247-252, 1998.

Huerta MF HJ. Comparative Neurology of Optic tectum. 1984.

Hughes HC, Nelson MD, and Aronchick DM. Spatial characteristics of visual-auditory summation in human saccades. *Vision Res* 38: 3955-3963, 1998.

Hughes HC, Reuter-Lorenz PA, Nozawa G, and Fendrich R. Visual-auditory interactions in sensorimotor processing: saccades versus manual responses. *J Exp Psychol Hum Percept Perform* 20: 131-153, 1994.

Iurilli G, Ghezzi D, Olcese U, Lassi G, Nazzaro C, Tonini R, Tucci V, Benfenati F, Medini P. Sound-driven synaptic inhibition in primary visual cortex. *Neuron* 73(4): 814-828, 2012.

Kadunce DC, Vaughan JW, Wallace MT, Benedek G, and Stein BE. Mechanisms of within- and cross-modality suppression in the superior colliculus. *J Neurophysiol* 78: 2834-2847, 1997.

Kadunce DC, Vaughan JW, Wallace MT, and Stein BE. The influence of visual and auditory receptive field organization on multisensory integration in the superior colliculus. *Exp Brain Res* 139: 303-310, 2001.

Krueger J, Royal DW, Fister MC, and Wallace MT. Spatial receptive field organization of multisensory neurons and its impact on multisensory interactions. *Hear Res* 258: 47-54, 2009.

Lakatos P, Chen CM, O'Connell MN, Mills A, Schroeder CE. Neuronal oscillations and multisensory interaction in primary auditory cortex. *Neuron* 53(2): 279-292, 2007

Macneilage PR, Zhang Z, Deangelis GC,Angelaki DE. Vestibular facilitation of optic flow parsing. PLoS One 7(7):e40264,2012.

Marino RA, Levy R, Boehnke S, White BJ, Itti L, Munoz DP. Linking visual response properties in the superior colliculus to saccade behavior. *Eur J Neurosci* 11: 1738-1752, 2012.

Marino RA, Trappenberg TP, Dorris M, Munoz DP. Spatial Interactions in the superior colliculus predict saccade behavior in a neural field model. *J Cogn Neurosci* 24(2): 315-336, 2012.

Marino RA, Rodgers CK, Levy R, Munoz DP. Spatial relationships of visuomotor transformations in the superior colliculus map. *J Neurophysiol* 100(5): 2564-2576, 2008.

Meredith MA, Nemitz JW, and Stein BE. Determinants of multisensory integration in superior colliculus neurons. I. Temporal factors. *J Neurosci* 7: 3215-3229, 1987.

Meredith MA, and Stein BE. Interactions among converging sensory inputs in the superior colliculus. *Science* 221: 389-391, 1983.

Meredith MA, and Stein BE. Spatial determinants of multisensory integration in cat superior colliculus neurons. *J Neurophysiol* 75: 1843-1857, 1996.

Meredith MA, and Stein BE. Spatial factors determine the activity of multisensory neurons in cat superior colliculus. *Brain Res* 365: 350-354, 1986.

Meredith MA, and Stein BE. Visual, auditory, and somatosensory convergence on cells in superior colliculus results in multisensory integration. *J Neurophysiol* 56: 640-662, 1986.

Meredith MA, and Stein BE. The visuotopic component of the multisensory map in the deep laminae of the cat superior colliculus. *J Neurosci* 10: 3727-3742, 1990.

Mucke L, Norita M, Benedek G, and Creutzfeldt O. Physiologic and anatomic investigation of a visual cortical area situated in the ventral bank of the anterior ectosylvian sulcus of the cat. *Exp Brain Res* 46: 1-11, 1982.

Munoz DP, and Guitton D. Fixation and orientation control by the tecto-reticulo-spinal system in the cat whose head is unrestrained. *Rev Neurol (Paris)* 145: 567-579, 1989.

Munoz DP, and Guitton D. Tectospinal neurons in the cat have discharges coding gaze position error. *Brain Res* 341: 184-188, 1985.

Perrault TJ, Jr., Vaughan JW, Stein BE, and Wallace MT. Neuron-specific response characteristics predict the magnitude of multisensory integration. *J Neurophysiol* 90: 4022-4026, 2003.

Perrault TJ, Jr., Vaughan JW, Stein BE, and Wallace MT. Superior colliculus neurons use distinct operational modes in the integration of multisensory stimuli. *J Neurophysiol* 93: 2575-2586, 2005.

Populin LC, Yin TC. Bimodal interactions in the superior colliculus of the behaving cat. *J Neurosci* 22(7): 2826-2834, 2002.

Populin LC. Anesthetics change the excitation/inhibition balance that governs sensory processing in the cat superior colliculus. *J Neurosci* 25(25): 5903-5914, 2005.

Rowland BA, Quessy S, Stanford TR, and Stein BE. Multisensory integration shortens physiological response latencies. *J Neurosci* 27: 5879-5884, 2007.

Rowland BA, Stanford TR, and Stein BE. A model of the neural mechanisms underlying multisensory integration in the superior colliculus. *Perception* 36: 1431-1443, 2007.

Rowland BA, and Stein BE. Multisensory integration produces an initial response enhancement. *Front Integr Neurosci* 1: 4, 2007.

Royal DW, Carriere BN, and Wallace MT. Spatiotemporal architecture of cortical receptive fields and its impact on multisensory interactions. *Exp Brain Res* 198: 127-136, 2009.

Sherman SM. Dual response modes in lateral geniculate neurons: mechanisms and functions. *Vis Neurosci* 13: 205-213, 1996.

Sparks DL, and Mays LE. Spatial localization of saccade targets. I. Compensation for stimulation-induced perturbations in eye position. *J Neurophysiol* 49: 45-63, 1983.

Stanford TR, Quessy S, and Stein BE. Evaluating the operations underlying multisensory integration in the cat superior colliculus. *J Neurosci* 25: 6499-6508, 2005.

Stanford TR, and Stein BE. Superadditivity in multisensory integration: putting the computation in context. *Neuroreport* 18: 787-792, 2007.

Stein BE MA. The Merging of the Senses. *Book* 1993.

Tortelly A, Reinoso-Suarez F, and Llamas A. Projections from non-visual cortical areas to the superior colliculus demonstrated by retrograde transport of HRP in the cat. *Brain Res* 188: 543-549, 1980.

Wallace MT, Meredith MA and Stein BE. Converging influences from visual, auditory, and somatosensory cortices onto output neurons of the superior colliculus. *J. Neurophysiol.* 69: 1797-1809, 1993.

Wallace MT, Stein BE. Cross modal synthesis in the midbrain depends on input from cortex. *J Neurophysiol* 71(1): 429-432, 1994.

Wallace MT, and Stein BE. Sensory organization of the superior colliculus in cat and monkey. *Prog Brain Res* 112: 301-311, 1996.

Wallace MT, Meredith MA, Stein BE. Multisensory integration in the superior colliculus of alert cat. *J Neurophysiol* 80(2): 1006-1010, 1998.

Wang Y, Celebrini S, Trotter Y, Barone P. Visuo-auditory interactions in the primary visual cortex of the behaving monkey: electrophysiological evidence. *BMC Neurosci*. 9: 79, 2008.

Xing J, and Andersen RA. Models of the posterior parietal cortex which perform multimodal integration and represent space in several coordinate frames. *J Cogn Neurosci* 12: 601-614, 2000.

CHAPTER IV

MULTISENSORY RESPONSE MODULATION IN THE SUPERFICIAL LAYERS OF THE SUPERIOR COLLICULUS

This chapter is a manuscript under preparation to be submitted to "Journal of Neuroscience" as: ***Ghose D, Maier A, Nidiffer AR and Wallace MT****. Multisensory integration in the superficial layers of the superior colliculus.*

Introduction

The mammalian superior colliculus (SC) has been shown to play an integral role in moving the eyes, ears and head toward a stimulus of interest (Huerta MF, 1984; Munoz and Guitton, 1985, 1989). Traditionally, the SC has been divided into two structural/functional distinctions – superficial and intermediate/deep layers. This classic distinction is based on observations that the superficial layers are exclusively visual while the intermediate and deep layers show visual, auditory and somatosensory responses as well as premotor activity (Casagrande et al., 1972; Ogasawara et al., 1984; Grantyn and Berthoz, 1985; Meredith and Stein, 1986a; Stein BE 1993; May, 2006). This functional dichotomy is also reflected in the respective input/output architecture of these two laminar compartments, which differ dramatically from one another (Edwards et al., 1979; Kudo and Niimi, 1980; Tortelly et al., 1980; Kudo, 1981;

Clemo and Stein, 1982; Mucke et al., 1982; Huerta MF, 1984; Segal and Beckstead, 1984).

Recent anatomical evidence has revealed reciprocal connections between the superficial and intermediate/deep layers of the SC, suggesting the presence of functional interactions previously thought to be limited across these layers. Most notably, neurons in the deeper SC layers have been shown to have axons and apical dendrites that extend up into the superficial layers, thus providing a possible substrate for functional interactions between these major laminar compartments (Behan et al., 1987; Behan and Appell, 1992; Behan and Kime, 1996; Hall and Lee, 1997; Doubell et al., 2003).This anatomical finding raises questions about the strict functional distinctions that have been drawn across the SC layers, including the absence of multisensory influences in the superficial layers. This question is particularly pressing as the vast majority of neurophysiological studies conducted within the superficial SC layers have used only visual stimuli.

In the current study we examine the impact of auditory stimuli on visual responses in the superficial layers of the cat SC. In addition to assessing if (and how) auditory stimuli impact visually evoked spiking responses, the analyses also tested for multisensory interactions in the local field potential (LFP), which has been shown to be sensitive to (subthreshold, weak and modulatory) synaptic processes. Our results show, for the first time, that auditory stimulation significantly alters the nature of visual information processing in the superficial layers of the mammalian SC.

Methods

General procedures: Experiments were conducted in adult cats (n=2) raised under standard housing conditions. All experiments were done in an anesthetized and paralyzed semi-chronic preparation (see below) and consisted of multi-unit and LFP extracellular recordings from the midbrain superior colliculus (SC). Experiments were run on a weekly basis on each of the animals. All surgical and recording procedures were performed in compliance with the Guide for the Care and Use of Laboratory Animals at Vanderbilt University Medical Center, which is accredited by the American Association for Accreditation of Laboratory Animal Care.

Implantation and recording procedures: For anesthesia during surgical procedures animals were initially induced with ketamine hydrochloride (20 mg/kg, administered intramuscularly (im)) and acepromazine maleate (0.04 mg/kg im). For implantation of the recording chamber over the SC, animals were transported to a central surgical suite, where they were intubated and artificially respired. A stable plane of surgical anesthesia was achieved using inhalation of isoflurane (1%-3%). Body temperature, expiratory CO^2, blood pressure and heart rate were continuously monitored (VSM7, Vetspecs/SCIL), recorded and maintained within ranges consistent with a deep and stable plane of anesthesia. A craniotomy was made to allow access to SC and a head holder was attached to the skull using stainless steel screws and orthopedic cement to hold the animal during recording sessions without obstructing the face and ears. Post-

operative care (antibiotics and analgesics) was done in close consultation with veterinary staff.

For neurophysiological recordings, animals were anesthetized with ketamine (20mg/kg im) and acepromazine maleate (0.04mg/kg im) and maintained throughout the procedure with a constant rate infusion of ketamine (5mg/kg/hr iv), delivered through a cannula placed in the saphenous vein. The head holding system was used to keep the animal comfortably in a recumbent position. In order to prevent ocular drift, animals were paralyzed using pancuronium bromide or vecuronium bromide (0.1mg/kg/hr, iv), and artificially respired for the duration of recording. On completion of experiments, animals were subcutaneously given 60-100 ml of lactated Ringer solution to facilitate recovery. Parylene-insulated tungsten electrodes (initial impedance at 1kHz = 4-5 MΩ) were advanced into the SC using an electronically controlled mechanical microdrive. Multi-unit neural activity (MUA), defined as voltage peaks crossing a pre-set threshold (2 standard deviations from the mean), and LFP (1-300 Hz) were recorded, amplified and routed to an oscilloscope, audio monitor and computer for performing online and offline analysis (see below for details).

Stimulus presentation, receptive field mapping and search strategy*:* The superficial layers of the SC were identified by their characteristic burst-like firing (Wurtz and Albano, 1980; Grantyn et al., 1983; Lo et al., 1998). The visual receptive fields of the MUA were mapped via a Keeler Pantoscope using rectangular bars and moving spots of light (1-6° in diameter) until reliable boundaries of the minimal response field could be discerned. Receptive fields and associated recordings were performed at three different depths during each electrode penetration.

First, the top of SC (just beneath the pial surface) was identified by the initial appearance of the characteristic robust responses elicited by moving visual stimuli. Once identified, the receptive field(s) at this location was mapped. Following this determination of receptive field borders, stimuli were presented from an array of locations both within and outside of the receptive field in an randomly interleaved fashion while both MUA and LFP responses were recorded. Once data was recorded from this most superficial location, the electrode was advanced by 200-300 μm, the receptive field was mapped again, and a stimulus battery was presented as above. This procedure was repeated at a depth an additional 700-1000 μm below the location of the second recording.

Visual stimuli consisted of the illumination of stationary light emitting diodes (LEDs: 100 ms duration, luminance = 104cd/m^2). Auditory stimuli were delivered through speakers, (DigiKey, impedance = 8Ω) and consisted of 100 ms duration broadband (20Hz-20KHz) noise bursts with an intensity of 67dB SPL on a background of 45 dB SPL, measured at the head of the animal with a sound level meter (Larson Davis SoundTrack LxT, Depew, NY). Both the LED and the speakers were mounted on a hoop placed 60 cm in front of the animal at azimuthal locations ranging from 0-90° on either side of the midline, in 10° increments. The hoop was rotated along different elevations that allowed sampling of locations from 90° above to 40° below the interaural plane, again in 10° increments. The physical characteristics of the stimuli were identical in all respects, except for the spatial location at which they were presented. Multisensory combinations consisted of visual and auditory stimuli presented at the same spatial location. The order in which stimulus locations were tested was pseudo-

randomized along a single elevation. A minimum of 60 trials (i.e., 20 visual, 20 auditory, 20 multisensory) was collected for any given stimulus location. In most cases, 40 trials per condition were obtained. Consecutive stimulus presentations were separated by at least 1.5 s and randomly jittered to avoid neural response habituation.

Two different conditions of stimulus timing (stimulus onset asynchrony, or SOA) were used throughout the study - simultaneous visual and auditory stimulation (V0A0) and with the visual stimulus preceding the auditory stimulus by 50 ms (V0A50). These intervals were chosen based on prior data suggesting that these SOAs optimize the opportunity for multisensory interactions (Meredith et al., 1987; Stein BE 1993; Ghose et al., 2012).

Data acquisition and analysis: A custom built PC-based real time data acquisition system controlled the structure of the trials and the timing of the stimulus, using custom scripts written in Labview (National Instruments, Austin, TX). The analog waveform of the extracellular voltage fluctuations picked up by the electrode were transferred to a Plexon MAP system (Plexon Inc., Dallas, TX) where they were high-pass filtered and digitized at 40kHz (for spikes) and low-pass filtered and digitized at 1kHz (for LFP). MUA responses were thresholded and sorted online using the Sort Client software (Plexon Inc., Dallas, TX). Spike time stamps were recorded and stored digitally for offline analysis. Using custom MATLAB scripts, (Mathworks, Natick, MA), neuronal responses were characterized through construction of peristimulus time histograms (PSTHs) and rasters for each condition [visual only (V), auditory only (A), visual-auditory together (AV)] and for each location tested within the spatial receptive field (SRF). Baseline activity for each PSTH was calculated as mean firing rate during the 500 ms

period immediately preceding stimulus onset. Stimulus-evoked response onset was defined as the first spike within the bin at which i) the PSTH crossed above a virtual threshold of two standard deviations (SD) above baseline and ii) remained above this value for at least 30 ms. Response offset was defined as the latest time at which the PSTH remained belowhe two SD threshold for >=30 ms. Mean spontaneous firing rate was subtracted from responses to obtain the mean stimulus evoked response for all the three conditions. Data was collected for a total of 55 recording sessions. Latency was calculated as the difference between time of stimulus onset and response onset.

Measures for quantifying multisensory integration: Two separate statistical measures were used to assess multisensory integration. The first measure, called the interactive index (ii), measures how the multisensory response differs from the largest evoked unisensory response. The magnitude of this change was calculated as:

$$ii = \frac{CM - SM_{max}}{SM_{max}} \times 100$$

where *CM* is the mean response evoked by the combined modality stimulus, and SM_{max} is the mean response evoked by the most effective single modality stimulus (Meredith and Stein, 1983, 1986b, a). Statistical comparisons between these conditions were done using a non-parametric Wilcoxon Rank Test. Response *enhancement* was defined as statistically significant positive ii values, whereas response *depression* was defined as statistically significant negative ii values. All cases where ii values were statistically non-significant were deemed as showing *no interaction*.

The second measure is termed mean statistical contrast (msc). This metric evaluates whether the multisensory response exceeds the response predicted by summation of the two component unisensory responses. Multisensory contrast is calculated using the formula:

$$msc = \frac{\sum AV_i - (A_i + V_i)}{n}$$

where, A_i is the evoked auditory response on a given trial (i), V_i is the evoked visual response on a given trial, AV_i is the evoked multisensory response on a given trial and n is the number of trials. The msc model assumes independence between the visual and auditory inputs and uses additive factors logic to distinguish between subadditive (contrast < 0), additive (contrast = 0) and superadditive (contrast > 0) modes of integration (Perrault et al., 2003, 2005; Stanford et al., 2005; Stanford and Stein, 2007). Significant differences from a contrast value of 0 were determined by the Wilcoxon Rank test.

Evoked LFP analyses: LFPs were sampled at 1000 Hz and converted to voltage as a function of time. To quantify the peak LFP amplitude, for both of the recorded SOAs (V0A0 and V0A50 respectively), the evoked LFP response for all stimulus locations showing response enhancements in the spiking data (see above) were averaged to produce a grand average Event-Related Potential (ERP). This procedure was repeated for all stimulus locations showing response depression as well as those showing no interaction. To quantify the changes in LFP amplitude in response to the stimuli, we compared LFP amplitude pre- and post-stimulus onset using Student's t-test (using Bonferroni correction for multiple comparisons) for each condition. More specifically, the

mean voltage within a 150 ms pre-stimulus window was taken as the baseline. Peak voltage changes within a window 300 ms post-stimulus presentation were then compared against this baseline in order to assess stimulus related changes in the LFP. Next, mean peak voltages within the response window were compared between visual and multisensory conditions using a t test to determine whether the visually-evoked LFP amplitude differed significantly from the multisensory LFP amplitude.

In addition to these peak-based analyses, the area under the curve for the averaged evoked LFPs over the interval spanning 0-200 ms post-stimulus were computed for the three stimulus conditions (V, A, AV) for each of the different types of interactions (response enhancement, response depression and no interaction) and for both SOAs (V0A0 and V0A50). Next, for each of the different types of interactions, the area under the curve for the visual condition was statistically compared to that of the multisensory condition using t tests. The choice of the 200 ms post-stimulus analysis window was based on visual inspection of the data to capture the majority of the stimulus evoked changes. Additionally, to quantify the late changes observed in averaged evoked LFP traces, area under the curve was also computed for the interval 201-300 ms (middle epoch) and 301-1400 ms (late epoch) after stimulus onset. The middle epoch (200-300ms post stimulus exhibited positive deflections for all three modalities and hence analyzed separate from the early epoch which exhibited negative deflections for all three modalities. Similar statistical comparisons were made as described above.

Time Frequency Analysis of LFPs: To test for stimulus-induced LFP power changes in different frequency bands, spectrograms were computed using an Fast Fourier Transform (FFT) with a running (Hamming) window size of 256 ms and an overlap of

255 ms. Each spectrogram was normalized to a pre-stimulus baseline by subtracting the average baseline power for each frequency band from the entire spectrogram, and dividing the result by the same baseline power (thus yielding fractional change). Note that a 60 Hz notch filter was used during recordings in order to eliminate AC noise. As a consequence, we have no data for this frequency band. Spectrograms were computed separately for stimulus locations within the receptive field that evoked response enhancement, response depression, or no significant interaction as defined by the local spiking response (see above). Contrast plots were then computed by subtracting the respective spectrogram pairs in order to determine the effects of multisensory stimulation on LFP responses. More specifically, contrast was defined as the LFP power difference between the multisensory condition and the unisensory visual condition (AV > V). Results for both comparisons were converted to t-scores for statistical comparison using the following formula:

$$t = \frac{\overline{AV} - \bar{V}}{\frac{SD}{\sqrt{n_1 + n_2}}}$$

where *SD* is the standard deviation of responses across both conditions, and n_1 and n_2 are the number of trials for condition 1 and condition 2, respectively. False discovery rate (FDR) at a level of 0.01 was used to correct for multiple comparisons. Similar results were achieved when Bonferroni correction was applied.

A two-way ANOVA with factors of response category (e.g., enhancement vs. no interaction) and SOA (0 ms vs. 50 ms) was computed comparing significant changes in activation(using FDR as a correction to control false positives) for the regions of high

gamma activity (70-90 Hz) within 350 ms of stimulus onset in the contrast (AV > V) spectrograms. Follow-up t-tests were calculated to compare levels within individual factors (e.g., enhancement vs. no interaction within a single SOA).

Results

Receptive field size and response latency differ between the superficial and deeper layers of the SC

In an effort to restrict our analyses to neurons in the superficial layers of SC, we employed several electrophysiological criteria that have been previously shown to differentiate between the superficial and deeper layers (Sterling and Wickelgren, 1969; Sterling, 1971; Wurtz and Albano, 1980; Meredith and Stein, 1990). The two most informative of these measures are visual receptive field size and response latency. Single unit and multiunit activity (MUA) along with local field potentials (LFP) were recorded from three different depths along a total of 55 different electrode penetrations.

Consistent with prior work, a systematic increase in visual receptive field size was observed as the electrode advanced deeper into the SC (Fig. 4-1). Whereas depth 1 was always at the first appearance of the characteristic visual responses of the SC, depth 2 was 200-300 μm below this location, and depth 3 was 1000-1400 μm from the beginning of the evoked visual responses (i.e., top of SC). The relationship between RF

size and recording depth is quantified in figure 4-2A, and which reveals the systematic change in visual RF size as the electrode transitions from superficial to deeper layers. A one-way repeated-measures ANOVA confirmed that visual receptive field size (i.e., area) was significantly different for the different recording depths ($F_{(2,134)} = 474.15$, $P = 5.5 \times 10^{-61}$). Follow up t tests indicated that the visual RFs of neurons at each depth differed significantly (depth 1 vs. depth 2: t= -17.8, $p = 1.1 \times 10^{-21}$; depth 1 vs. depth 3: t = -26.7, $p = 7.8 \times 10^{-29}$; depth 2 vs. depth 3: t = 22.18, $p = 1.6 \times 10^{-25}$).

In addition to these differences in RF size, consistent changes in visual response latency were observed as a function of recording depth. The relationship between changes in response latency and changes in recording depth is illustrated in figure 2B. A one-way ANOVA found that visual response latency significantly increased with depth ($F_{(2,754)} = 90.1$, $p = 8.21 \times 10^{-36}$). Follow up t tests revealed that the latency of visual responses was significantly greater at depth 3 (75 + 28.5 ms) when compared to depth 1 (34 +4.3 ms,) and depth 2 (35 + 4.26 ms,; depth 1 vs. depth 3: t = -9.7, $p = 4.0 \times 10^{-21'}$; depth 2 vs. depth 3: t = -9.26, $p = 2.34 \times 10^{-19}$; depth 1 vs. depth 2: t = -0.78, p =0.43).

In addition to the one way analysis of visual response latencies, we also conducted a two way analysis including modality (visual alone vs. visual-auditory) as a factor. This analysis revealed a significant interaction of recording depth and stimulus modality on response latency ($F_{(2,1627)} = 7.2$, $p = 0.0007$). In the multisensory condition, mean response latencies were 33 ms (SD=4.77), 34 ms (SD=4.35) and 61 ms (SD=30.7) for depths 1, 2 and 3 respectively. We also compared the visual and multisensory response latencies for all three depths Student t tests. These comparisons revealed that the

interaction effect was driven by a difference in response latency to visual and multisensory stimuli at Depth 3 ($T = -9.4$, $p = 1.7 \times 10^{-20}$). In contrast, visual and multisensory response latencies did not differ significantly for depth 1 ($p=0.69$) and depth 2 ($p=0.42$).

The combination of small visual RFs coupled with short visual response latencies provided great confidence that the uppermost (i.e., depth 1) recording sites were located within the superficial layers. The remaining analyses focus exclusively on responses recorded from these depth 1 sites.

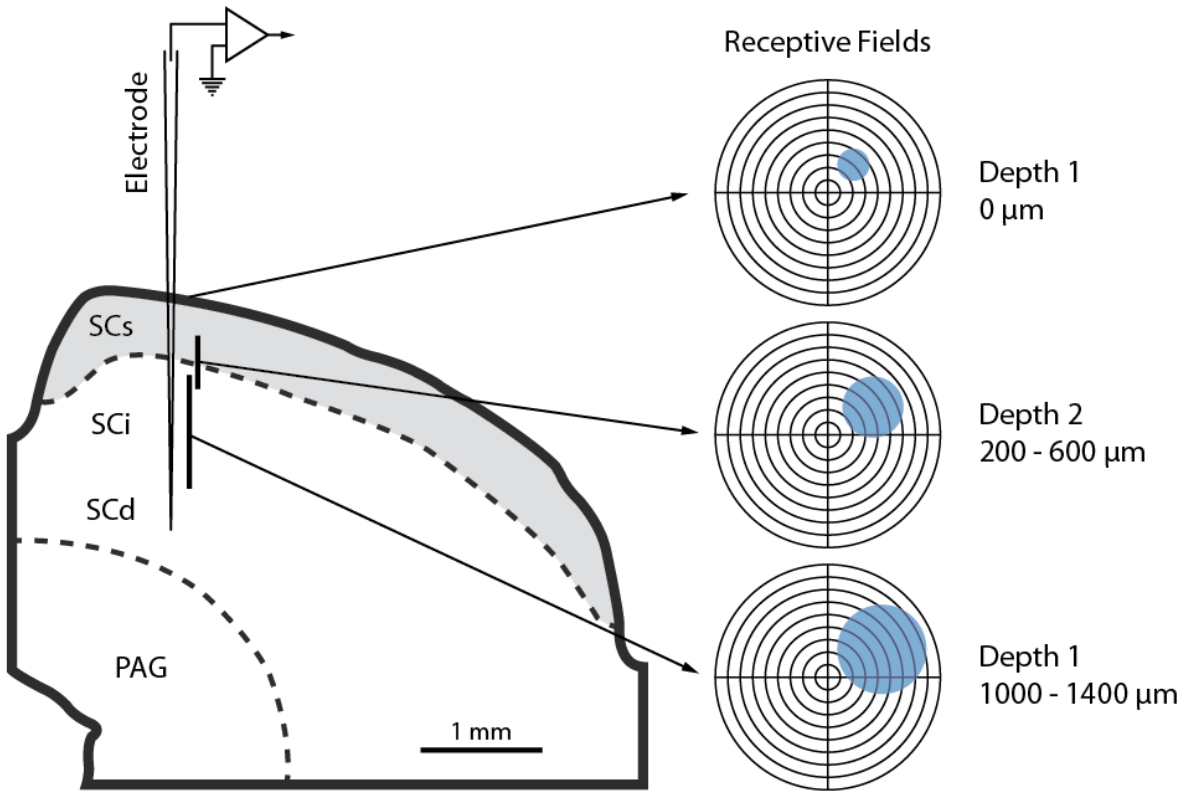

Figure 4-1: Changes in visual receptive fields size with increasing recording depth within the Superior Colliculus (SC).

Electrode position at different recording depths in SC is represented on a schematic cross section (for all experimental sessions n=55). Depth 1 represents recordings at the top of SC. Mappings and recordings at Depth 2 varied between 200-600µm from top of SC (mean depth across 55 sessions=353µm). Mappings and recordings at Depth 3 varied between 1000-1400µm from top of SC (mean depth across 55 sessions=1247µm). Blue circles at each of these depths represent the size of the mapped visual receptive fields (see Methods for mapping procedure). The size of visual receptive field increases with increase in depth within the SC.

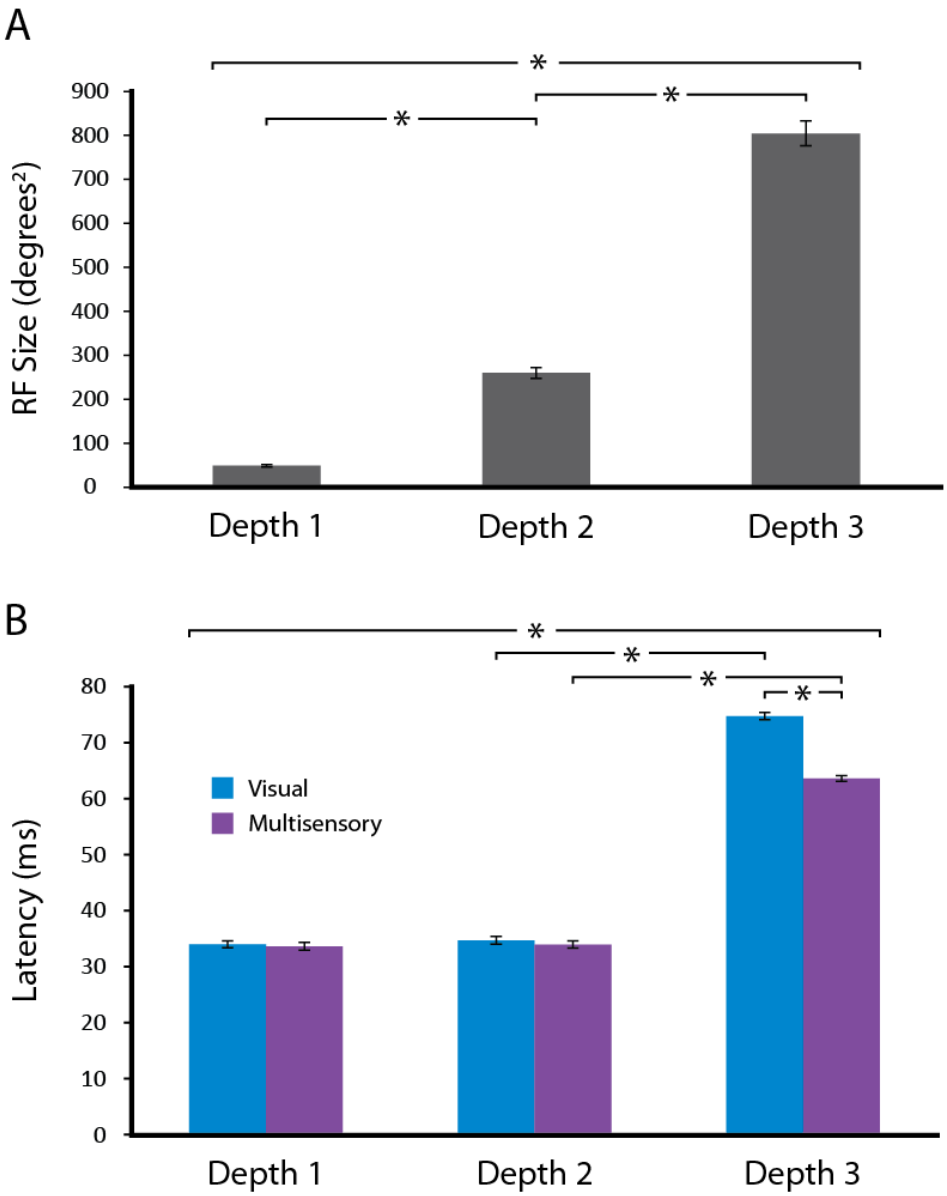

Figure 4-2: Quantification of receptive field (RF) size and response latency as a function of depth.

The size of visual RFs increases with increase in depth. **A.** Mean size at Depth 1= 48.4(deg)^2, Depth 2= 259.7(deg)^2 and Depth 3= 804.0(deg)^2 (n=55). Asterisks represent statistically significant differences between groups. **B.** Latency of responses at different Depths. Visual latencies at Depth 1 (n=47) and 2(n=44) are significantly shorter (represented by asterisks) than the visual latency at Depth 3(n=666). Also, for Depth 3 multisensory response latency (n=1119) is significantly shorter than visual response latency (Student t test $p<0.05$ shown by asterisks).

Auditory modulation of visually evoked spiking responses in the superficial layers of the SC

Once we established that a subset of our recording sites were restricted to the superficial layers, we tested for multisensory (i.e., visual-auditory) interactions. In these experiments, we first examined whether an auditory stimulus would either evoke overt responses or would modulate visual responses by examining the impact of the added auditory stimulus on spiking activity. Representative examples of visual, auditory and visual-auditory spiking responses from two different superficial recording sites are shown in figure 4-3. Although auditory stimuli never resulted in overt responses in superficial layer neurons, the presentation of an auditory stimulus could result in either an enhancement (Fig. 4-3A) or depression (Fig. 4-3B) of visual responses.

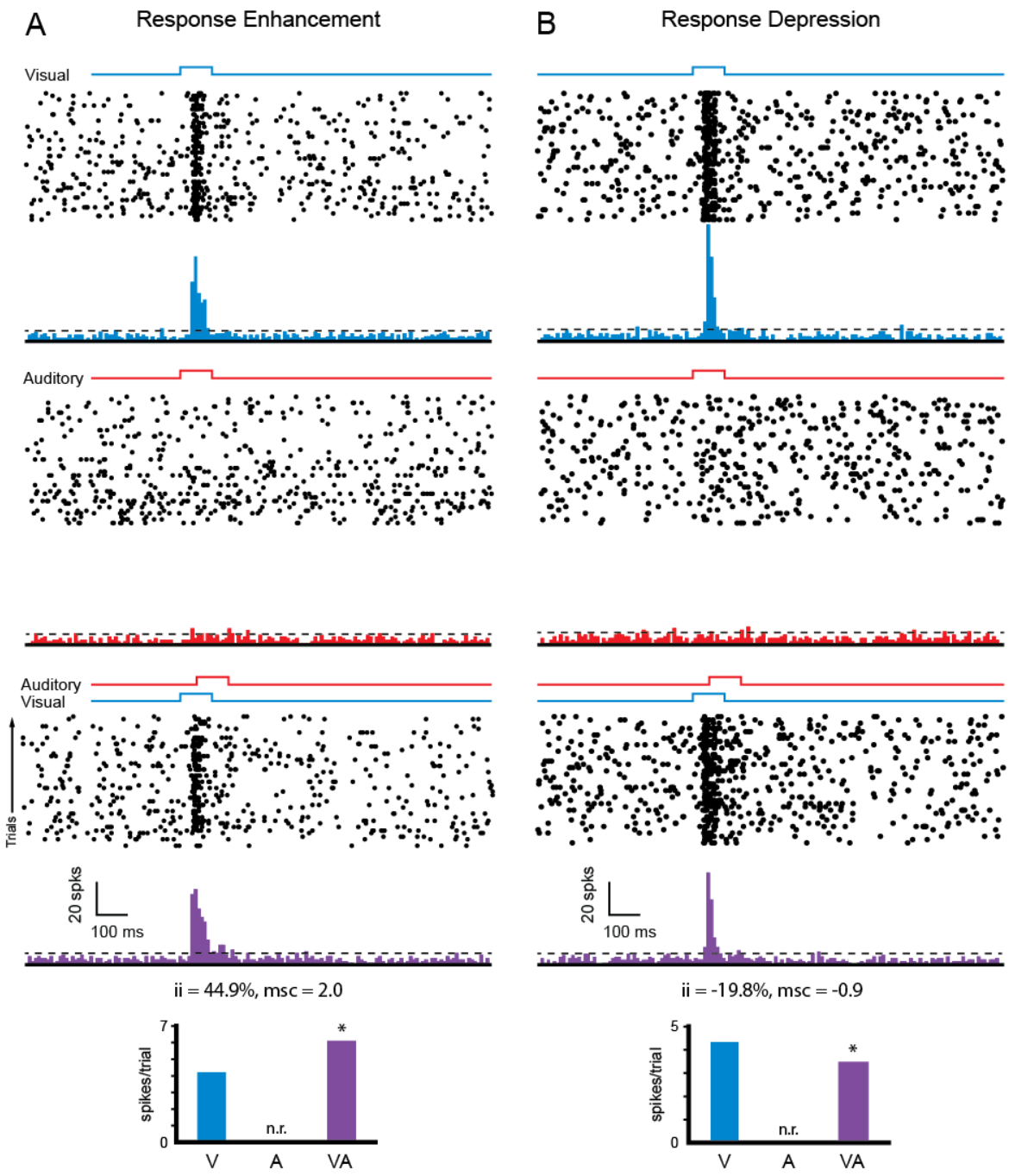

Figure 4-3: Multisensory spiking response modulation in the superficial layers of SC.

Representative example of multi-unit activity (MUA) recorded from the superficial layers of SC showing **A**] Response Enhancement (ii=44.9, p=0.002; msc=2.0, p=0.002; trials =40) and **B**] Response Depression (ii=-19.8, p=.008; msc=-0.9,p=0.008; trials =40). For both A and B rasters and post stimulus time

histograms (PSTHs) showing multi-unit responses for visual (blue), auditory (red) and multisensory (purple) stimulation are shown. For the raster plots, each row represents a trial and each dot represents a spike. Onset and duration of visual and auditory stimuli are represented by blue and red square waves on top of the raster plots for each condition. Dotted horizontal line represents the threshold for neuronal response. Quantification of neuronal responses (spikes/trial) for A] Response Enhancement and B] Response Depression under the 3 stimulus conditions [visual (V), auditory (A) and multisensory (VA)] as measured by interactive index(ii) and mean statistical contrast (msc).

To quantify these multisensory interactions at the population level, we performed two separate analyses. In the first, we detailed the presence or absence of multisensory interactions in multiunit activity (MUA) in the 55 sites recorded in the most superficial layers of the SC (Fig. 4-4A). This revealed that nearly all (53/55; 96.3%) of the recorded sites exhibited multisensory interactions at one or more of the tested locations within the receptive field. These interactions were further subdivided into sites showing only response enhancements (19/55; 34.5%), those showing only response depressions (7/55; 12.7%), or those showing both enhancements and depressions (27/55; 49.1%). The second population analysis quantified the total number of locations within the SRFs that showed significant multisensory interactions (Fig. 4-4B). For all of the tested sites, significant interactions were restricted to a few locations within the SRF. Interestingly, most of these interactions were seen at locations at the borders of the SRF and where visual sensitivity was weak (Fig 4-4C; see below). Out of the total of 1197 receptive field locations tested at the 55 superficial sites, 21.8% (261/1197) exhibited significant multisensory interactions. Approximately three-quarters of these interactions were response enhancements (212/261=81.2%).

Multisensory integration in the superficial SC abides by the principle of inverse effectiveness

One of the most robust characteristics of multisensory integration that has been demonstrated in the deeper layers of the SC (as well as in other structures) is the principle of inverse effectiveness (Meredith and Stein, 1986b).This principle refers to the finding that as the effectiveness of the individual unisensory stimuli decline, the gain that is obtained from their combination increases. We found a similar relationship for the superficial layers of the SC, where the magnitude of the visual response appeared to be a significant determinant of the multisensory gain obtained with the addition of an auditory stimulus. Fig 4-4D illustrates this relationship by plotting the interactive index as a function of the magnitude of the visual response, and reveals the largest gains at the lowest levels of visual response. As highlighted earlier, these weak visual responses were typically found near the borders of the receptive fields as shown in the example in Fig 4D.

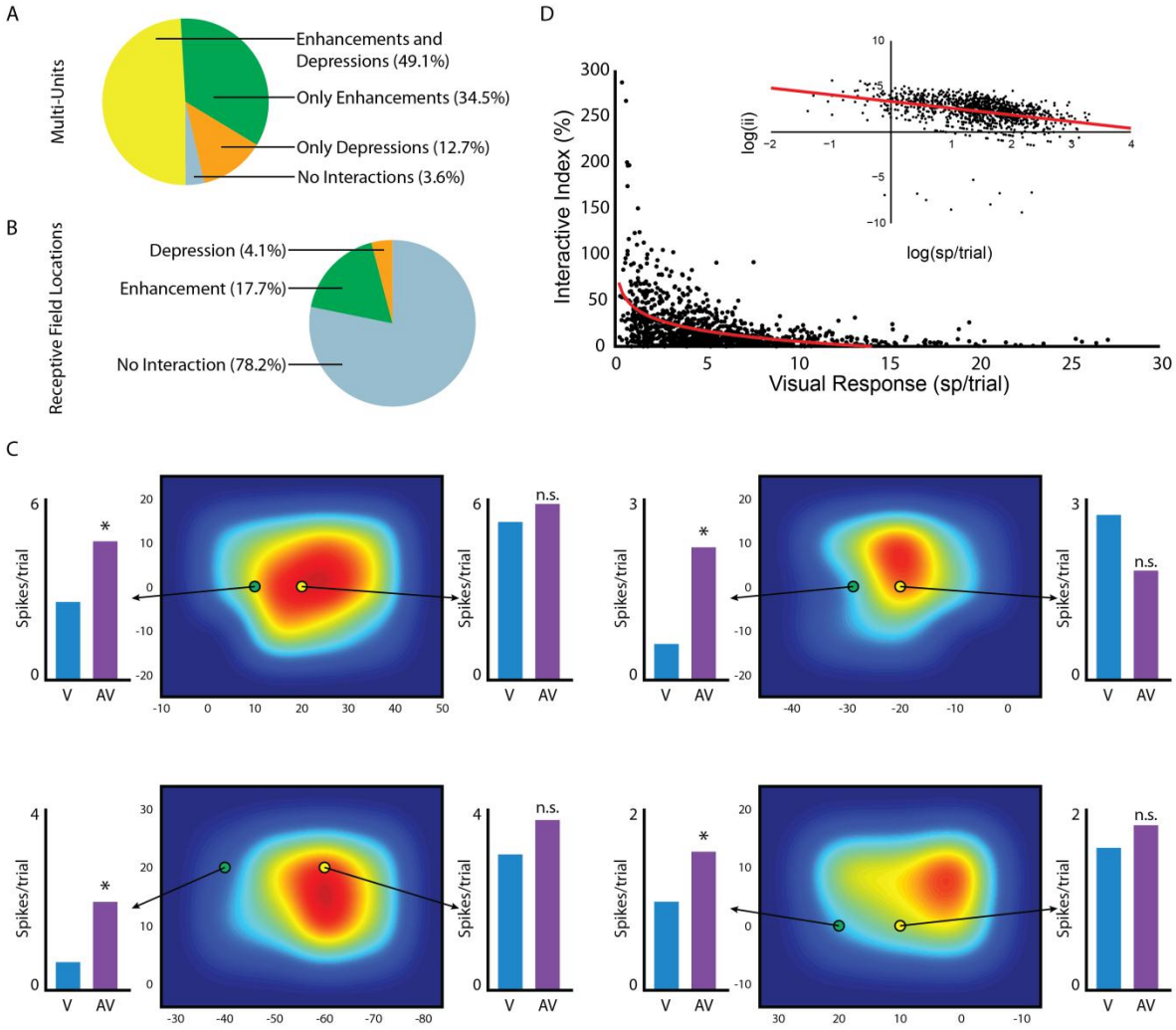

Figure 4-4: Quantification of population multi-unit activity.

A] Quantification of the proportion of multi units showing different types of multisensory interactions in the superficial layers of SC. **B**] Quantification of the nature of interaction across different receptive locations across all 55 recording sessions. **C]** Representative examples of Visual Spatial Receptive fields of 4 neurons showing significant modulations of visual activity by auditory stimulation (represented by the bar graphs) at borders of the visual receptive field but not at the hotspots. **D**] Principle of Inverse Effectiveness: Interactive index (ii) is plotted as a function of the visual response which shows that as visual responsiveness increases, amount of interaction decreases as represented more clearly in the inset where data is transformed to a logarithmic scale to show the negative correlation more clearly. The red curves represent the trend of the dataset and is represented by the equation $y=28.64x^{-0.735}$.

Multisensory modulation of the local field potential in the superficial SC

Low frequency (<100 Hz) voltage changes in the recorded signal, referred to as the local field potential (LFP), are commonly regarded as a reflection of synaptic activity in the immediate electrode vicinity (Katzner et al., 2009; Kajikawa and Schroeder, 2011). Importantly, under some circumstances, the LFP can deviate substantially from local spiking activity (Maier et al., 2008). This dissociation is believed to reflect sub-threshold activations that are the result of synaptic processes that fail to impact spiking responses (Buzsaki, 2002; Rasch et al., 2008). In an effort to expand our understanding of the observed multisensory effects on neuronal spiking in the superficial SC, we next focused on the LFP signal. Generally, two types of LFP activity can be distinguished: a) *evoked* activity that is strictly phase locked (time locked) to the onset of an event (in our case, the stimulus onset), and b) *induced* activity that is stimulus related but not phase locked to the onset of the stimulus. We computed both the evoked (i.e., phase-locked) and induced (i.e., non-phase-locked) LFP responses for all stimulus combinations and locations discussed above. Figure 4-5 shows representative examples of spiking and LFP responses for two locations in the superficial layers, one of which showed an enhancement of spiking activity (left) and the other of which showed a response depression (right). Note the stimulus evoked modulation of the LFP in the unisensory auditory condition in both instances (red traces in LFPs), a change that is not evident in the spiking responses.

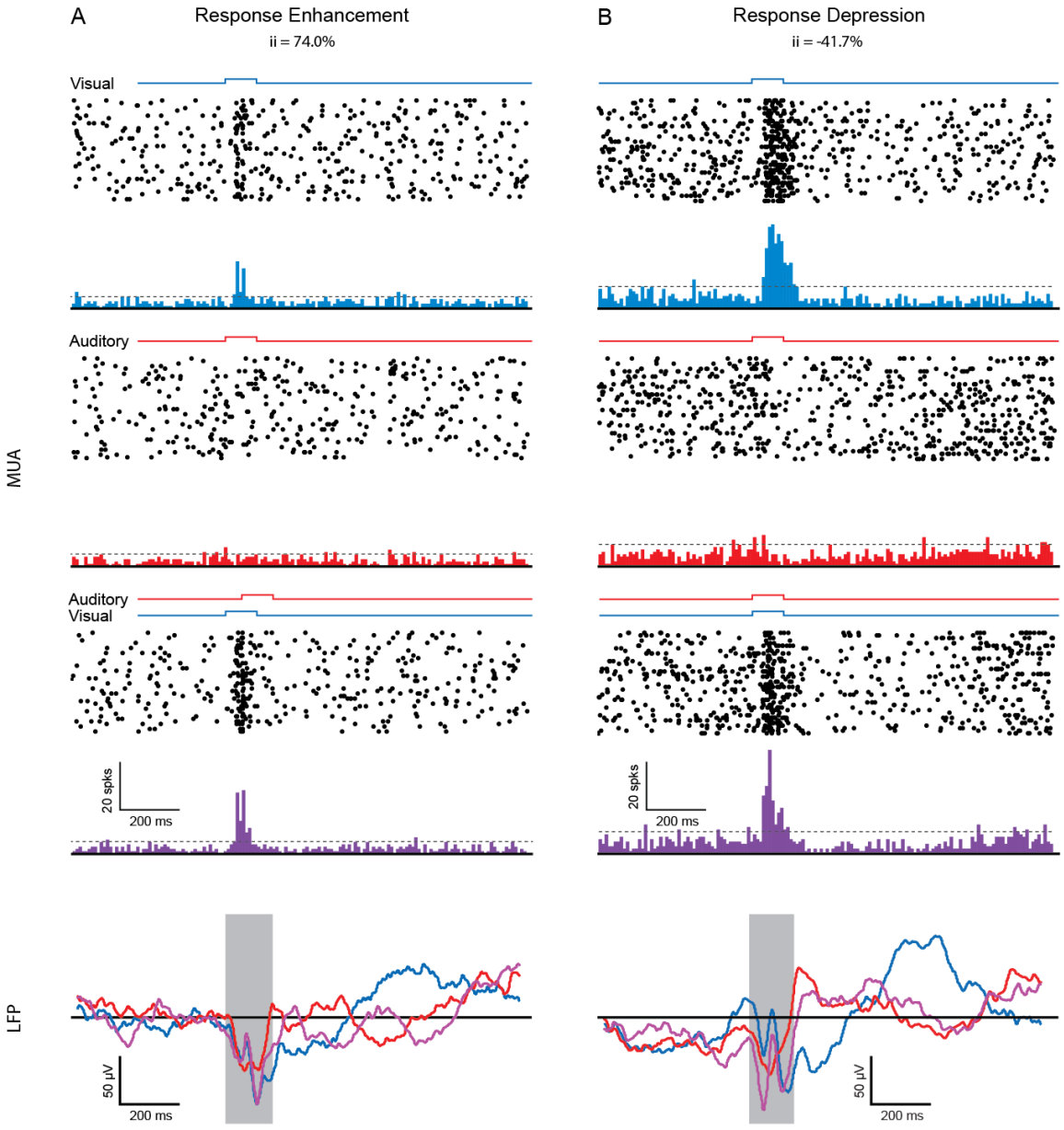

Figure 4-5: Local Field Potential (LFP) responses during multisensory stimulation.

PSTHs of MUA showing **A**] Response Enhancement (ii=74, p=0.01; msc=0.92, p=0.01 trials=40) and **B**] Response Depression(ii=-41.7, p=0.03; msc=-0.74, p=0.02 trials =40). Corresponding changes in LFPs are shown below. Blue represents the visual condition, red represents the auditory condition and purple represents the multisensory condition for both the PSTHs and the evoked LFP traces. Onset and duration of stimuli are represented by square waves over the PSTHs for the different stimulus conditions. The shaded box over the LFP traces represent the duration of the multisensory stimulus combination and =150ms.

To quantify the stimulus-related changes in the phase-locked LFP (the evoked potential or EVP) at the population level we compared the peak EVP and area under the curve for visual, auditory, and multisensory conditions. These LFP measures were carried out separately for the two tested temporal intervals (V0A0 and V0A50). We further divided the data according to stimulus locations showing enhancements, depressions, and no interactions in the spiking response (Fig.4- 6). These analyses revealed significant EVPs for each of the unisensory and for the multisensory stimulus conditions. The statistical details of these analyses are reported in Tables 1 and 2. The magnitude of the LFP signal as measured by both peak amplitude and area under the curve was significantly smaller for the auditory condition than for the visual and multisensory conditions – but still demonstrable in almost all circumstances. In comparing between the visual and multisensory conditions, it is of note that peak EVP amplitude was higher for the multisensory condition for all of the tested interactive conditions except for those showing response depression at V0A50 ($p = 0.07$). This lack of significance may be a result of the fact that the number of samples for this condition was substantially smaller ($n=20$) compared to all other conditions.

Comparing the area under the curve of the EVP for the early response epoch (0-200 ms, which exhibited prominent negative deflections for all three stimulus modalities see methods for details of analysis) revealed that for stimulus locations that yielded response enhancements and no interactions, the EVP area was significantly greater for the multisensory condition (both temporal intervals V0A0 and V0A50) when compared to the visual condition alone (response enhancement: V0A0: $T=3.7$,p3.6X10^{-4}, V0A50: $T=6.0$,$p=2.0X10^{-8}$ no interactions: V0A0: $T=4.1$,$p=3.9X10^{-5}$, V0A50: $T= 8.3$,$p=9.7X10^{-16}$)

(Fig. 6 lower bar graphs). In contrast, for the stimuli that resulted in response depressions, areal measurements did not differ between the visual and multisensory conditions (V0A0: T=1.1, p=0.2, V0A50: T=1.3, p=0.1). Once again, this lack of a difference may be due to the size of the sample and the associated lack of statistical power, since only 49 total observations (V0A0=29, V0A50=20) make up this data set.

For the middle epoch (200-300ms post stimulus which exhibited positive deflections for all three modalities and hence analyzed separate from the early epoch) for stimulus locations that yielded response enhancements, response depressions and no interactions for the SOA V0A50 trials, the EVP area was significantly greater for the multisensory condition when compared to the visual condition. For SOA V0A0, EVP area was significantly greater under multisensory conditions compared to visual condition for locations yielding response enhancements and no interactions but not for response depressions (again possibly due to the low sample size of n=29). Details of the statistical tests are provided in Tables 1 and 2.

Finally, for the late response epoch (300-1400 ms post-stimulus), the area under the curve was significantly smaller under multisensory conditions compared to the visual condition for all types of interactions and both SOAs tested (see Tables 1 and 2 for detailed statistical results).

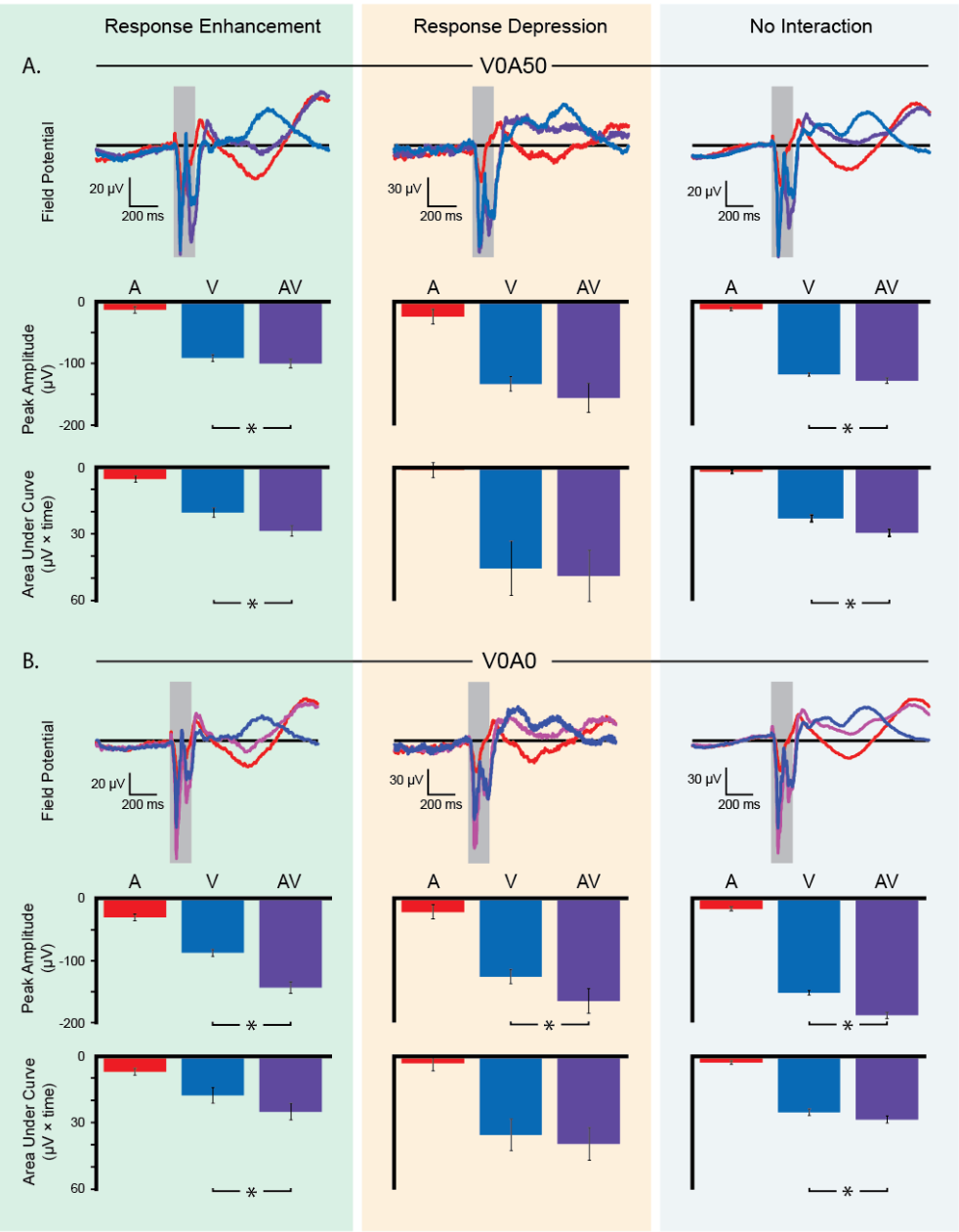

Figure 6: Quantification of evoked LFP amplitude in superficial layers of SC.

A] Averaged evoked LFP activity across all within-receptive field locations showing Response Enhancement, Response Depression and No Interaction respectively during visual (blue) , auditory(red), and multisensory stimulation (purple). The visual stimulus always preceded the auditory stimulus by 50ms (V0A50). Bar graphs represent the mean peak LFP amplitude and area under the curve for all the 3 stimulus conditions for Response Enhancement(n=122), Response Depression(n=20) and No Interaction (n=467) across all 55 sessions. **B]** Averaged evoked LFP activity for all stimulus locations showing Response Enhancement, Response Depression and No Interaction under visual (blue), auditory(red), and multisensory condition(purple). For these experiments, the visual and auditory stimulus were always presented simultaneously (V0A0). Bar graphs below represent the mean peak LFP amplitude and area under the curve for all the 3 stimulus conditions for Response Enhancement (n=90), Response

Depression(n=29) and No Interaction(n=469). For both A and B asterisks represent statistically significant differences between groups. Statistical details are reported in Table 1 and 2.

Table 4-1: Details of statistical tests for quantification of Mean Peak Amplitude and Area Under the Curve for SOA=V0A50

	Enhancement	**Depression**	**No Interaction**
Comparisons	**V vs. AV**	**V vs. AV**	**V vs. AV**
Mean peak amplitude T(p) (df)	2.11(0.03)(121)	1.87(0.07)(19)	3.39(7.3×10^{-4})(466)
AUC(early) T(p)(df)	6.01(2.0×10^{-8}) (121)	1.38(0.18)(19)	8.32(9.7×10^{-16})(466)
AUC(middle) T(p)	-7.17(6.47×10^{-11}) (121)	-2.38 (0.02)(19)	-7.46 (4.16×10^{-13}) (466)
AUC(late) T(p)(df)	6.88(2.7×10^{-10})(121)	2.75(0.01)(19)	7.32(1.0×10^{-12}) (466)
COMPARISONS WITH BASELINE ACTIVITY			
	V vs. baseline	**A vs. baseline**	**AV vs. baseline**
	Enhancement		
T(p)	-16.06(8.52×10^{-32})	-4.82(4.1×10^{-6})	-17.64(2.90×10^{-35})
	Depression		
T(p)	-4.50(2.41×10^{-4})	-1.72(0.01)	-6.5(3.15×10^{-6})
	No Interaction		
T(p)	-24.99(4.19×10^{-88})	-4.79(2.23×10^{-6})	-28.65(6.92×10^{-105})

Table 4-2: Details of statistical tests for quantification of Mean Peak Amplitude and Area Under the Curve for SOA=V0A0

	Enhancement	Depression	No Interaction
Comparisons	**V vs. AV**	**V vs. AV**	**V vs. AV**
Mean peak amplitude T(p)(df)	7.30(1.1×10^{-10})(89)	2.56(0.01)(28)	10.3(1.3×10^{-22})(468)
AUC(early) T(p)(df)	3.7(3.6×10^{-4})(89)	1.12(0.26)(28)	4.14(3.9×10^{-9})(468)
AUC(middle) T(p)(df)	-2.64 (0.009)(89)	-0.36 (0.72)(28)	-4.46 (1.0×10^{-5})(468)
AUC(late) T(p)(df)	3.31(0.001)(89)	1.59(0.12)(28)	2.27(0.02)(468)

COMPARISONS WITH BASELINE ACTIVITY

	V vs. baseline	A vs. baseline	AV vs. baseline
	Enhancement		
T(p)	-7.21(1.74×10^{-10})	-5.35(6.54×10^{-7})	-15.03(3.65×10^{-26})
	Depression		
T(p)	-5.55(6.12×10^{-6})	-1.65(0.10)	-8.20(6.20×10^{-9})
	No Interaction		
T(p)	-28.47(3.28×10^{-104})	-4.81(2.03×10^{-6})	-37.67(8.11×10^{-144})

Time frequency analysis for local field potentials in the superficial layers of SC

Next, spectral analysis was performed to investigate the stimulus-induced (i.e. phase-locked and non-phase locked) LFP responses as a function of time and frequency. In addition to revealing non-phase locked sensory responses, this analysis also allows for an investigation of the high frequency components of the LFP that can easily be masked by the far more dominant slow components. Computing normalized spectrograms (see Methods), we quantified the stimulus related LFP response across all frequency bands. Note that the qualitative structure of these time-frequency plots is similar for all three conditions as well as for both SOAs (Fig.4-7). Because the number of observations for stimulus locations resulting in response depressions was too low in the analyses outlined above, they were excluded from further analysis. As evident from the spectrograms shown in figure 4-7, the onset of unisensory visual stimulation was accompanied by an increase in power in the low frequency range up to 20 Hz (i.e., the theta, alpha and beta bands) as well as by an increase in the high gamma band (70-90 Hz). A smaller amplitude increase in power in the low gamma band (30-50 Hz) is also evident. Note the extended period of power change following stimulus onset (compared to the phase-locked EVP and spiking responses described above). For the unisensory auditory condition, we found short latency increases in LFP power in the low frequency range up to 10-12 Hz (theta and alpha bands) and also in the high gamma band (70-90 Hz), followed by a subsequent increase in power within the low (30-50 Hz) gamma bands. For the multisensory condition, we found that the onset of stimulation is accompanied by an increase in low frequency power and high gamma power similar to that seen in the visual and auditory conditions and a subsequent increase in low gamma power similar to that evoked by the unisensory auditory stimulus.

To better visualize the response differences between conditions, we generated contrast plots for each of the main stimulus comparisons (see Methods). Figure 4-8 (top) shows the spectral contrast plot comparing the multisensory condition to the visual condition (AV-V) for both the response enhancement and no interaction conditions and for the V0A0 (left) and V0A50 (right) temporal conditions. Note the increased LFP power for the multisensory condition within the low frequency bands (up to 20 Hz) and the high gamma band after stimulus onset. This is followed by a subsequent increase in power in the low gamma bands (30-50 Hz) and decreased power in the lower frequency bands and both high and low gamma bands. To quantify these differences in LFP power across conditions, we performed a statistical analysis comparing the visual and multisensory plots (Fig. 8 bottom). Of particular note in this analysis (and as is evident in the contrast plots in the top panel [arrow]), the multisensory-mediated difference in high gamma power was more robust for stimuli that elicited response enhancement when compared with the no interaction trials ($F_{(1,7155)}$ = 2552.3, p <0.0001). Collectively, these LFP analyses highlight significant differences between the visual-only and multisensory conditions, thus reinforcing the results of the spiking data and providing greater insight into the nature of the synaptic processes that may be underlying the spiking changes.

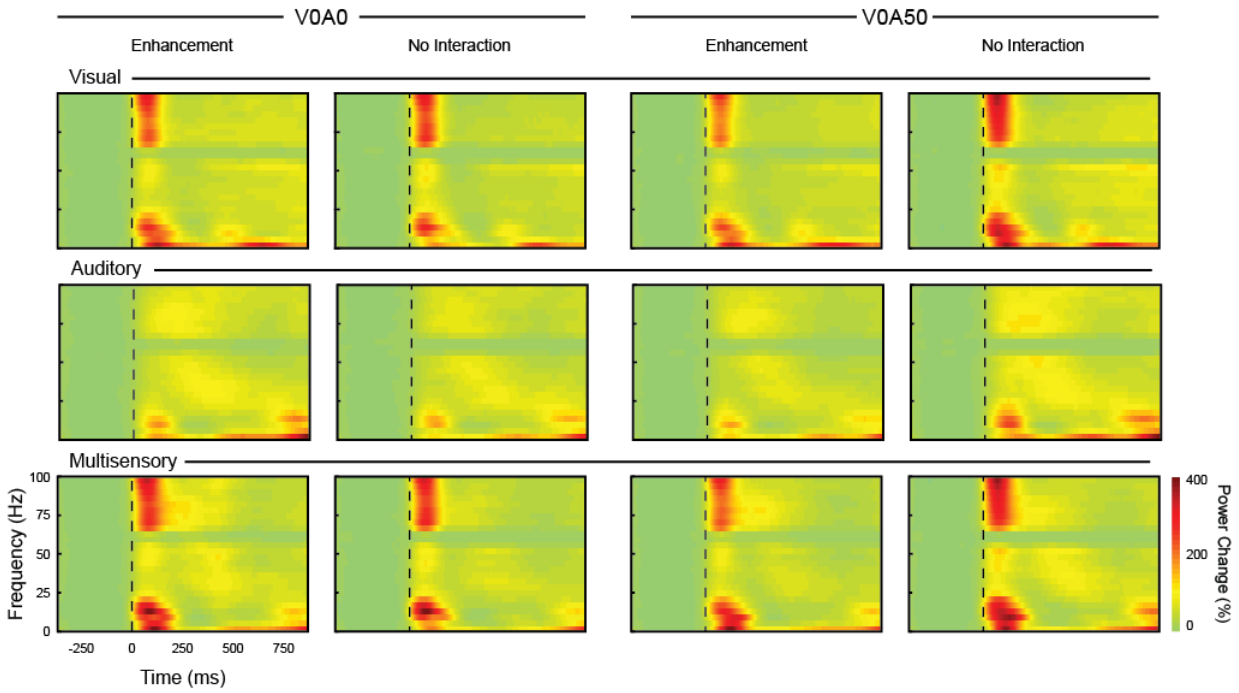

Figure 4-7: Time frequency analysis of LFP responses.

Averaged time-frequency representations (spectrograms) of LFP responses, showing power changes for Visual, Auditory and Multisensory stimulus conditions for all stimulus locations showing Response Enhancements and No Interactions, respectively. Visual and auditory stimulation was either simultaneous (V0A00, or the visual stimuli preceded auditory stimuli by 50ms (V0A50). Color bar at the bottom right represents the percentage of LFP power change compared to pre-stimulus baseline. The dashed vertical lines represent the onset of the visual stimulus.

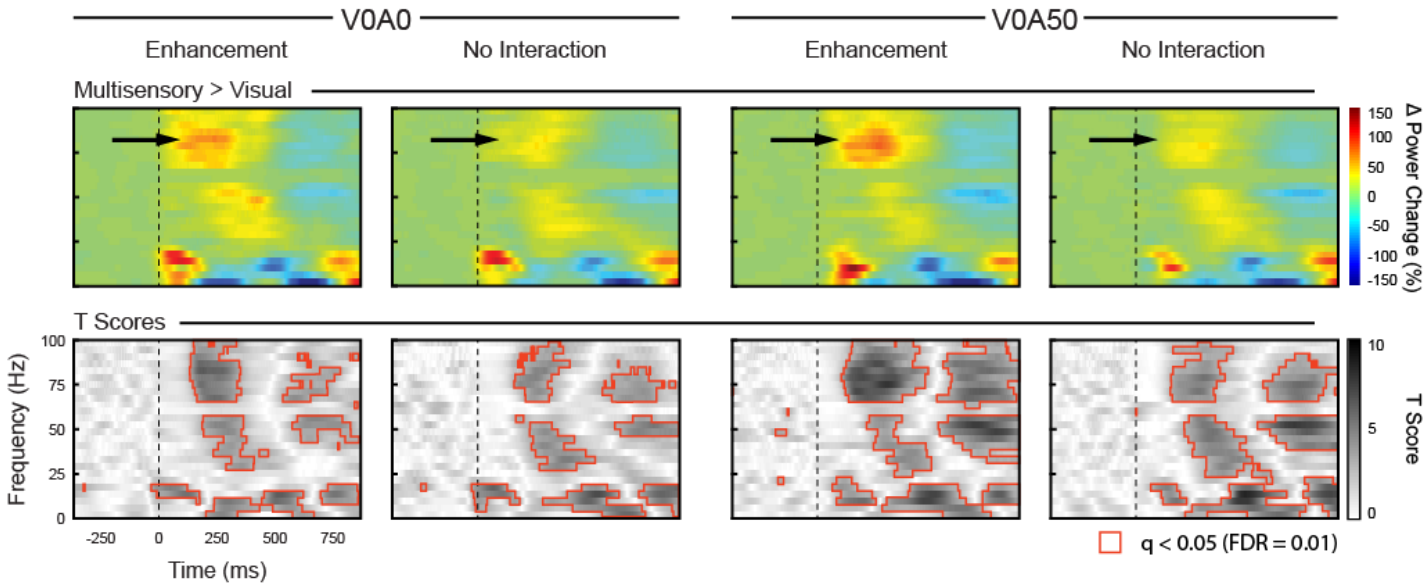

Figure 4-8: Statistical comparison of LFP responses to uni- and multisensory stimulation.

Top panel depicts difference plots obtained by subtracting the average LFP response for the visual-only condition (V) from the multisensory (AV) stimulation condition (AV-V) .The color bar on the right represents relative LFP power change (in %). The black arrow highlights modulation in the high gamma band (70-90Hz). The dotted vertical line represents visual stimulus onset.

Bottom panel shows respective t-scores for the contrast plots above. Darker shades represent higher t values. Regions outlined in red represent statistically significant t-scores, corrected for multiple comparisons using False Discovery Rate (FDR) = 0.01.

Discussion

The results of the current experiments demonstrate that neural processing of visual information in the superficial layers of the cat superior colliculus is modulated by the presence of auditory stimuli. This finding is the first data to our knowledge that provides neurophysiological evidence for multisensory integration within the superficial layers of the SC, reflected in both changes in local spiking activity as well as in the LFP signal. These results have important functional implications for furthering our understanding of sensory processing within the SC.

Auditory stimulation modulates visual spiking responses in the superficial layers of SC

We found robust responses of superficial SC neurons to both moving and stationary visual stimuli that match previous reports (Sterling and Wickelgren, 1969; Wurtz and Albano, 1980). However, in striking contrast to the view of the superficial layers as exclusively visual, addition of an auditory stimulus produced significant modulation of the visual responses. Further analysis revealed an inverse relationship between the strength of the visual response and the magnitude of these multisensory interactions. Specifically, regions within the receptive field with weak visual responses tended to show the greatest degree of gain when paired with an auditory stimulus, while regions with strong visual responses often failed to show any auditory response modulation. This finding is in accordance with the principle of “inverse effectiveness”, which was originally established for responses in the deep layers of the SC (Meredith and Stein,

1986b; Wallace and Stein, 1994; Meredith and Stein, 1996; Wallace et al., 1998; Perrault et al., 2003) and has since been extended to characterize multisensory responses in a number of neocortical areas [cats (Wallace et al., 1992; Carriere et al., 2008), monkeys (Barraclough et al., 2005; Ghazanfar et al., 2005; Kayser et al., 2005) and humans (Stevenson and James, 2009).

Multisensory interactions in the superficial SC reflected in the local field potential

In addition to the multisensory modulation of spiking activity in superficial SC, we also observed concurrent changes in the LFP. While auditory stimulation alone did not produce spiking activity in these layers, it did result in changes in LFP power. This finding is mirrored by the fact that increased LFP amplitude was seen for most of the multisensory conditions when compared with their visual correlates, while the multisensory modulation of the spiking responses was more restricted. One way to explain this dissociation between spiking activity and the LFP is that these two measures represent different aspects of neural mass action (Henze et al., 2000; Logothetis, 2008). Whereas multiunit activity (MUA) reflects the axonal output of a local neural population, LFPs are believed to be primarily related to synaptic processing (Mitzdorf, 1985, 1987; Kayser and Logothetis, 2007)

The physiological finding of auditory influences in the superficial layers may be mediated by the presence of processes from the intermediate and deep SC that ascend into the superficial layers (Behan et al., 1987; Behan and Appell, 1992; Hall and Lee, 1993; Behan and Kime, 1996; Hall and Lee, 1997; Isa and Hall, 2009). Alternatively, auditory influences may come via modulated cortical visual responses. The presence of

auditory influences in primary (and extraprimary) visual cortical fields has now been demonstrated and may provide the source for superficial SC auditory inputs (Falchier et al., 2002; Rockland and Ojima, 2003).

Most important in the current context is the fact that these auditory influences within the superficial layers can play an important modulatory role with regard to visual information processing. These “modulatory” multisensory influences are reminiscent of similar effects that have been described for higher level visual areas (Allman et al., 2008b; Allman et al., 2008a; Clemo et al., 2008) for regions of association cortex (Dehner et al., 2004; Avillac et al., 2005; Barraclough et al., 2005; Meredith et al., 2006; Avillac et al., 2007; Chandrasekaran and Ghazanfar, 2009)and for classic unisensory cortical domains (Schroeder et al., 2001; Schroeder and Foxe, 2002; Ghazanfar et al., 2005; Kayser et al., 2005; Lakatos et al., 2007; Lakatos et al., 2008; Kayser et al., 2010). Similar to the superficial SC data shown here, many of these areas show spiking responses only to the dominant modality but LFP responses that reveal subthreshold synaptic influences for other modalities.

Collectively, these results suggest that in addition to the overt convergence and integration of sensory inputs in multisensory brain areas, multisensory influences may extend to a host of structures that have been classically defined as components of a sensory specific axis. While evidence for this view has been growing rapidly in cortex (Falchier et al., 2002; Rockland and Ojima, 2003; Ghazanfar et al., 2005; Kayser et al., 2005; Lakatos et al., 2007; Lakatos et al., 2008; Kayser et al., 2010) ours is the first study to our knowledge that extends the prevalence of these modulatory effects into a subcortical structure.

Gamma activity and its relations to spiking activity and multisensory integrative capacity

We found an increase in high gamma (50-90 Hz) power in the superficial SC layers after visual stimulation. Increased activity in this frequency band has been reported following visual stimulation for a wide variety of visual areas and species in both anesthetized and awake preparations (Eckhorn et al., 1988; Gray et al., 1989; Gray and Singer, 1989; Engel et al., 1991b; Engel et al., 1991a; Frien et al., 1994; Kreiter and Singer, 1996; Fries et al., 1997; Rols et al., 2001; Berens et al., 2008). One plausible explanation for the increase in high gamma LFP power is that it is generally found to be closely related to (and indeed predictive of) local spiking activity (Rasch et al., 2008)(Berens et al 2010). This interpretation can also explain why increases in high gamma power were significantly larger for conditions yielding auditory-mediated response enhancements in the spiking data . Note that similar findings have been reported in monkey superior temporal sulcus where enhanced gamma band activity was found during the multisensory integration of faces and voices (Chandrasekaran and Ghazanfar, 2009).

Low frequency fluctuations in the multisensory LFP

Time-frequency analysis of the LFP signal further revealed that in addition to the changes in the high gamma band, the onset of visual stimulation is followed by an increase in LFP power of lower (<30Hz) frequency. Similarly, following auditory stimulation, there is an increase in low frequency LFP power. Combined visual-auditory stimulation resulted in an LFP response that shared the spectral characteristics of both

unisensory visual and auditory responses. Most notably, the increase in power within the low frequency bands during multisensory stimulation is greater than that which occurs during visual stimulation alone. As highlighted above, our assumption is that high gamma activity seen under the visual, auditory and multisensory conditions reflects synaptic drive in close proximity to the electrode, as it is tightly coupled to changes in spiking activity. In contrast, the lower frequency components of the LFP may be a broader reflection of synaptic processing, which may include auditory influences reaching superficial SC from primary visual cortex. This suggestion is based on the observation that differences between Response Enhancement and No Interaction are clearly seen in high gamma activity while such differences are not evident at lower frequencies.

Putative functional implications

The superficial layers of the SC have been implicated to play an important role in visual form discrimination (Sprague et al., 1970; Anderson et al., 1971; Berlucchi et al., 1972; Sprague et al., 1977; Tunkl and Berkley, 1977). The present results, by showing the presence of auditory influences in these layers, suggest that visual form discrimination (and other visual functions of the superficial SC) may be faciliated by the presence of concurrent auditory stimuli. This selective enhancement could be mediated through a gain control mechanism, for example, that serves to boost the salience of the visual signal when coupled with auditory cues. Such a mechanism may serve to amplify the visual signal under weak, ambiguous or noisy conditions, hence improving detection thresholds, discriminability and localization. Our finding that visual activity is modulated by auditory stimulation in the superficial SC may thus pave the way for future studies

examining the possible behavioral implications of these multisensory influences in the superficial layers.

Bibliography

Allman BL, Keniston LP, Meredith MA (2008a) Subthreshold auditory inputs to extrastriate visual neurons are responsive to parametric changes in stimulus quality: sensory-specific versus non-specific coding. Brain Res 1242:95-101.

Allman BL, Bittencourt-Navarrete RE, Keniston LP, Medina AE, Wang MY, Meredith MA (2008b) Do cross-modal projections always result in multisensory integration? Cereb Cortex 18:2066-2076.

Anderson ME, Yoshida M, Wilson VJ (1971) Influence of superior colliculus on cat neck motoneurons. J Neurophysiol 34:898-907.

Avillac M, Ben Hamed S, Duhamel JR (2007) Multisensory integration in the ventral intraparietal area of the macaque monkey. J Neurosci 27:1922-1932.

Avillac M, Deneve S, Olivier E, Pouget A, Duhamel JR (2005) Reference frames for representing visual and tactile locations in parietal cortex. Nat Neurosci 8:941-949.

Barraclough NE, Xiao D, Baker CI, Oram MW, Perrett DI (2005) Integration of visual and auditory information by superior temporal sulcus neurons responsive to the sight of actions. J Cogn Neurosci 17:377-391.

Behan M, Appell PP (1992) Intrinsic circuitry in the cat superior colliculus: projections from the superficial layers. J Comp Neurol 315:230-243.

Behan M, Kime NM (1996) Spatial distribution of tectotectal connections in the cat. Prog Brain Res 112:131-142.

Behan M, Lin CS, Hall WC (1987) The nigrotectal projection in the cat: an electron microscope autoradiographic study. Neuroscience 21:529-539.

Berens P, Keliris GA, Ecker AS, Logothetis NK, Tolias AS (2008) Feature selectivity of the gamma-band of the local field potential in primate primary visual cortex. Front Neurosci 2:199-207.

Berens P, Logothetis NK, Tolias AS (2010) Local field potentials, BOLD and spiking activity – relationships and physiological mechanisms. 2010

Berlucchi G, Sprague JM, Levy J, DiBerardino AC (1972) Pretectum and superior colliculus in visually guided behavior and in flux and form discrimination in the cat. J Comp Physiol Psychol 78:123-172.

Buzsaki G (2002) Theta oscillations in the hippocampus. Neuron 33:325-340.

Carriere BN, Royal DW, Wallace MT (2008) Spatial heterogeneity of cortical receptive fields and its impact on multisensory interactions. J Neurophysiol 99:2357-2368.

Casagrande VA, Harting JK, Hall WC, Diamond IT, Martin GF (1972) Superior colliculus of the tree shrew: a structural and functional subdivision into superficial and deep layers. Science 177:444-447.

Chandrasekaran C, Ghazanfar AA (2009) Different neural frequency bands integrate faces and voices differently in the superior temporal sulcus. J Neurophysiol 101:773-788.

Clemo HR, Stein BE (1982) Somatosensory cortex: a 'new' somatotopic representation. Brain Res 235:162-168.

Clemo HR, Sharma GK, Allman BL, Meredith MA (2008) Auditory projections to extrastriate visual cortex: connectional basis for multisensory processing in 'unimodal' visual neurons. Exp Brain Res 191:37-47.

Dehner LR, Keniston LP, Clemo HR, Meredith MA (2004) Cross-modal circuitry between auditory and somatosensory areas of the cat anterior ectosylvian sulcal cortex: a 'new' inhibitory form of multisensory convergence. Cereb Cortex 14:387-403.

Doubell TP, Skaliora I, Baron J, King AJ (2003) Functional connectivity between the superficial and deeper layers of the superior colliculus: an anatomical substrate for sensorimotor integration. J Neurosci 23:6596-6607.

Eckhorn R, Bauer R, Jordan W, Brosch M, Kruse W, Munk M, Reitboeck HJ (1988) Coherent oscillations: a mechanism of feature linking in the visual cortex? Multiple electrode and correlation analyses in the cat. Biol Cybern 60:121-130.

Edwards SB, Ginsburgh CL, Henkel CK, Stein BE (1979) Sources of subcortical projections to the superior colliculus in the cat. J Comp Neurol 184:309-329.

Engel AK, Kreiter AK, Konig P, Singer W (1991a) Synchronization of oscillatory neuronal responses between striate and extrastriate visual cortical areas of the cat. Proc Natl Acad Sci U S A 88:6048-6052.

Engel AK, Konig P, Kreiter AK, Singer W (1991b) Interhemispheric synchronization of oscillatory neuronal responses in cat visual cortex. Science 252:1177-1179.

Falchier A, Clavagnier S, Barone P, Kennedy H (2002) Anatomical evidence of multimodal integration in primate striate cortex. J Neurosci 22:5749-5759.

Frien A, Eckhorn R, Bauer R, Woelbern T, Kehr H (1994) Stimulus-specific fast oscillations at zero phase between visual areas V1 and V2 of awake monkey. Neuroreport 5:2273-2277.

Fries P, Roelfsema PR, Engel AK, Konig P, Singer W (1997) Synchronization of oscillatory responses in visual cortex correlates with perception in interocular rivalry. Proc Natl Acad Sci U S A 94:12699-12704.

Ghazanfar AA, Maier JX, Hoffman KL, Logothetis NK (2005) Multisensory integration of dynamic faces and voices in rhesus monkey auditory cortex. J Neurosci 25:5004-5012.

Ghose D, Barnett ZP, Wallace MT (2012) Impact of response duration on multisensory integration. J Neurophysiol 108:2534-2544.

Grantyn A, Berthoz A (1985) Burst activity of identified tecto-reticulo-spinal neurons in the alert cat. Exp Brain Res 57:417-421.

Grantyn R, Grantyn A, Schierwagen A (1983) Passive membrane properties, afterpotentials and repetitive firing of superior colliculus neurons studied in the anesthetized cat. Exp Brain Res 50:377-391.

Gray CM, Singer W (1989) Stimulus-specific neuronal oscillations in orientation columns of cat visual cortex. Proc Natl Acad Sci U S A 86:1698-1702.

Gray CM, Konig P, Engel AK, Singer W (1989) Oscillatory responses in cat visual cortex exhibit inter-columnar synchronization which reflects global stimulus properties. Nature 338:334-337.

Hall WC, Lee P (1993) Interlaminar connections of the superior colliculus in the tree shrew. I. The superficial gray layer. J Comp Neurol 332:213-223.

Hall WC, Lee P (1997) Interlaminar connections of the superior colliculus in the tree shrew. III: The optic layer. Vis Neurosci 14:647-661.

Henze DA, Borhegyi Z, Csicsvari J, Mamiya A, Harris KD, Buzsaki G (2000) Intracellular features predicted by extracellular recordings in the hippocampus in vivo. J Neurophysiol 84:390-400.

Huerta MF HJ (1984) Comparative Neurology of Optic tectum.

Isa T, Hall WC (2009) Exploring the superior colliculus in vitro. J Neurophysiol 102:2581-2593.

Kajikawa Y, Schroeder CE (2011) How local is the local field potential? Neuron 72:847-858.

Katzner S, Nauhaus I, Benucci A, Bonin V, Ringach DL, Carandini M (2009) Local origin of field potentials in visual cortex. Neuron 61:35-41.

Kayser C, Logothetis NK (2007) Do early sensory cortices integrate cross-modal information? Brain Struct Funct 212:121-132.

Kayser C, Logothetis NK, Panzeri S (2010) Visual enhancement of the information representation in auditory cortex. Curr Biol 20:19-24.

Kayser C, Petkov CI, Augath M, Logothetis NK (2005) Integration of touch and sound in auditory cortex. Neuron 48:373-384.

Kreiter AK, Singer W (1996) Stimulus-dependent synchronization of neuronal responses in the visual cortex of the awake macaque monkey. J Neurosci 16:2381-2396.

Kudo M (1981) Projections of the nuclei of the lateral lemniscus in the cat: an autoradiographic study. Brain Res 221:57-69.

Kudo M, Niimi K (1980) Ascending projections of the inferior colliculus in the cat: an autoradiographic study. J Comp Neurol 191:545-556.

Lakatos P, Chen CM, O'Connell MN, Mills A, Schroeder CE (2007) Neuronal oscillations and multisensory interaction in primary auditory cortex. Neuron 53:279-292.

Lakatos P, Karmos G, Mehta AD, Ulbert I, Schroeder CE (2008) Entrainment of neuronal oscillations as a mechanism of attentional selection. Science 320:110-113.

Lo FS, Cork RJ, Mize RR (1998) Physiological properties of neurons in the optic layer of the rat's superior colliculus. J Neurophysiol 80:331-343.

Logothetis NK (2008) What we can do and what we cannot do with fMRI. Nature 453:869-878.

Maier A, Wilke M, Aura C, Zhu C, Ye FQ, Leopold DA (2008) Divergence of fMRI and neural signals in V1 during perceptual suppression in the awake monkey. Nat Neurosci 11:1193-1200.

May PJ (2006) The mammalian superior colliculus: laminar structure and connections. Prog Brain Res 151:321-378.

Meredith MA, Stein BE (1983) Interactions among converging sensory inputs in the superior colliculus. Science 221:389-391.

Meredith MA, Stein BE (1986a) Spatial factors determine the activity of multisensory neurons in cat superior colliculus. Brain Res 365:350-354.

Meredith MA, Stein BE (1986b) Visual, auditory, and somatosensory convergence on cells in superior colliculus results in multisensory integration. J Neurophysiol 56:640-662.

Meredith MA, Stein BE (1990) The visuotopic component of the multisensory map in the deep laminae of the cat superior colliculus. J Neurosci 10:3727-3742.

Meredith MA, Stein BE (1996) Spatial determinants of multisensory integration in cat superior colliculus neurons. J Neurophysiol 75:1843-1857.

Meredith MA, Nemitz JW, Stein BE (1987) Determinants of multisensory integration in superior colliculus neurons. I. Temporal factors. J Neurosci 7:3215-3229.

Meredith MA, Keniston LR, Dehner LR, Clemo HR (2006) Crossmodal projections from somatosensory area SIV to the auditory field of the anterior ectosylvian sulcus (FAES) in Cat: further evidence for subthreshold forms of multisensory processing. Exp Brain Res 172:472-484.

Mitzdorf U (1985) Current source-density method and application in cat cerebral cortex: investigation of evoked potentials and EEG phenomena. Physiol Rev 65:37-100.

Mitzdorf U (1987) Properties of the evoked potential generators: current source-density analysis of visually evoked potentials in the cat cortex. Int J Neurosci 33:33-59.

Mucke L, Norita M, Benedek G, Creutzfeldt O (1982) Physiologic and anatomic investigation of a visual cortical area situated in the ventral bank of the anterior ectosylvian sulcus of the cat. Exp Brain Res 46:1-11.

Munoz DP, Guitton D (1985) Tectospinal neurons in the cat have discharges coding gaze position error. Brain Res 341:184-188.

Munoz DP, Guitton D (1989) Fixation and orientation control by the tecto-reticulo-spinal system in the cat whose head is unrestrained. Rev Neurol (Paris) 145:567-579.

Ogasawara K, McHaffie JG, Stein BE (1984) Two visual corticotectal systems in cat. J Neurophysiol 52:1226-1245.

Perrault TJ, Jr., Vaughan JW, Stein BE, Wallace MT (2003) Neuron-specific response characteristics predict the magnitude of multisensory integration. J Neurophysiol 90:4022-4026.

Perrault TJ, Jr., Vaughan JW, Stein BE, Wallace MT (2005) Superior colliculus neurons use distinct operational modes in the integration of multisensory stimuli. J Neurophysiol 93:2575-2586.

Rasch MJ, Gretton A, Murayama Y, Maass W, Logothetis NK (2008) Inferring spike trains from local field potentials. J Neurophysiol 99:1461-1476.

Rockland KS, Ojima H (2003) Multisensory convergence in calcarine visual areas in macaque monkey. Int J Psychophysiol 50:19-26.

Rols G, Tallon-Baudry C, Girard P, Bertrand O, Bullier J (2001) Cortical mapping of gamma oscillations in areas V1 and V4 of the macaque monkey. Vis Neurosci 18:527-540.

Schroeder CE, Foxe JJ (2002) The timing and laminar profile of converging inputs to multisensory areas of the macaque neocortex. Brain Res Cogn Brain Res 14:187-198.

Schroeder CE, Lindsley RW, Specht C, Marcovici A, Smiley JF, Javitt DC (2001) Somatosensory input to auditory association cortex in the macaque monkey. J Neurophysiol 85:1322-1327.

Segal RL, Beckstead RM (1984) The lateral suprasylvian corticotectal projection in cats. J Comp Neurol 225:259-275.

Sprague JM, Berlucchi G, Di Berardino A (1970) The superior colliculus and pretectum in visually guided behavior and visual discrimination in the cat. Brain Behav Evol 3:285-294.

Sprague JM, Levy J, DiBerardino A, Berlucchi G (1977) Visual cortical areas mediating form discrimination in the cat. J Comp Neurol 172:441-488.

Stanford TR, Stein BE (2007) Superadditivity in multisensory integration: putting the computation in context. Neuroreport 18:787-792.

Stanford TR, Quessy S, Stein BE (2005) Evaluating the operations underlying multisensory integration in the cat superior colliculus. J Neurosci 25:6499-6508.

Stein BE MA (1993) The Merging of the Senses. Book.

Sterling P (1971) Receptive fields and synaptic organization of the superficial gray layer of the cat superior colliculus. Vision Res Suppl 3:309-328.

Sterling P, Wickelgren BG (1969) Visual receptive fields in the superior colliculus of the cat. J Neurophysiol 32:1-15.

Stevenson RA, James TW (2009) Audiovisual integration in human superior temporal sulcus: Inverse effectiveness and the neural processing of speech and object recognition. Neuroimage 44:1210-1223.

Tortelly A, Reinoso-Suarez F, Llamas A (1980) Projections from non-visual cortical areas to the superior colliculus demonstrated by retrograde transport of HRP in the cat. Brain Res 188:543-549.

Tunkl JE, Berkley MA (1977) The role of superior colliculus in vision: visual form discrimination in cats with superior colliculus ablations. J Comp Neurol 176:575-587.

Wallace MT, Stein BE (1994) Cross-modal synthesis in the midbrain depends on input from cortex. J Neurophysiol 71:429-432.

Wallace MT, Meredith MA, Stein BE (1992) Integration of multiple sensory modalities in cat cortex. Exp Brain Res 91:484-488.

Wallace MT, Meredith MA, Stein BE (1998) Multisensory integration in the superior colliculus of the alert cat. J Neurophysiol 80:1006-1010.

Wurtz RH, Albano JE (1980) Visual-motor function of the primate superior colliculus. Annu Rev Neurosci 3:189-226.

CHAPTER V

SYNAPTIC PROCESSING IN THE DEEP LAYERS OF THE SUPERIOR COLLICULUS

This Chapter is a manuscript under preparation as: ***Ghose D, Maier A, Nidiffer AR and Wallace MT.*** *Synaptic processing in the deep layers of the superior colliculus.*

Introduction

The superior colliculus (SC) is a midbrain structure that plays an important role in eye movement and orientation behavior. The SC is a laminated structure divided into seven different layers LI-LVII (Huerta MF 1984; Kanaseki and Sprague 1974). The top three layers LI-III are grouped together as superficial layers while LIV-VII is grouped together as the intermediate/deep layers. This division into superficial and intermediate/deep layers is based on overall differences in neuronal morphology, afferent-efferent projections, physiological properties and behavioral involvements of the SC (Casagrande et al. 1972; Dreher and Hoffmann 1973; Huerta MF 1984; Stein BE 1993; Sterling and Wickelgren 1969). Most of the studies, done to date, show that the multisensory properties of the SC are restricted to its deeper layers while the superficial layers are visual in nature. However, the multisensory nature of the deep layers has been characterized by studying mainly spiking activity of neurons in the deep layers or in other words, essentially studying the ***outcome*** of the neural computations taking

place in this area. These multisensory neurons show profound increase in spiking activity when multisensory stimulus combination is presented compared to presentation of unisensory stimuli alone and such multisensory neuronal gains are reflected in behavior as well (Meredith et al. 1987; Meredith and Stein 1983; 1986a; b; Stein BE 1993). Animals show greater accuracy in localization behavior using multisensory cues compared to unisensory cues alone (Jiang W 2000; Wilkinson et al. 1996). However, majority of the studies that characterize “multisensory” nature of SC rely on overt responses of the neurons to more than one sensory modality. However, recent studies of multisensory processing in different brain areas suggest that neurons may not overtly respond to more than one sensory modality but their responses to the dominant sensory modality may be modulated by addition of stimuli from a non- dominant sensory modality, hence conferring multisensory properties to these neurons .For example, responses of auditory cortical neurons in non-human primates are modulated by visual stimulation (Ghazanfar and Schroeder 2006; Kayser and Logothetis 2007; Kayser et al. 2009; Schroeder and Foxe 2002). This is reflected not only in single and multi-unit spiking activity but also as sub-threshold changes in local field potentials (LFP). Similar kinds of modulatory influences have been reported in spiking activity of neurons in higher visual cortices in cats like the Posterolateral Lateral Suprasylvian Sulcus (PLLS) (Allman et al. 2008a; Allman et al. 2008b; Allman and Meredith 2007; Clemo et al. 2008) and traditional multisensory areas like anterior ectoslyvian sulcus (AES) and the intermediate/deep layers of the SC (Carriere et al. 2008; Dehner et al. 2004; Ghose et al. 2012; Meredith et al. 2006; Ghose and Wallace 2013 submitted). Intermediate/deep layers of SC are capable of demonstrating modulatory influences such that for example

a visual neuron with overt responses to presentation of visual stimulus alone but not auditory stimulus alone shows significant changes in visual response on presentation of visual-auditory stimulus combination (Ghose et al 2012; Ghose and Wallace 2013 submitted). Such modulatory changes may be brought about by sub threshold synaptic activity which can be studied by characterizing LFPs of the region. Moreover, since LFPs are essentially an index of local synaptic processing, they provide information about local inputs in a given brain area (Pesaran 2009) making the link between LFP and spiking activity an essential bridge between analyzing inputs to and outputs from the SC.

The intermediate/deep layers receive visual inputs from extra-primary visual cortical areas like the lateral suprasylvian area (Segal and Beckstead 1984; Tortelly et al. 1980) and anterior ectosylvian visual area (Mucke et al. 1982).Retinal input is sparse (Beckstead and Frankfurter 1983). In addition, the deep layers receive inputs from non-visual or auditory (Edwards et al. 1979; Kudo 1981; Kudo and Niimi 1980; Meredith and Clemo 1989) and somatosensory (Clemo and Stein 1982; McHaffie et al. 1988) brain areas as well. Auditory inputs are from Field AES region of the Anterior Ectosylvian sulcus (Meredith and Clemo 1989) while the ascending auditory inputs arise from dorsomedial periolivary nucleus (Edwards et al. 1979), inferior colliculus and nucleus of the lateral lemniscus (Henkel 1983; Kudo 1981; Kudo and Niimi 1980; Moore and Goldberg 1966). Somatosensory afferents are primarily from SIV cortex, the rostral part of lateral suprasylvian cortex (Clemo and Stein 1982; Meredith and Stein 1983), contralateral sensory trigeminal complex, dorsal column nuclei, lateral cervical nucleus and spinal cord (Edwards et al. 1979; Harting et al. 1980). In addition studies have

shown that the integrative abilities of these multisensory neurons are dependent on the cortical inputs from AES and rLS (Jiang W 2000; Wallace and Stein 1994; Wilkinson et al. 1996).Thus by studying LFPs in the deep layers of the SC and comparing it to spiking activity recorded from the same electrode we can understand the nature of sub-threshold synaptic processing (brought about by the wide variety of inputs to this region) and its relation to spiking activity (the final observed output of the region) in the SC and this will provide a better mechanistic view into multisensory processing in the SC.

Methods

General procedures: Experiments were conducted in adult cats (n=3) raised under standard housing conditions. A total of 72 single units were isolated but a detailed characterization was possible for 69 neurons. All experiments were done in an anesthetized and paralyzed semi-chronic preparation and consisted of single-unit and LFP extracellular recordings from the superior colliculus (SC) in the midbrain. Experiments were run on a weekly basis on each animal. All surgical and recording procedures were performed in compliance with the Guide for the Care and Use of Laboratory Animals at Vanderbilt University Medical Center, which is accredited by the American Association for Accreditation of Laboratory Animal Care.

Implantation and Recording procedures: For anesthesia during surgical procedures animals were initially induced with ketamine hydrochloride (20mg/kg, administered intramuscularly (im)) and acepromazine maleate(0.04mg/kg im). For implantation of the

recording chamber over the SC, animals were transported to a central surgical suite, where they were intubated and artificially respired. A stable plane of surgical anesthesia was achieved using inhalation of isoflurane (1%-3%). Body temperature, expiratory CO2, blood pressure and heart rate were continuously monitored (VSM7, Vetspecs/SCIL) recorded and maintained within ranges consistent with a deep and stable plane of anesthesia. A craniotomy was made to allow access to SC and a head holder was attached to the cranium using stainless steel screws and orthopedic cement to hold the animal during recording sessions without obstructing the face and ears. Post-operative care (antibiotics and analgesics) was done in close consultation with veterinary staff.

For recording animals were anesthetized with ketamine (20mg/kg im) and acepromazine maleate (0.04mg/kg im) and maintained throughout the procedure with constant rate infusion of ketamine (5mg/kg/hr iv) delivered through cannula placed in the saphenous vein. The head holding system was then used to keep the animal comfortably in recumbent position. To prevent ocular drifts animals were paralyzed using pancuronium/ vecuronium bromide (.1-.2 mg/kg/hr, iv) and artificially respired for the duration of recording. On completion of experiment animals were subcutaneously given 60-100ml of lactated Ringer solution to facilitate recovery. Parylene insulated tungsten electrodes (Z = 4-5 MΩ) were advanced into the SC using an electronically controlled mechanical microdrive. The top of SC was identified by its typical fast visual responses. Single- unit neural activity and local field potentials were recorded, amplified and routed to an oscilloscope, audio monitor and computer for performing online and offline analysis. Visual stimulus consisted of the illumination of stationary light emitting

diodes (LEDs: 100ms duration) while auditory stimulus were delivered through positionable speakers and consisted of 100ms duration broadband noise (20Hz-20KHz)with an intensity of 67dB SPL. Both the LED and speakers were mounted on a hoop placed 2ft in front of the cat at azimuthal locations 0-90 (10deg increments) on either side of the midline. The hoop could be rotated along different elevations that allowed sampling numerous locations within and just outside the receptive field of the cell creating Spatial Receptive Field architecture (SRF). The physical characteristics of the stimuli are identical in all respects except for the spatial location at which it is presented. Visual and auditory stimuli were presented in a randomized interleaved manner at multiple azimuthal locations along a single elevation at a time. Multisensory combinations consisted of visual and auditory stimuli presented at the same spatial location (ie spatial coincidence). The order in which stimulus locations were tested was determined randomly. Unisensory and multisensory stimulus conditions were randomly interleaved until a minimum of 60 trials (20 visual, 20 auditory, 20 multisensory) were collected for a given stimulus location. Consecutive stimulus presentations were separated by at least 1.5 secs to avoid response habituation.

Data acquisition and analysis: A custom built PC based real time data acquisition system controlled the structure of the trials and the timing of the stimulus (Labview. National Instruments). The analog waveform picked up by the electrode were transferred to the a Plexon MAP system (Plexon Inc.,Texas) where they are digitized at 40KHz. Single-unit activity was recorded online using Sort Client software (Plexon Inc., Texas)and also stored for further offline analysis. Neuronal responses were characterized through construction of peristimulus time histograms (PSTHs) for each

condition (visual (V) only, auditory only (A), visual-auditory together (VA)) for each location tested within the SRF. Baseline for each PSTH was calculated as mean firing rate during the 500ms immediately preceding the stimulus onset for each of the 3 conditions. The PSTHs were then set at a threshold, 2SD above their respective baselines to delimit the stimulus evoked response. After stimulus onset the time at which the PSTH crosses above the 2SD line (and remains so for at least 30ms) was noted as response onset. Response offset was the time at which the PSTH fell below the 2SD line and stayed below this line for >=30ms. Mean spontaneous firing rate is always subtracted from the response to get the mean stimulus evoked response for all the 3 conditions. Stimulus onset asynchrony (SOA) varied between V0A0 or V0A50 i.e., simultaneous visual and auditory stimulation or visual stimulus preceding the auditory stimulus by 50ms). The choice of the ideal SOAs was based on an initial analysis that tested neuronal responses to several SOA combinations and then the best SOA pair was chosen for further recordings.

Measures for testing multisensory integration: Two measures were used to test for multisensory integration. The first being the interactive index (ii) that measured quantitatively how the multisensory response differed from the best unisensory response. The magnitude of this change was calculated as [(CM-SMmax)/ SMmax)] X100 = % interaction where CM is the mean response evoked by combined modality stimulus, SMmax is the mean response evoked by the most effective single modality stimulus(Meredith and Stein 1983; 1986a; b). Statistical comparisons between the mean stimulus evoked responses of the multisensory condition and the strongest unisensory condition were done using a non-parametric Wilcoxon Rank Test. Response

enhancement was defined as statistically significant positive ii values, and no interaction was when ii values were statistically non-significant.

The second measure used is mean statistical contrast (msc). This metric evaluates the multisensory response as a function of the response predicted by the addition of the two unisensory. Multisensory contrast is calculated using the formula :∑[(SA-A)-(V-VA)]/n where SA is spontaneous activity, A is auditory response, V is visual response, VA is multisensory response and n is the number of trials. The model assumes independence between the visual and auditory inputs and uses additive factors logic to distinguish between subadditive (contrast<0), additive(contrast = 0) and superadditive (contrast >0)modes of response (Perrault et al. 2003; 2005; Stanford et al. 2005; Stanford and Stein 2007). Significant differences from a contrast value of 0 were determined by the Wilcoxon Rank test.

Based on these measures of multisensory integration, neurons were classified into two major groups: 1) Overt neurons: those which showed overt spiking activity in both visual and auditory conditions in at least 1 location within its spatial receptive field 2) Modulatory neurons: Those which showed overt spiking activity in **either** the visual (visual modulatory neuron) or the auditory condition (auditory modulatory neuron) but responses in the multisensory condition were significantly different from the best unisensory condition.

LFP analysis: LFP was sampled at 1000Hz and converted to millivolts as a function of time. For both SOAs (V0A0 and V0A50), the evoked LFP responses across all stimulus locations showing Response Enhancements (see above) were averaged to produce a

Grand Average LFP trace. This was repeated for all stimulus locations showing No Interactions as well. Number of locations showing Response Depression was very low so they were excluded from further analysis.

Evoked LFP amplitude was quantified using the two measures described below:

Mean peak LFP quantification: To quantify the changes in evoked LFP in response to the stimuli, the LFP amplitude pre and the post stimulus onset was compared using t tests (and corrected with Bonferroni correction for multiple comparisons) for each condition. More specifically, the mean voltage within 150-0ms pre-stimulus was taken as the baseline. Peak voltage change within a time window of 0-300ms post stimulus was compared to baseline in order to assess stimulus related changes for all conditions [visual, auditory and multisensory (V0A0/V0A50)]. Both time windows (pre and post stimulus) were chosen based on visual inspection of the data. The post stimulus window was chosen to encompass all stimulus-evoked LFP changes, including those lasting for several ms after stimulus presentation. Next, mean peak voltage within the response window was compared between visual , auditory and multisensory conditions for Overt neurons using a t test to determine whether the visually-evoked/ auditory evoked LFP amplitude differed significantly from multisensory LFP amplitude for stimulus locations showing Response Enhancement and No Interactions in their spiking responses, respectively. For modulatory neurons, mean peak voltages were compared between the dominant sensory modality and the multisensory condition. Correction for multiple comparisons was applied wherever necessary.

Area under the curve measure: Amplitude of evoked LFPs was also analyzed using Area under the curve measures. Area under the curve was computed from stimulus onset to 200ms post-stimulus for each of the stimulus conditions. These were then compared using t tests (corrected for multiple comparisons when necessary) for statistical significance. Choice of 200ms post stimulus was based on visual inspection of the data which showed that most of the changes phase locked to the stimulus could be captured within this post stimulus epoch.

Time frequency analysis: To test for phase locked and non- phase locked stimulus-induced LFP power changes in different frequency bands, spectrograms were computed using the Fast Fourier Transform with a running window size of 256ms and an overlap of 255ms. The spectrograms were computed separately for stimulus locations within the receptive field showing Response enhancement, and No significant Interaction as defined by the local spiking response (see above).

Contrast plots were computed to determine the effects of multisensory stimulation on LFP responses. The contrast plots quantified LFP power difference between the best unisensory (V or A) and the multisensory condition (AV). Results for the comparisons were converted to t-scores for statistical comparison using the following formula:

$t = (x1-x2)/ (SD/sqrt (n1+n2))$,

where x1 is the average response for condition 1 (such as AV), and x2 is the average response for condition 2 (such as V), SD is the standard deviation of responses across both conditions, sqrt is the square root, and n1 and n2 are the number of trials for condition 1 and condition 2, respectively.

False discovery rate (FDR) at a level of 0.01 was used to correct for multiple comparisons. Similar results were achieved when a Bonferroni correction was applied.

Results

Single unit activity and its relation to local field potentials in the intermediate/ deep layers of SC:

Intermediate/deep layer neurons of the SC can be divided into two broad categories: Overt neurons and modulatory neurons (for details see methods). Intermediate/deep layer multisensory neurons show changes in spiking activity when strongest unisensory and multisensory conditions are compared. Generally, when visual and auditory stimuli are presented in spatial and temporal congruence within the receptive fields of the multisensory neurons, spike counts are more under multisensory condition compared to the unisensory conditions. This is called Response Enhancement. To assess similarities/differences between spiking activity and sub-threshold changes evident in LFP activity under conditions of Response Enhancement, spikes and LFPs recorded from the same electrode were simultaneously analyzed. Fig 5-1 shows representative examples of spiking activity and local field potential for Response Enhancement at V0A50 SOA for an overt neuron and modulatory neurons (visual modulatory or auditory modulatory). For the overt neuron (Fig 5-1A) spiking activity can be seen after both visual alone and auditory alone stimulations. Moreover the multisensory response differs significantly from the best unisensory response (i.e, visual here) as reflected by

the significant interactive index (ii) value. The significant positive msc value (see methods for details) shows that the interaction is super-additive in nature. The corresponding LFP signal, though highly variable in nature, shows a clear stimulus related response for all 3 stimulus conditions. For the visual modulatory neuron (Fig 5-1B), spiking activity can be seen on presentation of visual stimulus alone but auditory stimulation alone does not produce spiking activity. However, response in the multisensory condition significantly differs from the best unisensory condition (visual) as reflected in the significant ii value and the interaction is super-additive in nature as depicted by the significant msc value. LFP responses recorded from the same electrode shows sub-threshold auditory responses in absence of spiking activity. Similarly for auditory modulatory neuron (Fig 5-1C) spiking activity occurs on presentation of auditory stimulus alone, not with visual stimulus alone but the multisensory response differs significantly from the auditory response as depicted in the ii and msc values. As for the LFP response, sub-threshold visual activity can be seen in absence of spiking on presentation of visual stimulus alone. Fig 5-2 (A and B) shows representative examples of overt and visual modulatory neuron at an SOA of V0A0. Findings are similar to Fig 5-1 where for the overt neuron spiking activity is seen for each of the unisensory conditions and the multisensory response differs from the best unisensory response. LFP activity is seen for all 3 stimulus conditions. For the visual modulatory neuron, sub-threshold auditory activity is seen in the LFP trace in absence of spiking activity. Thus, these examples highlight the fact that changes in evoked local field potentials can occur in absence of spiking activity in the intermediate/deep layers of SC.

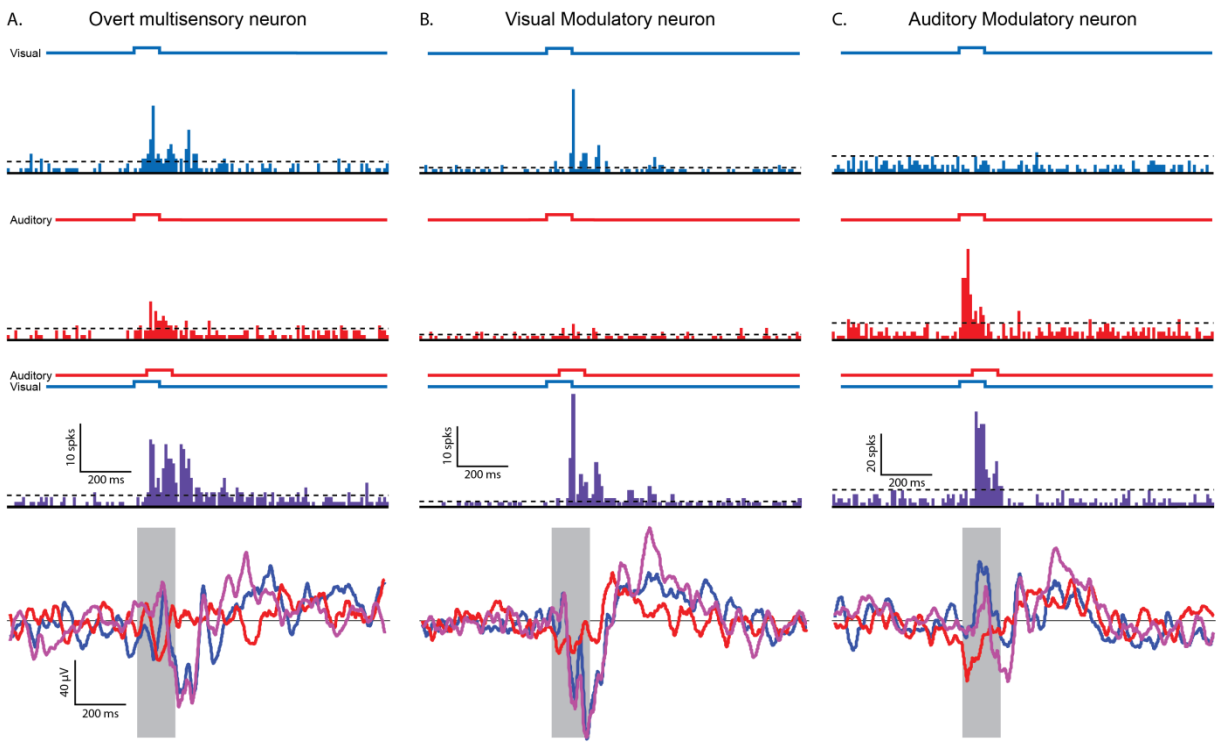

Fig 5-1: Representative examples of single unit activity and local field potential for different neuronal sub types in the intermediate/deep layers of the SC.

Representative example of single unit activity and local field potential recorded from the same electrode of an **A]** Overt Neuron **B]** Visual modulatory neuron and **C]** Auditory modulatory neuron in the intermediate/deep layers of SC showing Response Enhancement. For the multisensory stimulus condition Stimulus Onset Asynchrony (SOA) =V0A50, onset of the visual stimulus preceding the auditory stimulus by 50ms. Onset and duration of visual and auditory stimuli are represented by blue and red square waves on top of the raster plots for each condition. Dotted horizontal line represents the threshold for neuronal response. For the overt neuron in A. ii=130.6% p=0.0009, msc=3.5 p=0.008. For the visual modulatory neuron in B. ii=145.4%, $p = 9.9\times10^{-5}$; msc=3.9, $p=9.9\times10^{-5}$). For the auditory modulatory neuron in C. ii=40.8 p=0.01; msc=1.8 p=0.01).

Averaged LFP traces (averaged across trials) are shown below where blue: visual condition, red: auditory condition, purple: multisensory condition. The grey boxes on the LFP traces represent multisensory (V0A50) stimulus duration (150ms).

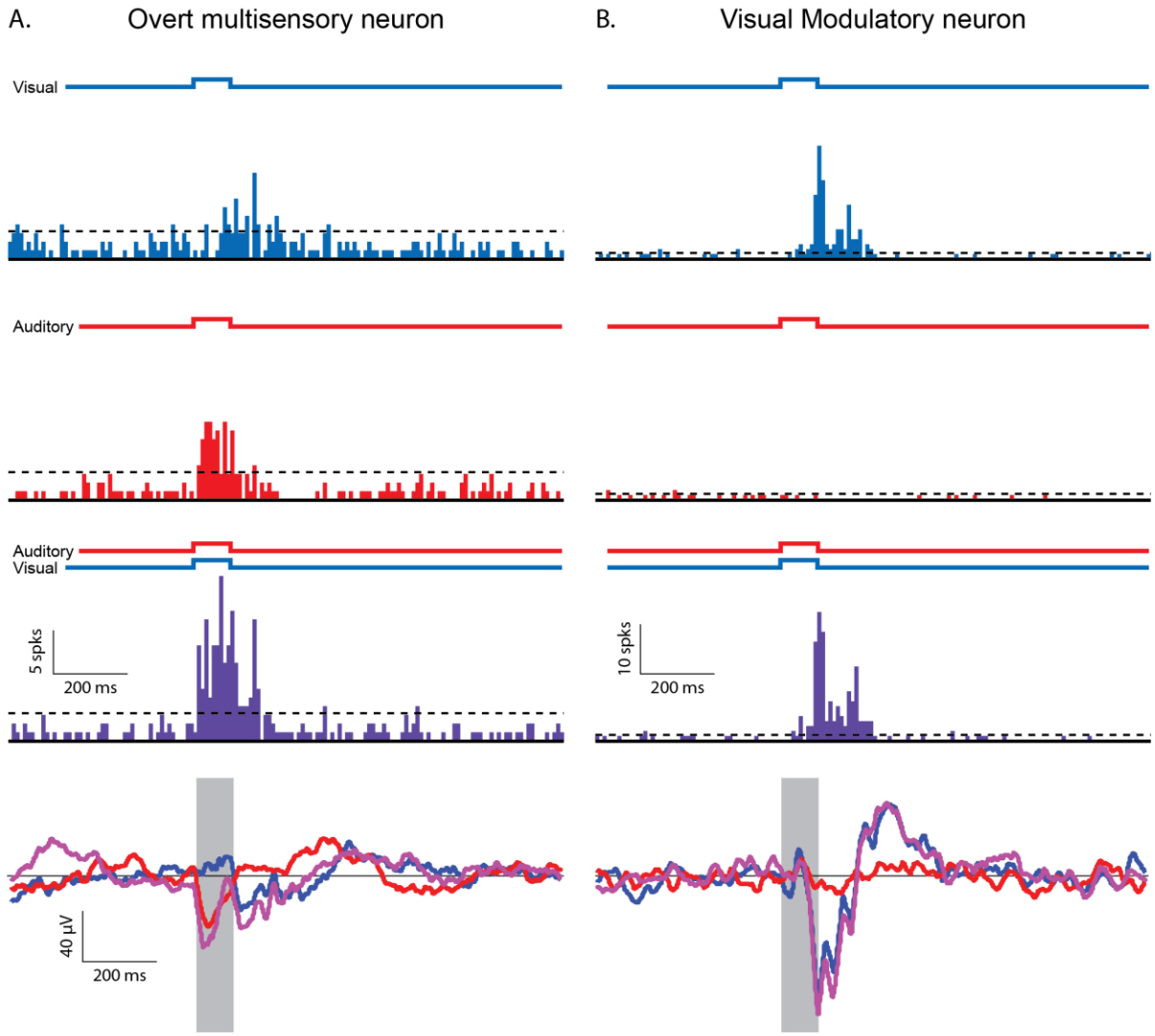

Fig 6-2: Representative examples of single unit activity and local field potential for different neuronal sub types in the deep layers of the SC.

Representative example of single unit activity and local field potential recorded from the same electrode of an **A]** Overt Neuron **B]** Visual modulatory neuron in the deep layers of SC showing Response Enhancement. For the multisensory stimulus condition, Stimulus Onset Asynchrony (SOA) =V0A0, simultaneous onset of visual and auditory stimulus. Onset and duration of visual and auditory stimuli are represented by blue and red square waves on top of the raster plots for each condition. Dotted horizontal line represents the threshold for neuronal response. For the overt neuron in A. ii=135.83 p=0.001; msc =2.3, p=0.02. For modulatory neuron in B. ii=48.5, p=0.015; msc=2.6, p= 0.015).

Averaged LFP traces (averaged across trials) are shown below where blue: visual condition, red: auditory condition, purple: multisensory condition. The grey boxes on the LFP traces represent multisensory (V0A0) stimulus duration (100ms).

Evoked LFPs in the intermediate/deep layers:

As mentioned earlier(see methods), Response Enhancements are accompanied by a statistical increase in spike count in the multisensory condition compared to the best unisensory condition while for No Interactions spike counts in the best unisensory and multisensory conditions do not differ significantly. Our next goal was to assess if such differences between Response Enhancement and No Interactions would be evident in evoked LFP responses as well for the different classes of neurons in the intermediate/deep layers of SC. To test this, the evoked LFPs for all locations within the receptive fields that showed Response Enhancements and No Interactions (based on spiking activity) for all 69 neurons (Overt and Modulatory, both SOAs V0A0 and V0A50) recorded were averaged separately to generate a Grand Average LFP trace for each of these conditions as shown in Fig 5-3 (SOA=V0A50) and Fig. 5-4(SOA=V0A0). Two measures were the used to quantify changes in the amplitude of evoked LFPs.

Mean Peak LFP amplitude: The mean peak voltage was then compared across different conditions. For details see methods. Fig 5-3 represents changes in mean peak voltage for overt and modulatory neurons when multisensory stimuli with an SOA=V0A50 was tested. Overall, mean peak voltage was highest for the multisensory condition for overt and modulatory neurons for both Response Enhancements and No Interactions. However, when the best unisensory and multisensory conditions were statistically compared, statistical significance was achieved for overt neurons and visual modulatory neurons but not for auditory modulatory neurons (Fig 5-3). Quantification of the mean peak amplitude for SOA =V0A0 (Fig 5-4) revealed that for the overt neurons the peak amplitudes were significantly different between the best unisensory and

multisensory condition (both Response Enhancement and No Interactions) while such differences could not be found in the peak amplitudes of visual modulatory neurons. The statistical details are reported in Table 1and 2.

Area under the curve: The second measure used to quantify evoked LFP amplitude was Area under the curve [Fig 5-3 (V0A50) and 5-4(V0A0) second set of bar graphs]. This analysis revealed that for both overt neurons and visual modulatory neurons (both SOAs V0A50 and V0A0) area under the curve for multisensory condition was significantly greater when compared to the best unisensory condition for both Response Enhancements and No Interactions. Though our sample included only 6 auditory modulatory neurons showing integration at V0A50 SOA only, area under the curve was significantly greater for spatial locations showing both Response Enhancement and No Interaction. Statistical details are reported in Tables 1 and 2.

LFP latency: Another interesting finding here is that the evoked visual LFP trace has the longest latency compared to the auditory and multisensory conditions (Fig 5-3 and 5-4). This could be because the driving visual inputs of deep SC are derived from cortical areas like posteromedial lateral suprasylvian sulcus (PMLS) and posterolateral lateral suprasylvian sulcus (PLLS) which take longer to reach SC than the driving auditory inputs that are derived from sub cortical auditory areas. Such differences in latencies are noted for spiking activity as well with the mean visual latency of deep layer neurons being about 75ms compared to the mean visual latency of 34ms in the superficial layers of SC that receive driving inputs directly from the retina.

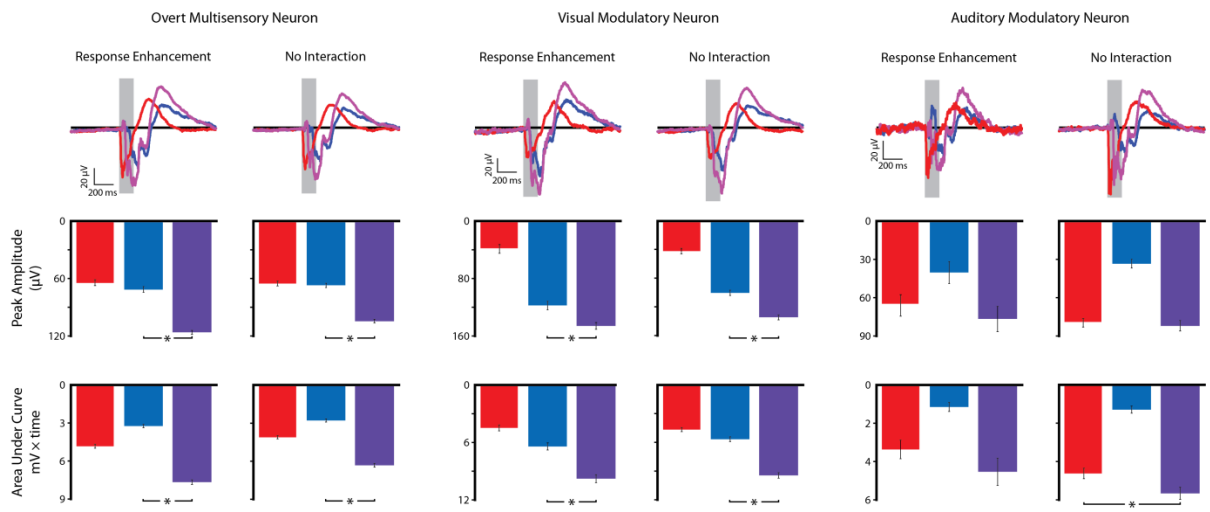

Fig 5-3: Averaged evoke LFPs and quantification of evoked LFP amplitude for the different neuronal subtypes for SOA=V0A50.

Evoked LFP responses for visual (blue) auditory (red) and multisensory (purple) stimulus (V0A50) conditions for Response Enhancements and No Interactions, for overt neurons, visual and auditory modulatory neurons (Top panel).

Quantification of mean peak amplitude and area under the curve for all three stimulus conditions and for both Response Enhancement and No Interactions are shown in the bottom two panels respectively. Asterisks represent statistically significant differences.

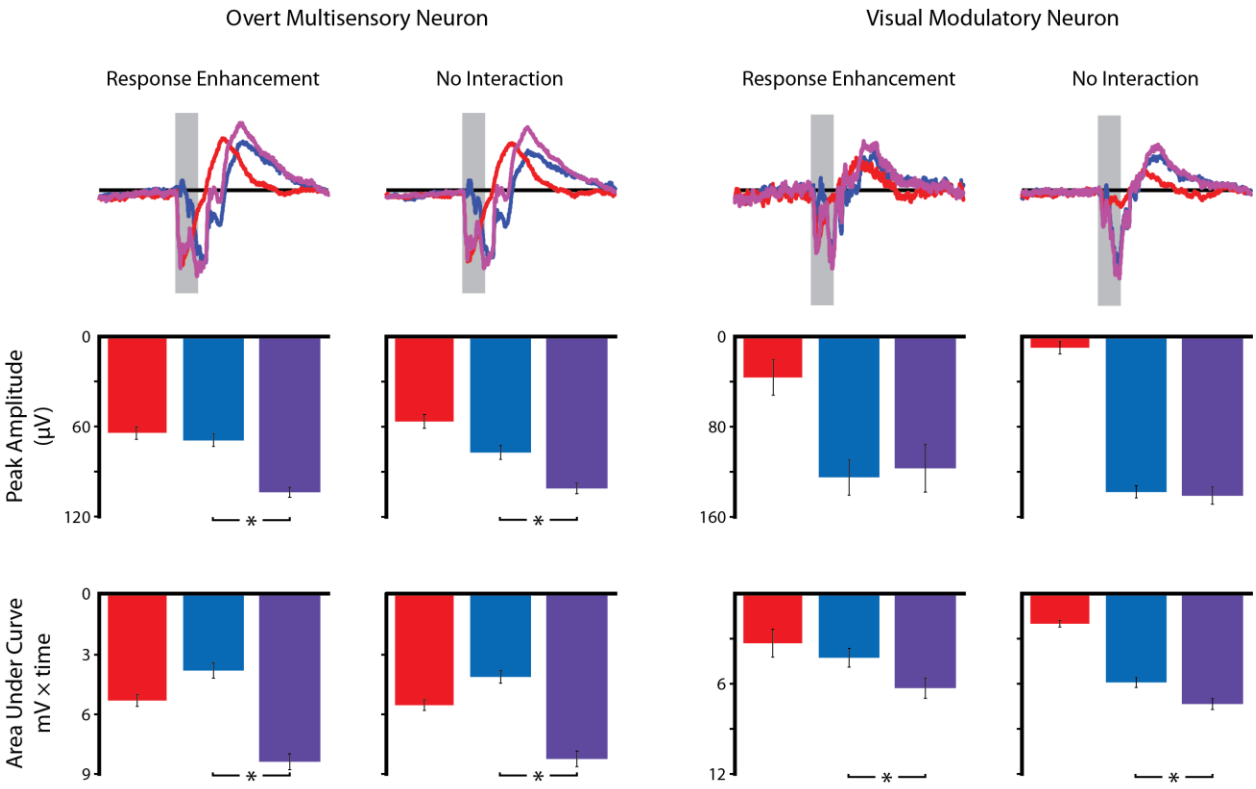

Fig 5-4: Averaged evoke LFPs and quantification of evoked LFP amplitude for the different neuronal subtypes for SOA=V0A0.

Evoked LFP responses for visual (blue) auditory (red) and multisensory (purple) stimulus (V0A0) conditions for Response Enhancements and No Interactions for Overt neurons and visual modulatory neurons (Top panel).

Quantification of mean peak amplitude and area under the curve for all three stimulus conditions and for both Response Enhancement and No Interactions are shown in the bottom two panels respectively. Asterisks represent statistically significant differences.

Table 5-1: Details of statistical tests for Mean Peak Amplitude and Area Under the Curve for the different neuronal subtypes for SOA=V0A50

	Overt neurons				Visual modulatory neurons		Auditory modulatory neurons	
	Enhancement		No Interaction		Enhancement	No Interaction	Enhancement	No Interaction
	V	A	V	A	V	V	A	A
Mean peak T(p)	15.48(2.2×10^{-42})	15.52(1.5×10^{-42})	14.89 (8.2×10^{-42})	15.32(8.6×10^{-44})	5.77(1.1×10^{-7})	10.73 (2.1×10^{-22})	1.09(0.28)	0.58(0.55)
AUC T(p)	26.08 (4.2×10^{-87})	17.99 (5.7×10^{-53})	24.01 (1.8×10^{-85})	16.06 (3.4×10^{-47})	10.86 (8.2×10^{-18})	16.01 (2.3×10^{-40})	2.38(0.05)	4.31(0.05)

Table 5-2: Details of statistical tests for Mean Peak Amplitude and Area Under the Curve for the different neuronal subtypes for SOA=V0A0

	Overt neurons				Visual modulatory neurons	
	Enhancement		No Interaction		Enhancement	No Interaction
	V	A	V	A	V	V
Mean peak T(p)	6.35(4.6×10^{-9})	8.16(4.9×10^{-13})	4.83(3.2×10^{-6})	7.93 (5.2×10^{-13})	-0.35 (0.72)	0.46 (0.64)
AUC T(p)	12.35(1.0×10^{-22})	9.06(4.5×10^{-15})	10.97(9.1×10^{-21})	8.71(6.1×10^{-15})	2.90(.008)	5.74(8.3×10^{-8})

Time frequency analysis of LFP signals in the intermediate/deep layers of SC

Next, to quantify the changes in LFP power across different frequency bands, averaged spectrograms were computed for Overt Neurons and Visual modulatory neurons as well. Since there were only 6 auditory modulatory neurons, spectrograms generated were very noisy and hence are not included for further analysis here. Generally, two types of LFP activity can be distinguished: a) evoked activity that is strictly phase locked and time locked to stimulus onset called evoked LFP response and b) induced activity that is stimulus related but not phase locked to the onset of the stimulus called non phase locked induced LFP response. Most of the power changes in the higher frequency bands shown here are phase locked to the stimulus while non-phase locked induced changes can be seen in the low frequency ranges where changes in LFP power is observed long after stimulus offset.

Fig 5-5 depicts the power changes across different frequency bands for Overt multisensory neurons at SOAs V0A50 and V0A0 after visual, auditory and multisensory stimulations. Changes in power are depicted as % change from baseline. Onset of auditory stimulus is followed by an increase in power in the low frequency bands (up to ~10-12Hz theta and alpha bands) and the high gamma band (70-90Hz) for both Response Enhancements and No Interactions for both SOAs. Visual stimulation was accompanied by an increase in power in the low frequency bands (theta and alpha) and low and high gamma bands as well (30-90Hz) for both SOAs. Similar increases in power were observed under multisensory conditions as well. Most of the power changes in the higher frequency bands shown here are phase locked to the stimulus while non-

phase locked induced changes can be seen in the low frequency ranges where changes in LFP power is observed long after stimulus offset.

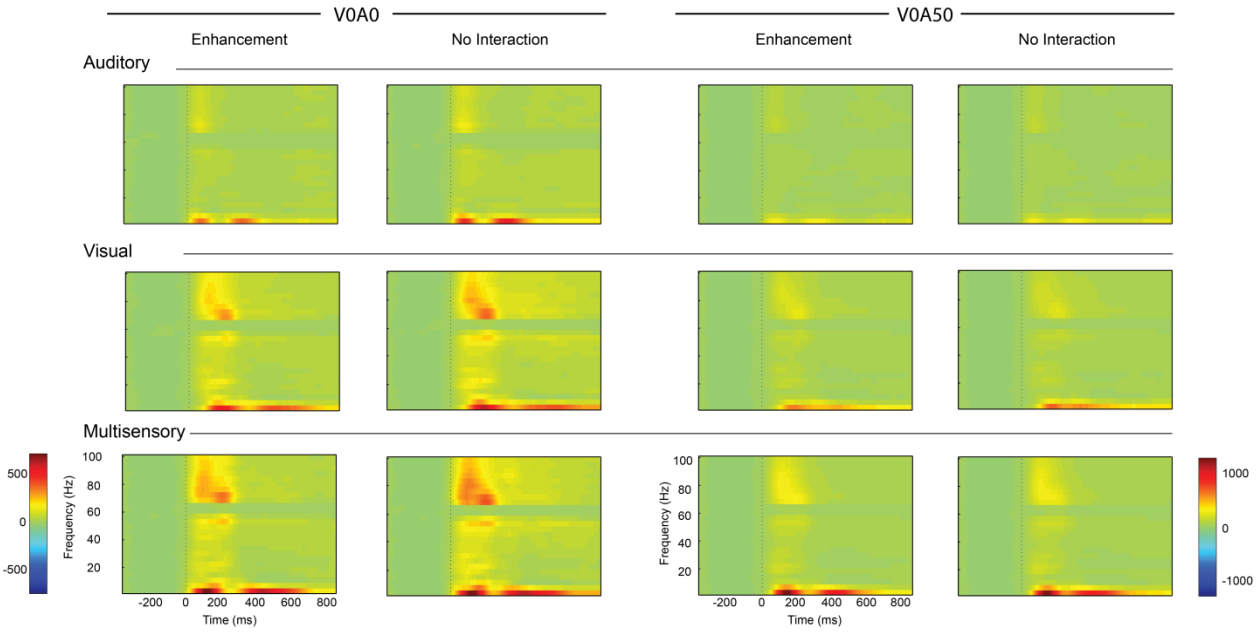

Fig 5-5: Time frequency plots for Overt Neurons in the intermediate/deep layers of the SC

Averaged Time frequency representations of LFPs showing power changes for Auditory, Visual and Multisensory stimulus conditions (V0A0: simultaneous visual and auditory stimulation or V0A50: visual preceding auditory by 50ms) for all stimulus locations showing Response Enhancements and No Interactions. Color bar at the bottom represents the percentage of power change compared to pre-stimulus baseline. The dashed vertical lines represent onset of the stimulus for each condition.

To compare differences between unisensory and multisensory conditions contrast plots were generated as described in Methods. Fig 5-6 shows the contrast plots generated by subtracting the unisensory condition from the multisensory condition for Overt multisensory neurons (depicted in Fig 5-5). Hence, the warmer colors represent greater power in the multisensory condition compared to the unisensory conditions. To quantify these changes in LFP power, statistical analysis was performed comparing the unisensory and multisensory plots. The resulting plots of t values as a function of time and frequency reveal the reliability of this power change (increased power in the multisensory condition). When comparing visual and multisensory power changes, Fig 5-6 (top panel) the increase in power in the multisensory condition was most reliable for the low frequency bands, the low and high gamma band as reflected in the higher and statistically significant t values across these frequency ranges. However, these power changes were stimulus evoked and occurred within a restricted time frame post stimulus. In contrast, when comparing auditory and multisensory conditions, (Fig 5-6 bottom panel) the increase in power in the multisensory condition across different frequency bands that encompassed low frequency ranges (alpha, theta, beta) and low and high gamma bands were seen to extend for longer time periods post stimulus. Though the strongest effects were seen just after stimulus onset (as evident in the darker shaded regions in the T maps showing higher T values), significant differences were still evident 500ms post stimulus.

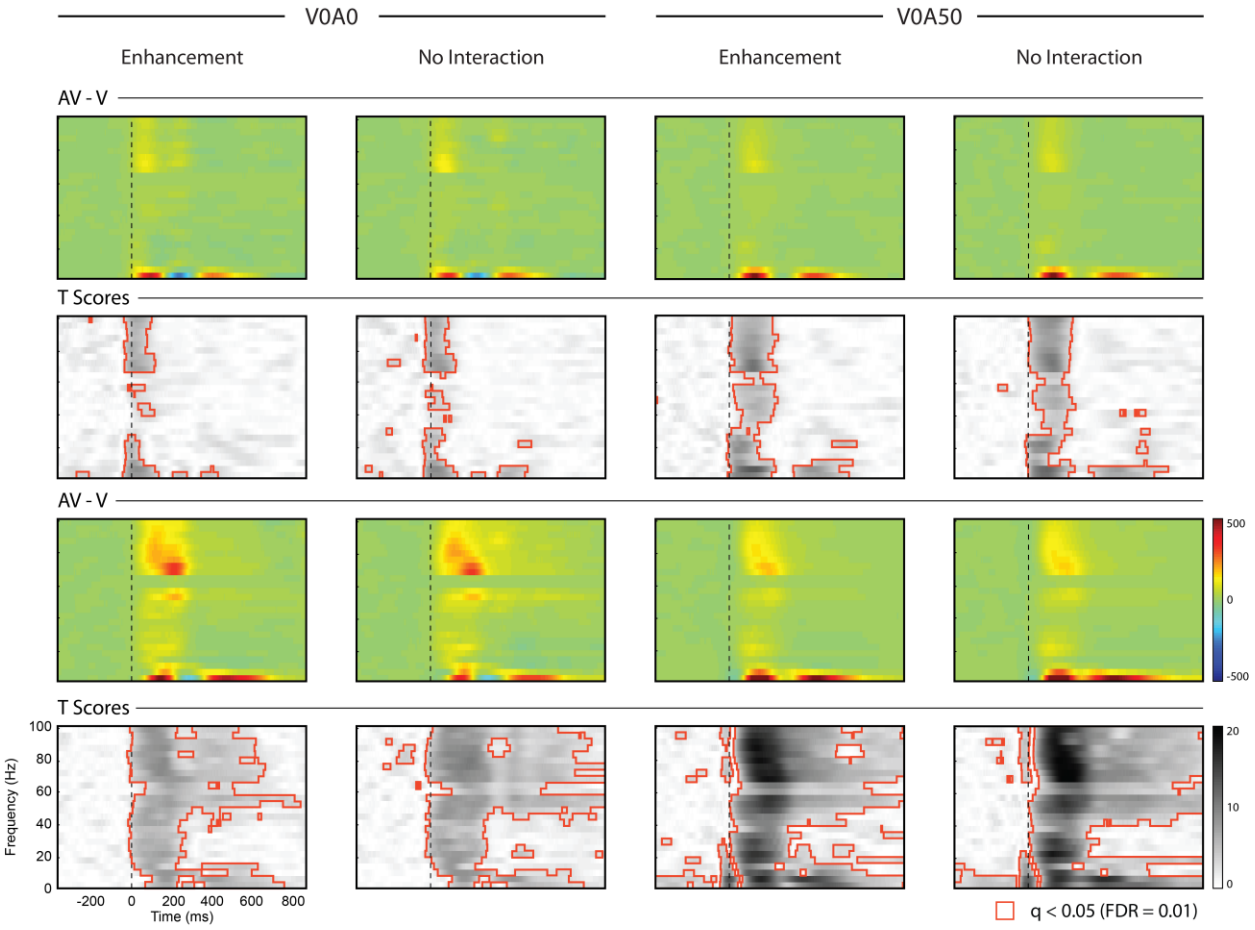

Fig 5-5: Contrast spectrograms and T score plots for LFP changes for Overt Neurons in the intermediate/deep layers of SC

Top panel depicts contrast plots obtained by subtracting the visual condition (V) from the multisensory (AV) condition (AV-V) .The color bar on the right represents the relative power changes (in %) comparing the visual (V) and the multisensory(AV) condition (top set of graphs) and the auditory and multisensory condition(bottom set of graphs). Bottom panel shows time frequency representation of T scores statistically quantifying the reliability of the change seen in the contrast plot above. Darker shades represent higher T score values. The red outlined regions represent statistically significant t scores quantified using the criterion False Discovery Rate (FDR) = 0.01.

For visual modulatory neurons (Fig 5-7) auditory and visual stimulation was accompanied by an increase in power in the low frequency and high gamma bands. Power changes in the multisensory condition were similar to the visual condition. To compare the differences in power between the best unisensory (visual) and multisensory conditions, contrast plots were generated. This is shown in Fig 5-8 for both SOAs. A slight increase in power in the low frequency ranges and the high gamma band was seen for both SOAs. The reliability of this change (increased power) was measured by plotting the T scores over time. Interestingly it was found that, in contrast to the large multisensory effects seen for the overt multisensory neurons, power changes in any frequency band for the visual modulatory neurons failed to reach statistical significance.

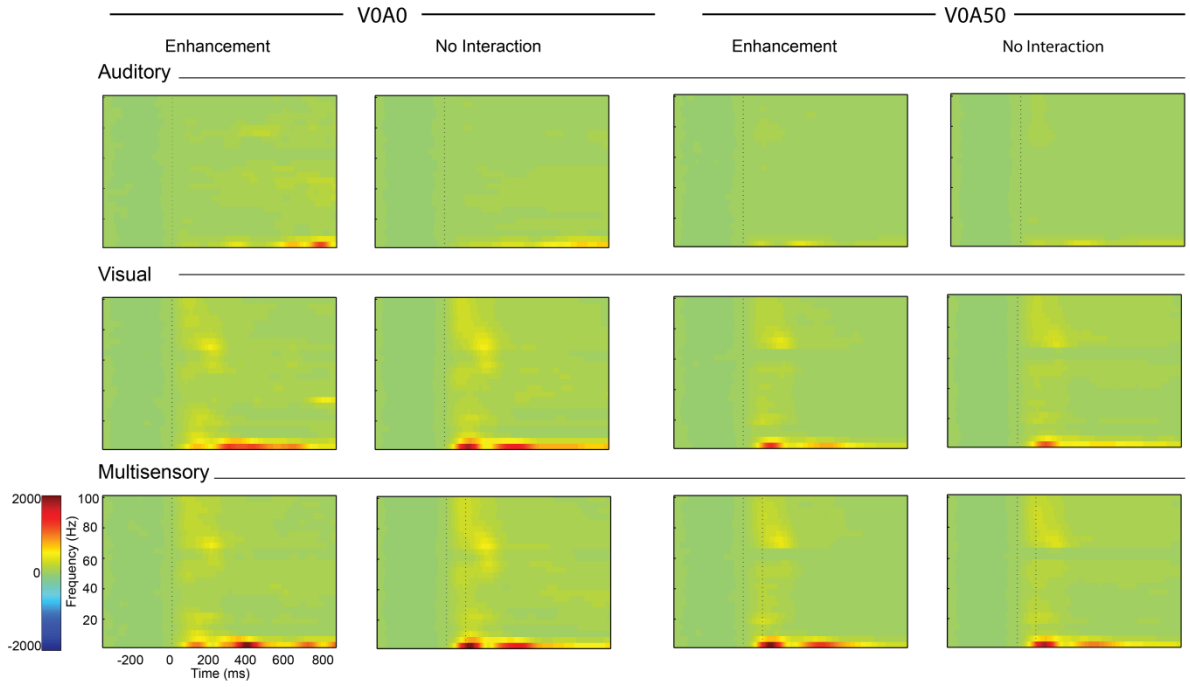

Fig 5-7: Time frequency plots for Visual Modulatory Neurons in the intermediate/deep layers of the SC

Averaged Time frequency representations of LFPs showing power changes for Auditory, Visual and Multisensory stimulus conditions (V0A0: simultaneous visual and auditory stimulation or V0A50: visual preceding auditory by 50ms) for all stimulus locations showing Response Enhancements and No Interactions. Color bar at the bottom represents the percentage of power change compared to pre-stimulus baseline. The dashed vertical lines represent onset of the stimulus for each condition.

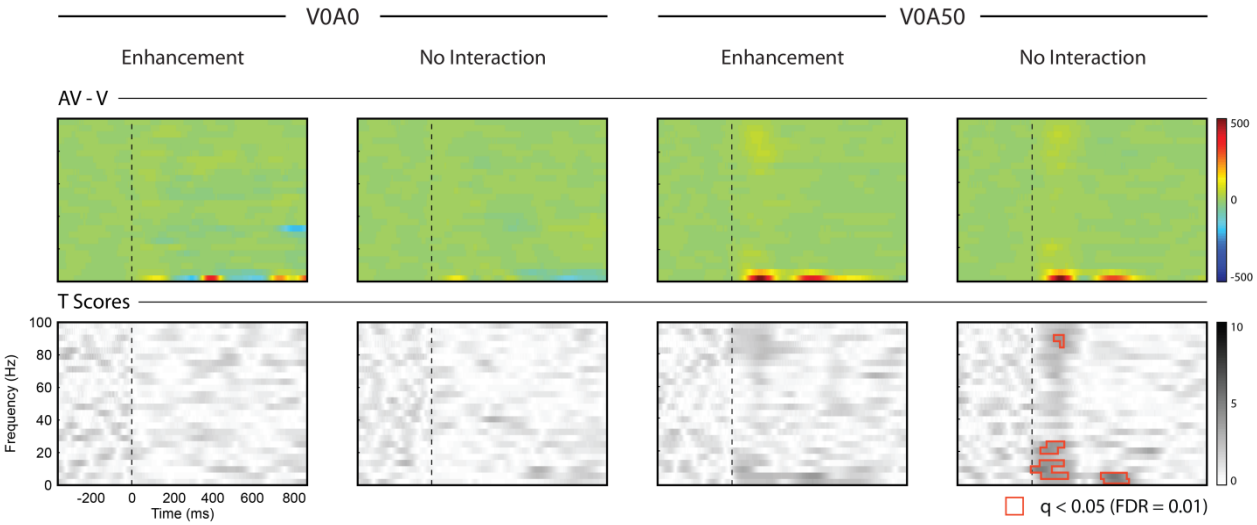

Fig 5-8: Contrast spectrograms and T score plots for LFP changes for Visual Modulatory Neurons in the intermediate/ deep layers of SC

Top panel depicts contrast plots obtained by subtracting the visual condition (V) from the multisensory (AV) condition (AV-V) .The color bar on the right represents the relative power changes (in %) comparing the visual (V) and the multisensory(AV) condition. Bottom panel shows time frequency representation of T scores statistically quantifying the reliability of the change seen in the contrast plot above. Darker shades represent higher T score values. The red outlined regions represent statistically significant t scores quantified using the criterion False Discovery Rate (FDR) = 0.01.

Discussion

This is the first study that reports sub threshold local field potential changes in the intermediate/ deep layers of the superior colliculus in cat SC. The multisensory nature of the deep layers of SC has been the subject of studies for several decades now, but this multisensory nature has been characterized solely by studying changes in spiking activity. Here we show that the multisensory nature of the deep layers of SC is also evident in synaptic processing as reflected in LFP changes under multisensory stimulus conditions and this may have important mechanistic implications for multisensory processing in the SC.

Dissociations between spiking activity and local field potential changes

For Overt neurons with spiking activity under both visual and auditory conditions, multisensory integrative ability is classified into 2 major types: Response Enhancement and No Interactions based on spiking criteria (ii values, see methods). For Response Enhancements spiking activity in the multisensory condition is different from the best unisensory condition while for No Interaction spiking under unisensory and multisensory conditions are similar with no statistical differences. Quantification of evoked LFP amplitude as measured by mean peak voltage changes and changes in area under the curve show increased activity under multisensory conditions for both Response Enhancement and No Interactions. Thus, though spiking activity remains the same for unisensory and multisensory conditions for No Interactions, differences are evident at the synaptic level. This may be because spiking activity reflects axonal output of local

neural population while LFPs are thought to be related to processing on the soma and dendrites (Henze et al. 2000; Logothetis 2008; Mitzdorf 1985; 1987; Berens et al 2010). The final outcome of net changes at the synaptic level is finally reflected in spiking activity. Hence studying LFPs help us understand the mechanisms underlying changes in spiking output of the neurons. Additionally, this supports the use of LFPs as a more sensitive measure of multisensory processing especially when revealing changes that are sub-threshold in nature.

For modulatory neurons (visual modulatory and auditory modulatory) overt spiking activity was not observed on presentation of the non-dominant modality alone but sub-threshold changes in synaptic processing were evident in evoked LFP responses. Quantification of evoked LFP amplitude revealed similar results as discussed for Overt neurons. Peak voltage changes and area under the curve were highest under multisensory stimulation conditions for both Response Enhancements and No Interactions suggesting dissociations between synaptic processing and spiking activity for the modulatory class of neurons as well. For visual modulatory neurons, multisensory integration (Response Enhancement) was observed much more frequently for SOA V0A50 (100 locations) compared to SOA V0A0 (37locations) and this may account for the fact that evoked mean peak LFP was not statistically different between the visual and multisensory conditions. This was also true for auditory modulatory neurons where only 6 neurons (36 locations) were recorded and hence data was not enough to generate statistical power. However, the second measure that we used to quantify evoked LFP amplitude i.e., area under the curve showed significant statistical differences between the best unisensory and multisensory conditions for the modulatory

neurons as well. Thus, both mean peak amplitude and area under the curve together helped us best quantify the changes in evoked LFP amplitudes.

Similar sub-threshold influences have been reported in the auditory cortex of primates on presentation of visual stimulus where presentation of visual stimulus alone does not result in spiking activity but sub-threshold changes are evident in LFP changes and visual- auditory stimulus combination produces highest changes in LFP amplitude compared to auditory stimulation alone (Ghazanfar et al. 2005; Kayser et al. 2009).

Spectral changes in LFP power in the intermediate/deep layers: Possible mechanisms underlying multisensory integration

Changes in LFP power across different frequency bands was quantified separately for Overt neurons and Visual Modulatory neurons of the deep layers of SC and are shown in Figs 5-5 - 5-8.

Overt neurons: For Overt neurons, increase in power after visual stimulation spanned a broader frequency range compared to auditory stimulation as shown in Fig 5-5. However, increase in power in the low frequency bands and high gamma band after multisensory stimulation was significantly higher when compared to visual stimulation alone or auditory stimulation alone for both SOAs and for both Response Enhancement and No Interactions. This is reflected in the significant t score values depicted in Fig 5-6. However, the duration of these power changes varied greatly depending on whether visual or auditory condition was compared to the multisensory condition. Power changes were prolonged for (AV-A) conditions compared to (AV-V) conditions. This may suggest that the prolonged increase in power is largely brought about by visual

stimulation. The true multisensory effects are hence restricted in the early increase in power that occurs 250ms within stimulus onset for both AV-V and AV-A contrast conditions. These long duration changes have also been shown in the visual and multisensory spiking responses of the multisensory neurons in these layers (Ghose et al 2012) the functional role of which remains to be deciphered. However, recent studies of visuomotor processing have suggested the involvement of intermediate and deep layer SC neurons in higher order functions like target selection, reward expectation, covert visuospatial orienting (Horwitz and Newsome 1999; 2001; Kim and Basso 2008; Krauzlis et al. 2004; Li and Basso 2005; McPeek and Keller 2002; Shen and Pare 2007). These higher order functions have sensory components that are linked to SC. (Dorris et al. 2002; Fecteau and Munoz 2005). Though, our study used anesthetized preparations and so we cannot implicate any such higher order processing from our data but it is possible that these long lasting synaptic changes and in turn longer spiking responses may be a part of bottom up stimulus processing that may be involved in such higher order functions of the SC.

Modulatory neurons: In contrast to our findings for overt neurons, for the visual modulatory neurons, auditory stimulation is accompanied by sub-threshold changes in LFP amplitude but time frequency analysis failed to reveal any statistically significant increase in power under multisensory conditions (compared to visual alone condition) in any frequency bands. This finding may have important mechanistic implications which warrant future investigation.

This may suggest that these two different classes of multisensory neurons employ different mechanisms for integrating multimodal information at the synaptic level. It has

been suggested that multisensory integration at the population level may be achieved by a) an increase in broadband synaptic activity that helps the membrane potential to reach threshold or by b) stimulus induced phase resetting of ongoing neuronal oscillations or by c) a combination of the two (Lakatos et al. 2007; Makeig et al. 2004a; Makeig et al. 2004b; Shah et al. 2004; Sewenski and Engel 2012). Our data suggests that the overt multisensory neurons in the intermediate/deep layers of SC combine information from multiple modalities in a way that is reflected at least partly by an increase in the power of neuronal oscillations in different frequency bands. This increase in power may be brought about by power changes across different frequency bands alone, changes in phase of neuronal oscillations alone or some combination of the two. This warrants future studies to tease apart the exact mechanisms underlying multisensory processing by the overt neurons in the intermediate/deep layers of SC.

However, this data also suggests that the modulatory neurons in these layers do not cause significant increase in broadband power in any particular frequency band when combining information from multiple modalities. This may suggest that for this neuronal class, multisensory integration is achieved largely by a “phase reset” mechanism. Such a mechanism underlying multisensory integration has been demonstrated in the auditory cortex of non-human primates and involves a resetting of phase of ongoing neuronal oscillations by the non-dominant modality (Lakatos et al. 2007; Lakatos et al. 2008). These studies demonstrated that in A1 of macaque monkeys the phase of ongoing oscillations is reset by somatosensory inputs (Lakatos et al. 2007). Thus, the activity of subsequent auditory inputs can be either enhanced or suppressed depending on their timing relative to the oscillatory cycle. Each oscillation cycle of field potentials

has periods of high and low excitability, thus presenting transient windows of opportunity during which the phase of oscillation in the local neuronal ensemble can phase-lock to relevant stimulus inputs. Such phase-locking (i.e., synchronization) is very powerful, ultimately serving to amplify neuronal representations, facilitate sensory discrimination, and increase response speed and accuracy (O'Connell et al. 2011). Auditory cortical neurons and the modulatory neurons in SC are similar because both classes have a dominant driving modality with the non-dominant modality modulating the driving responses. Hence it is possible that the modulatory neurons in SC largely use a “phase reset” mechanism to combine information from multiple modalities rather than frequency dependent power changes as seen in auditory cortical neurons. This remains to be explored in future studies.

Implications for studying synaptic processing in the intermediate/deep layers of SC

Here, in this study, an important difference between measures of synaptic processing (LFP activity) and spiking activity is seen for both Overt multisensory neurons and Visual modulatory neurons. The evoked LFP amplitude under multisensory conditions was significantly higher than the best unisensory condition for both Response Enhancement and No Interaction. This observation may have important implications for multisensory processing in the SC as discussed below.

Multisensory interactions classified as Response Enhancement and No Interactions using spike based measures are similar with respect to LFP power changes i.e., for both Response Enhancements and No Interactions, increase in power in the different

frequency bands is more after multisensory stimulation when compared to unisensory stimulation alone. LFP power changes represent ongoing synaptic processing while spiking activity represents the final outcome of such a process. LFPs are thought to represent inputs to a particular brain area (Khawaja et al. 2009; Berens et al 2010). The deep layers of the SC receive inputs from a wide variety of visual, auditory and somatosensory brain areas (see Introduction) and this may be responsible for the power changes across wide frequency ranges. Moreover, it is known that the integrative capacity of the deep layer neurons (i.e., the ability of the deep layer neurons to show Response Enhancements/ Response depressions) depends on the cortical inputs from AES and rLS (Jiang W 2000; Wallace and Stein 1994; Wilkinson et al. 1996). Deactivation of AES and /rLS abolishes the capacity of these neurons to show response enhancement or response depression(Jiang W 2000; Wallace and Stein 1994) and the benefits in orientation behavior(i.e., greater accuracy under multisensory conditions) are also abolished (Wilkinson et al. 1996). But the exact synaptic mechanism by which these cortical afferents confer integrative abilities (reflected in spiking output) to the deep layer neurons is still not known.

Recent studies have started elucidating the underlying anatomical circuitry that confers integrative abilities to the deep layer multisensory neurons but our understanding is still far from complete (Fuentes-Santamaria et al. 2009; Fuentes-Santamaria et al. 2008; Fuentes-Santamaria et al. 2006). It has been shown that there are 2 major types of cortical afferents that target multisensory neurons in the deep layers of SC: Type I and Type II fibers that make direct contacts with the distal and primary dendrites of the deep layer SC neurons respectively (Fuentes-Santamaria et al. 2009; Fuentes-Santamaria et

al. 2008). These fibers also target nitrergic interneurons present in the deep layers (Fuentes-Santamaria et al. 2008) providing an indirect route for multisensory processing. Preliminary studies also suggest the existence of different groups of interneurons in the deep layers of the SC (McHaffie et al 2012). It has been suggested that these interneurons are likely candidates to form intrinsic networks that are capable of generating spontaneous oscillations and in turn stimulus driven changes in oscillatory activity that affect multisensory integration similar to findings in cortex(Schroeder and Foxe 2002; Senkowski et al. 2008; McHaffie et al 2012). The present study is the first of its kind that provides empirical evidence for the existence of oscillatory activity and stimulus driven changes in such activity within the deep layers of the SC. This suggests that indeed multisensory integration in the deep layers may be mediated by oscillatory activity brought about by activation of cortical afferents that directly or indirectly (via inter-neuronal networks) affect integrative properties of neurons in these layers. Future studies should be directed to understand **"how"** these cortical inputs mediate such changes. The idea is that, the increase in power across different frequency bands that occur after multisensory stimulation (shown here in Fig 5-6) is likely due to activation of various inputs to the deep layer SC neurons that in turn activates the inter-neuronal network as well. In future, efforts should be directed to study multisensory synaptic processing in the deep layers by deactivation of AES and/or rLS and thereafter studying the changes in LFP activity. Now that we know the nature of evoked LFP and spectral nature of LFP when all inputs are present, by deactivating specifically those inputs that confer multisensory integrative abilities to the SC neurons (inputs from AES and rLS), will now help to pinpoint the synaptic changes that are brought about specifically by

activation of those cortical afferents thereby shedding light on the underlying mechanistic basis of multisensory processing in the SC. Additionally, it may be even possible to selectively block the nitrergic interneurons while keeping the cortical inputs intact and record the changes synaptic activity by way of LFP recordings. Such a manipulation will help understand the role of these interneurons (if any) in conferring integrative abilities to the deep layer multisensory neurons.

Bibliography

Allman BL, Bittencourt-Navarrete RE, Keniston LP, Medina AE, Wang MY, and Meredith MA. Do cross-modal projections always result in multisensory integration? *Cereb Cortex* 18: 2066-2076, 2008a.

Allman BL, Keniston LP, and Meredith MA. Subthreshold auditory inputs to extrastriate visual neurons are responsive to parametric changes in stimulus quality: sensory-specific versus non-specific coding. *Brain Res* 1242: 95-101, 2008b.

Allman BL, and Meredith MA. Multisensory processing in "unimodal" neurons: cross-modal subthreshold auditory effects in cat extrastriate visual cortex. *J Neurophysiol* 98: 545-549, 2007.

Beckstead RM, and Frankfurter A. A direct projection from the retina to the intermediate gray layer of the superior colliculus demonstrated by anterograde transport of horseradish peroxidase in monkey, cat and rat. *Exp Brain Res* 52: 261-268, 1983.

Berens P, Logothetis NK, Tolias AS. Local field potentials, BOLD and spiking activity – relationships and physiological mechanisms. 2010
Available from Nature Precedings http://hdlhandlenet/10101/npre201052161>

Carriere BN, Royal DW, and Wallace MT. Spatial heterogeneity of cortical receptive fields and its impact on multisensory interactions. *J Neurophysiol* 99: 2357-2368, 2008.

Casagrande VA, Harting JK, Hall WC, Diamond IT, and Martin GF. Superior colliculus of the tree shrew: a structural and functional subdivision into superficial and deep layers. *Science* 177: 444-447, 1972.

Clemo HR, Sharma GK, Allman BL, and Meredith MA. Auditory projections to extrastriate visual cortex: connectional basis for multisensory processing in 'unimodal' visual neurons. *Exp Brain Res* 191: 37-47, 2008.

Clemo HR, and Stein BE. Somatosensory cortex: a 'new' somatotopic representation. *Brain Res* 235: 162-168, 1982.

Dehner LR, Keniston LP, Clemo HR, and Meredith MA. Cross-modal circuitry between auditory and somatosensory areas of the cat anterior ectosylvian sulcal cortex: a 'new' inhibitory form of multisensory convergence. *Cereb Cortex* 14: 387-403, 2004.

Dorris MC, Klein RM, Everling S, and Munoz DP. Contribution of the primate superior colliculus to inhibition of return. *J Cogn Neurosci* 14: 1256-1263, 2002.

Dreher B, and Hoffmann KP. Properties of excitatory and inhibitory regions in the receptive fields of single units in the cat's superior colliculus. *Exp Brain Res* 16: 333-353, 1973.

Edwards SB, Ginsburgh CL, Henkel CK, and Stein BE. Sources of subcortical projections to the superior colliculus in the cat. *J Comp Neurol* 184: 309-329, 1979.

Fecteau JH, and Munoz DP. Correlates of capture of attention and inhibition of return across stages of visual processing. *J Cogn Neurosci* 17: 1714-1727, 2005.

Fuentes-Santamaria V, Alvarado JC, McHaffie JG, and Stein BE. Axon morphologies and convergence patterns of projections from different sensory-specific cortices of the anterior ectosylvian sulcus onto multisensory neurons in the cat superior colliculus. *Cereb Cortex* 19: 2902-2915, 2009.

Fuentes-Santamaria V, Alvarado JC, Stein BE, and McHaffie JG. Cortex contacts both output neurons and nitrergic interneurons in the superior colliculus: direct and indirect routes for multisensory integration. *Cereb Cortex* 18: 1640-1652, 2008.

Fuentes-Santamaria V, Stein BE, and McHaffie JG. Neurofilament proteins are preferentially expressed in descending output neurons of the cat the superior colliculus: a study using SMI-32. *Neuroscience* 138: 55-68, 2006.

Ghazanfar AA, Maier JX, Hoffman KL, and Logothetis NK. Multisensory integration of dynamic faces and voices in rhesus monkey auditory cortex. *J Neurosci* 25: 5004-5012, 2005.

Ghazanfar AA, and Schroeder CE. Is neocortex essentially multisensory? *Trends Cogn Sci* 10: 278-285, 2006.

Ghose D, Barnett ZP, and Wallace MT. Impact of response duration on multisensory integration. *J Neurophysiol* 108: 2534-2544, 2012.

Harting JK, Huerta MF, Frankfurter AJ, Strominger NL, and Royce GJ. Ascending pathways from the monkey superior colliculus: an autoradiographic analysis. *J Comp Neurol* 192: 853-882, 1980.

Henkel CK. Evidence of sub-collicular auditory projections to the medial geniculate nucleus in the cat: an autoradiographic and horseradish peroxidase study. *Brain Res* 259: 21-30, 1983.

Henze DA, Borhegyi Z, Csicsvari J, Mamiya A, Harris KD, and Buzsaki G. Intracellular features predicted by extracellular recordings in the hippocampus in vivo. *J Neurophysiol* 84: 390-400, 2000.

Horwitz GD, and Newsome WT. Separate signals for target selection and movement specification in the superior colliculus. *Science* 284: 1158-1161, 1999.

Horwitz GD, and Newsome WT. Target selection for saccadic eye movements: prelude activity in the superior colliculus during a direction-discrimination task. *J Neurophysiol* 86: 2543-2558, 2001.

Huerta MF HJ. Comparative Neurology of Optic tectum. 1984.

Jiang W JH, Stein BE. Influences from the anterior ectosylvian sulcus and rostral lateral suprasylvian sulcus are critical for multisensory orientation behavior. *Soc Neurosci Abstr 26 : 1220* 2000.

Kanaseki T, and Sprague JM. Anatomical organization of pretectal nuclei and tectal laminae in the cat. *J Comp Neurol* 158: 319-337, 1974.

Kayser C, and Logothetis NK. Do early sensory cortices integrate cross-modal information? *Brain Struct Funct* 212: 121-132, 2007.

Kayser C, Petkov CI, and Logothetis NK. Multisensory interactions in primate auditory cortex: fMRI and electrophysiology. *Hear Res* 258: 80-88, 2009.

Khawaja FA,Tsui JMG,Pack CC. Pattern motion selectivity of spiking outputs and local field potentials in macaque visual cortex. *J Neurosci* 29: 13702-13709, 2009

Kim B, and Basso MA. Saccade target selection in the superior colliculus: a signal detection theory approach. *J Neurosci* 28: 2991-3007, 2008.

Krauzlis RJ, Liston D, and Carello CD. Target selection and the superior colliculus: goals, choices and hypotheses. *Vision Res* 44: 1445-1451, 2004.

Kudo M. Projections of the nuclei of the lateral lemniscus in the cat: an autoradiographic study. *Brain Res* 221: 57-69, 1981.

Kudo M, and Niimi K. Ascending projections of the inferior colliculus in the cat: an autoradiographic study. *J Comp Neurol* 191: 545-556, 1980.

Lakatos P, Chen CM, O'Connell MN, Mills A, and Schroeder CE. Neuronal oscillations and multisensory interaction in primary auditory cortex. *Neuron* 53: 279-292, 2007.

Lakatos P, Karmos G, Mehta AD, Ulbert I, and Schroeder CE. Entrainment of neuronal oscillations as a mechanism of attentional selection. *Science* 320: 110-113, 2008.

Li X, and Basso MA. Competitive stimulus interactions within single response fields of superior colliculus neurons. *J Neurosci* 25: 11357-11373, 2005.

Logothetis NK. What we can do and what we cannot do with fMRI. *Nature* 453: 869-878, 2008.

Makeig S, Debener S, Onton J, and Delorme A. Mining event-related brain dynamics. *Trends Cogn Sci* 8: 204-210, 2004a.

Makeig S, Delorme A, Westerfield M, Jung TP, Townsend J, Courchesne E, and Sejnowski TJ. Electroencephalographic brain dynamics following manually responded visual targets. *PLoS Biol* 2: e176, 2004b.

McHaffie JG, Kruger L, Clemo HR, and Stein BE. Corticothalamic and corticotectal somatosensory projections from the anterior ectosylvian sulcus (SIV cortex) in neonatal cats: an anatomical demonstration with HRP and 3H-leucine. *J Comp Neurol* 274: 115-126, 1988.

McHaffie JG, Fuentes-Santamaria V,Alvarado JC, Fuentes-Farias AL,Gutierrez-Opsina G, Stein BE. Anatomical features of the intrinsic circuitry underlying

multisensory integration in the superior colliculus. Chapter 2 In: *The New Handbook of Multisensory Processing.* 2012.

McPeek RM, and Keller EL. Saccade target selection in the superior colliculus during a visual search task. *J Neurophysiol* 88: 2019-2034, 2002.

Meredith MA, and Clemo HR. Auditory cortical projection from the anterior ectosylvian sulcus (Field AES) to the superior colliculus in the cat: an anatomical and electrophysiological study. *J Comp Neurol* 289: 687-707, 1989.

Meredith MA, Keniston LR, Dehner LR, and Clemo HR. Crossmodal projections from somatosensory area SIV to the auditory field of the anterior ectosylvian sulcus (FAES) in Cat: further evidence for subthreshold forms of multisensory processing. *Exp Brain Res* 172: 472-484, 2006.

Meredith MA, Nemitz JW, and Stein BE. Determinants of multisensory integration in superior colliculus neurons. I. Temporal factors. *J Neurosci* 7: 3215-3229, 1987.

Meredith MA, and Stein BE. Interactions among converging sensory inputs in the superior colliculus. *Science* 221: 389-391, 1983.

Meredith MA, and Stein BE. Spatial factors determine the activity of multisensory neurons in cat superior colliculus. *Brain Res* 365: 350-354, 1986a.

Meredith MA, and Stein BE. Visual, auditory, and somatosensory convergence on cells in superior colliculus results in multisensory integration. *J Neurophysiol* 56: 640-662, 1986b.

Mitzdorf U. Current source-density method and application in cat cerebral cortex: investigation of evoked potentials and EEG phenomena. *Physiol Rev* 65: 37-100, 1985.

Mitzdorf U. Properties of the evoked potential generators: current source-density analysis of visually evoked potentials in the cat cortex. *Int J Neurosci* 33: 33-59, 1987.

Moore RY, and Goldberg JM. Projections of the inferior colliculus in the monkey. *Exp Neurol* 14: 429-438, 1966.

Mucke L, Norita M, Benedek G, and Creutzfeldt O. Physiologic and anatomic investigation of a visual cortical area situated in the ventral bank of the anterior ectosylvian sulcus of the cat. *Exp Brain Res* 46: 1-11, 1982.

O'Connell MN, Falchier A, McGinnis T, Schroeder CE, and Lakatos P. Dual mechanism of neuronal ensemble inhibition in primary auditory cortex. *Neuron* 69: 805-817, 2011.

Perrault TJ, Jr., Vaughan JW, Stein BE, and Wallace MT. Neuron-specific response characteristics predict the magnitude of multisensory integration. *J Neurophysiol* 90: 4022-4026, 2003.

Perrault TJ, Jr., Vaughan JW, Stein BE, and Wallace MT. Superior colliculus neurons use distinct operational modes in the integration of multisensory stimuli. *J Neurophysiol* 93: 2575-2586, 2005.

Pesaran B. Uncovering the mysterious origins of local field potentials. *Neuron* 61: 1-2, 2009.

Schroeder CE, and Foxe JJ. The timing and laminar profile of converging inputs to multisensory areas of the macaque neocortex. *Brain Res Cogn Brain Res* 14: 187-198, 2002.

Segal RL, and Beckstead RM. The lateral suprasylvian corticotectal projection in cats. *J Comp Neurol* 225: 259-275, 1984.

Senkowski D, Schneider TR, Foxe JJ, and Engel AK. Crossmodal binding through neural coherence: implications for multisensory processing. *Trends Neurosci* 31: 401-409, 2008.

Senkowski D and Engel AK. Oscillatory activity and multisensory processing. Chapter 11 In: *The New Handbook of Multisensory Processing*. 2012.

Shah AS, Bressler SL, Knuth KH, Ding M, Mehta AD, Ulbert I, and Schroeder CE. Neural dynamics and the fundamental mechanisms of event-related brain potentials. *Cereb Cortex* 14: 476-483, 2004.

Shen K, and Pare M. Neuronal activity in superior colliculus signals both stimulus identity and saccade goals during visual conjunction search. *J Vis* 7: 15 11-13, 2007.

Stanford TR, Quessy S, and Stein BE. Evaluating the operations underlying multisensory integration in the cat superior colliculus. *J Neurosci* 25: 6499-6508, 2005.

Stanford TR, and Stein BE. Superadditivity in multisensory integration: putting the computation in context. *Neuroreport* 18: 787-792, 2007.

Stein BE MA. The Merging of the Senses. *Book* 1993.

Sterling P, and Wickelgren BG. Visual receptive fields in the superior colliculus of the cat. *J Neurophysiol* 32: 1-15, 1969.

Tortelly A, Reinoso-Suarez F, and Llamas A. Projections from non-visual cortical areas to the superior colliculus demonstrated by retrograde transport of HRP in the cat. *Brain Res* 188: 543-549, 1980.

Wallace MT, and Stein BE. Cross-modal synthesis in the midbrain depends on input from cortex. *J Neurophysiol* 71: 429-432, 1994.

Wilkinson LK, Meredith MA, and Stein BE. The role of anterior ectosylvian cortex in cross-modality orientation and approach behavior. *Exp Brain Res* 112: 1-10, 1996.

CHAPTER VI

RESPONSE VARIABILITY AND MULTISENSORY INTEGRATION

Introduction

Combining information from different sensory modalities has been shown to have important behavioral benefits such as speeded reaction times (Corneil and Munoz 1996; Diederich and Colonius 2004; Frens et al. 1995; Harrington and Peck 1998; Hughes et al. 1994) greater accuracy in detection (Lovelace et al. 2003) and orientation behavior (Stein et al. 1988). At the neuronal level, the benefits of combining information from multiple modalities has been demonstrated in various brain areas (Meredith and Stein 1983; Wallace et al. 1992) and these gains are typically represented as a function of various aspects of neuronal firing rate (e.g., interactive index, multisensory contrast). However, reliable transmission of sensory information depends not only on the average response to stimuli but also on the variability of response (Kara et al. 2000). Hence, benefits of synthesizing information from multiple modalities may also be reflected in other ways such as by changes in response variability under multisensory conditions. Changes in neuronal response variability in different sensory systems have been shown to have various functional implications. In the visual system, response variability has been shown to increase at higher hierarchical levels in the geniculostriate system with the retinal response being least variable and the visual cortical response being most variable, the differences at each level being attributed to decreasing firing rates and

decreasing absolute and relative refractory periods at higher levels of the hierarchy (Kara et al 2000). Changes in response variability has been shown to code for stimulus features like stimulus velocity in the superficial layers of the superior colliculus where trial by trial variability of neuronal response as measured by Fano Factor (FF) correlated negatively with firing rate for fast moving stimuli while for slow moving stimuli FF was positively correlated with firing rate (Mochol et al 2010). In awake behaving primates neural variability has been shown to decrease during motor preparation in neurons of the Premotor cortex with little change in mean firing rates (Churchland et al. 2006). Similar findings have been reported for area V4 during preparation of saccadic eye movements (Steinmetz and Moore 2010). In prefrontal cortex of macaques, FF values change with components of a motion discrimination task as well as with behavioral performance (Hussar and Pasternak 2010). Attention dependent decreases in response variability was observed in neurons of area V4 of monkeys performing an attention demanding task and was interpreted to increase sensory processing for behaviorally relevant stimuli (Mitchell et al. 2007). Thus, changes in response variability have been shown to have important implications for sensory processing in individual sensory systems. Recent work by (Kayser et al. 2010) showed that reduction in response variability results in multisensory information gain in the auditory cortex of rhesus monkeys.

In addition, response variability changes with response mode as shown in cat lateral geniculate nucleus (LGN) where burst mode has been linked to less variability, increased signal to noise ratio and better signal detection compared to tonic mode of firing (Guido et al. 1995; Guido and Sherman 1998). Recent work from our lab (Ghose

et al 2012) also demonstrates two different response modes, short response duration mode and long response duration mode, for the multisensory neurons in the intermediate and deep layers of superior colliculus, with the short discharge duration being associated with high integration and the long discharge duration with low integrative abilities. Since numerous unisensory studies have demonstrated that response variability represents an important aspect of neuronal coding in various brain areas, we hypothesized that response variability might also change according to response modes (short versus long) and in turn multisensory integrative capacity.

Methods

General procedures: Experiments were conducted in adult cats (n=2) raised under standard housing conditions. All experiments were done in an anesthetized and paralyzed semi-chronic preparation and consisted of single unit extracellular recordings from the superior colliculus (SC). Experiments were run on a weekly basis on each animal. All surgical and recording procedures were performed in compliance with the Guide for the Care and Use of Laboratory Animals at Vanderbilt University Medical Center, which is accredited by the American Association for Accreditation of Laboratory Animal Care. All procedures were approved by the Vanderbilt Institutional Animal Care and Use Committee.

Implantation and Recording procedures: For surgical anesthesia, animals were induced with ketamine hydrochloride (20 mg/kg, and acepromazine maleate (0.04

mg/kg) administered intramuscularly (im). For implantation of the recording chamber over the SC, animals were intubated and artificially respired. A stable plane of surgical anesthesia was achieved using inhalation isoflurane (1%-3%). Body temperature, expiratory CO2, blood pressure and heart rate were continuously monitored (VSM7, Vetspecs/SCIL), recorded and maintained within ranges consistent with a deep and stable plane of anesthesia. A craniotomy was made to allow access to the SC and a head holder was attached to the cranium using stainless steel screws and orthopedic cement to hold the animal during recording sessions without obstructing the face and ears. Post-operative care (antibiotics and analgesics) was done in close consultation with veterinary staff.

For recording experiments, animals were anesthetized with ketamine (20mg/kg im) and acepromazine maleate (0.04 mg/kg im) and maintained throughout the procedure with a constant rate infusion of ketamine (5mg/kg/hr iv) was delivered intravenously through a cannula placed in the saphenous vein. The head holding system maintained the animal in a comfortable recumbent position throughout the recording procedure. To prevent ocular drift, animals were paralyzed using pancuronium bromide (0.1mg/kg/hr, iv) and artificially respired for the duration of the recording. Parylene insulated tungsten electrodes (Z = 1-5 MΩ) were advanced into the SC using a mechanical microdrive. Single unit neural activity (signal to noise ratio >= 3:1) was recorded (Sort client software, Plexon Inc. ,Texas), amplified and routed to an oscilloscope, audio monitor and computer for performing online) and offline analysis. At the end of the recording session (approximately 8-10 hours), paralysis was reversed and the animal was weaned from the ventilator. Anesthesia was discontinued, and upon return of stable

respiration and locomotion the animal was returned to its home cage. Animals were given 60-100ml of lactated Ringer solution subcutaneously in order to facilitate recovery.

Stimulus presentation and search strategy: Extracellular single unit recordings targeted visual-auditory (VA) multisensory neurons in the deep layers of the SC. A multisensory neuron was defined as one in which the firing rate in the multisensory condition was statistically different from the best unisensory condition as determined by the Wilcoxon Rank test ($p < 0.05$). Once a neuron was isolated, the borders of its receptive field were coarsely mapped. Visual stimuli consisted of the illumination of stationary light emitting diodes (LEDs: 100 ms duration) while auditory stimuli were delivered through speakers and consisted of 100 ms duration broadband noise (20Hz-20KHz) ranging in intensity from 50-70 dB SPL. Both the LEDs and speakers were mounted on a hoop 0.6 m away from the center of the animal's head, with locations spanning azimuthal space from 0-90° on either side of the midline. The hoop could also be rotated to map different elevations. This stimulus configuration allowed for the sampling of numerous locations within and just outside of the coarsely-delimited receptive fields, creating a spatial receptive field (SRF) characterization for each of the effective modalities as well as for the multisensory condition. The physical characteristics of the stimuli were always identical in all respects except for spatial location. Visual and auditory stimuli were presented in a randomized interleaved manner at multiple azimuthal locations along a single elevation at a time. Multisensory combinations always consisted of visual and auditory stimuli presented at the same spatial location (i.e., spatial coincidence). A total of 60 trials (20 visual, 20 auditory, 20

multisensory) were collected for each stimulus location. Consecutive stimulus presentations were separated by a minimum of 1.5 s to avoid response habituation.

Data acquisition and analysis: A custom built PC-based real time data acquisition system controlled the structure of the trials and the timing of the stimuli (Labview. National Instruments). Analog waveforms were transferred to a Plexon MAP system (Plexon Inc.,Texas) where they were digitized at 40kHz. Single units were isolated online using Sort Client software (Plexon Inc., Texas) and also stored for further offline analysis. Neuronal responses were characterized through construction of peristimulus time histograms (PSTHs) for each condition (visual (V) only, auditory only (A), visual-auditory (VA)) and for each location tested within the SRF. The response baseline (spontaneous firing rate) was calculated as the mean firing rate during the 500 ms immediately preceding the stimulus onset for each of the 3 conditions and was subtracted from each stimulus evoked response. Thresholds for the PSTHs were set at 2 standard deviations (SD) above the respective baselines to delimit the stimulus evoked response. Following stimulus onset, the time at which the PSTH exceeded the the 2SD criterion (and remained so for at least 30ms) was noted as the response onset. Response offset was the time at which the PSTH fell below the 2SD criterion for >=30ms. Response duration was defined as the time interval between response onset and offset. Mean stimulus evoked response was calculated as the average number of spikes elicited per trial during the defined response duration interval.

Measure of multisensory integration: The measure used to quantify multisensory integration was the interactive index (ii), which measures how the multisensory response (firing rate) differs from the best unisensory response. The magnitude of this

change was calculated as [(CM-SMmax)/SMmax)] X100 = % interaction where CM is the mean response evoked by the combined modality (i.e., visual-auditory) stimulus and SMmax is the mean response evoked by the most effective single modality stimulus (Meredith and Stein 1983; 1986a). Statistical comparisons between the mean stimulus evoked responses of the multisensory condition and the best unisensory condition were done using a non-parametric Wilcoxon Rank Test ($p<0.05$).

Measure of response variability: Neuronal response variability was measured by Fano Factor analysis. Fano Factor (FF) is the ratio of variance to mean spike counts computed across trials averaged over a specified time window. In this study, FF was computed for each of the unisensory (visual or auditory) and the multisensory (visual-auditory) conditions. Generally, a lower FF value indicates decreased variability or increased reliability. To compare changes across different conditions, the FF value for the multisensory condition was subtracted from that of the best unisensory condition producing a ∆FF or change in FF value. Thus, when ∆FF is positive the multisensory condition is *less variable* or *more reliable* than the best unisensory condition. When ∆FF is negative the reverse is true. In addition we compared the effects of variability of response alone, separate from firing rate influences (since FF includes both) using standard deviation values computed for the different conditions as well as the change in SD (∆SD). A positive ∆SD also indicates less variability in the multisensory condition compared to the best unisensory condition.

Results

Multisensory neurons in the SC exhibit distinct firing modes that show different integrating abilities:

As reported previously (Ghose et al 2012) multisensory neurons in the intermediate and deep layers of the SC exhibit both short (<250ms) and long discharge durations (>250ms).In addition, response duration was a good determinant of the integrative capacity of the neurons with short discharge durations showing higher integrative abilities while longer discharge durations showed low integrative abilities. Moreover, the same neuron could exhibit both short and long response durations depending on the spatial location of the stimulus within the receptive field.

Relationship between response mode and response variability:

To test if the two different response modes with varying integrative abilities also differ in response variability, we used Fano Factor as a measure of response variability and computed the change in Fano Factor (∆FF) between the best unisensory and multisensory conditions for both short and long discharge durations (Fig 6-1A). A total of 51 multisensory neurons were collected. Since spatial locations with long response durations were rare so all spatial locations with long discharge durations were included in the analysis. Spatial locations with short discharge durations were randomly chosen for inclusion in this variability analysis (so as to keep the number of spatial locations with short and long response durations approximately equal). In addition, change in standard deviation (∆SD) was also computed to ensure that the changes in Fano factor

represented changes in response variability separate from firing rate (Fig 6-1B). Fig 6-1(A and B) shows that ΔFF and ΔSD values are generally negative for the long responses indicating increased response variability in the multisensory condition compared to the best unisensory condition. The shorter responses were characterized by both positive and negative ΔFF and ΔSD values in approximately equal measure.

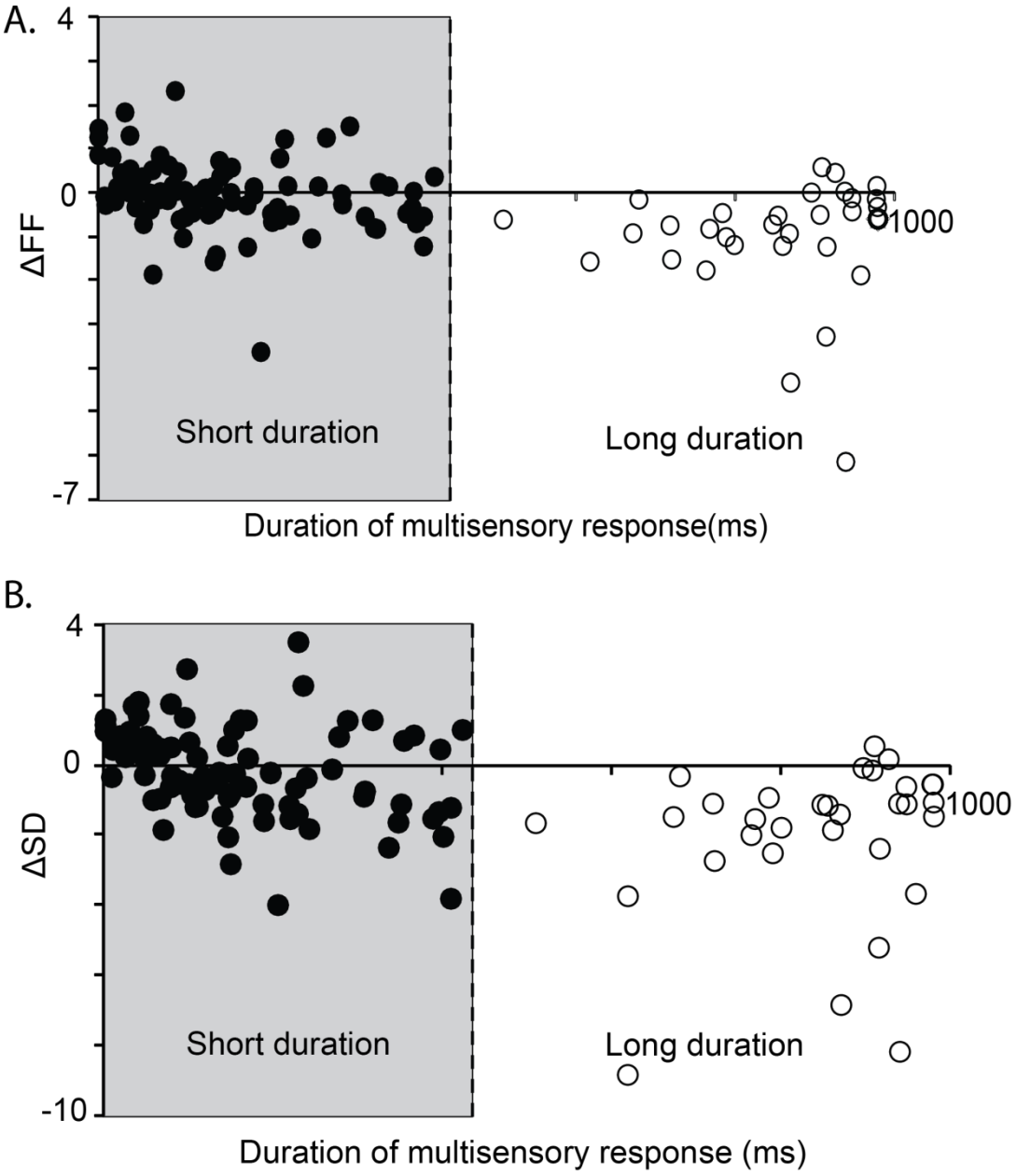

Figure 6-1: Changes in Response Variability.

A. Change in Fano Factor (Δ FF) or **B**. change in standard deviation (ΔSD) plotted as a function of multisensory response duration. For both, long duration responses are associated with negative ΔFF and ΔSD values signifying increased variability in the multisensory condition. However, short duration responses have both positive and negative ΔFF and ΔSD values.

Relationship between response variability and integrative capacity:

Since the responses with short discharge duration exhibits both positive and negative ∆FF values and is also the mode that is associated with high integrative abilities (both response enhancement and response depression), we analyzed whether the change in response variability varied according to the nature of multisensory integration (enhancement vs depression) under multisensory conditions. Figure 6-2 (A and B) demonstrates the relationship between ∆FF, ∆SD values and measure of multisensory integration or interaction index (ii). Positive ii values (response enhancements) are associated with negative ∆FF and ∆SD values while negative ii values (response depressions) are associated with positive ∆FF and ∆SD values. This means that for response enhancements variability increases whereas for response depressions, variability decreases in the multisensory condition compared to the best unisensory condition.

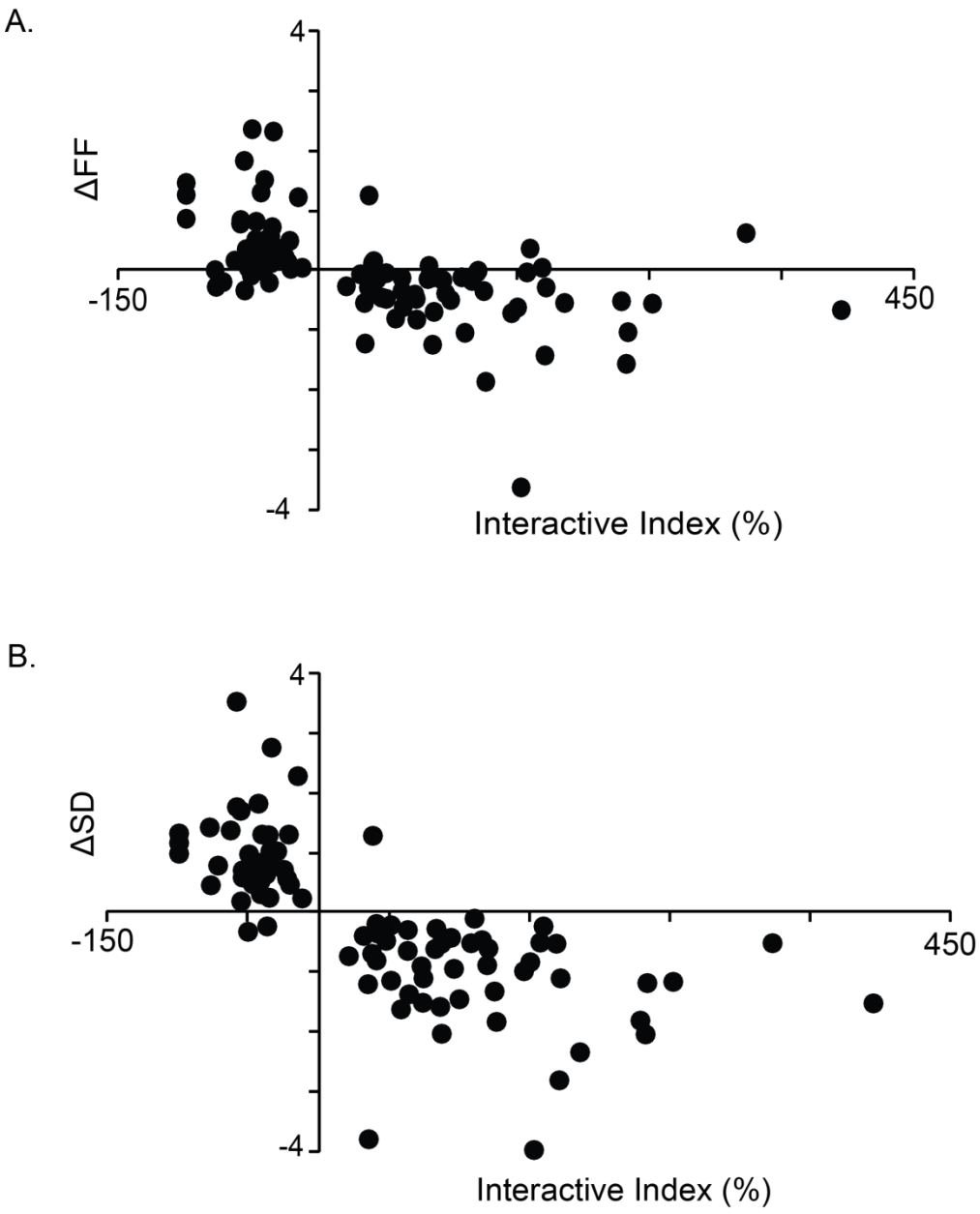

Figure 6-2: Changes in Fano Factor and standard deviation as a function of interactive index for short duration responses.

Interactive indices of short duration responses were plotted as a function of **A**. ΔFF **B**. ΔSD. Response Depressions (or negative ii values) in the multisensory condition were associated with decreased variability/increased reliability (positive ΔFF and ΔSD values) while response enhancements were associated with increased variability/decreased reliability(negative ΔFF and ΔSD values).

This trend is also reflected in the mean ΔFF and ΔSD values associated with degree of integrative capacity (Fig 6-3). Long responses (associated with no significant multisensory interactions, as noted above) demonstrated mean ΔFF values that were negative (Figure 6-3A) indicating increased variability under multisensory conditions. Short responses, included both response enhancements which exhibited a negative mean ΔFF and response depressions which exhibited a positive mean ΔFF value (Figure 6-3A). These trends in variability were also reflected by quantification of ΔSD values according to degree of integrative capacity (Figure 6-3B). This demonstrates that increases in response variability under multisensory conditions are observed for both long responses and also the short responses that resulted in response enhancements. In contrast, decreased response variability (increased reliability) was observed for short responses that demonstrated response depressions under multisensory conditions. Thus, similar to studies in individual sensory systems, response variability seems to be an important neural measure for information processing in the multisensory realm.

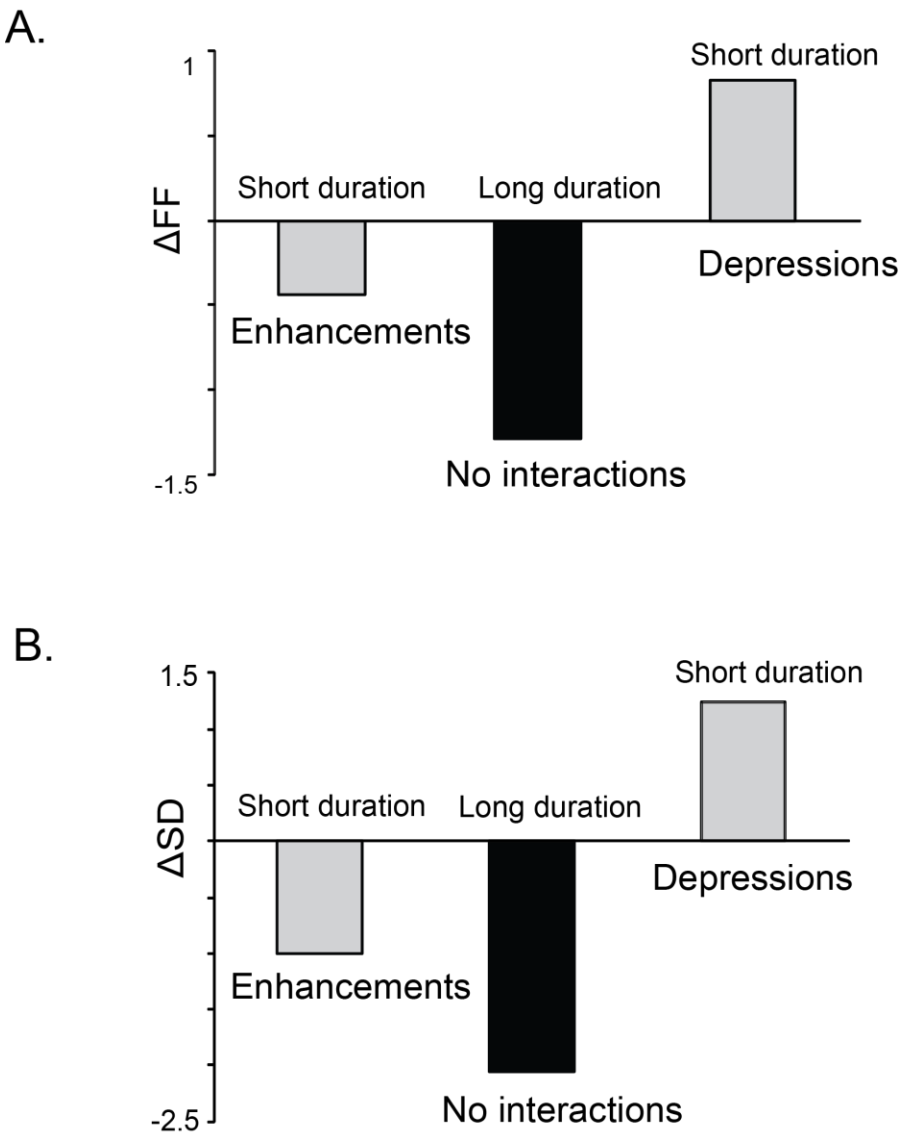

Figure 6-3: Mean trends for changes in Response variability as a function of nature of multisensory integration.

Trends in A. mean ΔFF and B. ΔSD values for different modes of multisensory integration. Gray bars represent short duration mode while black bars represent long duration mode.

Discussion

It has been shown that SC multisensory neurons exhibit both long and short discharge durations with response duration being an important determinant of integrative capacity. Short discharge durations are associated with high integrative abilities as measured by changes in firing rates and long discharge durations show mostly no integration. It has been suggested that, similar to visual processing, phasic mode (short duration) may be related to better stimulus detection while tonic mode (long duration) is associated with stimulus analysis (Guido et al. 1995; Ghose et al 2012). Here we show that in addition to changes in firing rates, shorter responses are associated with lower response variability in the multisensory condition which is a function of the nature of multisensory integration, the effect being different for response enhancement versus response depression.

Changes in response variability and its implications in multisensory processing

In addition to exhibiting almost no significant changes in its firing rate between the best unisensory and multisensory conditions, the long responses or tonic response mode is also associated with higher response variability in the multisensory condition compared to the best unisensory condition which may not be ideal for integrating capacity of the neuron either. These together may be responsible for the low integrating abilities observed for the long responses/ tonic mode. However, the shorter responses/ phasic mode of response mostly show significant changes in firing rates between the best unisensory and multisensory conditions. This is reflected in its high integrative index

values. In the visual system, relay cells of the cat's lateral geniculate nucleus (LGN) has been shown to exhibit both phasic and tonic response modes to visual stimulation, the type of response mode being dependent on the stage of voltage gated low threshold calcium conductance(Sherman 1996; 2001). In addition, considerable nonlinear distortions in firing patterns have been observed during phasic firing compared to effective linear summation during tonic firing (Guido et al. 1992; Mukherjee and Kaplan 1995). This is somewhat similar to the nonlinear increases in firing rates observed in the phasic mode of the SC multisensory neurons reflected as superadditive / subadditive interactions (Ghose et al 2012). The burst mode of LGN neurons have also been suggested to be beneficial for signal detection with increased signal to noise ratios, lower variability and greater ability to efficiently drive postsynaptic cells (Guido and Sherman 1998; Lu et al. 1992). Similarly, the multisensory responses reported to date in the superior colliculus (Meredith et al. 1987; Meredith and Stein 1983; 1986a; b) is predominantly phasic in nature and these multisensory responses and their integrative abilities have been implicated in the benefits observed in localization and orientation behavior under multisensory conditions (Burnett et al. 2004; Stein et al. 1988; Wilkinson et al. 1996). Spatially and temporally coincident multisensory stimulus combinations lead to response enhancements (Meredith et al. 1987; Meredith and Stein 1996; 1986a) and helps us to know that they belong to the same unitary event while spatially or temporally disparate stimuli (Meredith et al 1996; Meredith et al 1987; Kadunce et al. 2001) result in response depressions and in turn helps us to know that the stimulus combination should not be linked together and most likely belongs to two discrete events. However, recent studies characterizing the spatial receptive field architecture of

multisensory neurons in the superior colliculus (Krueger et al. 2009; Ghose et al 2012; Ghose and Wallace 2013 submitted) demonstrate that spatially and temporally coincident multisensory stimulus combinations can also produce response depressions. In other words, the nature of multisensory integration varies as a function of stimulus location within the neuronal receptive field. In addition, spatial location within the receptive field also affects the mode of response which in turn affects the integrative abilities of the multisensory neurons (Ghose et al 2012). As discussed above phasic mode is associated with high integrative abilities which may be enhancement or depression, in both cases all stimulus parameters except spatial location within the receptive field remains the same, or in other words the stimuli are spatially and temporally coincident and yet result in both response enhancement and response depression depending on its location within the receptive field of the neuron. However, response enhancements differ from response depressions in that they show increased response variability in the multisensory condition while response depressions show decreased response variability. It was also noted that for spatial locations showing response depressions, in most cases, firing rates were high in the unisensory conditions, so addition of a second modality not only resulted in a significant decrease in firing rates but also exhibited a decrease in response variability as measured by changes in Fano Factor and standard deviation measures between the different conditions. In other words, regions of the receptive field that have high unisensory firing rate values may require additional coding strategies (other than the rate code, because according to principle of inverse effectiveness, interactive indices which is based on the rate code, are higher and hence more beneficial when unisensory responses are low),

for driving multisensory integration and its resultant behavioral benefits. One of the ways this may be achieved is by decreasing the response variability. At the population level, decreased response variability, increases the probability of multisensory neurons producing coincident discharge patterns thereby providing an efficient temporal coding strategy which along with the rate code, may lead to behavioral benefits. However, this remains to be empirically tested in awake behaving cat preparations in multisensory neurons of the superior colliculus. That being said, it is important to note that response depression with congruent audiovisual stimulus combinations have been reported in auditory cortex (Ghazanfar et al. 2005; Kayser et al. 2010) and ventrolateral prefrontal cortex (VLPFC)(Sugihara et al. 2006) in primates. Interestingly, Kayser et al (2010) reports reduced response amplitude for strong auditory responses when visual and auditory stimuli are presented which also show a decrease in response variability in auditory cortex of alert monkeys. This is very similar to our current findings reported here. In addition, recent human evoked potential studies report that face plus voice integration is represented by suppressed auditory N100 responses (Besle et al. 2004; van Wassenhove et al. 2005)(Besle et al 2004; van Wassenhove et al 2005). Decreased activation with congruent audiovisual stimulus has also been reported in few neuroimaging studies (Miller and D'Esposito 2005) . It will be interesting to test for changes in response variability in these brain regions under conditions of response depression to see if they are accompanied by similar changes in response variability as reported in this current study and by Kayser et al (2010). More importantly, these decreases in response variability should be related to behavioral or perceptual benefits under multisensory conditions. This will help to elucidate if changes in response

variability, in addition to changes in firing rates, forms a part of the general neural code for multisensory integration under conditions of response depression.

Conclusion

Thus, this study describes the different changes in response variability with changes in response mode and its effects on multisensory integration in multisensory neurons of superior colliculus. It suggests that changes in response variability in addition to firing rate changes may form a neural code for the nature of multisensory integration.

Bibliography

Besle J, Fort A, Delpuech C, and Giard MH. Bimodal speech: early suppressive visual effects in human auditory cortex. *Eur J Neurosci* 20: 2225-2234, 2004.

Burnett LR, Stein BE, Chaponis D, and Wallace MT. Superior colliculus lesions preferentially disrupt multisensory orientation. *Neuroscience* 124: 535-547, 2004.

Churchland MM, Yu BM, Ryu SI, Santhanam G, and Shenoy KV. Neural variability in premotor cortex provides a signature of motor preparation. *J Neurosci* 26: 3697-3712, 2006.

Corneil BD, and Munoz DP. The influence of auditory and visual distractors on human orienting gaze shifts. *J Neurosci* 16: 8193-8207, 1996.

Diederich A, and Colonius H. Bimodal and trimodal multisensory enhancement: effects of stimulus onset and intensity on reaction time. *Percept Psychophys* 66: 1388-1404, 2004.

Frens MA, Van Opstal AJ, and Van der Willigen RF. Spatial and temporal factors determine auditory-visual interactions in human saccadic eye movements. *Percept Psychophys* 57: 802-816, 1995.

Ghazanfar AA, Maier JX, Hoffman KL, and Logothetis NK. Multisensory integration of dynamic faces and voices in rhesus monkey auditory cortex. *J Neurosci* 25: 5004-5012, 2005.

Ghose D, Barnett ZP , and Wallace MT. Impact of respone duration on multisensory integration. *J Neurophysiol* 108: 2534-2544, 2012.

Guido W, Lu SM, and Sherman SM. Relative contributions of burst and tonic responses to the receptive field properties of lateral geniculate neurons in the cat. *J Neurophysiol* 68: 2199-2211, 1992.

Guido W, Lu SM, Vaughan JW, Godwin DW, and Sherman SM. Receiver operating characteristic (ROC) analysis of neurons in the cat's lateral geniculate nucleus during tonic and burst response mode. *Vis Neurosci* 12: 723-741, 1995.

Guido W, and Sherman SM. Response latencies of cells in the cat's lateral geniculate nucleus are less variable during burst than tonic firing. *Vis Neurosci* 15: 231-237, 1998.

Harrington LK, and Peck CK. Spatial disparity affects visual-auditory interactions in human sensorimotor processing. *Exp Brain Res* 122: 247-252, 1998.

Hughes HC, Reuter-Lorenz PA, Nozawa G, and Fendrich R. Visual-auditory interactions in sensorimotor processing: saccades versus manual responses. *J Exp Psychol Hum Percept Perform* 20: 131-153, 1994.

Hussar C, and Pasternak T. Trial-to-trial variability of the prefrontal neurons reveals the nature of their engagement in a motion discrimination task. *Proc Natl Acad Sci U S A* 107: 21842-21847, 2010.

Kadunce DC, Vaughan JW, Wallace MT, and Stein BE. The influence of visual and auditory receptive field organization on multisensory integration in the superior colliculus. *Exp Brain Res* 139: 303-310, 2001.

Kara P, Reinagel P, and Reid RC. Low response variability in simultaneously recorded retinal, thalamic, and cortical neurons. *Neuron* 27: 635-646, 2000.

Kayser C, Logothetis NK, and Panzeri S. Visual enhancement of the information representation in auditory cortex. *Curr Biol* 20: 19-24, 2010.

Krueger J, Royal DW, Fister MC, and Wallace MT. Spatial receptive field organization of multisensory neurons and its impact on multisensory interactions. *Hear Res* 258: 47-54, 2009.

Lovelace CT, Stein BE, and Wallace MT. An irrelevant light enhances auditory detection in humans: a psychophysical analysis of multisensory integration in stimulus detection. *Brain Res Cogn Brain Res* 17: 447-453, 2003.

Lu SM, Guido W, and Sherman SM. Effects of membrane voltage on receptive field properties of lateral geniculate neurons in the cat: contributions of the low-threshold Ca2+ conductance. *J Neurophysiol* 68: 2185-2198, 1992.

Meredith MA, Nemitz JW, and Stein BE. Determinants of multisensory integration in superior colliculus neurons. I. Temporal factors. *J Neurosci* 7: 3215-3229, 1987.

Meredith MA, and Stein BE. Interactions among converging sensory inputs in the superior colliculus. *Science* 221: 389-391, 1983.

Meredith MA, and Stein BE. Spatial determinants of multisensory integration in cat superior colliculus neurons. *J Neurophysiol* 75: 1843-1857, 1996.

Meredith MA, and Stein BE. Spatial factors determine the activity of multisensory neurons in cat superior colliculus. *Brain Res* 365: 350-354, 1986a.

Meredith MA, and Stein BE. Visual, auditory, and somatosensory convergence on cells in superior colliculus results in multisensory integration. *J Neurophysiol* 56: 640-662, 1986b.

Miller LM, and D'Esposito M. Perceptual fusion and stimulus coincidence in the cross-modal integration of speech. *J Neurosci* 25: 5884-5893, 2005.

Mitchell JF, Sundberg KA, and Reynolds JH. Differential attention-dependent response modulation across cell classes in macaque visual area V4. *Neuron* 55: 131-141, 2007.

Mukherjee P, and Kaplan E. Dynamics of neurons in the cat lateral geniculate nucleus: in vivo electrophysiology and computational modeling. *J Neurophysiol* 74: 1222-1243, 1995.

Sherman SM. Dual response modes in lateral geniculate neurons: mechanisms and functions. *Vis Neurosci* 13: 205-213, 1996.

Sherman SM. Tonic and burst firing: dual modes of thalamocortical relay. *Trends Neurosci* 24: 122-126, 2001.

Stein BE, Huneycutt WS, and Meredith MA. Neurons and behavior: the same rules of multisensory integration apply. *Brain Res* 448: 355-358, 1988.

Steinmetz NA, and Moore T. Changes in the response rate and response variability of area V4 neurons during the preparation of saccadic eye movements. *J Neurophysiol* 103: 1171-1178, 2010.

Sugihara T, Diltz MD, Averbeck BB, and Romanski LM. Integration of auditory and visual communication information in the primate ventrolateral prefrontal cortex. *J Neurosci* 26: 11138-11147, 2006.

van Wassenhove V, Grant KW, and Poeppel D. Visual speech speeds up the neural processing of auditory speech. *Proc Natl Acad Sci U S A* 102: 1181-1186, 2005.

Wallace MT, Meredith MA, and Stein BE. Integration of multiple sensory modalities in cat cortex. *Exp Brain Res* 91: 484-488, 1992.

Wilkinson LK, Meredith MA, and Stein BE. The role of anterior ectosylvian cortex in cross-modality orientation and approach behavior. *Exp Brain Res* 112: 1-10, 1996.

CHAPTER VI

General Discussion

Summary of results

The overall goal of this thesis was to provide a detailed description of the receptive field architecture of multisensory neurons in the deep layers of the superior colliculus with the hope of shedding additional light as to “how” these neurons combine information from multiple modalities. To that end, we describe the heterogeneous nature of the receptive fields of multisensory neurons in SC in Chapter II and show that these neurons are characterized by complex receptive field architecture. Despite the complexity of this organization, a single underlying computational principle appears to govern the integrative features of these neurons. Thus, sensory responsiveness to both unisensory and multisensory stimulus combination changes depending on spatial location of the stimuli within the receptive field. These changes in sensory responsiveness appear to be primary determinants of multisensory integration, such that regions of the receptive field that are *less* responsive to unisensory stimuli show *higher* multisensory gains, a finding in accordance with the principle of inverse effectiveness. In addition to sensory responsiveness, Chapter III focuses on the temporal characteristics of these multisensory responses, which also vary depending on

the region of the receptive field that is stimulated, and which in turn also affects the nature of multisensory integration. Here we provide evidence for a complex temporal architecture to these receptive fields, such that some regions showing short response durations while others show long response duration. Once again, this duration impacts the multisensory response, largely through its effects on the overall efficacy of the sensory responses.

In addition to using classical spike-based measures (e.g., firing rates) to study multisensory processing in the SC as done in Chapters II and III, Chapters V and VI investigated mechanisms of multisensory processing in the deep layers of the SC using two novel approaches. Chapter V studies multisensory processing in the deep layers of the SC by examining local field potentials, and provides some of the first evidence for the nature of synaptic processing in these layers. This study, for the very first time, shows the greatest increase in LFP amplitude after multisensory stimulation, a change that is accompanied by increased power in different frequency bands. Furthermore, changes in the LFP in the absence of overt spiking activity provide a novel tool to better examine sensory convergence and integration in the SC. Chapter VI shows that response variability changes under multisensory conditions compared to the best unisensory condition, the nature of this change being dependent on the type of multisensory integration. Thus, for response enhancements, variability increases under multisensory stimulus conditions, whereas for response depressions variability decreases during multisensory stimulation. This suggests that, along with changes in firing rate, changes in response variability may be an additional mechanism by which neurons convey information as to the nature of the multisensory stimulus. Finally,

although the focus of this thesis is on the deep (i.e., multisensory) layers of the SC, we also uncovered evidence that multisensory activity may extend into the superficial SC layers as well. Such a finding represents a major conceptual shift in thinking about the superficial layers, which have been traditionally viewed as exclusively visual layers. In Chapter IV, we describe evidence for multisensory processing in the superficial layers in both spiking and LFP records, as well as provide support for the concept of inverse effectiveness.

Implications of the key findings

The important implications of the key findings of the different studies described in this thesis have been discussed in the individual chapters. However, below are some of the major implications of these results (as well as linkages between them) that can collectively bear on future studies of multisensory processing in the SC.

Implications of heterogeneous receptive fields of multisensory neurons in SC

The thesis work underscores the heterogeneous nature of the large receptive fields of multisensory SC neurons, a previously underappreciated aspect of these neurons. The heterogeneity characterizes both the spatial and temporal aspects of these receptive fields, reinforcing the view that we need to think about receptive fields in multiple dimensions – a view encapsulated in the concept of the spatiotemporal receptive field (STRF). Furthermore, this STRF structure is a key determinant in the multisensory integration exhibited by these neurons. Collectively, these findings have strong mechanistic and behavioral implications. In an effort to highlight these issues, we have recently published a report attempting to make the field aware of these important issues

[see (Sarko and Ghose 2012)].In light of the evidence provided here, it is suggested that while designing experiments testing for multisensory integration at the neuronal level, care should be taken to ascertain that factors such as sensory responsiveness and response duration are accounted for in any analyses. Otherwise the differences in integrative abilities cannot be attributed solely to the experimental manipulation and could result from the inherent differences in receptive field architecture. As a tangible example of this issue, consider if we want to study the effects of noise rearing on integrative abilities of multisensory neurons in the SC. To do this experiment we would need two groups of animals: controls and a noise reared group. When comparing multisensory integration of a neuron from the control group to that of a neuron in the noise reared group, care should be taken to ensure that the location of the stimuli within the receptive field is comparable across the two groups. In other words, for both groups the most responsive region within the neuronal RF (say unisensory hotspots) must be compared. However, if the unisensory hotspot of a neuron in one group (say noise reared group) is compared to a less unisensory responsive region within the RF of a neuron in the other group (control group), then the differences in integrative abilities may not be a true reflection of the experimental manipulation (i.e., noise rearing). It may simply result from the fact that due to sampling of the higher unisensory responsive region of the RF of the neuron in the noise reared group, the amount of multisensory integration appears to be less than the control group where a less unisensory responsive region of the RF was sampled. Thus, the possibility remains that if for both neurons the unisensory hotspots/unisensory coolspots were compared, the integrative

ability could be same. Thus, by ignoring the heterogeneous nature of these receptive fields it could be easy to arrive at erroneous conclusions.

In addition, the spatial and temporal heterogeneity evident within the receptive field architecture of these neurons are important factors that will help create better neuronal models of multisensory integration that will ultimately help us understand the mechanistic underpinnings of the integrative capacity of multisensory neurons. Neuronal models provide an opportunity to understand some of the mechanisms underlying neuronal functions. There has been an upsurge in interest in recent times in modeling multisensory processes (Anastasio and Patton 2003; Anastasio et al. 2000; Avillac et al. 2005; Diederich and Colonius 2004; Rowland et al. 2007).As described in detail earlier in this thesis, numerous studies have been done that have described various factors that affect the nature and magnitude of integrative abilities of multisensory neurons (Kadunce et al. 1997; Kadunce et al. 2001; Meredith et al. 1987; Meredith and Stein 1996; 1986a; b; Perrault et al. 2003; 2005; Wallace and Stein 1996) and creating a successful model for multisensory processing would require inclusion of these factors to create a neuronal model that can predict the integrative abilities of the multisensory neurons. Though a recent study (Cuppini et al. 2010) uses some of these factors among others to create a model for SC multisensory neurons, it is by no means a complete one. Most of the factors that have been empirically shown to affect the magnitude of integration have not been incorporated in the model but it does provide the first step in creating such models and understanding the power of their predictive nature. The empirical evidence showing interdependency of space, response duration and neuronal responsiveness in this thesis will help in future modeling studies. Incorporating

response duration as a predictor for amount and nature of multisensory integration may help to create models with higher predictive powers. Ina addition, future modeling studies can consider using space and stimulus effectiveness as a single component of the model where altering one changes the other in a predictable manner and that in turn alters the magnitude of integration in a predictable way. This will help to limit the unnecessary increase in the degrees of freedom for the model which in turn will improve its predictive capacity.

It is important to mention here, that heterogeneity of receptive fields, both in space and time is not a unique feature of multisensory neurons alone. It has been shown that heterogeneous receptive fields help in spatiotemporal processing of information that has important functional implications in different sensory systems. For example, in the auditory system, information that is embedded in the duration, interval and temporal order of the acoustic stimuli are important parameters for signal processing. Characterization of auditory neurons is best accomplished by combining spectral and temporal features when compared to mapping frequency sensitivity and temporal response properties separately (Eggermont et al 1981). The spectrotemporal RF of an auditory neuron represents the specific characteristics of a sound stimulus in both the time and frequency domain that affect the firing probability of the neuron (Ghazanfar and Nicolelis 2001).The classical and most studied example of time varying auditory RF has been the echo delayed neurons of the bat (Suga et al 1983). Studies show that bat auditory cortical neurons best respond to one frequency at one time and then to another frequency at a later time (Fitzpatrick et al 1998) and it has been suggested that these frequency and time delays correspond to the species specific vocal signals used for

echolation of prey and /or communication among conspecifics (Suga et al 1987; Kanwal 1999). In cat auditory cortex neurons may show excitatory responses to more than one frequency range and these ranges may be separated by ranges of no excitation or inhibition (Oonishi and Katuski 1965; Abeles and Goldstein 1972). In primates the existence of spectrotemporal RF was demonstrated by deCharms et al (1998) in the A1 cortex of awake owl monkeys. The auditory stimuli consisted of rapid sequences of tones or chords and reverse correlation was used to relate neuronal firing pattern with the sound sequences. It was found that most neurons in A1 cortex have RF whose best frequency varies as a function of time. Majority of the neurons have complex RFs that included regions of excitation and inhibition and time varying frequency tuning. Some neurons had narrow regions of excitation flanked by regions of inhibition above (i.e. at a relatively high frequency range) and below (i.e. at a relatively low frequency range). Others had excitatory or inhibitory responses to one frequency range at one time and another frequency range at a later time. It was suggested by the authors that spectrotemporal RF of auditory neurons in A1 cortex of owl monkeys may indicate preferences for stimulus edges, stimulus transitions in frequency or intensity and conjunctions of different stimulus features. This hypothesis was tested by using the RF of auditory neurons as guides in construction of the stimuli. When matched to their appropriate spectrotemporal RF, such stimuli elicited robust responses from the auditory cortical neurons (deCharms et al 1998). Stimuli which deviated spectrally or temporally from the RF elicited weaker responses.

In the visual system early work characterized the receptive fields of LGN neurons in purely spatial terms with an on center that responds to onset of a bright stimulus and off

surround that responds to onset of a dark stimulus (or offset of a bright stimulus) (Hubel and Weisel 1961). The spatiotemporal organization of the LGN RFs was first studied by Steven and Gerstein (1976). They used response plane method to characterize the LGN RF in joint space and time domain. Two different types of LGN RFs were revealed. One type exhibited excitatory and inhibitory domains that remained stable over time (heterogeneous response plane). They exhibited antagonism (excitatory vs inhibitory) in space while the second type exhibited excitatory and inhibitory domains that shifted as a function of time (homogenous response plane). These exhibited antagonism (excitatory vs inhibitory) in time. The authors suggested that this RF architecture might reflect that the heterogeneous cells act as spatial filters while the homogenous cells act as temporal filters. Thus the heterogeneous cells might optimally respond to an object of specific size while homogenous cells would respond to temporal properties like velocity of movement of the stimulus. In practice, however, most LGN cells were to some extent both spatially and temporally antagonistic which led the authors to conclude that each cell might respond optimally to a certain range of object sizes and velocities and the homogenous and heterogeneous planes represent the two extreme ends of this range. (Stevens and Gerstein 1976). Thus it is clear that even in the visual system the complex spatiotemporal RF architecture of different visual structures (LGN being an example structure discussed above) help to encode important features of the stimulus that helps in effective processing of information about the natural surroundings.

In the somatosensory system, similar studies were conducted in various structures such as the VPM nucleus of thalamus and the primary somatosensory cortex in rats and primates which elucidated the functional significance of spatiotemporal RFs. Nicolelis et

al (Nicolelis et al 1993a; Nicolelis and Chapin 1994) used methods similar to the response plane technique. They recorded single neuron's response to the stimulation of 5X5 matrix of whiskers (deflected one at a time) and divided the response into 5ms post stimulus epochs. For each epoch the whisker that elicited the greatest response (in spike counts) was defined as RF center for that time epoch. It was revealed that single VPM neurons have large multiwhisker RF whose center is defined by one whisker called the principal whisker (PW) whose stimulation elicits strongest response. The location of the PW of a given VPM neuron could vary as a function of post stimulus time (Nicolelis and Chapin 1994). VPM neurons could be classified into 2 classes according to time dependency of their RF centers. In one class the spatial position of the RF center shifted over post stimulus time. In the other class neurons exhibited RF centers that remained in the same whisker over time (Nicolelis and Chapin 1994). This complex spatiotemporal RF architecture in the rat somatosensory system may serve to integrate time varying multiple whisker inputs. This may have important behavioral implications for the rats in that this information may be used for performing discrimination tasks or identifying patterns of tactile stimulation.

Similar heterogeneous SRF and STRF has also been reported in classical multisensory cortical areas such as the anterior ectosylvian cortex (AES) in cats (Carriere et al 2008; Royal et al 2009). Similar to our findings in SC, it has been shown that AES multisensory neurons have complex heterogeneous receptive field architecture and changes in the efficacy of the unisensory responses at different locations plays a key role in dictating the multisensory interactions generated by their combination. Though the functional role of AES still remains enigmatic, it has been suggested that, receptive

field heterogeneity and the multisensory interactive profiles derived from such an organization play an important role in the coding and binding of multisensory motion (Carriere et al 2008). RF heterogeneity provides an excellent substrate for construction of unisensory motion selectivity (Clifford and Ibbotson 2002; Wagner et al 1997; Witten 2006) and the “gain” that occurs under multisensory conditions may aid in providing uniformity in the coding of moving visual and auditory stimuli with similar dynamics that are likely derived from the same multisensory event (Carriere et al 2008).

Thus, in the light of our present study described in Chapter II here and the study of Carriere et al 2008, it can be concluded that there are striking similarities in the construction of SRF architecture of both SC and AES multisensory neurons. In both SC and AES, multisensory neurons exhibit single or multiple hotspots of activity (both under unisensory and multisensory conditions) that bear important predictable consequences on their integrative abilities. Moreover, the regions of high activity for different effective modalities could be well aligned or strikingly misaligned both in SC and AES. This suggests that the principles underlying the generation of complex heterogeneous RF architecture of multisensory neurons is ubiquitous in cortical and sub cortical structures. This may be partly because SC and AES both function as parts of the same neuronal network that is involved in providing multisensory benefits in localization and orientation behaviors as discussed earlier.

However, the STRF architecture differs in SC and AES multisensory neurons. In AES neurons, two temporal epochs in which multisensory integration occurs has been described – an early phase and a late phase (Royal et al 2009). However, results of our studies described here in Chapter III and studies by Rowland et al 2007; Rowland and

Stein 2008 demonstrate that SC multisensory neurons exhibit multisensory integration during the early phase of the response but not at a later phase. Based on such difference in STRF architecture of SC and AES neurons it may be reasonable to suggest that AES, being a high order association area may be involved in higher order perceptual processes such as coding and binding of multisensory motion, coordinate transformations between the different sensory systems (Wallace et al 1992,2006) and hence necessitating longer periods of integration while SC plays a larger role in stimulus directed action or orientation which is reflected in the initial response enhancements that are seen in SC multisensory neurons that may be behaviorally reflected in faster reaction times that have been reported under multisensory conditions.

Another important consideration here is that, SC is not exclusively involved in sensory processing. Rather, it is an elegant sensorimotor structure that plays an important role in visuomotor control and gaze shifts. It is well known that SC has a motor map. Moreover, the representation of sensory information in SC is in motor co-ordinates (Sparks and Mays 1983; Munoz and Guitton 1989; Harris 1980). Most of the multisensory neurons in SC are also motor in nature and are thought to provide a command signal to move the eyes and/or head. This signal plays a part both in initiating and in specifying the vector of a movement. Vector of SC mediated saccadic eye movements is determined by the weighted average of activity across the motor map rather than by the activity of any restricted group of neurons within the topographic map. Thus the desired gaze change is represented by the spatial distribution of activity across a substantial fraction of the SC motor map (Stein and Meredith 1993). It can be suggested that, since the sensory information in SC is represented in motor

coordinates, the heterogeneous nature of the sensory receptive fields and their resultant effects on multisensory integration that creates “smoothing” of the spatial response profile described in detail in Chapter II here, may aid in generation of more accurate spatial localization (in the sensory domain) and in turn more accurate gaze shifts (in the motor domain, that definitely depends on accurate spatial localization of the sensory stimuli) under multisensory conditions. However this remains to be empirically tested in awake behaving animals.

Implications of the multisensory nature of the superficial layers of SC:

Another major finding of this thesis is the multisensory nature of the superficial layers of the SC. We provide evidence for both sub- and supra-threshold audiovisual processing in the superficial layers of cat SC. The long standing notion about the superior colliculus has been that the superficial layers are solely involved in visual processing while the deep layers are multisensory in nature and play an important role in orientation behavior (Casagrande et al. 1972; Schneider 1969; Sprague 1996; 1991; Sprague et al. 1970; Sprague and Meikle 1965; Stein et al. 1988; Tunkl and Berkley 1977; Wilkinson et al. 1996). The purely visual nature of the superficial layers is called into question by the current findings of this thesis and recent anatomic evidence for intrinsic connectivity of the SC (Behan and Appell 1992; Behan and Kime 1996; Hall and Lee 1993; 1997; May 2006) and it is possible that the superficial and deep layers of the SC are not completely separate entities after all. As discussed in detail in Chapter I and Chapter IV, the auditory influences reach the superficial layer neurons most likely via dendrodendritic connections between the superficial and intermediate layer neurons. These superficial layer neurons, in turn, project to the dorsal lateral geniculate nucleus of the thalamus

which in turn provides the major driving input to V1(review see Hackett TA 2012). Thus, now that we have demonstrated auditory influences on visual processing in the superficial layers of SC, this may serve as a pathway for multisensory information to reach the LGN and in turn V1, V2 and higher visual cortical areas. The influence of such multisensory information may help to improve processing of visual information providing multisensory benefits in processing visual motion, object perception and spatial localization or in other words both the “what” and “where” pathways. As discussed in details in Chapter 1, superficial SC neurons are known to play an important role in visual form discrimination [(Berlucchi et al. 1972; Casagrande et al. 1972; Schneider 1969; Sprague 1991; Sprague et al. 1977; Tunkl and Berkley 1977)] and presence of auditory influences in the superficial layers may help to confer multisensory benefits in form perception/discrimination. For example, based on the current findings, it can be speculated that pairing an auditory stimuli with the visual stimulus may help in better and/or faster form discriminative abilities in awake behaving animals. In addition, the superficial layers of SC also project to the lateral posterior (LP) / pulvinar nucleus of the thalamus which is known to have multisensory properties (for a recent review see Hackett TA 2012). Thus, the superficial SC input may serve as one of the potential candidates for conferring multisensory properties to the LP/pulvinar neurons. The LP/pulvinar, in turn, is extensively connected to sensory cortices of all modalities as well as much of prefrontal, orbital and cingulate cortex. The densest connections involve non primary sensory and association areas and it has been suggested that LP/pulvinar may serve as a higher order relay of information between cortical areas (Guillery and Sherman 2002; Sherman 2001a; 2007; 2001b; Sherman and Guillery 2002). More

specifically, LP/pulvinar may receive driving inputs from one cortical area and relay those inputs to another area forming a cortico-thalamo-cortical (CTC) loop (Hackett TA 2012) . Given, that the LP/pulvinar is heavily connected with sensory and multisensory areas of cortex, the CTC loops involving the LP/pulvinar may play an important role in mediating multisensory integration in cortex.

Another important role attributed to the superficial layers of SC is that in visual attention. The complexity of the visual world around us forces us to select one or a few objects in the scene for detailed analysis at the expense of others (Fecteau and Munoz 2006; 2007; White and Munoz 2011) and the object that is selected is considered to be most salient. Salience refers to the sensory qualities of the object that makes it more distinct compared to its surroundings such as its color, size, orientation, shape, movement (Fecteau and Munoz 2006, 2007; White and Munoz 2011). The concept of a salience map has been proposed in recent times and is such that, on this map, each object competes for selection. More distinct the object, greater is its representation and more chances of its selection. Several brain areas including the superficial SC has been suggested to be a part of the neural network for creating such visual salience maps (Fecteau and Munoz 2006, White and Munoz 2011).It has been suggested that the superficial SC neurons is well suited towards this role because of the following properties discussed below (White and Munoz 2011). First, the neurons constituting the salience map should participate in bottom up processing of objects in the scene as opposed to goal directed processing. Secondly, they should be spatially selective but otherwise capable of identifying the most distinct object, independent of the features that it possesses by receiving inputs from different feature maps that represent different

qualities of the scene and then computing the relative distinctiveness of the object in a featureless manner (Itti and Koch 2001; 2000; Treisman and Gelade 1980; Wolfe et al. 1989). Thirdly, lesions of these neurons should result in deficits in attentional selection. Fourthly, electrical stimulation of these neurons should facilitate attentional selection of objects. Finally, these neurons should receive inputs from the ventral visual pathways about specific object features that will help them compute the salience map. The superficial SC neurons receive projections from higher visual areas as described in Chapter 1 and hence are ideally suited to play an important role in construction of visual salience maps. Moreover, neurons coding for stimulus salience should have extensive feedback to higher levels of visual processing, and hence superficial SC with its extensive connections with pulvinar projects to multiple extrastriate visual areas as discussed above. Lesions of the SC result in profound sensory neglect without any motor impairment suggesting its role in visual attention as well (Sprague and Meikle 1965). Hence, all these evidences suggest that the superficial layers of SC is well suited to be a part of the neural network for generation of visual salience maps that in turn helps in visual target selection. Appropriate visual target selection in cluttered visual environments is important in our daily lives. In addition to the role of superficial layers of SC in generating salience maps, the intermediate layers of SC have been shown to play a role in target selection and visuospatial attention (review see Fecteau and Munoz 2006, White and Munoz 2011).

Our current results, showing auditory influences in the superficial layers suggest that the role of SC in generation of salience map for target selection in a cluttered environment may not be restricted to the visual modality. Such salience maps may be multimodal in

nature. The CTC loops involving the superficial SC and LP/pulvinar described above are in a position to convey multisensory information to higher cortical areas (not only visual but auditory and somatosensory cortices as well) forming multisensory salience maps. This will help in target selection in a “supramodal” manner which may be a more efficient way of neural coding given that stimuli in our daily environment are not unimodal but mostly multimodal in nature. In addition to the possible role of superficial SC in formation of such multimodal salience maps ,the intermediate SC neurons project to multisensory thalamic nuclei such as the suprageniculate which in turn project to the striatum, amygdala, secondary sensory and association areas as well as multisensory cortical areas such as retroinsular area, insula, FEF (Hackett TA 2012). These projections may be involved in multisensory target selection which may be more common in our natural environments as well. Thus, this would support the idea that the superficial and intermediate/deep layers of SC are not completely separate entities. Rather they function together to some extent, to mediate multisensory target representation and selection in our noisy natural environment.

Implications of using novel methods to study multisensory processing in the SC:

Another major implication of the studies described in this thesis is the idea of studying multisensory processing in the superior colliculus using methods other than ones that rely solely on spiking activity and firing rate changes. Strength of a response (measured by spike counts and firing rates) is only one of the relevant parameters that determine how well and with what fidelity neurons can represent the sensory environment. Changes in neuronal response variability may be another mechanism by which information is relayed in the brain. Decreased response variability under multisensory

conditions has been shown when congruent audiovisual stimuli are decoded in auditory cortex (Kayser et al. 2010). This decreased variability has been suggested to enhance the reliability or precision of sensory representations and hence result in multisensory benefits in behavior/perception. Similarly, our findings in Chapter VI show decreased variability of multisensory responses in the SC under conditions of response depression. It is important to bear in mind that classically response depression has been shown to occur in SC neurons when spatially disparate audiovisual stimuli are presented. This helps to prevent unwanted binding of multimodal stimuli that may not belong to the same event. However, in our study, response depression was produced with spatially congruent audiovisual stimuli (similar to that shown in auditory cortex by Kayser et al 2010), most commonly in regions of the receptive field that exhibited high unisensory firing rates. Thus, due to biological constraints, it is possible that on presentation of multisensory stimulus combinations, these regions of the RF may not be able to increase their firing rates further. Under such conditions, spatially congruent audiovisual stimulation results in response depression. Moreover, in addition to decreasing its firing rate under multisensory conditions, the neurons also show a decrease in response variability. Together, this decrease in firing rate and variability may serve to increase the reliability of stimulus representation under multisensory conditions, hence facilitate binding of the audiovisual stimulus pair (which is spatially and temporally congruent and hence should be bound together). Moreover, this decreased variability, at the population level, may help to increase neuronal synchrony which in turn may result in benefits in orientation behavior that has been reported under multisensory conditions for spatiotemporally congruent multisensory stimuli. Thus, in

addition to carrying information by changes in firing rates, SC neurons may transmit extra information by precise temporal patterns of activity. This may also be important for building future neuronal models of multisensory processing in SC neurons where in addition to firing rates, changes in temporal patterns of activity should be borne in mind when accounting for mechanisms underlying multisensory integration.

Such considerations are important because recent studies have shown that precise spike timing and low frequency network oscillations together provide information about sensory stimuli that is additional to that conveyed by spike firing rate (for review see King and Walker 2012). For example, using information theoretic approaches, (Montemurro et al 2008) demonstrated that in visual cortex, the timing of spikes relative to the phase of LFP oscillations in the delta band carries information about the contents of naturalistic images. Similarly in the auditory cortex, the timing of spikes with respect to LFP phase in the theta frequency range carries information about the type of sound presented to awake, passively listening monkeys (Kayser et al 2009b). Both these studies show that the information provided by the “phase of firing” is complementary to that of the spike rate code, thus enhancing the sensory acuity of the spike code through global network activation (King and Walker 2012).

Similarly, it can be envisioned that by decreasing the response variability under multisensory conditions as described in Chapter VI here, SC neurons are able to align the temporal spiking pattern across the population to a more “ideal” phase of ongoing neuronal oscillations hence providing more information under multisensory conditions and possible behavioral benefits such as decreased saccadic reaction time and

increased accuracy. Such a hypothesis remains to be tested using information theoretic measures in awake behaving animal models.

As alluded to previously, the most common form of multisensory integration studied in the SC is that represented solely by changes in spiking activity or more specifically solely based on firing rate changes under different stimulus conditions. However, recent research mainly in the cortical domains suggest that sub threshold mechanisms underlying multisensory integration are most commonly found in different brain areas. Our findings suggest that sub threshold multisensory processing is not unique to cortical structures alone. Using local field potential recordings we were able to demonstrate multisensory processing at the synaptic level in both the superficial and intermediate/deep layers of the SC. However, before we discuss the important implications of sub-threshold multisensory processing in the SC, due to the inherent nature of the LFP signal it is important to discuss here the spatial nature of our LFP signals and pieces of converging evidence in our data that assured us that we were successfully sampling the superficial and intermediate/deep layers largely independently.

Though the spatial extent of the spread of LFP signals due to volume conduction is still controversial, the upper range has been estimated to be about 500-800μm (Katzner et al. 2009; Liu and Newsome 2006; Xing et al. 2009; Berens et al 2010). Thus, when we recorded LFPs with our electrode on the top of SC (details of identification of top of SC responses are discussed in Chapter IV), even if we were sampling 500-800μm, the signals were mainly from the superficial layers (comprising of SZ, SGS, SO), the depth of which ranges from 800-1000μm in cats (Huerta MF 1984; May 2006). In addition all

our intermediate/deep layer LFP recordings were sampled at depths of 1000-1200μm from top of SC (at least). In addition, the nature of evoked LFPs was dramatically different in the superficial and intermediate/deep layers. A clear distinction was seen in the latency of visual responses in the superficial and deep layers (see Fig 4-6, 5-3, 5-4). The visual responses in the superficial layers occurred much faster than the deep layer visual responses. This is in accordance with the differences in driving visual inputs to these layers. As described extensively in Chapter I, the superficial layers receive majority of their driving inputs from the retina and primary visual cortex while the driving inputs to the intermediate/deep layers are derived from extra-striate visual cortical areas. Moreover, the spectral nature of the LFPs was vastly different in these layers as well. This is clearly seen in Figs 4-7, 5-5, 5-7. Finally, we suggest that auditory influences reaching the superficial layers are mediated predominantly via dendrodendritic connections between the superficial and intermediate layer neurons that have been described in recent anatomical studies. The auditory influences in the intermediate/deep layers are directly derived via synapses of auditory inputs on the multisensory neurons that reside in these layers. Also, as discussed extensively in Chapter IV, in our data, the activity in high gamma band was found to correlate with multi-unit/single unit spiking activity. Thus we suggested that high gamma band activity, like spiking responses, may be a read out of multisensory integrative capacity of the local neuronal population. Based on this logic, the “multisensory gain” in the high gamma band activity should occur earlier in the LFP responses of the intermediate/deep layers (since it is mediated by direct synapses of auditory inputs on the multisensory neurons) compared to the superficial layers (which receive this auditory input later via

the dendro-dendritic synapses described earlier). This is clearly evident in the contrast plots shown in figs 4-8 and 5-6 that quantify multisensory gains in the superficial and intermediate/deep layers of SC respectively. Thus, all these pieces of converging evidence reassured us that we were correctly sampling superficial and deep layer responses largely in an independent manner.

Evidence for sub-threshold multisensory processing in the superficial/visual layers of SC can be of utmost functional importance as described in detail earlier. In addition, studying LFPs in the deep layers of SC helps to understand the nature of synaptic inputs in these layers. The multisensory nature of the intermediate/deep SC has been known for decades but relationship between processing of multisensory information at the input level (as reflected in LFPs) and the output level(as reflected in spiking activity) still remains largely ignored. The study described in Chapter V attempts to bridge the gap and demonstrate the nature of synaptic processing in these layers. This will help us understand the mechanistic basis of multisensory processing in these layers.

Two types of multisensory neuronal populations are described in the intermediate/deep layers of SC: overt neurons and modulatory neurons. Though evoked LFP amplitude was significantly different under multisensory conditions for both these classes of neurons, we are able to demonstrate spectral differences in sub threshold processing in these two classes of neurons. Sub threshold multisensory processing as reflected in power changes across different frequency bands was much more widespread across different frequencies for overt multisensory neurons while the modulatory neurons showed significant changes in power mostly in the low frequency bands. This finding

may have several implications. It is possible that the underlying mechanism for multisensory integration is different for overt and modulatory multisensory neurons.

It has been suggested that multisensory integration can be achieved by changes in the power of ongoing neuronal oscillations or changes in phase of ongoing oscillations or some combination of the two processes (Lakatos et al. 2008; Senkowski and Engel 2012) Recent studies in auditory cortex (Lakatos et al. 2007; Lakatos et al. 2008) demonstrate that neurons in the auditory cortex use a “phase reset” mechanism for integrating multisensory information. The driving input sets the rhythm across ensembles of oscillating neurons. Presentation of the modulatory input resets the phase of such ongoing neuronal oscillations. Such a mechanism helps to adjust the timing of neuronal activity related to specific inputs thus providing means of enhancing/ suppressing spiking responses. Such a mechanism of multisensory integration may not be reflected in power changes of the LFP signal but may be reflected in phase changes. Such changes in phase can be quantified by using inter-trial phase coherence measures or measures that quantify changes in phase angle (Lakatos et al. 2007; Lakatos et al. 2008; Zion Golumbic et al. 2013a; Zion Golumbic et al. 2013b). Such phase-locking (i.e., synchronization) ultimately serves to amplify neuronal representations, facilitate sensory discrimination, and increase response speed and accuracy (Lakatos et al. 2008; Schroeder and Lakatos 2009a; b).

In the light of our current findings described in Chapter V, it is possible that the overt multisensory neurons in SC engage in multisensory integration by changing the power of neuronal oscillations across different frequency bands as shown here while the lack of such evidence for the modulatory neurons may suggest that for this class of neurons,

changes in phase of oscillation may be an alternative mechanism by which they engage in multisensory integration. Whether the overt multisensory neurons also use such phase resetting mechanisms in addition to the power changes reported here remains an open question. Nonetheless, we clearly demonstrate that using LFPs to study multisensory processing in the SC may shed new lights on the underlying mechanisms of multisensory integration which remains elusive to date.

Conclusions

1. Multisensory neurons in the deep layers of the SC have complex heterogeneous receptive fields.
2. This complex spatial architecture appears to play an important role in dictating a resultant multisensory interaction
3. Sensory responsiveness appears to be a primary determinant for multisensory interactions.
4. Neuronal response durations also vary across these heterogeneous spatial receptive fields such that regions with short response durations show higher integrative abilities.
5. In addition to firing rate changes, changes in response variability may be another mechanism by which cross modal information is processed in the SC.
6. Superficial layers of the SC show evidence of multisensory processing both in spiking activity and in synaptic mechanisms
7. Study of local field potentials provide evidence for synaptic mechanisms of multisensory processing in the deep layers of the SC.

Based on the work in this thesis, some future directions are discussed below.

Future directions

Future studies should be directed towards understanding the functional implications of heterogeneous receptive field architecture by designing experiments in awake behaving animals. Future work in our laboratory is using operant conditioning methods to train animals to fixate on a single location while audiovisual stimuli are presented in order to study SRF/STRF architecture and its potential implications on behavior. Now that we know the heterogeneity inherent within the receptive field architecture of normal reared animals(essentially the control group), future experiments can be designed to test for changes in receptive field architecture that occur after sensory deprivation (like dark rearing, noise rearing, adult onset blindness) and how that affects multisensory processing and behavior.

Our finding that response variability decreases under multisensory conditions for response depressions leads us to suggest that this decreased variability at the population level may improve neuronal synchrony and hence may be a mechanism by which behavioral benefits of multisensory integration can occur even when the strength of response is actually decreasing. This idea can be tested in future studies by employing multi electrode recordings in the deep layers of the SC and comparing coincident firing of neuronal pairs under conditions of response enhancement and response depression to test if neuronal synchrony is more when response depressions occur compared to response enhancements which will provide evidence for the idea that decreased response variability is part of a temporal code (spike timing) for

multisensory processing in the SC. This can then be extended in awake behaving paradigms to test for behavioral benefits as well.

We show sub threshold auditory influences in the superficial layers of the SC, possibly being mediated by intrinsic connections within the SC. Future studies should be directed to understand the detailed anatomical circuitry and functional implications of the existence of such modulatory influences and how that would affect downstream visual processing. Also, attempts should be made to uncover the underlying cellular mechanisms that bring about these modulations.

We know from previous studies that cortical inputs from AES and /rLS are critical for multisensory integrative abilities of the deep layer neurons (Jiang et al 2001) and recent studies have also elucidated the anatomical circuitry that mediates this effect (Fuentes-Santamaria et al 2008). Anatomical evidence suggests that cortical afferents act on the multisensory neurons directly or indirectly through interneurons to bring about multisensory integration. Here in this thesis we provide evidence for deep layer synaptic processing and the activity generated by the wide variety of inputs that the deep layer receives including the critical inputs from cortex. By recording local field potentials in the deep layers and characterizing the amplitude changes in evoked LFPs under different stimulus conditions and power changes in different frequency bands we characterize the input activity in this region. This sets the stage for future studies which can now elucidate the exact contribution of the cortical inputs by a) deactivating AES and rLS and then observing changes in LFP activity and comparing it to LFPs when all inputs are present (as described here) b) specifically deactivate the interneurons by GABA antagonists leaving all other inputs intact and observe the changes in LFP. These

studies will help us elucidate the exact mechanisms underlying multisensory integration in the deep layers of SC.

Bibliography

Abeles M, and Goldstein MH, Jr. Responses of single units in the primary auditory cortex of the cat to tones and to tone pairs. *Brain Res* 42: 337-352, 1972.

Anastasio TJ, and Patton PE. A two-stage unsupervised learning algorithm reproduces multisensory enhancement in a neural network model of the corticotectal system. *J Neurosci* 23: 6713-6727, 2003.

Anastasio TJ, Patton PE, and Belkacem-Boussaid K. Using Bayes' rule to model multisensory enhancement in the superior colliculus. *Neural Comput* 12: 1165-1187, 2000.

Avillac M, Deneve S, Olivier E, Pouget A, and Duhamel JR. Reference frames for representing visual and tactile locations in parietal cortex. *Nat Neurosci* 8: 941-949, 2005.

Behan M, and Appell PP. Intrinsic circuitry in the cat superior colliculus: projections from the superficial layers. *J Comp Neurol* 315: 230-243, 1992.

Behan M, and Kime NM. Intrinsic circuitry in the deep layers of the cat superior colliculus. *Vis Neurosci* 13: 1031-1042, 1996.

Berlucchi G, Sprague JM, Levy J, and DiBerardino AC. Pretectum and superior colliculus in visually guided behavior and in flux and form discrimination in the cat. *J Comp Physiol Psychol* 78: 123-172, 1972.

Carriere BN, Royal DW, and Wallace MT. Spatial heterogeneity of cortical receptive fields and its impact on multisensory interactions. *J Neurophysiol* 99: 2357-2368, 2008.

Casagrande VA, Harting JK, Hall WC, Diamond IT, and Martin GF. Superior colliculus of the tree shrew: a structural and functional subdivision into superficial and deep layers. *Science* 177: 444-447, 1972.

Clifford CW, and Ibbotson MR. Fundamental mechanisms of visual motion detection: models, cells and functions. *Prog Neurobiol* 68: 409-437, 2002.

Cuppini C, Ursino M, Magosso E, Rowland BA, and Stein BE. An emergent model of multisensory integration in superior colliculus neurons. *Front Integr Neurosci* 4: 6, 2010.

deCharms RC, Blake DT, and Merzenich MM. Optimizing sound features for cortical neurons. *Science* 280: 1439-1443, 1998.

Diederich A, and Colonius H. Bimodal and trimodal multisensory enhancement: effects of stimulus onset and intensity on reaction time. *Percept Psychophys* 66: 1388-1404, 2004.

Eggermont JJ, Aertsen AM, Hermes DJ, and Johannesma PI. Spectro-temporal characterization of auditory neurons: redundant or necessary. *Hear Res* 5: 109-121, 1981.

Fecteau JH, and Munoz DP. Salience, relevance, and firing: a priority map for target selection. *Trends Cogn Sci* 10: 382-390, 2006.

Fecteau JH, and Munoz DP. Warning signals influence motor processing. *J Neurophysiol* 97: 1600-1609, 2007.

Fitzpatrick DC, Olsen JF, and Suga N. Connections among functional areas in the mustached bat auditory cortex. *J Comp Neurol* 391: 366-396, 1998.

Ghazanfar AA, and Nicolelis MA. Feature article: the structure and function of dynamic cortical and thalamic receptive fields. *Cereb Cortex* 11: 183-193, 2001.

Guillery RW, and Sherman SM. Thalamic relay functions and their role in corticocortical communication: generalizations from the visual system. *Neuron* 33: 163-175, 2002.

Hackett TA .Multisensory convergence in the thalamus. *The New Handbook of Multisensory Processing.* Edited by Stein BE. 2012:

Hall WC, and Lee P. Interlaminar connections of the superior colliculus in the tree shrew. I. The superficial gray layer. *J Comp Neurol* 332: 213-223, 1993.

Hall WC, and Lee P. Interlaminar connections of the superior colliculus in the tree shrew. III: The optic layer. *Vis Neurosci* 14: 647-661, 1997.

Harris LR. The superior colliculus and movements of the head and eyes in cats. *J Physiol* 300: 367-391, 1980.

Hubel DH, and Wiesel TN. Integrative action in the cat's lateral geniculate body. *J Physiol* 155: 385-398, 1961.

Huerta MF HJ. Comparative Neurology of Optic tectum. 1984.

Itti L, and Koch C. Computational modelling of visual attention. *Nat Rev Neurosci* 2: 194-203, 2001.

Itti L, and Koch C. A saliency-based search mechanism for overt and covert shifts of visual attention. *Vision Res* 40: 1489-1506, 2000.

Kadunce DC, Vaughan JW, Wallace MT, Benedek G, and Stein BE. Mechanisms of within- and cross-modality suppression in the superior colliculus. *J Neurophysiol* 78: 2834-2847, 1997.

Kadunce DC, Vaughan JW, Wallace MT, and Stein BE. The influence of visual and auditory receptive field organization on multisensory integration in the superior colliculus. *Exp Brain Res* 139: 303-310, 2001.

Kanwal JS, Fitzpatrick DC, and Suga N. Facilitatory and inhibitory frequency tuning of combination-sensitive neurons in the primary auditory cortex of mustached bats. *J Neurophysiol* 82: 2327-2345, 1999.

Katzner S, Nauhaus I, Benucci A, Bonin V, Ringach DL, and Carandini M. Local origin of field potentials in visual cortex. *Neuron* 61: 35-41, 2009.

Kayser C, Logothetis NK, and Panzeri S. Visual enhancement of the information representation in auditory cortex. *Curr Biol* 20: 19-24, 2010.

Kayser C, Petkov CI, and Logothetis NK. Multisensory interactions in primate auditory cortex: fMRI and electrophysiology. *Hear Res* 258: 80-88, 2009.

King AJ, and Walker KM. Integrating information from different senses in the auditory cortex. *Biol Cybern* 106: 617-625, 2012.

Lakatos P, Karmos G, Mehta AD, Ulbert I, and Schroeder CE. Entrainment of neuronal oscillations as a mechanism of attentional selection. *Science* 320: 110-113, 2008.

Lakatos P, Chen CM, O'Connell MN, Mills A, and Schroeder CE. Neuronal oscillations and multisensory interaction in primary auditory cortex. *Neuron* 53: 279-292, 2007.

Lakatos P, Karmos G, Mehta AD, Ulbert I, and Schroeder CE. Entrainment of neuronal oscillations as a mechanism of attentional selection. *Science* 320: 110-113, 2008.

Liu J, and Newsome WT. Local field potential in cortical area MT: stimulus tuning and behavioral correlations. *J Neurosci* 26: 7779-7790, 2006.

May PJ. The mammalian superior colliculus: laminar structure and connections. *Prog Brain Res* 151: 321-378, 2006.

Meredith MA, Nemitz JW, and Stein BE. Determinants of multisensory integration in superior colliculus neurons. I. Temporal factors. *J Neurosci* 7: 3215-3229, 1987.

Meredith MA, and Stein BE. Spatial determinants of multisensory integration in cat superior colliculus neurons. *J Neurophysiol* 75: 1843-1857, 1996.

Meredith MA, and Stein BE. Spatial factors determine the activity of multisensory neurons in cat superior colliculus. *Brain Res* 365: 350-354, 1986a.

Meredith MA, and Stein BE. Visual, auditory, and somatosensory convergence on cells in superior colliculus results in multisensory integration. *J Neurophysiol* 56: 640-662, 1986b.

Montemurro MA, Rasch MJ, Murayama Y, Logothetis NK, and Panzeri S. Phase-of-firing coding of natural visual stimuli in primary visual cortex. *Curr Biol* 18: 375-380, 2008.

Munoz DP, and Guitton D. Fixation and orientation control by the tecto-reticulo-spinal system in the cat whose head is unrestrained. *Rev Neurol (Paris)* 145: 567-579, 1989.

Nicolelis MA, and Chapin JK. Spatiotemporal structure of somatosensory responses of many-neuron ensembles in the rat ventral posterior medial nucleus of the thalamus. *J Neurosci* 14: 3511-3532, 1994.

Nicolelis MA, Lin RC, Woodward DJ, and Chapin JK. Dynamic and distributed properties of many-neuron ensembles in the ventral posterior medial thalamus of awake rats. *Proc Natl Acad Sci U S A* 90: 2212-2216, 1993a.

Nicolelis MA, Lin RC, Woodward DJ, and Chapin JK. Induction of immediate spatiotemporal changes in thalamic networks by peripheral block of ascending cutaneous information. *Nature* 361: 533-536, 1993b.

Oonishi S. KY. Functional organization and integrative mechanism on the auditory cortex of cat. *JPN J Physiol* 15: 342-365, 1965.

Perrault TJ, Jr., Vaughan JW, Stein BE, and Wallace MT. Neuron-specific response characteristics predict the magnitude of multisensory integration. *J Neurophysiol* 90: 4022-4026, 2003.

Perrault TJ, Jr., Vaughan JW, Stein BE, and Wallace MT. Superior colliculus neurons use distinct operational modes in the integration of multisensory stimuli. *J Neurophysiol* 93: 2575-2586, 2005.

Rowland BA, Stanford TR, and Stein BE. A model of the neural mechanisms underlying multisensory integration in the superior colliculus. *Perception* 36: 1431-1443, 2007.

Royal DW, Carriere BN, and Wallace MT. Spatiotemporal architecture of cortical receptive fields and its impact on multisensory interactions. *Exp Brain Res* 198: 127-136, 2009.

Sarko DK, and Ghose D. Developmental plasticity of multisensory circuitry: how early experience dictates cross-modal interactions. *J Neurophysiol* 108: 2863-2866, 2012.

Schneider GE. Two visual systems. *Science* 163: 895-902, 1969.

Senkowski D and Engel AK . Oscillatory activity and multisensory processing. *The New Handbook of Multisensory Processing.* Edited by Stein BE. 2012:

Sherman SM. Thalamic relay functions. *Prog Brain Res* 134: 51-69, 2001a.

Sherman SM. The thalamus is more than just a relay. *Curr Opin Neurobiol* 17: 417-422, 2007.

Sherman SM. A wake-up call from the thalamus. *Nat Neurosci* 4: 344-346, 2001b.

Sherman SM, and Guillery RW. The role of the thalamus in the flow of information to the cortex. *Philos Trans R Soc Lond B Biol Sci* 357: 1695-1708, 2002.

Sprague JM. Neural mechanisms of visual orienting responses. *Prog Brain Res* 112: 1-15, 1996.

Sprague JM. The role of the superior colliculus in facilitating visual attention and form perception. *Proc Natl Acad Sci U S A* 88: 1286-1290, 1991.

Sprague JM, Berlucchi G, and Di Berardino A. The superior colliculus and pretectum in visually guided behavior and visual discrimination in the cat. *Brain Behav Evol* 3: 285-294, 1970.

Sprague JM, Levy J, DiBerardino A, and Berlucchi G. Visual cortical areas mediating form discrimination in the cat. *J Comp Neurol* 172: 441-488, 1977.

Sprague JM, and Meikle TH, Jr. The Role of the Superior Colliculus in Visually Guided Behavior. *Exp Neurol* 11: 115-146, 1965.

Stein BE, Huneycutt WS, and Meredith MA. Neurons and behavior: the same rules of multisensory integration apply. *Brain Res* 448: 355-358, 1988.

Treisman AM, and Gelade G. A feature-integration theory of attention. *Cogn Psychol* 12: 97-136, 1980.

Tunkl JE, and Berkley MA. The role of superior colliculus in vision: visual form discrimination in cats with superior colliculus ablations. *J Comp Neurol* 176: 575-587, 1977.

Wallace MT, and Stein BE. Sensory organization of the superior colliculus in cat and monkey. *Prog Brain Res* 112: 301-311, 1996.

White BJ and Munoz DP. The Superior Colliculus.*Oxford Handbook of eye movements.*2011.

Wilkinson LK, Meredith MA, and Stein BE. The role of anterior ectosylvian cortex in cross-modality orientation and approach behavior. *Exp Brain Res* 112: 1-10, 1996.

Wolfe JM, Cave KR, and Franzel SL. Guided search: an alternative to the feature integration model for visual search. *J Exp Psychol Hum Percept Perform* 15: 419-433, 1989.

Xing D, Yeh CI, and Shapley RM. Spatial spread of the local field potential and its laminar variation in visual cortex. *J Neurosci* 29: 11540-11549, 2009.

Zion Golumbic E, Cogan GB, Schroeder CE, and Poeppel D. Visual input enhances selective speech envelope tracking in auditory cortex at a "cocktail party". *J Neurosci* 33: 1417-1426, 2013a.

Zion Golumbic EM, Ding N, Bickel S, Lakatos P, Schevon CA, McKhann GM, Goodman RR, Emerson R, Mehta AD, Simon JZ, Poeppel D, and Schroeder CE. Mechanisms underlying selective neuronal tracking of attended speech at a "cocktail party". *Neuron* 77: 980-991, 2013b.